

RESILIENCE PLANNING AND OPTIMIZATION OF ELECTRIC POWER  
SYSTEMS AGAINST EXTREME WEATHER EVENTS

By

ABODH POUDYAL

A dissertation submitted in partial fulfillment of  
the requirements for the degree of

DOCTOR OF PHILOSOPHY

WASHINGTON STATE UNIVERSITY  
School of Electrical Engineering and Computer Science

MAY 2024

© Copyright by ABODH POUDYAL, 2024  
All Rights Reserved

© Copyright by ABODH POUDYAL, 2024  
All Rights Reserved

To the Faculty of Washington State University:

The members of the Committee appointed to examine the dissertation of ABODH POUDYAL find it satisfactory and recommend that it be accepted.

Anamika Dubey, Ph.D., Chair

Anjan Bose, Ph.D.

Noel Schulz, Ph.D.

## **ACKNOWLEDGMENT**

I recognize that my Ph.D. journey is not solely my own. Without the support of my family, professors, mentors, and friends, getting closer to graduation would have been much more challenging. I would like to express my sincere gratitude towards my thesis advisor Dr. Anamika Dubey for her continuous guidance, support, and encouragement. She has always supported me whether it is in discussing new ideas, getting out of a research problem, or providing suggestions to succeed as a graduate student.

I would also like to thank Dr. Anjan Bose and Dr. Noel Schulz, my dissertation committee, for providing valuable comments and suggestions in various steps of my Ph.D. journey that have further improved my research contributions. I am very thankful to Dr. Shiva Poudel, who has not only guided me during my initial Ph.D. years but also helped me as a friend throughout this journey. Special thanks to Charlotte, Shishir, and Sajjad for collaborating on a few of my projects. I am grateful to my friends Deepak, Saugat, Menuka, Habib, Surendra, Rabayet, Daniel, Aryan, Anup, Ninad, Athul, and Kunal for bolstering my efforts and research goals.

I owe my deepest gratitude to my family – especially my mother, Aruna Upadhyay – for her unconditional love and for providing me with continuous encouragement and support. I would have been far from this feat had it not been her sacrifice and hard work. Lastly, I cannot thank my wife, Shristi, enough for her unwavering support and encouragement. Her presence has been a constant source of motivation, inspiring me to strive for greater heights in life.

# RESILIENCE PLANNING AND OPTIMIZATION OF ELECTRIC POWER SYSTEMS AGAINST EXTREME WEATHER EVENTS

## Abstract

by Abodh Poudyal, Ph.D.  
Washington State University  
May 2024

Chair: Anamika Dubey

The socioeconomic losses from the recent unprecedented incidents in the electric power systems suggest the need for alternative planning strategies that account for the expected and extreme events that are less likely to occur. Such high impact low probability (HILP), or black swan, events are typically weather-related, have accounted for billions of dollars in economic losses, and left customers in the dark for several days. Furthermore, the proliferation of distributed energy resources (DERs) on the distribution grid indicates that system operators can also plan resilience from the customer's end, forming intentional microgrid islands when needed. However, existing planning strategies only minimize the expected operating cost and do not explicitly include the risk of extreme events. With the increasing frequency of black swan events in the current scenario, system operators should focus on the HILP events and find the optimal trade-off decision to maximize resilience with available resources. This

dissertation aims to investigate the impact of extreme weather events, hurricanes, and floods on the power grid and propose planning solutions to enhance the grid's resilience.

*First*, we highlight the need for resilience planning and assessment against extreme weather events. Here, we detail the resilience analysis process, characterize several attributes and performance-based resilience metrics, and identify measures to enhance the resilience of existing power distribution systems. *Second*, we develop a risk-averse two-stage stochastic optimization framework for resilience planning power distribution systems against extreme weather events. The resource planning strategy involves minimizing a risk metric, conditional value-at-risk (CVaR), while adhering to budget constraints for planning. Furthermore, the framework evaluates trade-offs among various factors, including resource availability, data availability, budget constraints, and risks. This facilitates the selection of specific planning decisions from a range of planning portfolios that can optimally restore critical loads during the realization of a HILP event. *Third*, we extend the risk-based planning framework for bulk power systems. The planning decisions include resilient dispatch of existing generators, line capacity upgrade, line hardening, DG siting, and sizing. *Fourth*, we decompose the planning problem into several sub-problems that can be solved in parallel. With the proposed approach, the solving time for a reasonably sized planning problem is reduced drastically without significantly compromising the planning solution's quality. *Finally*, we propose a modeling framework to assess the spatiotemporal compounding effect of hurricanes and storm surges on electric power systems. The spatiotemporal probabilistic loss metric helps system operators identify the potential impact and vulnerable components as the storm approaches. Additionally, we characterize the

impact of extreme weather events on socioeconomically vulnerable communities due to extended power outages induced by extreme weather events.

## TABLE OF CONTENTS

	Page
ACKNOWLEDGMENT . . . . .	iii
ABSTRACT . . . . .	iv
LIST OF TABLES . . . . .	xvii
LIST OF FIGURES . . . . .	xxi
CHAPTER	
1    INTRODUCTION . . . . .	1
1.1    Background . . . . .	1
1.1.1    Impact of Extreme Weather on the Power Grid . . . . .	1
1.1.2    Grid Modernization and Automation . . . . .	4
1.2    Motivation . . . . .	6
1.3    Contributions . . . . .	7
1.4    Dissertation Organization . . . . .	9
1.5    Publications and Software Packages . . . . .	10
1.5.1    Journals . . . . .	10
1.5.2    Conferences . . . . .	11
1.5.3    Software Packages . . . . .	12
REFERENCES . . . . .	13
2    RESILIENCE ASSESSMENT AND PLANNING IN POWER DISTRIBUTION SYSTEMS . . . . .	16
2.1    Introduction . . . . .	16

2.1.1 Motivation . . . . .	16
2.1.2 Related Literature and Gaps . . . . .	18
2.1.3 Contribution . . . . .	23
2.2 Framework for Resilience Evaluation in Power Distribution Systems	25
2.2.1 Reliability Vs. Resilience . . . . .	25
2.2.2 Resilient Power Distribution Systems . . . . .	27
2.2.3 Qualitative and Quantitative Assessment of Resilience . . . . .	30
2.2.4 Resilience analysis process . . . . .	31
2.2.5 Resilience metrics . . . . .	35
2.3 Power distribution resilience – Tools for planning & enhancement . .	42
2.3.1 Event forecast . . . . .	43
2.3.2 Load prioritization . . . . .	43
2.3.3 Situational awareness . . . . .	45
2.3.4 Resilience planning and restoration . . . . .	47
2.4 Interdependence with other critical infrastructures . . . . .	51
2.4.1 Information and communication technologies . . . . .	51
2.4.2 Transportation . . . . .	53
2.4.3 Natural gas . . . . .	55
2.4.4 Water distribution systems . . . . .	57
2.5 Research gaps and opportunities . . . . .	60
2.5.1 Proactive decision-making/operational planning . . . . .	60
2.5.2 System planning for resilience/long-term planning . . . . .	62

2.5.3	Modeling and forecasting the impact of natural disasters . . . . .	64
2.5.4	Smart grid operation for enhanced resilience . . . . .	65
2.5.5	Compound effect of extreme events and equity . . . . .	66
2.6	Summary . . . . .	68
	REFERENCES . . . . .	69
3	RESILIENCE QUANTIFICATION USING MULTI-CRITERIA DECISION MAKING . . . . .	95
3.1	Introduction . . . . .	95
3.1.1	Motivation . . . . .	95
3.1.2	Related Literature and Gaps . . . . .	96
3.1.3	Contribution . . . . .	97
3.2	Event and Impact Modeling . . . . .	98
3.2.1	Modeling Probabilistic Events . . . . .	98
3.2.2	Line Fragility Models . . . . .	98
3.3	Resilience of Power Distribution Grid . . . . .	99
3.3.1	Resilience Curve . . . . .	99
3.3.2	Resilience-driven Parameters . . . . .	100
3.3.3	Risk-based Resilience Measures . . . . .	104
3.4	Multi-criteria Decision Making using Choquet Integral . . . . .	104
3.4.1	$\lambda$ -Fuzzy Measures . . . . .	105
3.4.2	Behavioral Analysis of Fuzzy Measures . . . . .	106
3.4.3	Choquet Integral . . . . .	107

3.5	Resilience Metric Evaluation Framework . . . . .	107
3.5.1	Evaluating Resilience-driven Parameters . . . . .	108
3.5.2	Risk-driven Resilience Quantification . . . . .	108
3.6	Results and Analysis . . . . .	109
3.6.1	Calculating CVaR of Parameters . . . . .	109
3.6.2	Quantifying Resilience using Choquet Integral . . . . .	110
3.7	Summary . . . . .	113
	REFERENCES . . . . .	114
4	RISK-BASED ACTIVE DISTRIBUTION SYSTEMS PLANNING FOR RESILIENCE AGAINST EXTREME WEATHER EVENTS . . . . .	117
4.1	Introduction . . . . .	117
4.1.1	Motivation . . . . .	117
4.1.2	Related Literature and Gaps . . . . .	118
4.1.3	Contribution . . . . .	122
4.2	Mathematical Background . . . . .	124
4.2.1	Long-Term Planning Model Representation . . . . .	124
4.2.2	Two-stage Stochastic Optimization . . . . .	125
4.2.3	Optimization of Conditional Value-at-Risk . . . . .	126
4.2.4	Risk-based Stochastic Optimization . . . . .	129
4.3	Risk-based Resilience-oriented Distribution System Planning . . . . .	129
4.3.1	Probabilistic scenario generation and reduction . . . . .	130
4.3.2	Two-Stage Stochastic Optimization Problem Formulation . . . . .	134

4.4	Results and Analysis . . . . .	141
4.4.1	Scenario Generation and Reduction . . . . .	143
4.4.2	Risk-Averse Long-Term Planning . . . . .	144
4.4.3	Sensitivity analysis . . . . .	150
4.5	Summary . . . . .	156
	REFERENCES . . . . .	157
5	RESILIENCE PLANNING TRADE-OFFS IN POWER DISTRIBUTION SYSTEMS . . . . .	164
5.1	Introduction . . . . .	164
5.1.1	Motivation . . . . .	164
5.1.2	Related Literature and Gaps . . . . .	165
5.1.3	Contribution . . . . .	167
5.2	System Modeling Requirements for Resilience Planning . . . . .	168
5.2.1	Extreme Weather Events Simulator . . . . .	168
5.2.2	Distribution Systems Impact Model . . . . .	170
5.2.3	Modeling Different Uncertainties . . . . .	171
5.2.4	Risk Analysis . . . . .	172
5.3	Methodology . . . . .	172
5.3.1	Planning Decisions and Assumptions . . . . .	173
5.3.2	Problem Formulation . . . . .	174
5.3.3	Scenario Generation and Reduction . . . . .	185
5.4	Results and Analysis . . . . .	186

5.4.1	Wind and Fragility Models . . . . .	188
5.4.2	Planning Model Trade-offs . . . . .	189
5.5	Summary . . . . .	195
	REFERENCES . . . . .	197
6	RESILIENCE PLANNING OF BULK POWER SYSTEMS AGAINST EXTREME WEATHER EVENTS . . . . .	201
6.1	Introduction . . . . .	201
6.1.1	Motivation . . . . .	201
6.1.2	Related Literature and Gaps . . . . .	203
6.1.3	Contribution . . . . .	204
6.2	Resilience-driven Planning Modeling . . . . .	206
6.2.1	Two-stage Stochastic Planning Model . . . . .	206
6.3	Probabilistic Scenario Generation and Selection . . . . .	211
6.3.1	Scenario Generation . . . . .	211
6.3.2	Scenario Selection . . . . .	214
6.4	Results and Analysis . . . . .	215
6.4.1	Test Case and Parameters . . . . .	215
6.4.2	Scenario Generation and Selection . . . . .	216
6.4.3	Resilience Planning . . . . .	217
6.5	Summary . . . . .	224
	REFERENCES . . . . .	225
7	SCALABLE PLANNING FRAMEWORK FOR RESILIENCE PLANNING IN POWER DISTRIBUTION SYSTEMS . . . . .	229

7.1	Introduction . . . . .	229
7.1.1	Motivation . . . . .	229
7.1.2	Related Literature and Gaps . . . . .	230
7.1.3	Contribution . . . . .	230
7.2	Scalable Framework for Power Systems Planning . . . . .	231
7.2.1	Dual-decomposition with Progressive Hedging . . . . .	231
7.2.2	Progressive Hedging Extensions . . . . .	232
7.3	Results and Analysis . . . . .	237
7.3.1	9500-Node Model . . . . .	237
7.3.2	Analysis of Model Complexities . . . . .	239
7.3.3	Scalability of Planning Models . . . . .	240
7.3.4	PH Extensions . . . . .	242
7.4	Summary . . . . .	245
	REFERENCES . . . . .	246
8	EXTREME WEATHER EVENTS-INDUCED OUTAGES AND THEIR SOCIOECONOMIC IMPACT . . . . .	249
8.1	Introduction . . . . .	249
8.1.1	Motivation . . . . .	249
8.1.2	Related Literature and Gaps . . . . .	251
8.1.3	Contribution . . . . .	253
8.2	Extreme Weather Events and Impact Model . . . . .	253
8.2.1	Hurricane Wind Field Model . . . . .	253

8.2.2 Storm Surge Model . . . . .	255
8.2.3 Power Systems Impact Model . . . . .	256
8.2.4 Power Systems Impact Model . . . . .	257
8.2.5 Community Impact Assessment . . . . .	259
8.3 Vulnerability Assessment . . . . .	260
8.3.1 Power System Vulnerability . . . . .	260
8.3.2 Community Vulnerability . . . . .	263
8.4 Simulation Framework . . . . .	265
8.5 Results and Analysis . . . . .	267
8.5.1 Hurricane and Storm Surges Impact Assessment . . . . .	268
8.5.2 Vulnerability Assessment . . . . .	268
8.6 Summary . . . . .	275
REFERENCES . . . . .	277
<b>9 CONCLUSIONS AND FUTURE WORK . . . . .</b>	<b>282</b>
9.1 Summary of Contributions . . . . .	282
9.1.1 Resilience Assessment and Planning for Power Distribution . .	283
9.1.2 Risk-based Planning Framework of Electric Power Systems .	283
9.1.3 Large-Scale Planning using Dual Decomposition Approach .	284
9.1.4 Spatiotemporal Impact Assessment of Hurricanes and Storm Surges . . . . .	284
9.2 Future Research Directions . . . . .	285
9.2.1 Modeling Critical Infrastructures Interdependence . . . . .	285

9.2.2 Multi-stage Planning . . . . .	286
9.2.3 Defensive Islanding and Restoration of Electric Power Systems Against Extreme Weather Events . . . . .	286
9.2.4 Use of Artificial Intelligence Techniques for Realistic Scenario Generation . . . . .	287
9.3 Publications and Software Packages . . . . .	288
9.3.1 Journals . . . . .	288
9.3.2 Conferences . . . . .	288
9.3.3 Software Packages . . . . .	289
REFERENCES . . . . .	290

## LIST OF TABLES

TABLE	Page
2.1 Comprehensive resilience study in the existing literature in different domains, their contributions, and limitations. . . . .	19
2.2 Some widely used examples of the category of consequences and resilience metrics. . . . .	36
2.3 State-of-the-art– Resilience planning and enhancement strategies for power distribution systems. . . . .	42
3.1 $CVaR_\alpha$ of normalized resilience-based parameters for base and smart network . . . . .	110
3.2 Initial fuzzy weights of parameters for resilience metric calculation . .	112
3.3 Shapely values of each parameters based of their initial weights. . . .	112
3.4 Choquet Integral values based on Shapely values of each parameters .	113
4.1 Summary of existing literature for resilience-oriented planning of power distribution systems . . . . .	120
4.2 Base case expected value and $CVaR_\alpha$ of prioritized load loss. . . . .	146
4.3 Expected value and $CVaR_\alpha$ of prioritized load loss and prioritized critical load (PCL) picked up for different values of $\lambda$ . . . . .	147
4.4 95% confidence interval of the solution obtained using different scenario sets for each number of scenarios. . . . .	155
5.1 Resilience Planning Investment Costs . . . . .	188
6.1 Cost for each planning measure. . . . .	216
6.2 Expected load shed and CVaR for various planning strategies, risk	

aversion, and budget. . . . .	220
7.1 Comparison of model complexities with the number of scenarios. . . . .	239
7.2 Solve time and solution for EF and solution with relative gap and parameters for PH algorithm. . . . .	241
8.1 Voltage level-based critical and collapse sustained wind speed values for each line segment for fragility analysis . . . . .	267

## LIST OF FIGURES

FIGURE	Page
1.1 Weather and non-weather-related US power outages from 2000-2021 [9]. . . . .	2
1.2 Billion dollar disaster events in the US from 1980-2023 [9]. . . . .	3
1.3 Microgrid with several distributed resources [19]. . . . .	5
2.1 a) The number of extreme events and publication trends in energy and resilience. b) Extreme events and their frequency in the US . . . . .	17
2.2 Similarities and differences between reliability and resilience. . . . .	27
2.3 Response of power distribution system during HILP events. . . . .	29
2.4 The resilience analysis process – Setting up resilience goals, measuring resilience, and planning for resilience enhancement. . . . .	32
2.5 Different stages of resilience planning and enhancement strategies. . . . .	44
2.6 Interdependence among various critical infrastructures, namely ICT, transportation, natural gas, and physical power grid networks. . . . .	52
3.1 Typical resilience assessment curve based on the number of weighted CL online. The time variables refer to the smart network . . . . .	101
3.2 Simulation-based framework for resilience metric computation . . . . .	105
3.3 Modified IEEE-123 test case with DGs, tie switches, and CLs. . . . .	110
3.4 PDF of availability for base and smart network. . . . .	111
4.1 Two-stage planning framework example for a specific scenario. . . . .	124
4.2 VaR and CVaR representation for a discrete loss function. HILP events are the ones with $(1 - \alpha)$ probability of occurrence. . . . .	128

4.3	Overall architecture of risk-averse two-stage planning problem. . . . .	128
4.4	Regional wind profile. . . . .	131
4.5	a) Component and b) system-level fragility model for an extreme event	132
4.6	A set of 49 representative scenarios with respective probabilities. . . . .	134
4.7	Modified IEEE 123-bus test case . . . . .	142
4.8	Moving average of loss of load for 1000 Monte-Carlo trials a) without hardening b) with line hardening. . . . .	144
4.9	Comparison of prioritized load loss obtained for two sets of reduced scenarios a) without hardening b) with hardening. . . . .	145
4.10	DG sizing and siting solution for a scenario with additional hardening measures for a) risk-neutral and b) risk-averse planning. . . . .	149
4.11	Comparison of $CVaR_\alpha$ of prioritized loss of load for different values of $\alpha$ and risk preference. . . . .	150
4.12	$CVaR_\alpha$ for different DG investment strategies for a) risk-neutral and b) risk-averse planning. . . . .	151
4.13	Different number of scenarios with respective probabilities of occur- rence: (a) 7, (b) 21, (c) 49, (d) 98, and e) 147 scenarios. . . . .	151
4.14	Comparison of objective value and solve time for a different number of scenarios. . . . .	154
4.15	Comparison of objective value on a different set of scenarios for each number of scenarios sampled. . . . .	155
5.1	Resilient distribution systems planning framework. . . . .	168
5.2	Planning decisions and strategies for resilience enhancement in power distribution systems. . . . .	175
5.3	Switch operation and status for normal and damaged conditions. . . . .	179
5.4	Modified IEEE-123 bus test system. . . . .	187
5.5	a) Historical wind gust data in Fort Myers, Florida, and its Gaussian density estimate. b) Wind gust scenario probability estimation. . . . .	189

5.6	a) Fragility models of 1-phase and 3-phase line segments. b) Sensitivity of $CVaR_\alpha$ with change in fragility models. . . . .	191
5.7	Sensitivity of $CVaR$ of the prioritized load loss with respect to $\alpha$ and risk preference. . . . .	191
5.8	Multi-resource trade-offs for $\mathcal{C}_{max}^T = \$2$ M. The size represents the expected, whereas the color represents the $CVaR_{0.95}$ of load loss. . . . .	192
5.9	Budget distribution in various planning decisions with respect to risk preferences. . . . .	195
6.1	Overall framework of risk-based planning model. . . . .	212
6.2	Regional wind profile [19]. . . . .	213
6.3	Loss distribution of overall scenarios for each wind speed. . . . .	218
6.4	Comparison of total and % load shed for various planning strategies. . . . .	219
6.5	Variation of expected load shed and CVaR of load shed for varying planning portfolios risk-neutral decisions. . . . .	221
6.6	Variation of expected load shed and CVaR of load shed for varying planning portfolios risk-averse decisions. . . . .	222
6.7	Budget distribution for multiple planning decisions. . . . .	223
7.1	Scenario decomposition and non-anticipativity relaxation . . . . .	233
7.2	Progressive Hedging Algorithm . . . . .	233
7.3	Two scenario bundles with two scenarios each . . . . .	234
7.4	9500-node test system. . . . .	238
7.5	Increase in model complexity with the increase in the number of scenarios. The base with factor 1 is represented by 5 scenarios. . . . .	240
7.6	a) Normalized term-difference convergence metric b) Primal-dual residual convergence metric. . . . .	243
7.7	Convergence bounds and mip gap for PH and post PH operation. . . . .	244
8.1	Distribution of wind field of a hurricane at a fixed time. . . . .	254

8.2	a) Wind field of Hurricane Harvey and b) Substation flooding scenario, above ground level, for Texas basins. . . . .	261
8.3	CDC's social vulnerability index . . . . .	263
8.4	Overall framework of assessing hurricane and storm surge-induced power system vulnerabilities and their socioeconomic impact. . . . .	265
8.5	a) Line outage probability for selected lines Harvey's track. b) Substation outage probability for all storm surge scenarios. . . . .	269
8.6	Overall loss comparison between the impact of hurricane alone and the compound impact of the hurricane and coastal flood for $\zeta = 1$ . . . . .	270
8.7	Time-varying loss for each hurricane track. The loss at each time step also includes the expected value of loss over entire flood basins. . . .	271
8.8	Vulnerability indices based on the percentile rank of the average outage probability of a) branches and b) substations for all hurricanes. . . .	272
8.9	Bar chart depicting an overall load loss in the study area caused by historical hurricanes. . . . .	273
8.10	a) Outage Vulnerability Index (OVI) and b) Integrated Community Vulnerability Index (ICVI) around the ERCOT region. . . . .	274

## **Dedication**

*To my Mother*

# CHAPTER 1

## INTRODUCTION

### 1.1 Background

#### 1.1.1 Impact of Extreme Weather on the Power Grid

Extreme weather events can have a devastating impact on the electric power grid, posing serious concerns for personal safety and national security. These events pose severe challenges to the operation and supply of the electric grid, affecting millions of customers [1]. For example, Hurricane Ian in 2022 affected approximately 2.7 million customers in Florida [2], while Europe experienced an energy crisis during the 2022 heatwave, with France witnessing a drastic increase in electricity prices, reaching a record of €700/MWh [3]. In 2022, extreme drought and heatwave in China caused a 50% drop in hydropower generation from 900 GWh to 450 GWh upstream of the Yangtze River. This led to extended power outages in the Sichuan region, where 80% of electricity generation depended on hydropower [4]. The power outage in Texas in February 2021 left more than ten million people without power, causing a financial impact of about \$4 billion on wind farms, significantly more than their annual gross revenue [5]. Iran experienced a summer heatwave in 2021 with temperatures exceeding 122 F; a deficit of almost 11 gigawatts of electricity was reported [6]. In 2021, Hurricane Ida caused widespread outages in the Northeastern US, affecting 1.2 million people, and it took almost fifteen days to restore electric power entirely [7]. In 2022, there were eighteen different billion-dollar disasters in the United States alone, with an estimated loss of approximately \$172 billion [8]. Critical customers, such as hospitals and transportation systems, endure substantial economic losses during such

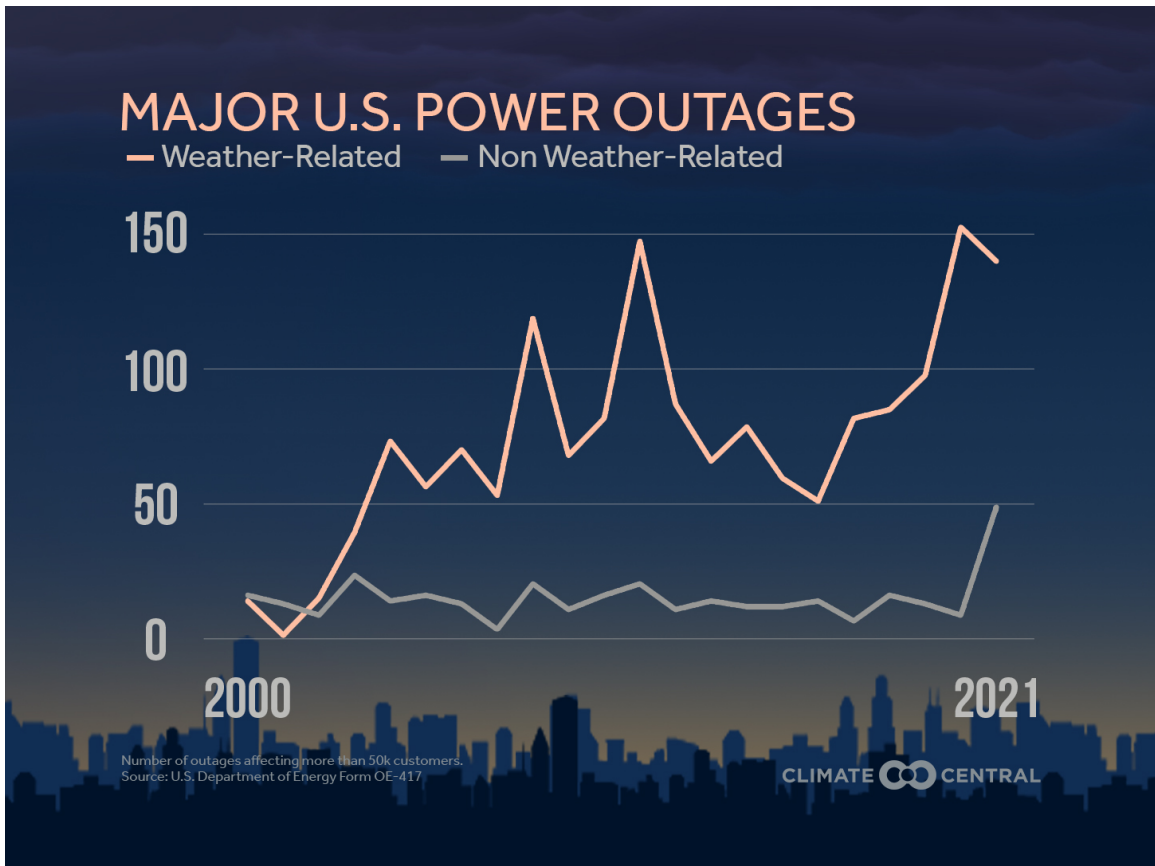


**Figure 1.1** Weather and non-weather-related US power outages from 2000-2021 [9].

calamities. Prolonged power outages also exacerbate personal safety and security vulnerabilities, highlighting the need to increase grid resilience to extreme weather events.

Fig. 1.1 represents the weather and non-weather-related power outages in the United States from 2000 - 2021 [9]. The figure shows that weather-related outages have increased significantly in recent years. Hurricanes, in particular, account for over a trillion dollars in economic losses and are responsible for significant power outages in the US [10, 11]. During landfall, as the strong hurricane wind field traverses inland,

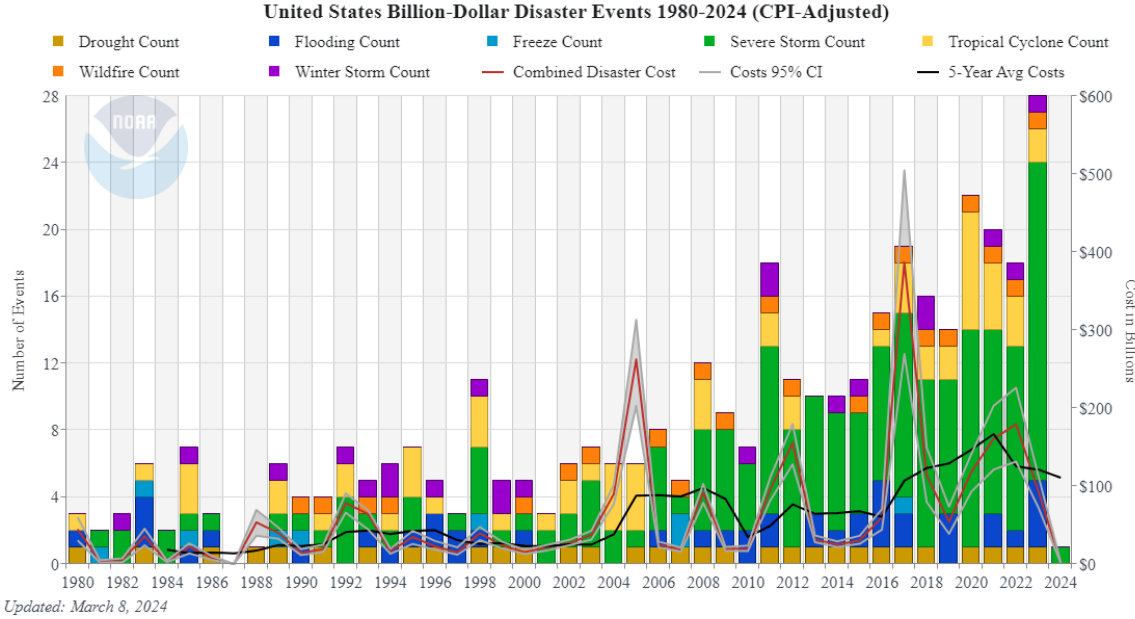


**Figure 1.2** Billion dollar disaster events in the US from 1980-2023 [9].

it propels a huge water body known as a storm surge, flooding the coastal regions. The storm surge is sometimes the most destructive part of a hurricane and accounts for considerable damage [12]. For instance, Hurricane Ida caused about \$55 billion in damages in Louisiana alone due to wind and storm surge damage, with additional flooding damage of about \$23 billion in the Northeastern US [13]. Almost 1.2 million customers experienced power outages across eight different states. Hurricane Ian recently had a devastating impact in Florida and is expected to have incurred billions of dollars in losses, with a peak of about 2.7 million customers in a power outage [14]. The frequency of such high-impact, low-probability (HILP) events has increased at an alarming rate, costing about \$152.6 billion in climate-related disasters in 2021 alone in the US. The US Department of Energy (DOE) estimated that the total cost of power outages can reach up to \$150 billion per year [15]. Fig. 1.2 shows the number of events per year and their associated damages from 1980 - 2023 [9].

The resulting socio-economic losses and the power grid's vulnerability to extreme weather events necessitate the incorporation of resilience in system planning to account for not only the expected events but also the extreme events that are less likely to occur. Towards this goal, different utilities have spent millions of dollars deploying smart grid technologies such as distribution automation with automated feeder switching, intentional islanding (microgrid), and upgrading vulnerable feeders and substations [16]. However, with the increasing frequency and severity of weather-related events, a more systematic approach to smart grid expenditures is required to identify appropriate system upgrade solutions for strengthening system resilience.

*This dissertation work aims to develop an end-to-end framework that can assist electric grid planners in assessing and quantifying the impact of extreme weather events and making risk-averse planning decisions that can enhance the resilience of existing electric grid against extreme weather events in the future.*

### 1.1.2 Grid Modernization and Automation

Recently, the US government announced billions of dollars of investment in making the electric power grid more reliable, resilient, and secure [17]. Although the existing power grid is somewhat reliable in its current form, the socioeconomic losses due to the increasing frequency and intensity of extreme weather conditions pushed the government and grid planners to invest in making it more resilient. In the US alone, extreme weather events between 2003 and 2012 caused nearly 700 power outages, with 80-90% of these outages resulting from power distribution system failures [18]. In the last decade, these numbers have grown exponentially; hence, the effort on resilience enhancement has shifted focus to the distribution side.

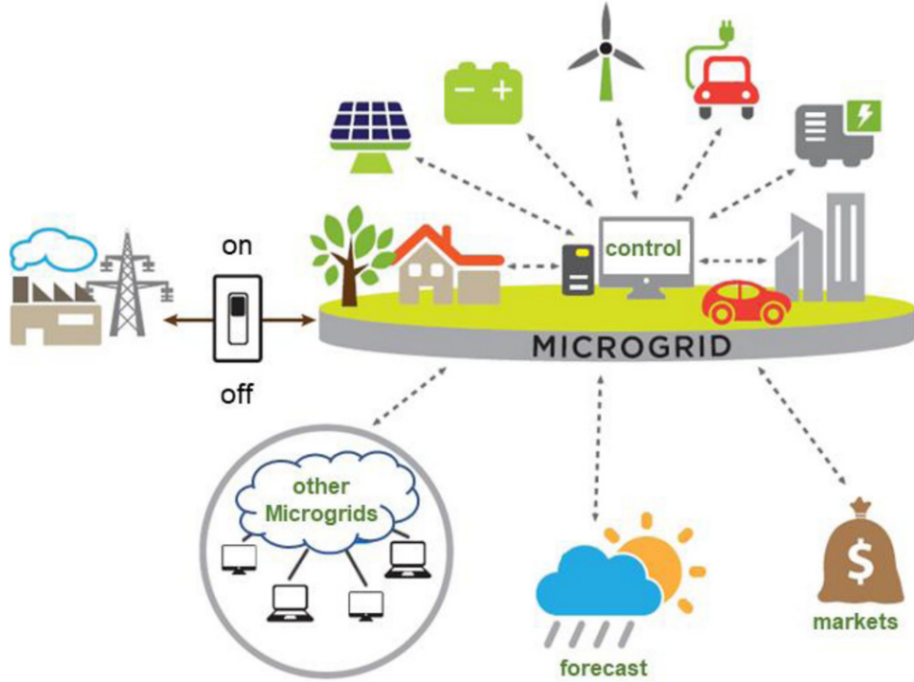


**Figure 1.3** Microgrid with several distributed resources [19].

The growth of distributed energy resources (DER) has paved a new way for resilience enhancement in the power grid via microgrid formation such that the electric grid can be segregated into multiple smaller grids that can operate independently or in a networked fashion. Fig. 1.3 shows a general representation of a microgrid [19]. During normal conditions, the microgrid operates in a grid-connected mode and receives continuous electric power from the upstream generation. However, in emergency conditions, the microgrid can operate as a self-sustained island. Installing remote-controlled sensors and switches can assist utility crews in quickly identifying outage locations and enhance situational awareness. Remotely controlled automatic switches can temporarily reroute the power supply route to maintain an uninterrupted power supply for customers. Traditionally, utility crews need to manually identify the source of outages and isolate them with manual switch operations. Furthermore, utilities and

DOE are actively identifying ways for grid hardening such as undergrounding systems affected by high-speed winds or weatherizing poles and conductors to prevent extreme cold and wildfire impact. Such investments can boost the grid resilience goals for both transmission and distribution systems.

## 1.2 Motivation

In recent years, there have been several advancements in weather prediction models. Still, they have not been adequately utilized to analyze the potential impact of upcoming natural hazards on the power grid. Such predictive information is essential to power grid planners and operators to reduce the effects when an event is realized [20, 21]. For instance, system operators can identify potential substations that could be inundated due to storm surges and proactively disconnect them to avoid equipment damage and facilitate fast restoration. These long-term planning strategies can help planners identify vulnerable transmission lines and propose line-hardening strategies. However, there are several challenges in developing a resilience planning model for the electric power grid against extreme weather conditions. The motivation of this dissertation is based on these specific challenges. *First*, there is a lack of resilience assessment and planning principles for grid planners specific to extreme weather events. Grid planners can benefit from the resilience analysis process, characterization of resilience metrics, and identification of resilience planning methods to enhance the resilience of the electric power grid. *Second*, although advanced and accurate, physics-based weather models are complex, require extensive computational resources, and take extensive time to run, making them unsuitable for grid planners. Hence, there is a need for data-driven weather models that can suitably represent the

physics of the actual weather models and assist grid planners in assessing the spatiotemporal impact of these events on the power grid and associated socioeconomic vulnerabilities of related communities. *Third*, existing planning-based methods address the impact of expected events but not HILP events and their associated risks. Hence, it is desirable to incorporate the risks and minimize them in the planning stage so that more customers can either be restored or have an uninterrupted power supply when such HILP scenarios are realized. Moreover, grid planners are undecided on the planning portfolios as some decisions are guided by policy and regulations rather than resilience and risk. Hence, there is a need for extensive trade-off analysis on several planning decisions, which can assist the grid planners in making an informed decision without compromising the risk and resilience of the system. *Fourth*, planning problems become increasingly difficult to solve with the increase in uncertainty, number of decision spaces, number of scenarios, and size of the system. Hence, there is a need for a scalable solution that can alleviate the computational challenges of the planning problem without compromising solution quality.

### 1.3 Contributions

Broadly, this dissertation aims to create a framework for multi-resource planning that improves the resilience of electric power systems using optimization tools. The major contributions of this dissertation are detailed below:

The first contribution is to provide a detailed overview of the standard resilience analysis process and its assessment methods for power distribution systems. Through this work, we differentiate resilience from reliability and characterize the resilience of the power distribution systems in terms of several attribute-based and performance-

based metrics. We also provide insights into how these metrics are formulated and used in the current resilience enhancement practices. Additionally, we identify the interdependencies of power distribution systems with other critical infrastructures and provide long-term and operational planning solutions that can enhance the resilience of the distribution grid against extreme weather conditions.

As a second contribution, we develop a risk-averse active distribution system planning framework to enhance resilience against extreme weather events. We propose a resilience metric considering conditional value-at-risk (CVaR) and the multi-criteria decision-making process. Then, we formulate a risk-averse stochastic planning framework with distributed generator siting and sizing decisions using a two-stage stochastic programming method. The framework is extended to include multiple planning resources, including line hardening, tie switch placements, and DG siting and sizing, to analyze the trade-offs among different planning decisions. The trade-off parameters considered are fragility models, risk preference, multiple planning resources, and planning budget allocation. Additionally, we develop a risk-averse planning framework for bulk power systems with investment decisions considering line hardening, line capacity upgrade, DG siting and sizing, and proactive dispatch set points of the generators to minimize the expected load shed and CVaR of load shed for high wind speed conditions.

The third contribution of this work is to propose a scalable framework based on a dual decomposition algorithm to solve the stochastic planning model in parallel. The planning problem is decomposed into each scenario-based sub-problem and solved in parallel using progressive hedging (PH). The non-anticipative nature of the first stage decisions is relaxed and rather introduced as a penalty function in the objective.

Finally, this dissertation develops a spatiotemporal impact assessment framework and analyzes the socioeconomic vulnerabilities due to power outages induced by extreme weather events. The hurricane is modeled using a statistical method, and an existing storm surge model is leveraged to assess the compound impact of hurricanes and storm surges on the power grid. Probabilistic simulations are conducted to observe the spatiotemporal losses due to the combined impact of hurricanes and storm surges. The work is extended to translate the extreme event-induced outages with the socioeconomic vulnerability of the residing population in the affected area.

#### **1.4 Dissertation Organization**

The overall dissertation is organized into nine chapters. The resilience planning and assessment methods are described in Chapter 2. The chapter also discusses the resilience metrics and identifies several research directions pertaining to long and short-term planning for resilience enhancement in power distribution systems.

Chapter 3 presents a resilience metric in power distribution systems using a multi-criteria decision-making process. The metric incorporates both the attribute-based and performance-based aspects of the system and uses a risk-based approach to quantify the resilience into a single score.

Chapter 4 details a mathematical risk-based resilience planning model for power distribution systems using two-stage stochastic programming. A risk-based planning model is formulated, and case studies with sensitivity analyses are provided to validate the proposed model.

Chapter 5 of this dissertation extends the planning model presented in Chapter 4 to include multiple planning resources and details the trade-offs of various planning

decisions and solution space. The trade-off analyses are conducted on several system parameters and planning strategies.

Chapter 6 focuses on resilience-based planning for bulk power systems against extreme weather conditions. The planning model is described, and several planning strategies are proposed and compared to identify optimal planning portfolios for grid planners. The proposed model is validated on a realistic test system.

Chapter 7 presents a scalable power distribution planning model based on the model decomposition technique. Additionally, the chapter includes a comparative study of the decomposition-based model with the extensive form-based planning model with simulation results.

Chapter 8 provides a spatiotemporal hurricane and storm surge impact assessment framework for bulk power grids. Later in the chapter, the community-level vulnerability assessment metric is proposed to identify customers' vulnerability due to power outages due to extreme weather conditions.

Chapter 9 concludes the dissertation and summarizes the major contribution. Furthermore, potential future research directions are also highlighted to extend the research presented here.

## 1.5 Publications and Software Packages

### 1.5.1 Journals

1. A. Poudyal, S. Poudel, and A. Dubey, “Large-scale Resilience Planning in Power Distribution Systems against Extreme Weather Events,” IEEE Transactions on Power Systems (in preparation)

2. A. Poudyal, S. Lamichhanne, J. Campos do Prado, and A. Dubey, “**Resilience-driven Planning of Electric Power Systems Against Extreme Weather Events**,” *Sustainable Energy, Grids and Networks* (in preparation)
3. A. Poudyal, and A. Dubey, “**Multi-resource Trade-offs in Resilience Planning Decisions for Power Distribution Systems**,” *IEEE Transactions on Industry Applications* (under review)
4. A. Poudyal, S. Paul, S. Poudel, and A. Dubey, “**Resilience assessment and planning in power distribution systems: Past and future considerations**,” *Renewable and Sustainable Energy Reviews*, Jan. 2024
5. A. Poudyal, S. Poudel, and A. Dubey, “**Risk-Based Active Distribution System Planning for Resilience Against Extreme Weather Events**,” *IEEE Transactions on Sustainable Energy*, Nov. 2022

### 1.5.2 Conferences

1. A. Poudyal, S. Lamichhane, C. Wertz, S. Uddin Mahmud, and A. Dubey. “**Hurricane and Storm Surges-Induced Power System Vulnerabilities and their Socioeconomic Impact**,” *2024 IEEE Power & Energy Society General Meeting*, Seattle, WA, Jul. 2024 (accepted)
2. A. Poudyal, and A. Dubey. “**Understanding Trade-Offs in Resilience Planning Decisions for Power Distribution Systems**,” *2023 IEEE Industry Applications Society Annual Meeting (IAS)*, Nashville, TN, Oct. 2023.
3. A. Poudyal, C. Wertz, A. Mi Nguyen, S. Uddin Mahmud, V. Gunturi and A. Dubey. “**Spatiotemporal impact assessment of hurricanes and storm**

**surges on electric power systems,” 2023 IEEE Power & Energy Society General Meeting**, Orlando, FL, Jul. 2023.

4. A. Poudyal, V. Iyengar, D. Garcia-Camargo, and A. Dubey. “**Spatiotemporal Impact Assessment of Hurricanes on Electric Power Systems**,” *2022 IEEE Power & Energy Society General Meeting*, Denver, CO, Jul. 2022.
5. A. Poudyal, S. Poudel, and A. Dubey. “**A risk-driven probabilistic approach to quantify resilience in power distribution systems**,” *2022 17th international conference on probabilistic methods applied to power systems (PMAPS)*, Manchester, UK, Jun. 2022.

### 1.5.3 Software Packages

1. <https://abodh.github.io/LinDistRestoration/>
2. <https://github.com/abodh/LinDistRestoration>
3. [https://github.com/abodh/proactive\\_resilience\\_planning](https://github.com/abodh/proactive_resilience_planning)

## REFERENCES

- [1] S. Paul, A. Poudyal, S. Poudel, A. Dubey, and Z. Wang, “Resilience assessment and planning in power distribution systems: Past and future considerations,” *Renewable and Sustainable Energy Reviews*, vol. 189, p. 113991, 2024.
- [2] NASA Earth Observatory, “Power outages after hurricane ian,” tech. rep., NASA Earth Observatory, Sep. 2022. <https://earthobservatory.nasa.gov/images/150431/power-outages-after-hurricane-ian>.
- [3] I. Binnie and K. Abnett, “Heatwave puts Europe’s energy systems to the test,” *Reuters*, Jun. 2022. Last accessed 18 April 2023.
- [4] M. Ma, Y. Qu, J. Lyu, X. Zhang, Z. Su, H. Gao, X. Yang, X. Chen, T. Jiang, J. Zhang, *et al.*, “The 2022 extreme drought in the yangtze river basin: Characteristics, causes and response strategies,” *River*, vol. 1, no. 2, pp. 162–171, 2022.
- [5] G. S. Poulos, W. Johnson, J. Crescenti, M. Stoelinga, and J. Bosche, “Ercot market cold weather failure 10-19 february 2021: wind energy financial loss and corrective actions,” *ArcVera Renewables*, Apr. 2021.
- [6] S. J. Frantzman, “Iran power outage crisis leads politicians to slam their own policy,” *The Jerusalem Post*, Jul. 2021.
- [7] J. L. Beven II, A. Hagen, and R. Berg, “National hurricane center tropical cyclone report: Hurricane Ida (AL092021),” tech. rep., National Oceanic and Atmospheric Administration, Apr. 2022.

- [8] A. B. Smith, “2021 U.S. billion-dollar weather and climate disasters in historical context,” *National Oceanic and Atmospheric Administration*, Jan. 2022.
- [9] “Surging weather-related power outages,” September 2022.
- [10] NOAA National Centers for Environmental Information (NCEI), “U.S. Billion-Dollar Weather and Climate Disasters,” 2021.
- [11] N. Alemazkoor, B. Rachunok, D. R. Chavas, A. Staid, A. Louhghalam, R. Nateghi, and M. Tootkaboni, “Hurricane-induced power outage risk under climate change is primarily driven by the uncertainty in projections of future hurricane frequency,” *Nature Scientific Reports*, vol. 10, Sep. 2020.
- [12] N. Bradford, “The empowered storm surge.”
- [13] J. L. Beven II, A. Hagen, and R. Berg, “HURRICANE IDA,” Tech. Rep. AL092021, National Hurricane Center, Apr. 2022.
- [14] “Hurricane Ian | Update #21 - Final,” Oct. 2022.
- [15] The White House, “FACT SHEET: Biden-Harris Administration Announces Historic Investment to Bolster Nation’s Electric Grid Infrastructure, Cut Energy Costs for Families, and Create Good-paying Jobs.” <https://shorturl.at/jJMv7>, October 2023.
- [16] R. Moreno, M. Panteli, P. Mancarella, H. Rudnick, T. Lagos, A. Navarro, F. Ordonez, and J. C. Araneda, “From Reliability to Resilience: Planning the Grid Against the Extremes,” *IEEE Power and Energy Magazine*, vol. 18, no. 4, pp. 41–53, 2020.

- [17] Department of Energy, “Biden-harris administration announces \$3.5 billion for largest ever investment in america’s electric grid, deploying more clean energy, lowering costs, and creating union jobs.” <https://shorturl.at/ampBQ>, October 18 2023.
- [18] J. Furman, “Economic Benefits of Increasing Grid Resilience to Weather Outages,” tech. rep., US Department of Energy, Aug. 2013.
- [19] M. Stadler and A. Naslé, “Planning and implementation of bankable microgrids,” *The Electricity Journal*, vol. 32, no. 5, pp. 24–29, 2019.
- [20] A. Poudyal, S. Poudel, and A. Dubey, “Risk-based active distribution system planning for resilience against extreme weather events,” *IEEE Transactions on Sustainable Energy*, pp. 1–14, 2022.
- [21] A. Poudyal, A. Dubey, and S. Poudel, “A risk-driven probabilistic approach to quantify resilience in power distribution systems,” in *2022 17th International Conference on Probabilistic Methods Applied to Power Systems (PMAPS)*, pp. 1–6, 2022.

## CHAPTER 2

# RESILIENCE ASSESSMENT AND PLANNING IN POWER DISTRIBUTION SYSTEMS

### 2.1 Introduction

This chapter introduces the concept and necessity of resilience assessment and planning specific to power distribution systems. The resilience of the grid is characterized by reliability, and a detailed resilience analysis process is described. Furthermore, resilience metrics are characterized, and critical infrastructures interdependent with power distribution systems are identified. Finally, various long-term and short-term planning measures are described for present and future research directions.

#### 2.1.1 Motivation

Over the past decade, the frequency and intensity of extreme weather events have significantly increased worldwide, leading to widespread power outages and blackouts. As these threats continue to challenge power distribution systems, mitigating the impacts of extreme weather events has become paramount. Consequently, resilience has become crucial for designing and operating power distribution systems. A resilient system can withstand severe disturbances, recover quickly to its normal operating state, and ensure uninterrupted power supply. It is worth noting that power distribution grids account for more than 80% of power outages due to disruptions caused by extreme weather events [1]. Furthermore, due to the grid modernization initiatives, the bidirectional energy flow architecture of power grids, and the increasing impact of extreme weather events, ensuring the resilience of power distribution systems has

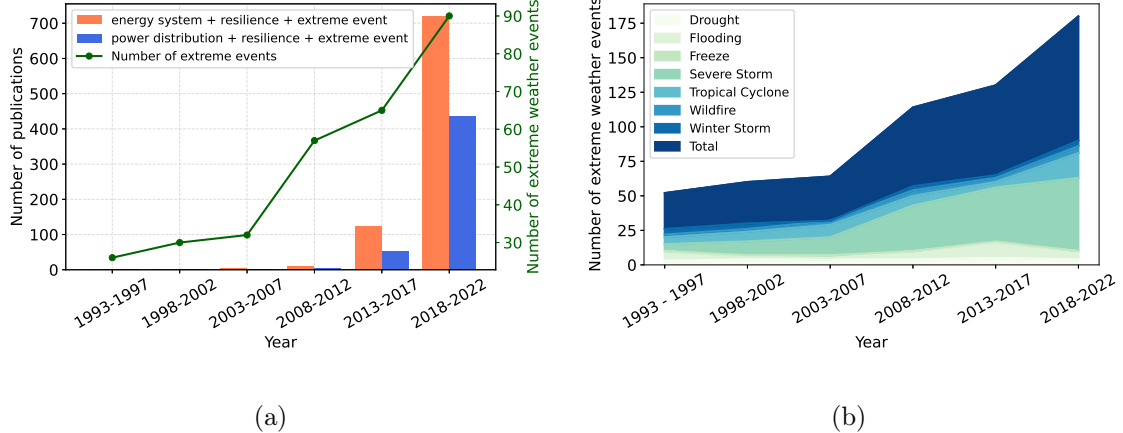


**Figure 2.1** a) The number of extreme events and publication trends in energy and resilience. b) Extreme events and their frequency in the US [3].

become a pressing priority [2]. Although several questions and challenges remain, significant research efforts have been devoted to understanding and improving the resilience of power distribution grids.

Figure 2.1 a) shows the increasing number of research publications since 1993 on the impact of extreme events on energy systems, specifically related to power distribution systems. Figure 2.1 b) illustrates the frequency of various extreme events in the United States [3]. It should be noted that the increase in the frequency of extreme events is not limited to the US alone and is a global concern. The rise in publications reflects the urgency and importance of addressing the resilience of energy systems to extreme weather events. In particular, research on power distribution systems has gained prominence recently, with advances in controllable distribution systems. Therefore, a comprehensive understanding of current state-of-the-art resilience assessment and planning methods in power distribution systems is crucial to realize practical implications, including enhanced operational resilience, effective risk management strategies, and informed infrastructure planning. This work also

plays an important role in forming the development of regulations, standards, and guidelines related to resilience planning, emergency response, and strategic infrastructure investments. This allows policymakers, industry stakeholders, and researchers to address extreme weather events' challenges effectively.

### **2.1.2 Related Literature and Gaps**

Table 2.1 summarizes some of the existing review studies on resilience-related topics in different critical infrastructure systems, including power distribution systems, and outlines their contributions and limitations. These survey articles include related work on resilience quantification and planning applied to different domains. A holistic framework for the development of critical infrastructure resilience interrupted by external and unexpected forces is discussed in [4]. The described framework builds the foundation for resilience on a set of resilience policies, considering the influences of policies on the damage prevention, absorption, and recovery stages, and presents implementation methodologies. Similarly, in [5], a review of the resilience of six critical infrastructures is presented, including electric, water, gas, transportation, drainage, and communication networks. The resilience of critical infrastructure elements and their main factors are studied in [6] involving electricity, gas, information and communication technology (ICT), and road transportation networks. The deployment of deep learning techniques for critical infrastructure resilience is presented in [7]. Similarly, [8, 9, 10] presents a comprehensive review of different critical infrastructure resilience, including, but not limited to, transportation, geology, and water-distribution system. However, none of the existing works specifically addresses resilience enhancement or assessment methods for electric power distribution systems, including the

associated infrastructural and operational considerations.

**Table 2.1** Comprehensive resilience study in the existing literature in different domains, their contributions, and limitations.

References	Domain	Summary	Drawbacks
[4]	Critical infrastructure systems (CIS)	Holistic frameworks for developing critical infrastructure resilience	Missing distribution system resilience discussion
[5, 6]		Resilience assessment of multi-domain infrastructure systems	Very little analysis on power distribution system resilience, missing discussion of interdependencies
[7]		Discusses the deployment of deep learning techniques in critical infrastructure resilience	Missing thorough and focused analysis of distribution system resilience, characterization, and interdependencies
[8, 9, 10]		Discusses critical infrastructure resilience including transportation, geoscience, and water distribution system	None of them have focused on electric power distribution systems resilience and their in-depth analysis

Continued on next page

Table 2.1 – continued from previous page

References	Domain	Summary	Drawbacks
[11]	Bulk power systems (BPS)	Discusses resilience enhancement strategies using microgrids	Missing focuses of distribution system resilience, resilience metric characterization, understanding the interdependencies of the infrastructures
[12]		Analyze a load restoration framework to enhance the resilience of the power system against an extreme event	Lacks metrics analysis, characterizing resilience, and other resilience enhancement strategies
[13, 14]		Comprehensive studies on power system resilience against natural disasters focusing on forecast models, corrective actions, and restoration strategies	Missing characterization of resilience metrics
[15]		Discusses the resilience and security of smart grid infrastructures	Missing the interdependence and metric analysis

Continued on next page

Table 2.1 – continued from previous page

References	Domain	Summary	Drawbacks
[16]	Power distribution systems (PDS)	Comprehensively summarizes the distribution system resilience assessment frameworks and metrics.	Lacks characterization of resilience and resilience enhancement methods
[17]		Discusses the definition, frameworks, resilience frameworks development, etc.	Missing the discussion of critical understanding of interdependencies for multi-domain resilience assessment and enhancement
[18]		Discusses resilience enhancement utilizing microgrids in distribution systems and definitions of resilience	Lacks understanding of the resilience characterization in distribution systems, other strategies of resilience enhancements, and understanding of the interdependencies

Continued on next page

Table 2.1 – continued from previous page

References	Domain	Summary	Drawbacks
[19, 20]	PDS	Comprehensive study of resilience assessment on the power distribution systems.	Missing characterization, discussion on interdependencies of critical infrastructures, resilience analysis process, and enhancement strategies

In the domain of power systems, existing articles extensively cover the resilience of the high-voltage bulk power grid [11, 12]. However, there is a noticeable gap in discussing resilience considerations for medium-voltage and low-voltage power distribution systems. Bulk power grids and power distribution systems drastically differ in structure and operation. Thus, the general understanding of the bulk grid system does not translate directly to distribution systems that require specialized analysis. Although some review works touch on the resilience of smart grid infrastructures [15], resilience metric and quantification [17, 16], microgrid-based resilience assessment and enhancement [18], resilience planning against extreme weather events [21], and resilience assessment framework in power distribution systems [22], there is a lack of comprehensive work which compiles the major aspects of resilience analysis, quantification, mitigation, enhancement, and multidomain interdependencies in power distribution systems.

Existing reviews on the resilience of the power distribution system lack several key aspects. First, there is a lack of a systematic framework for evaluating resilience. The

existing works do not provide a comprehensive process for resilience analysis, which is one of the most important aspects for characterizing the resilience of any critical infrastructure, including power distribution systems. Furthermore, these works do not highlight resilience metrics specific to power distribution systems. Secondly, these review articles do not provide insight into the interdependencies among critical infrastructures that can significantly impact the resilience of the power distribution grid. The impact of extreme weather events on one critical infrastructure can have a drastic effect on the other, which can negatively impact the community. Finally, the research gaps and limitations discussed in existing works are broad, making it challenging to identify specific research directions.

### 2.1.3 Contribution

The objective of this chapter is to review all aspects of resilience in power distribution systems comprehensively. We aim to provide valuable information to the scientific and engineering community to address the resilience challenges posed by extreme weather events. The discussions underscore the critical role of a resilient power distribution grid in advancing the sustainable development goals (SDG) of the United Nations, such as affordable and clean energy, sustainable cities and communities, and climate action, thereby contributing to the broader agenda of sustainable and inclusive development [23]. It is essential to clarify that this study is focused solely on the resilience of the power distribution system and does not address other aspects of the resilience of the power system. By narrowing the scope, this work aims to provide a comprehensive analysis and practical recommendations tailored to enhance the resilience of power distribution systems. Specifically, the major contributions of

this chapter are as follows.

1. The conceptual necessity for the resilience of the power distribution system is detailed, specifically in anticipation of HILP events, while also discussing the significance of existing definitions and their relevance.
2. A characteristic representation of distribution system resilience is provided. This includes classifying assessments into qualitative and quantitative evaluations and attribute and performance-based metrics. Furthermore, a systematic resilience analysis process is detailed for power distribution systems.
3. A comprehensive survey of existing strategies to enhance the resilience of power distribution systems is presented. These strategies are categorized into event forecasting, load prioritization, situational awareness (SA), repair and resource allocation, and utilization of microgrids and distributed energy resources (DER) for resilience enhancement.
4. The interdependencies among power distribution systems and various critical infrastructure systems, such as ICT, transportation, natural gas, and water distribution systems, are reviewed for their impacts on the resilience of the power distribution system.
5. Research gaps and potential opportunities for further exploration in power distribution system resilience are identified and reviewed. These focus areas encompass proactive outage management, long-term resilience investment frameworks, investments in smart grid infrastructure, and modeling and forecasting the impact of extreme weather events.

## 2.2 Framework for Resilience Evaluation in Power Distribution Systems

The resilience evaluation of power distribution systems is challenging due to their complex nature. Due to such intricacy, it is crucial to adopt a comprehensive approach that considers both qualitative and quantitative perspectives [24, 25]. The resilience analysis process is vital in assessing the system's ability to maintain specific objectives during adverse grid conditions. Typically, the evaluation is quantified using some metric that aims to capture the system's resilience. However, it is widely acknowledged that a single metric cannot fully capture all the diverse resilience characteristics of power distribution systems [26]. This section provides a comprehensive framework that explores various aspects of power distribution systems resilience, evaluation approaches, analysis process, and assessment metrics, aiming to facilitate a holistic understanding of resilience in power distribution systems.

### 2.2.1 Reliability Vs. Resilience

Reliability and resilience are the most commonly used performance criteria for assessing and planning critical infrastructure systems. Specific to power distribution systems, the quantification and characterization of reliability and resilience have gained significant attention with the increasing complexities of distribution systems and the growing need for a higher level of service quality. Typically, resilience is discussed in relation to reliability. Before that, it is imperative to clearly define the context of reliability and resilience concerning power distribution systems.

According to the North American Electric Reliability Corporation (NERC), the power grid reliability is defined as the ability of the system to supply electric power at all times while incorporating routine or unexpected outages and withstand sudden

disturbances such as short circuits or unanticipated loss in system components [27]. Thus, a system is reliable if it can continue providing service in case of previously known contingencies [28]. Resilience is the characteristic of any infrastructure that describes how fast the infrastructure can recover from an unexpected and catastrophic event [27, 28]. In contrast with reliability, the focus of resilience is not only on its impact on the affected customers (e.g., evaluating the duration of interruptions or the energy not supplied) but also on the ability of the infrastructure to rapidly and effectively recover to its pre-disaster operational state.

Although reliability and resilience are frequently used together, they are conceptually different. Typically, reliability refers to the capability of the power grid to deliver a continuous power supply to its customers. On the other hand, resilience is the ability of the infrastructure to withstand and recover from extreme events, such as natural disasters and cyber-physical attacks. Although different in definition and usage, resilience directly impacts the reliability of the concerned infrastructure system. Fig. 2.2 shows some general differences and similarities between resilience and reliability. Adaptability is the crucial quality of resilience that distinguishes it from reliability. Additionally, system reliability incorporates highly probable events with low severity, whereas resilience is considered for extreme events that create a more significant impact but have a low probability of occurrence. Regardless, resilience and reliability definitions target avoiding system outages, minimizing the risk of those outages, and restoring the system quickly and efficiently.

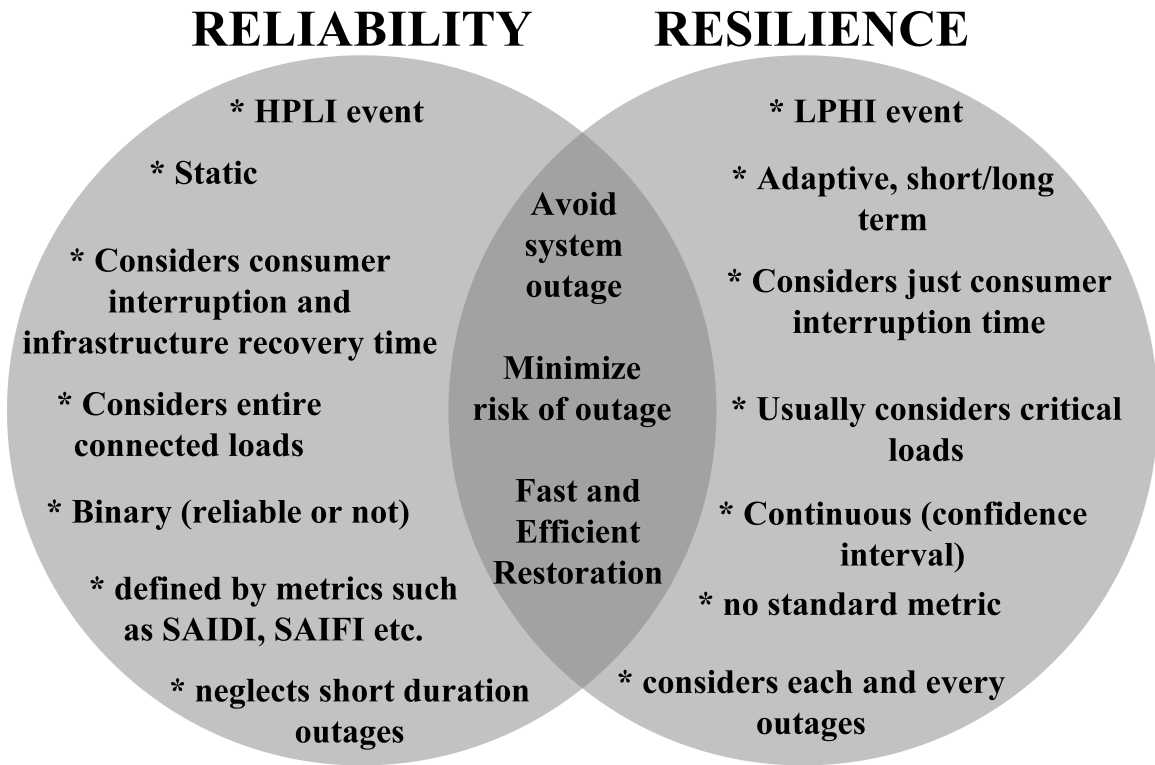


**Figure 2.2** Similarities and differences between reliability and resilience.

### 2.2.2 Resilient Power Distribution Systems

The response of a power distribution system when impacted by an extreme weather event is detailed in this section along with how it affects grid resilience. Figure 2.3 illustrates an overall response of the power distribution system, including some corrective actions after an HILP event. The top left portion of Figure 2.3 illustrates a general curve to show the response of a system towards an event. The vertical axis is the figure of merit (FOM) that accounts for the overall resilience of the system, and the horizontal axis represents time. FOM can be the number of customers online, the number of connected components, the electrical load fed by the system, etc. FOM is observed in every instance – before, during, and after an extreme event and

is commonly referred to as the system’s resilience in this work. From Figure 2.3, it can be seen that the system’s resilience drastically decreases immediately after the event occurs. The appropriate infrastructure planning and hardening measures can slow down the rate of decrements in the system’s resilience. When the system approaches the emergency response stage, a system with planned infrastructure shows better resilience than the traditional one with limited or no infrastructural development. An adequately hardened system with the knowledge of previous events that can effectively counteract the unwanted changes and restore the disrupted system in the lowest possible time is assumed to have higher resilience than the system that lacks these capabilities. Here, for the traditional system,  $FOM^-$  represents FOM before the event,  $FOM_D$  represents FOM before any remedial actions are taken, and  $FOM^+$  represents FOM after corrective actions are taken.

To strengthen the effective response of the system to an event and minimize the potential impacts and necessary investments, it is essential to have an efficient long-term plan. One such investment is grid hardening [29], which refers to making physical changes in its structure, e.g., replacing overhead lines with underground lines, elevating substations to prevent them from being flooded, and so forth. Although the effective response of the system might improve with planning measures, the occurrence, impact, and location of events are still not certain. Therefore, immediate corrective actions or emergency responses are needed during or after an event. Corrective action can include dispatch of mobile energy resources [30], load shedding [31], and intentional islanding [32]. Intentional islanding can effectively provide continuous supply to critical loads in the system with the help of distributed generators (DG) while isolated from the main grid [33]. While critical loads are islanded, the operators can

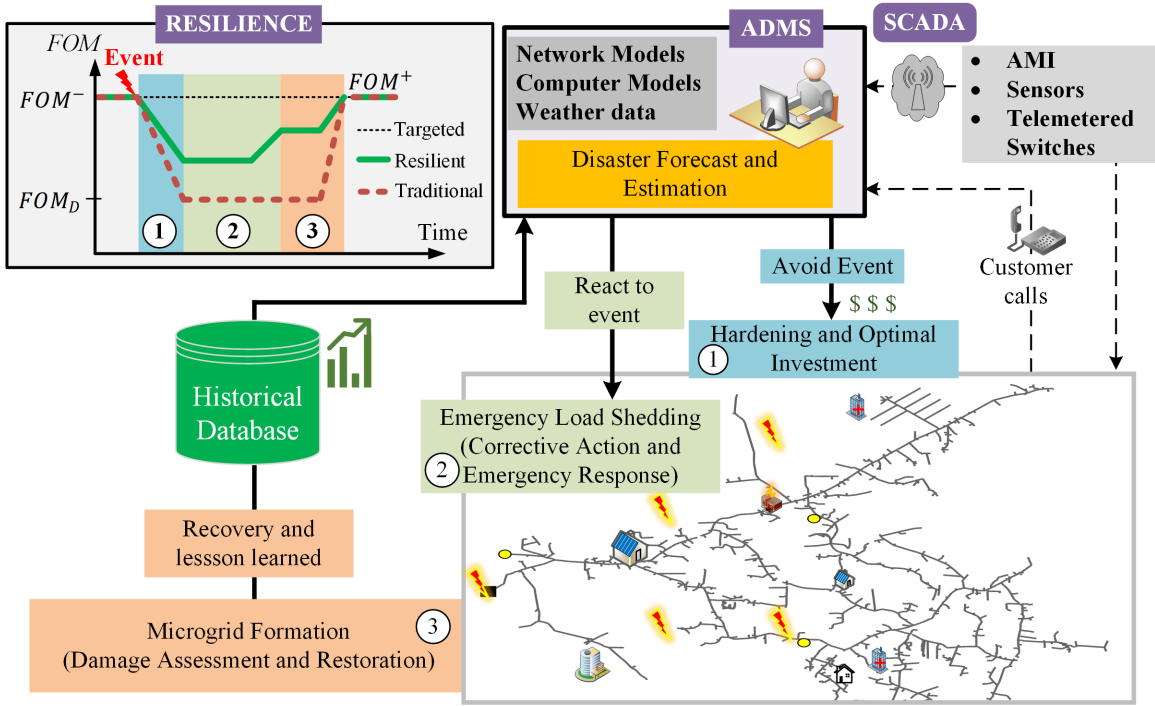


**Figure 2.3** Response of power distribution system during HILP events.

dispatch other generating units to pick up additional system loads. With improved impact modeling, the appropriate system response can be proposed to counteract the negative effect of the event. As seen in Figure 2.3, all the impact modeling, long-term planning, and emergency response processes are interconnected and work together to improve the resilience of the distribution system. Advanced distribution management systems (ADMS) facilitate the interconnection of these processes by continuously interacting with the distribution grid through supervisory control and data acquisition (SCADA) [34]. Furthermore, the system operators are directly connected to the customers, who can provide additional information about the current situation of the distribution grid when an extreme event hits the grid.

### **2.2.3 Qualitative and Quantitative Assessment of Resilience**

Qualitative assessment of resilience considers aspects of energy infrastructure, information systems, fuel supply chain, business structure, etc. The capabilities of the system involved in the qualitative resilience assessment include preparedness, mitigation, response, and recovery. Qualitative resilience assessment frameworks can guide policymakers in implementing long-term energy policies [12]. Existing work includes numerous qualitative resilience assessment methods. For example, the work in [35] assesses the resilience of the system and the regional level using questionnaires, investigations, and individual ratings to address individual, industrial, federal, and infrastructural resilience. A scoring matrix is developed in [36] to evaluate the functionality of the system from different perspectives. The analytical hierarchy process is employed in [37] to convert subject opinions into comparable quantities, eventually aiding operational decision-making.

Quantitative assessment methods aim to numerically assess the resilience of critical infrastructure systems such as the power grid [38]. Specific to power distribution systems, many studies have been conducted to assess system resilience quantitatively. The intrinsic characteristics of resilience can be defined as stress resistance and strain compensation. Later, the stress resistance is split into hardness and asset health. In contrast, strain compensation is characterized by capacity and efficacy [39]. Another way to measure the resilience in the electric power grid that quantifies the efficacy of the recovery process is the ratio of recovered functionality to the system [40]. The resilience analysis process can be interpreted in multiple steps depending on time. The indices include expected hazard frequency, initial failure scale, maximum level of impact, recovery time, and recovery cost according to stages. A functional

description of resilience is obtained in terms of initial failure scales, maximum impact level, and recovery time [41]. When considering extreme weather events, the resilience assessment metric can be expressed as a function of the expected number of power grid outages during the event, the probability of loss of load, the expected demand not served, and the level of difficulty of the grid recovery processes [42]. Similarly, other resilience measures emphasize multiple system properties, including recovery time, loads not served, etc., [43].

#### **2.2.4 Resilience analysis process**

This section briefly discusses and extends the resilience analysis process, initially introduced for the 2015 quadrennial energy review in [44]. The analysis framework evaluates the power system's capacity to handle potential future disturbances. Based on this assessment, it helps to prioritize planning decisions, investment endeavors, and response actions. In doing so, this study also highlights the available research and techniques that concentrate on every aspect of the analysis procedure to define resilience goals for utilities, choose suitable metrics that align with those objectives, collect essential data for the metrics, and ultimately determine the optimal approach to making resilience-based decisions. The conceptual framework and analysis process for creating forward-looking resilience metrics, which are based on extensive simulations that measure the impact on grid operations and power delivery, are shown in Figure 2.4. It provides a clear roadmap that outlines the journey from establishing resilience goals to effectively achieving them, with multiple interconnected components in between.

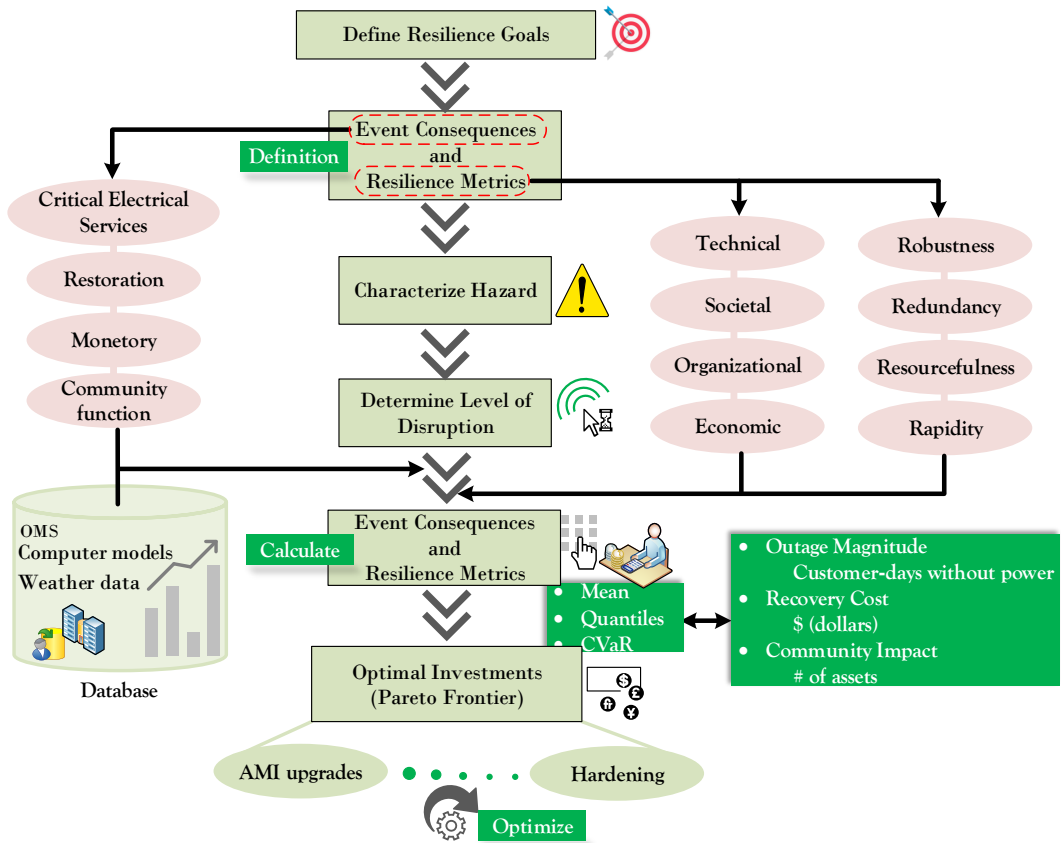


**Figure 2.4** The resilience analysis process – Setting up resilience goals, measuring resilience, and planning for resilience enhancement.

## Resilience goals/objectives

The resilience analysis process starts with defining resilience goals. The goal could be to improve the resistance and capability of a regional electric grid to withstand extreme events, evaluate a utility's investment plan for resilience enhancement, reduce the cost of recovery (monetary and time), ensure power availability to critical services, and/or reduce the overall interruption cost. For example, in [24], resilience is defined as the sum of the availability of individual critical loads during an event. In [45], the

focus is on optimal investment decision-making capability to enhance resilience. Other studies have suggested various indicators of resilience, such as the optimal duration for repairing critical components [46], disruptions in the energy supply following extreme events [47], the general delivery of essential resources and uninterrupted power supply to critical customers after a disaster [48], and the recovery of infrastructure and operations [49]. Table 2.2 summarizes these indicators, and a comprehensive list of examples is available in [50]. These indicators can be instrumental in defining resilience goals and developing relevant metrics to measure them.

### **Hazard characterization**

The grid disturbance event could be initiated by various natural threats. Several efforts have been made to create better ways to evaluate the impacts of these threats. It is worth noting that different threats to energy infrastructure vary in probability and impact. For instance, a wind storm can cause significant damage to overhead structures but may not impact underground systems such as cables and substations. Consequently, it is critical to understand the hazard characterization as part of the resilience analysis process. Hazard US (HAZUS) or CLIMate ADaptation (CLIMADA) tool can be used effectively to model or simulate extreme weather events, including but not limited to hurricanes, floods, and earthquakes [51, 52]. When evaluating resilience against multiple hazards effectively, it is crucial to consider two key factors: (1) the probability of each potential threat scenario and (2) how the intensity of an event maps onto the resulting consequences at the system level.

## **Event to impact mapping**

Once the onset of the event is identified, the next step is to use the characteristics or attributes of the event to determine the impact at the component level. Different components in the power grid have predefined thresholds (intrinsic property of a device) to handle the subjected disturbances. These thresholds depend on the type of component and the duration of exposure. Although the thresholds are not directly measurable, historical data can be used to derive the failure probabilities [53]. These component-level failure probabilities can then be mapped to characterize system-level impacts. For example, a Monte Carlo simulation approach can be used to assess the spatiotemporal impacts of grid disturbances using fragility curves [54]. Grid disturbance theory and functional form modeling capture the spatiotemporal effects of any possible scenarios [55]. Although functional models can describe grid disturbance, event onset must be carefully analyzed to demonstrate the most meaningful impact and responses. This is crucial because different disruptive events can have varying effects on a system, requiring specific strategies for resistance and recovery. The work in [56] reviews some widely used impact models in energy systems planning and operations due to extreme weather events.

## **Calculate consequence– performance measure and resilience metrics**

In this stage of the resilience analysis process, the consequence category is defined, which forms the basis for the development of the metrics. Resilience metrics are then determined for each category of consequences related to the technical, societal, organizational, or economic impacts of an event. Some commonly used metrics are demand/energy not served, recovery time and cost, load recovery factor, revenue loss,

and customers not served [57]. Other indices, such as restoration efficiency, vulnerability index, degradation index, and microgrid resilience index, are also widely studied [58]. It should be noted that the impact of potential threats is dependent on the system's capacity to (1) anticipate, prevent, and mitigate them before being affected by the event, (2) adapt to, absorb, and survive the threat when it occurs, and (3) recover, restore, reconfigure, and repair itself afterwards [22]. Since a single resilience metric cannot capture all possible aspects of the threat response, these metrics are a function of resilience goals, the operating conditions and intrinsic characteristics of the system, and new investment planning initiatives.

### **Evaluate resilience improvements**

Once the resilience metrics are established, the potential investment for resilience enhancement is studied. Given limited resources and high risk, resilience can be improved by focusing on low-probability events, investment prioritization, and consequence management. These studies allow system analysts to decide on investments based on evolving research to identify the most impactful decision in improving resilience while minimizing long-term costs and stranded investment [60]. In recent years, it has been realized that investments should focus on quantitative analysis, the ability to incorporate the uncertainty of grid disturbance, and bottom-up approaches where efforts for resilience enhancement should start from the grid-edge [61].

#### **2.2.5 Resilience metrics**

This section details the desired characteristics of a metric defining distribution system resilience and the categories of resilience metrics for distribution system resilience

**Table 2.2** Some widely used examples of the category of consequences and resilience metrics [59].

Category of consequence	Resilience metrics
Electric service	Total customer-hours of outage Total customer energy demand not served Average/percentage of customers experiencing a power outage during a specified period
Recovery	time and cost of recovery
Monetary	Loss of revenue, cost of damages, repair and resource allocation Loss of assets and business interruption cost Impact on gross municipal/regional product
Community function	Critical services without power Critical customer energy not served

planning. A metric is essential for resilience planning, as it quantifies the impacts of potential HILP events on the grid and helps evaluate and compare planning alternatives to improve operational resilience [62]. Measuring progress towards a more resilient infrastructure requires developing and deploying metrics that can be used to assess infrastructure planning, operations, and policy changes [63]. The resilience metric should focus on HILP events, consider the likelihood and consequences of threats, and evaluate the system's performance. Furthermore, the metric should con-

sider the uncertainties inherent in response and planning activities while quantifying the consequences of power grid failures [44].

It is incredibly challenging to adopt a unified metric that can capture several contributing factors such as uncertainty, spatiotemporal features of a threat, and intrinsic system properties to deal with possible threats [64]. Current resilience measures can be classified into two main types: a) attribute-based metrics, which assess the attributes of the power system such as adaptiveness, resourcefulness, robustness, SA, and recoverability [22], and b) performance-based metrics, which evaluate the ability of the system to remain energized (commonly referred to as availability [65]), often represented by the conceptual resilience curve [66].

### **Attribute-based metrics**

Attribute-based metrics are relatively simple in mathematical formulation, and the required data collection is also easier than performance-based metrics. The fundamental question that attribute-based metrics aim to answer is “What makes the system more/less resilient than other systems?”. Attribute-based metrics are used to provide a baseline understanding of the system’s current resilience and are driven by the properties that increase the resilience of the concerned system. The properties of the system comprise robustness, resourcefulness, adaptivity, recoverability, and SA. For example, the ratio of underground feeders to overhead feeders, the proportion of distributed resources to critical consumers, the number of advanced metering infrastructures/sensors, path redundancy, and overlapping branches result in increased robustness, resourcefulness, and SA, thus improving the resilience of the system to HILP events [24]. Some of the widely used attribute-based resilience metrics are

described below:

1. System robustness: This metric evaluates the ability of the power distribution system to withstand shocks or disturbances without failure. For example, the robustness of the system can be evaluated based on the strength of the system infrastructure, such as the resilience of poles, wires, and transformers to severe weather events [67].
2. System flexibility: This metric evaluates the system's ability to adapt to changes or disturbances. For example, the flexibility of the system can be evaluated based on its ability to manage power supply and demand during peak hours, integrate renewable energy sources, and/or extract demand flexibility during scarcity [68].
3. System redundancy: This metric evaluates the system's ability to maintain power supply even when one or more system components fail. For example, redundancy can be evaluated based on the number of backup power sources, such as generators or batteries, available to maintain the power supply during outages [69] or tie switches to utilize the power from the feeder [48].
4. Customer satisfaction: This metric evaluates the ability of the power distribution system to meet customer expectations during and after disruptions. For example, customer satisfaction can be evaluated based on the system's ability to provide timely and accurate information during outages and the quality of customer service provided by the system's operators.

The definition of resilience plays an important role in the evaluation of resilience metrics based on the attributes of the system [44]. When forming the attribute-based

resilience metric, the spatiotemporal features of an HILP event on power distribution systems are also taken into account [12]. The uncertainty associated with HILP events is a critical attribute that is often represented using probabilistic measures [70]. These attributes, incorporated into the metric, are valuable for decision-making in planning and policy-making processes [44]. When utilizing attribute-based metrics, it becomes possible to compare different systems, both with and without resilience enhancement strategies. Attribute-based resilience enhancement metrics need to be able to adapt to advances in technology, ensuring their continued relevance and effectiveness.

### **Performance-based metrics**

It is recommended that the grid resilience metrics are defined based on system performance. They should be (1) forward-looking, (2) quantify the consequences of disruptions, (3) incorporate uncertainties that can affect the response of the system and planning decisions, and 4) be flexible enough to use data from historical analysis and system models [59]. Such performance-based metrics follow the approaches in evaluating system resilience quantitatively. The performance of the electric grid during major shocks, such as natural disasters, can be described by outage frequency, the number of customers impacted, outage duration, or a combination of these. The National Energy Regulatory Commission (NERC) published separate metrics to evaluate system performance against reliability standards [71]. The growing occurrence of extreme events has emphasized the importance of developing metrics to assess the performance of the power system during HILP events. Eventually, entities are expected to appropriately include all events that affect the power system, considering the event's probability and impact on the communities. Some of the widely used

performance-based resilience metrics are described below:

1. Energy at risk: Energy at risk is a metric that quantifies the amount of energy that may not be supplied during extreme events. It provides a forward-looking assessment of the potential consequences of disruptions by estimating the amount of energy that can be lost due to outages during extreme events [72].
2. Probabilistic assessment risk: Probabilistic assessment risk is a metric that assesses the likelihood and consequences of disruptions due to various failure scenarios. It reflects inherent uncertainties by considering the probability of various failure scenarios and the potential consequences of these failures [54]. It can use historical analysis and system modeling to quantify the likelihood of different scenarios and the potential consequences of these events.
3. Flexibility margin: This metric measures the ability of the system to respond to changes in demand and supply. It is forward-looking and reflective of inherent uncertainties by assessing the system's ability to respond to unexpected changes in demand and supply, especially during scarcity and emergency conditions [73].
4. Restoration time: Restoration time is a metric that measures the time it takes for the power system to restore power following a disruption [74]. It is forward-looking and quantifies the consequences of disruptions by assessing the time required to restore service to customers. Historical analysis and system modeling can be used to estimate the time required to restore customer service in various scenarios.

A resilience performance curve is widely used to define performance-based metrics [75]. Several studies have adopted a resilience triangle in the past to determine the system performance where only two different states are presented [20]. Lately, it has been realized that the one-dimensional character of the resilience triangle is not very helpful and can only capture the recovery from an event. It is equally important to capture other highly critical resilience dimensions such as "how fast resilience degrades and how long the system remains in the degraded state before the recovery stage" [76]. A conceptual resilience curve has recently been used to assess and define performance-based metrics [77].

In conclusion, performance-based approaches are commonly used in cost-benefit analysis and planning studies to assess the advantages and drawbacks of proposed resilience improvements and investments. While attribute-based and performance-based approaches have distinct definitions and can be used independently depending on utility preferences, combining these approaches allows for a more comprehensive analysis of grid resilience, considering the potential consequences of disturbances. Attribute-based metrics broadly characterize grid resilience, while performance-based approaches assess tailored options for enhancing resilience, integrating economic, social, and regional factors. By combining attribute-based and performance-based metrics, a baseline evaluation of resilience, recovery efforts, planning, and investment activities can be effectively maximized, leading to improved grid resilience [78]. Unlike these methods, some recent works also explore a data-driven method, using publicly available data, to characterize resilience in power distribution systems [79]. Data-driven approaches are likely to be popular as critical information from the electric utility is less likely to be publicly available.

**Table 2.3** State-of-the-art – Resilience planning and enhancement strategies for power distribution systems.

References	Resilience category	Planning & enhancement strategy
[80]	Operational resilience	Load prioritizing
[81]		Situational awareness
[82]		Microgrids and DERs-based load restoration
[83]		Mobile energy resources
[84]	Infrastructural resilience	Deployment of soft open point technology
[85]		Remote units deployment
[86]		Deployment of mobile energy resources
[87]		Smart distribution systems
[88]	Both operational & infrastructural resilience	Repair scheduling, Optimal switching, crew dispatching
[89]		Networked microgrid
[90]		Repair and restoration using DGs, switches, and crews

### 2.3 Power distribution resilience – Tools for planning & enhancement

The resilience enhancement of power distribution systems depends on various tools and strategies. These include accurately forecasting natural events, recognizing critical loads that require uninterrupted power supply, maintaining situational awareness, and implementing proper planning and restoration measures. The combination of these measures and tools contributes to the overall enhancement of system resilience. These measures can be further categorized into operational and infrastructural resilience, as detailed in Table 2.3. The stages of a resilience curve — avoid, react, and recover — are illustrated in Figure 2.5, indicating where these tools can be applied

to enhance resilience [55]. This section details related work on critical measures and tools for resilience planning and enhancement in power distribution systems.

### **2.3.1 Event forecast**

Extreme weather forecasting helps utility planners make appropriate operational decisions to reduce damage to the power grid. Recently, advances in observation networks such as satellite remote sensing have significantly improved the accuracy of short-term weather forecasting models [91]. Additionally, advances in data analytics, accurate weather modeling, and enhanced computing resources make extreme weather forecasting efficient and reliable. However, long-horizon weather prediction is still an active area of research and requires further consideration when used for infrastructural planning purposes. Nevertheless, with advancements in short-term predictions, utility planners can take advantage of accurate event forecasting to make appropriate operational decisions. These decisions may include resource scheduling, dispatching crews and other resources for maintenance, and stocking backup resources. Essentially, a weather-grid impact model can be developed to understand and simulate the effects of an extreme weather event on the power grid. The existing research on the weather-grid impact model can be categorized into statistical and simulation-based models. These models include a detailed modeling of power systems, extreme weather events, damage assessment, and restoration after extreme natural events [92].

### **2.3.2 Load prioritization**

Hazardous incidents that impact the operation of the distribution system disrupt the supply to critical loads, thus affecting grid resilience. To ensure a high level of re-

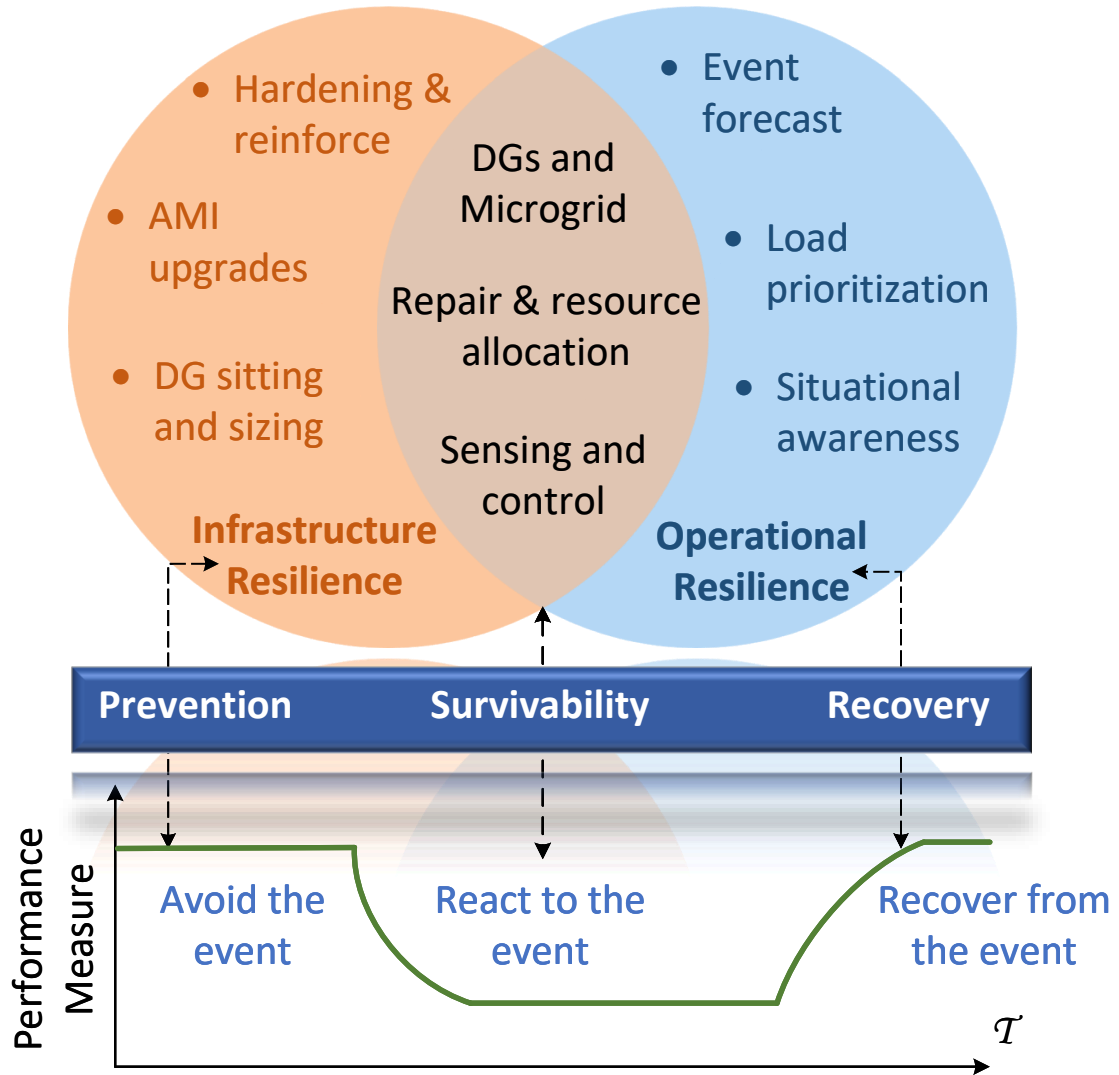


**Figure 2.5** Different stages of resilience planning and enhancement strategies.

silience for critical infrastructures, federal and state authorities are actively working to identify and provide guidance for enhancing critical infrastructure security [93]. Critical customers such as hospitals, fire departments, water suppliers, and other emergency units are recognized and prioritized for the prompt restoration of power supply within the utility's service area. This underscores the significance of enhancing

the resilience of critical infrastructures through the increased availability of essential customers and their critical loads. The objective is threefold: 1) facilitate a rapid response to grid disturbances, 2) reduce the magnitude of harm and challenges experienced by communities, and 3) accelerate the restoration of critical functions [94]. Moreover, due to the significant amount of grid outages caused by catastrophic events, it is impossible to prevent threats to all assets. Therefore, prioritizing the critical assets of the grid becomes a clear choice for utilities [50]. Critical loads identification allows operators to selectively disconnect low-priority loads and maintain backup resources within their generation capacity while sustaining vital facilities for an extended duration [95]. In such cases, various advanced techniques can be employed to restore the prioritized loads while considering topology and operational constraints, thereby enhancing the overall system resilience [96].

### 2.3.3 Situational awareness

It is crucial to have adequate SA of the system conditions for effective and timely decision-making to counteract the impacts of the HILP event [81]. Several incidents discussed in Chapter 1.1.1 illustrate the severity when the system operators are not fully aware of relevant information. Inadequate SA increases the probability that the system enters the cascading blackout phase [81]. In light of these events, several industrial stakeholders have significantly advanced information systems to enhance SA. One key element of this is state estimation, which is critical to enabling continuous and reliable monitoring and control of the distribution systems, particularly in the presence of DER penetration [97]. To date, the observability of the system downstream of the substations is very limited. Only a limited number of utility companies

have implemented control room applications, including, but not limited to, state estimation, topology identification, fault management, and cyber attack mitigation [98]. Furthermore, it is unclear how to adapt existing SA technologies from the bulk power system to power distribution due to unknown network models, poor observability, and incorrect measurements [99].

Nevertheless, progress in power distribution systems has brought together various innovative technologies like digital relays, phasor measurement units, intelligent electronic devices, automated feeder switches, voltage regulators, and smart inverters for DER. These advancements pave the way for improved end-to-end awareness and visualization of the network. Furthermore, the regular polling and on-demand retrieval of customer interval demand data through the advanced metering infrastructure contribute to enhancing the accuracy of the online model for the distribution network [100]. The integration of advanced metering infrastructure information in SA tools is supplemented with conventional supervisory control and data acquisition, which provides additional data to improve the system's SA [101, 102]. In the future, most of the electric power grid will have installed communication networks, intelligent monitoring, and distributed sensors along feeders to provide additional data for an improved SA [103]. It is also envisioned that such digital networks will ultimately lead to greater levels of communication between the end-users, the utilities, and with other physical infrastructures [104]. The use of drones and unmanned air vehicles for damage assessments is also gaining popularity [105]. The improved SA and increased automation in a smart grid paradigm will assist the control room operators with real-time decision-making, thus improving the grid resilience.

#### **2.3.4 Resilience planning and restoration**

Resilience planning and restoration involve various strategies and actions aimed at improving the ability of a distribution system to withstand and recover from extreme events. These strategies can be broadly categorized into three main areas: long-term resilience investment, short-term pre-event preparation, and post-event restoration.

##### **Long-term resilience investment**

Long-term resilience investment involves strategic planning to make the distribution system more resilient to uncertain and extreme events. This includes infrastructure reinforcements or system hardening methods such as installing underground lines, elevating substations, and other upgrades to improve the system's reliability and robustness [106]. However, unlike transmission systems, distribution systems have unique characteristics, such as radial topology, low redundancy, and inability to incorporate DC power flow methods, which require specific considerations in resilience planning [107]. Distribution systems have received less attention compared to transmission systems, with limited literature on resilient distribution system design [108].

Most of the studies in resilience planning and upgrades apply two different types of modeling techniques, namely robust [107] and stochastic modeling [109]. The scenario-based stochastic methods and other network interdiction models facilitate optimal hardening strategies in the distribution system [107]. In other works, DGs siting/sizing and automatic switch placement strategies are simultaneously formulated to minimize the overall expected cost [110]. However, with the growing need of resilience enhancement, investment decisions should be based on HILP events rather than the expected cost of several possible events. Furthermore, resource planning

should be carried out to fulfill the need for operational flexibility, and specialized power distribution system models should be integrated with advanced operations [44]. Works have shown that sensing and control technologies can also be deployed in the planning phase to enhance the resilience of the distribution system [111]. Integrating these resources in the planning phase and observing the trade-off between these resources against uncertain or extreme events can provide a better planning portfolio.

### **Short-term pre-event preparation**

Short-term pre-event preparation focuses on resource allocation and planning strategies that can be implemented just before an extreme weather event to enhance the resilience of the distribution system. This includes activities such as pre-staging of resources, crew dispatching, and network reconfiguration to minimize the impact of the event and expedite restoration. One approach to short-term pre-event preparation is the strategic placement of resources, such as emergency response generators and crews, in strategic locations before an extreme weather event occurs. This allows for quicker deployment and utilization of resources immediately after the event, reducing the time required for restoration. For example, the U.S. Federal Emergency Management Agency (FEMA) pre-stages emergency response generators before hurricanes or other major events, but the effectiveness of this strategy depends on the accuracy of the event forecast and the optimal placement of resources [112]. Mathematical models, such as mixed-integer linear programming models, can be used to optimize the pre-staging of resources based on various factors, such as forecasted event severity, expected outage duration, and available resources [88].

Short-term preparation also involves proactive network reconfiguration, where the

distribution system is strategically reconfigured so that the damaged sections can be quickly isolated and power can be restored to unaffected areas once the event occurs. This can be achieved through automated switching actions or remote-controlled switches that can be operated remotely, allowing for quicker restoration without needing physical presence on site [87]. Optimization models can be used to determine the optimal switching actions and reconfiguration plans considering system topology, available resources, and outage duration [82, 88]. Furthermore, repair crew deployment and coordination is an essential preparation plan to ensure efficient restoration efforts. Crews must be strategically deployed to affected areas based on event severity, expected restoration time, and available resources. Mathematical models can be used to optimize crew deployment and scheduling to minimize restoration time and maximize the utilization of available resources [90]. There are other efforts in pre-allocating mobile resources as a short-term preparation process [86]. The main idea is to restore critical loads by forming small MGs with the available mobile resources for a resilient emergency response to natural disasters. Such intentionally islanded MGs will have voltage support grid-forming resources that can energize the islanded loads until the restoration and repair tasks are completed.

### **Post-event restoration**

Post-event restoration involves activities carried out after an extreme weather event to restore the distribution system to normal operation. It is one of the most critical components of a system's resilience, as quick and effective restoration justifies an efficient planning strategy. Hence, planning and pre-event preparation are vital in ensuring a quick and efficient restoration process. Restoration includes repairing damaged infras-

ture, re-configuring the network, and optimizing allocated resources to expedite restoration [48]. The repair crews must assess the damage, repair or replace damaged components, and restore the system to its normal operating condition following an event to minimize downtime and expedite restoration. Network reconfiguration also plays a crucial role in post-event restoration. The distribution system must be reconfigured to restore power to affected areas and isolate damaged sections. This can be achieved through automated switching actions or remote-controlled switches. Mixed integer programming models can be leveraged to optimize the repair and restoration process by coordinating crew assignments, resource allocation, and network reconfiguration to minimize restoration time and ensure efficient utilization of available resources [88].

Post-event restoration research also focuses on resilience enhancement against natural disasters using DERs and MGs, with varying restoration objectives [113]. MGs provide an effective DERs management and utilization solution for system restoration after extreme weather events [114]. Networked MGs are considered dispatchable as well as non-dispatchable resources for service restoration in power distribution during long-duration outages [89]. MGs can also be adaptive in which the formation of MG and load switching sequence is guided by the nature of extreme events [115]. MGs and DERs can also be used for sequential service restoration [116]. The DG dispatch and network switching can be coordinated well to generate a feasible restoration sequence. Furthermore, such restoration can also be performed in multiple or hierarchical stages [90]. Service restoration can be achieved via dynamic changes in the boundaries of MGs within a distribution network that includes synchronous-machine DGs [117]. It is vital to maintain the grid frequency throughout the restoration

process [118]. The correlation between switching actions and frequency deviations is considered and a suitable switching sequence is formulated that meets the essential requirement of adhering to the dynamic frequency nadir limit. Some controllers, such as grid-friendly appliance controllers, can avoid large transients in low inertia microgrids associated with switching operations for coordination [119].

## 2.4 Interdependence with other critical infrastructures

The inherent interdependencies between power distribution systems and other critical infrastructures contribute to the resilience of the community [120]. Figure 2.6 shows a high-level overview of the interdependencies of critical infrastructures with the power distribution system. It is crucial to understand these interdependencies for effective disaster response and recovery planning, as disruptions in the power distribution system can have cascading effects on other critical infrastructures, amplifying the overall impact on the community [121]. However, there is little understanding of the complex dynamics, vulnerabilities, and emerging threats associated with these interdependences. This section investigates and analyzes these infrastructure interdependencies, highlights the contributions that have been made so far in this problem space, and addresses some open challenges.

### 2.4.1 Information and communication technologies

Interdependent power distribution systems and ICT networks offer opportunities to mitigate vulnerabilities and leverage infrastructural convergence. Key trends in analyzing their interdependencies include increasing data volumes, faster system dynamics, hidden feedback, renewable portfolio standards, variable energy resources

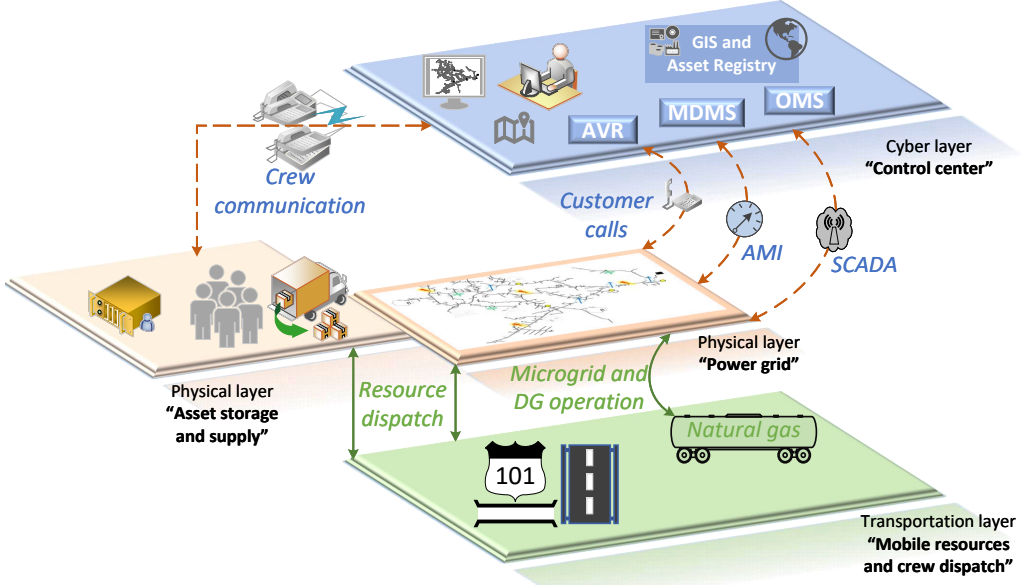


**Figure 2.6** Interdependence among various critical infrastructures, namely ICT, transportation, natural gas, and physical power grid networks.

penetration, network cybersecurity, co-simulation needs, reliability coordination, and real-time/data-in-motion analytics. Figure 2.6 illustrates the interdependencies between cyber layers and other physical layers of the power distribution system. Prioritizing cybersecurity is crucial for federal research and industry. Investigating these interdependencies helps to develop assessment tools to specify ICT requirements for advanced grid functionalities and build a strong foundation for new grid management tools. The deployment of advanced sensing and measurement technologies facilitates data collection and understanding while improving the resilience of the system with strategic decisions. The transmission of data streams, such as measurement data, from field devices to the control center for monitoring, analysis, and control purposes

faces security risks, including data leaks, hacks, and adversarial intrusion [122, 123]. There are four domains — cyber, social, energy market, and distribution system networks — that interact to enable advanced grid functionalities and revolutionize grid modernization. However, such interaction also exposes the network to severe security threats.

Failure or hacking in the cyber layer can have cascading effects on the physical layer, affecting equipment and services. Understanding the relationship between the distribution grid’s architecture and control systems is crucial. During extreme weather events, the power grid becomes highly vulnerable. If cyber intruders breach the control and communication system when impacted by an extreme event, it can critically collapse the power grid [124]. Loss of communication makes damage assessment and asset management nearly impossible, leading to incomplete situational awareness. Limited situational awareness during extreme events hinders decision-making. Additionally, considering cyber layer constraints can enhance the resilience of the power system, as the cyberinfrastructure is interconnected with the physical layer [125]. Advanced distribution management systems and networked microgrid control paradigms should coordinate to address operational conflicts and reconnect microgrids to the distribution networks after events. In addition, the future of distribution management systems will see an increased dependence on distributed resources and distributed architecture, necessitating robust communication capabilities [126].

#### **2.4.2 Transportation**

It is essential to model the critical infrastructure dependency between power distribution and transportation, as the dispatch of the crew and other mitigation processes

can be delayed if the transportation network is not accessible when the region is affected by an extreme event. In Figure 2.6, the interdependency between the transportation layer and the physical layer (power grid) is represented. The transportation system and the operational dependency of the power grid play a critical role in the resilience enhancement during extreme weather events, especially when preparing for an upcoming storm by allocating mobile resources (mobile energy storage, poles, distribution lines, etc.) and dispatching repair crews for optimal service restoration, calling for thorough research in understanding and modeling the related interdependencies. During extreme weather events, critical operations, such as optimal resource planning for rapid system restoration and emergency evacuation mechanisms, require proper modeling of the transportation network associated with the power distribution system. To investigate the critical elements that need upgrading or expansion, the study of the influence of contingency on traffic flow and power flow can be a great addition to interdependence modeling [127]. Additionally, the optimal selection of emergency stations (including distribution centers, power supply recovery, emergency supplies, medical centers, etc.) requires specific attention during interdependence modeling considering disaster management [128]. Such an interdependence assessment can greatly help disaster-impacted areas develop a rapid recovery plan. For example, after Hurricane Maria in Puerto Rico, it took 11 months to fully restore the power back to its nominal state. One of the primary reasons for such a lengthy restoration was the lack of proper modeling of the transportation systems, preventing efficient crew dispatch [129].

### **2.4.3 Natural gas**

The primary reasons for the interdependence between natural gas pipelines and power distribution systems are attributed to the space and water heating in residential, commercial, and industrial buildings. In the U.S. residential sector, there is a sharp decline in the use of natural gas from 58% in 2015 to 42% in 2021 while the use of electricity has increased to 43% surpassing natural gas usage for the first time [130]. However, a substantial amount of electricity generation is still dependent on natural gas, which creates a supply conflict during extreme cold conditions due to scarce natural gas pipeline capacity. Considering the historical usage of natural gas for heating purposes, local distribution companies, the primary supplier of natural gas to end users, receive higher supply priority than natural gas-based generation units in case of extreme cold events. Due to increasing dependence on electricity for space and water heating, the supply deficit of natural gas puts electricity-dependent customers at a disadvantage as the natural gas-based generating units may be curtailed in order to prioritize supply to local distribution companies. In the 2004 New England cold snap, the real-time price of electricity rose the ISO-New England's bid cap [131]. The day-ahead gas prices at New England's gas system were increased by nearly ten times their normal price range along with an increase in electricity price. Similarly, natural gas supply disruption was identified as the major cause of power outage due to Texas winter storm Uri in February 2021 [132]. Almost 50% of Texas residents use electricity for heating, and most of the casualties due to Winter Storm Uri were caused by hypothermia and conditions worsened by freezing conditions. Hence, it is evident that the supply chain bias of natural gases creates equity concerns about customers using electricity as opposed to customers using natural gas only for heating.

The interdependence should be modeled to jointly identify the overall patterns of electricity generation and distribution, focusing on the energy requirements of electricity and natural gas. The existing works on the integrated study of gas and electric system networks focus mainly on the transmission of electric power and natural gas [133]. In [134], a modeling strategy is introduced to enhance the coordination between natural gas and the bulk power system, specifically to assess and improve day-ahead and intraday market coordination. Similarly, the work in [135] presents a combined expansion planning model for gas and electric networks by analyzing the fluctuations in gas prices during congestion. Although relevant, these studies overlook the challenges associated with natural gas pipelines and power distribution systems. Due to the increasing dependency of end users on electricity and their inadvertent disadvantage during extreme cold events, it is essential to incorporate power distribution models, building models, and equity-based policy into the simulation study to represent the overall interdependence accurately. The framework for interdependence between natural gas and power distribution systems requires an assessment of integration and automation in these infrastructures, such as threat/hazard identification and data acquisition, identification of potential impact zones, initial and cascading effects on infrastructural assets from failure events, and identification of propagation paths of this disruptive events [136]. Furthermore, power distribution systems energize the constituent components of the gas distribution system. The operation of natural gas processing plants and other relevant assets, including electricity-powered compressor stations, depends on the power distribution networks [137]. Failures in the corresponding power distribution network may propagate to the gas distribution network due to the strong interdependencies [138]. Therefore, simultaneous damage to both

networks due to a natural disaster can cause severe concern to affected communities and overall resilience of the critical infrastructures.

#### **2.4.4 Water distribution systems**

The manageability and resilience of power and water distribution system are challenged by their increasing interdependence and inter-connectivity, as widely studied within water-energy/power nexus activities [139]. While power system research has made considerable progress over the years through dedicated research efforts and active community participation, the tools used in existing studies on water distribution networks are comparatively less advanced [140]. The key challenges in managing the increasing interdependence between the power and water distribution systems include complex coordination between stakeholders, resource availability and operating expenses, and increasing pressures of drought and population growth [141]. Additionally, there is a traditional view of water and power distribution systems as separate and uncoupled systems, resulting in a lack of coordination between them and the absence of a comprehensive framework for modeling and optimizing their coupled operation and functionalities [142]. Moreover, there are concerns that the coupled operation of these two systems may adversely impact the reliable and quality operation and distribution of water and power systems [143]. Critical infrastructures such as water and power distribution systems are widely interdependent since they share energy, computing, and communication resources. In heavily loaded power distribution systems, failures on distant power lines can cause severe water supply shortages. The water distribution network is heavily energy-intensive, which uses electrical power to treat, store, and distribute water, and comprises several hydraulic

components, including pipes, pumps, and tanks. The power system energizes some of these elements. Operational failure in one of these two systems can impact the operation of the other system. For instance, a power outage can impact the water treatment, storage, and distribution operations since these processes require electrical power. This interdependence propagates to health care units and other local businesses requiring a continuous water supply for their normal operation. For wastewater treatment units, a discontinuous operation of the machines can cause serious consequences of contamination of the non-treated wastewater. Conversely, water shortage can impact many power system operations as generators require water for cooling. For example, Europe's 2022 heatwave and drought, considered the worst in 500 years, resulted in a significant loss of nuclear generation due to water shortage for cooling and hydro generation. Among others, France lost 23% of nuclear and 24% of hydro generation while Germany lost 50% of its nuclear generation [144]. The energy crisis affected the electricity markets significantly, ultimately affecting the end users. Similarly, after the 2021 winter storm, Texas faced a severe drinking water shortage as utilities suffered long-duration power outages. As per the Texas Commission of Environmental Quality, millions of customers were under the boil water notice while people were boiling snow to quench their thirst or carry out normal activities [145]. Thus, failure in one system can cause cascading impacts in the other systems, damaging operational integrity and causing social and economic impacts [142]. Any failure will trigger cascaded loss and interrupt the electrical power supply to the hydraulic components.

Similar to the challenges in the interdependence of other infrastructures, there is a lack of a proper model to characterize the interdependence between water and power

distribution systems [146]. It is important to characterize extreme events that can impact one or both of the infrastructures and include them in the interdependence model. In [147], an integrated power and water distribution model is formulated to identify the propagating impact of power outages on the water distribution system. A study in [148] provides an insight into the operational cost and effect on distribution marginal prices due to coordination between water and power distribution systems. Additionally, the work provides case studies on potentially using water tanks as a means to offset congestion and voltage violations in the distribution grid in the future. Existing studies focus on an independent research problem of interdependence. The holistic model, however, should capture normal and extreme weather or temperature conditions, infrastructural markets, and economics. The importance of coordination is paramount in extreme conditions; hence, it is essential to develop such a model that captures the aspect of resilience in normal and extreme conditions. Similarly, research is being carried out to understand and assess this interdependence using different performance metrics [147]. One such metric is the demand satisfaction ratio, which measures the impact of power failure on the interconnected water distribution network [149]. The security framework of such critical interdependent infrastructures must be modeled using different state-of-the-art techniques, such as game-theoretic methods [150]. The operation of multi-purpose reservoirs in water distribution networks requires interdependent resource allocation between water and power distribution networks; it can be solved as a multi-objective optimization problem [151]. Furthermore, multi-infrastructure interdependence modeling paves the way for a more sophisticated resilience analysis for power distribution systems [120].

## **2.5 Research gaps and opportunities**

There is a significant research gap in standardizing resilience quantification, modeling, and planning for critical infrastructures such as power distribution systems. There are several areas where extensive research can improve the resilience quantification and analysis process. The research gaps specific to the analysis and enhancements of power distribution system resilience are summarized in the following sections.

### **2.5.1 Proactive decision-making/operational planning**

From the utility's perspective, planning for an upcoming HILP event is desirable to enhance resilience proactively. Planning includes mechanisms to reduce the impacts of an upcoming event or resource allocation to assist in faster recovery. For instance, staging the repair crews at appropriate locations, analyzing the availability of supply resources, and deciding on an appropriate restoration scheme before the event can help reduce their impacts on the system and help accelerate recovery [90]. The necessity and effectiveness of proactive decision-making have been extensively discussed for both the bulk grid [152] and distribution systems [153]. In general, proactive outage management can help the system recover and restore faster in the aftermath of an event, thus reducing the overall impact of the HILP event. However, such a decision-making process involves a high degree of uncertainty, including extreme weather uncertainty, damage uncertainty, availability of resources, system loading conditions, and so forth. The uncertain and time-varying nature of HILP events must be appropriately modeled in the problem formulation for resilience considerations. The efficacy of proactive planning depends on the accuracy of models used to account for these uncertainties and infrastructure considerations. Enhancing

forecasting models is a key avenue for improving planning strategies, as it aids system operators in narrowing down uncertainty bounds and anticipating future scenarios. Proactive measures operate on shorter planning horizons, demanding swift decision-making. Given the complexity of these models, achieving quick solutions is often a significant challenge. Therefore, methods that prioritize near-optimal approximations and relaxations can prove effective in refining planning models.

While high-dimensional, nonlinear models can represent intricate physical details, they also introduce several algorithmic challenges. Even mixed-integer linear models, while more tractable, remain computationally demanding due to their non-convex nature. Robust algorithms are needed to solve related decision-making problems that typically involve solving stochastic non-linear (often) mixed-integer optimization problems, which are computationally expensive. It is also important to model the spatiotemporal characteristics of the available resources (both human and automated) in the proactive decision-making process. For instance, fully utilizing a currently available resource for a specific outage can impact the operation in the future due to the inherent stochasticity of the resource and the changing nature of the event. In such a case, an optimal solution will include multi-stage planning to obtain optimal allocation at a given time step, considering future requirements and uncertainties. This is an even more complex problem to scale computationally for large-scale nonlinear systems such as the power grid. Additional research is needed to efficiently solve the resulting problem considering all the uncertainties related to the event and resources while appropriately modeling the complex operational decision-making problems of large-scale power systems.

### **2.5.2 System planning for resilience/long-term planning**

Resilience planning is a long-term goal for the efficient and robust operation of electric power distribution systems. Investment plans are required for infrastructure hardening, including vegetation management, smart device installations, pole maintenance, upgrades, etc. Investments are required to install weather stations in high-risk areas to avoid high-impact extreme events. State-level regulators need to reevaluate their efforts in prioritizing investments for resilience enhancement by utility companies and reassess several techniques of resilience assessment from the perspective of regulatory decisions which might impact state-level grid investments (such as DERs). Although electric utilities are supposedly investing approximately \$1 trillion in the U.S. electric power grid between 2020 and 2030, investments must be implemented so that economic and national security perspectives can promote resilience by design. Utility companies require significant investment to improve security against potential vulnerabilities in distribution systems. These investments can make the distribution grid more resilient to HILP events [154].

However, several uncertainties are associated with the planning process; inappropriately incorporating those can lead to sub-optimal investment decisions. Therefore, the planning problem should appropriately model such uncertainties and the associated risks imposed on the power delivery systems. Additionally, it is also important to model those risks in the optimization framework to achieve realistic outcomes from the planning process. Recently, some current work incorporates a convex risk measure, namely conditional value-at-risk, when solving the distribution system restoration problem [155]. Similarly, other works explore the uncertainties associated with the system in the development of restoration approaches [156]. However, the risk

associated with the uncertainties should also be determined for a more accurate resilience assessment. Hence, while modeling the stochastic nature of events or available resources, it is equally important to model associated risks [157].

The long-term planning problem presents significant challenges in terms of modeling, solving, and scalability [158]. Unlike operational planning, long-term planning requires the consideration of multiple scenarios and depends on the number of scenarios and time horizon being considered. Additionally, long-term planning decisions must account for the full profile of extreme weather events, necessitating a multi-hazard model that encompasses various events occurring independently or simultaneously [159]. Furthermore, it is crucial to have a robust forecast model with minimal errors to justify future planning decisions [160]. However, one major challenge in multi-hazard modeling and forecasting is the need for a large number of scenarios to represent such hazards. Balancing computational efficiency and accuracy is critical, as incorporating sufficient scenarios is necessary to capture the high uncertainty associated with HILP events. The long-term planning model typically includes stages before, during and after the event, but the complexity grows exponentially with the time horizon, number and nature of resources, and size of the power grid under consideration. Uncertainties arise from factors such as future weather conditions, solar irradiance, battery state-of-charge, and operating conditions of DERs. To address these challenges, sophisticated tools for scenario generation and reduction are required to model the problem while retaining essential information effectively. Future research should also focus on scalable algorithms and leveraging high-performance computing resources to enhance computational tractability [161].

### **2.5.3 Modeling and forecasting the impact of natural disasters**

The recent and rapid changes in weather and the frequent occurrence of natural disasters are alarming, as these events can have long-lasting impacts. Therefore, modeling and forecasting the effects of extreme weather events play a major role in the resilient operation of the power distribution system. Most of the previous works consider hurricanes as extreme events while assessing the resilience of the distribution system. On the contrary, the different types of extreme weather events differ significantly in their impact on power distribution systems, making it challenging to develop a generalized impact modeling framework. Hence, considering all the parameters affecting the distribution system resilience, a generalized impact modeling framework is challenging. Additionally, there is a gap in appropriately modeling the impacts of extreme weather events on power distribution systems when designing system hardening solutions. Most impact models are based on the topology of the power system, lacking details about localized geographical information [13]. Weather forecasting is vital for routine operations, balancing production and demand. It is essential to warn of extreme events, making it possible to better manage demand and supply, prepare a response, and accelerate recovery times. Utilities lack improved models that downscale global information to the local level. Comprehensive research is required to develop tools and skills to interpret the data and understand how meteorological uncertainty affects current and future operations. Moreover, since the frequency of these events is extremely low, the available data to characterize these events are limited. Novel methods are needed to use limited data to model the impacts of extreme weather events at the component and system level. There is also a critical need for accurate predictive event and damage models that use limited data. Weather, meteo-

rological, historical outage reports, and other useful data sources must be integrated to improve resilience planning and preparation models for an upcoming event. Furthermore, the study should also have provisions for integrated studies with multiple critical infrastructures [150].

#### **2.5.4 Smart grid operation for enhanced resilience**

Improved SA and controllability at the distribution level provide an additional venue to enhance resilience through smart grid operations. In recent years, advanced metering infrastructure and intelligent electronic devices such as sensors and telemetered controllers have been deployed in distribution systems, providing utilities with access to large and increasing amounts of data [162]. Furthermore, phasor measurement units, which provide real-time synchrophasor data, are expected to be widely deployed in distribution grids [163]. These innovative grid-edge technologies enhance SA compared to traditional approaches, which are labor-intensive and time-consuming. However, it is not practical to successfully deploy such devices across the network due to the associated cost and geographical difficulties [164]. Therefore, a cost-benefit analysis is needed for the design and deployment of improved state estimation technologies. This can enhance system monitoring performance and facilitate model validation with post-event analysis, allowing for accurate decision-making [165].

Another aspect of resilient smart grid operation is enabling non-traditional ways of operating grids using microgrids and other DER such as PV, storage, and flexible loads. Recently, DERs have been extensively examined for resilience enhancement because they support critical loads during extreme events independent of the bulk power system in an islanded mode. These DERs can also be effectively engaged with

the help of transactive energy systems. Transactive energy systems can address operational challenges during abnormal conditions when new mechanisms are designed for contingencies [166]. Although conventional approaches for resilience enhancement are usually prepared from the system operator's standpoint, the transactive energy systems mechanism, if appropriately designed, can be utilized to incentivize customers to engage in activities that shift load to where it is needed the most and reduce the peak loads, thus relieving stress on the grid during scarcity [167].

#### **2.5.5 Compound effect of extreme events and equity**

Extensive research efforts have been dedicated to assessing the planning, operation, and valuation of power system resilience when confronted with the independent occurrence of extreme events, such as hurricanes, earthquakes, floods, as well as various human-induced threats like cyberattacks and physical threats [168]. Nonetheless, the assessment of power system resilience within the context of the compounding effect of extreme events, specifically those related to temperature fluctuations like heatwaves and cold waves, introduces distinct challenges [169]. These challenges stem from the compounding effects of temperature extremes, which can result in increased mortality rates and a cascade of other severe consequences, including reduced productivity and property damage [170]. Furthermore, such extreme temperature-related events can significantly stress the power distribution grid, increasing electricity demand and leading to brownouts or blackouts if not managed properly. While there is a growing practice of managed power outages during severe weather events, there is limited empirical evidence regarding the impartiality and fairness with which these planned outages and subsequent restoration efforts are executed [171]. For instance, research

centered on the rolling blackouts implemented in Texas during the winter storm Uri in 2021 has revealed a substantial disparity in the scope and duration of these outages [172] and areas with a high share of minority population were greater than four times as likely to suffer a blackout than other areas. Furthermore, during the same event, as discussed in Section 4.3, customers using electricity for space heating were at a disadvantage as natural gas supply was prioritized to customers using natural gas for heating. The power outage's major cause was natural gas supply disruption [132]. While events such as natural disasters, extreme weather conditions, or resource shortages are inevitable, the distribution of essential resources must be done in a way that minimizes disparities and ensures that disadvantaged communities — defined using indicators such as socioeconomic, demographic, financial, and health — are not disproportionately affected. Equity-informed metrics should be augmented with traditional practices that consider system-wide averages (e.g., energy-not-served, cumulative customers-hours of outages, loss of revenue, and recovery time) in the planning and operation of distribution utilities. In terms of recovery and resilience planning for future events, there is no concrete understanding of how the planning costs should be distributed, as the economics of resilience is yet to be defined. A study focusing on the wildfire-resilient distribution system suggested socializing the cost of resilience as a means of achieving equitable cost distribution [173]. However, communities with higher median income are identified as higher wildfire risk zones in California, which has suffered from frequent wildfire events now [174]. Therefore, adopting a socialized resilience cost approach, especially in a diverse community-based area like California, could disproportionately benefit higher-income communities. Thus, it is essential to characterize this disparity by integrating equity considerations into the resilience

planning model.

## 2.6 Summary

This chapter highlights the significance of examining the resilience analysis process of power distribution networks during extreme weather events. As it evolved with the strategic discussion and analysis of the resilience assessment and analysis process and the relevant challenges associated with different domains, it became increasingly evident that ensuring a robust and resilient power grid is not only an expected characteristic but also an absolute requirement. The outcomes of this chapter have significant implications for multiple stakeholders in the energy sector. Industry stakeholders can leverage the resilience analysis framework to enhance their resilience planning, infrastructure investments, and operational strategies to mitigate the impacts of extreme events, as existing utility planning measures do not incorporate risks. Policymakers can utilize the insights to shape regulations, standards, and policies that promote the resilience of power distribution systems, aligning with global energy, environment, and sustainability goals. Furthermore, the research underscores the urgency of coordinated action at the international level to address the increasing frequency and severity of extreme events, emphasizing the need for collaborative efforts to build resilient energy systems, thus fostering a sustainable and climate-resilient future that prioritizes equitable access and benefits for all.

## REFERENCES

- [1] G. Hou, K. K. Muraleetharan, V. Panchalogarajan, P. Moses, A. Javid, H. Al-Dakheeli, R. Bulut, R. Campos, P. S. Harvey, G. Miller, *et al.*, “Resilience assessment and enhancement evaluation of power distribution systems subjected to ice storms,” *Reliability Engineering & System Safety*, vol. 230, p. 108964, 2023.
- [2] Government Accountability Office, “Electricity grid resilience,” Tech. Rep. GAO-21-423T, United States Government Accountability Office, Mar. 2021.
- [3] National Centers for Environmental Information, “U.S. billion-dollar weather and climate disasters 1993-2022,” 2023.
- [4] L. Labaka, J. Hernantes, and J. M. Sarriegi, “A holistic framework for building critical infrastructure resilience,” *Technological Forecasting and Social Change*, vol. 103, pp. 21 – 33, 2016.
- [5] W. Liu and Z. Song, “Review of studies on the resilience of urban critical infrastructure networks,” *Reliability Engineering & System Safety*, vol. 193, p. 106617, 2020.
- [6] D. Rehak, P. Senovsky, and S. Slivkova, “Resilience of critical infrastructure elements and its main factors,” *Systems*, vol. 6, no. 2, 2018.
- [7] K. Dick, L. Russell, Y. Souley Dosso, F. Kwamena, and J. R. Green, “Deep learning for critical infrastructure resilience,” *Journal of Infrastructure Systems*, vol. 25, no. 2, p. 05019003, 2019.

- [8] T. J. Nipa, S. Kermanshachi, and I. J. Ramaji, “Comparative analysis of strengths and limitations of infrastructure resilience measurement methods,” in *7th CSCE International Construction Specialty Conference (ICSC)*, p. 6, 2019.
- [9] B. Petrenj, E. Lettieri, and P. Trucco, “Information sharing and collaboration for critical infrastructure resilience—a comprehensive review on barriers and emerging capabilities,” *International journal of critical infrastructures*, vol. 9, no. 4, pp. 304–329, 2013.
- [10] C. Pursiainen and P. Gattinesi, “Towards testing critical infrastructure resilience,” *EUR—Scientific and Technical Research reports, European Commission, Joint Research Center*, 2014.
- [11] A. A. Bajwa, H. Mokhlis, S. Mekhilef, and M. Munibin, “Enhancing power system resilience leveraging microgrids: A review,” *Journal of Renewable and Sustainable Energy*, vol. 11, no. 3, p. 035503, 2019.
- [12] Z. Bie, Y. Lin, G. Li, and F. Li, “Battling the extreme: A study on the power system resilience,” *Proceedings of the IEEE*, vol. 105, no. 7, pp. 1253–1266, 2017.
- [13] Y. Wang, C. Chen, J. Wang, and R. Baldick, “Research on resilience of power systems under natural disasters—a review,” *IEEE Transactions on Power Systems*, vol. 31, no. 2, pp. 1604–1613, 2016.
- [14] H. Cai, N. S. Lam, Y. Qiang, L. Zou, R. M. Correll, and V. Mihunov, “A synthesis of disaster resilience measurement methods and indices,” *International Journal of Disaster Risk Reduction*, vol. 31, pp. 844 – 855, 2018.

- [15] P. Eder-Neuhäuser, T. Zseby, and J. Fabini, “Resilience and security: a qualitative survey of urban smart grid architectures,” *IEEE Access*, vol. 4, pp. 839–848, 2016.
- [16] Y. Chi, Y. Xu, C. Hu, and S. Feng, “A state-of-the-art literature survey of power distribution system resilience assessment,” in *2018 IEEE Power Energy Society General Meeting (PESGM)*, pp. 1–5, 2018.
- [17] H. H. Willis and K. Loa, “Measuring the resilience of energy distribution systems,” *RAND Corporation: Santa Monica, CA, USA*, 2015.
- [18] S. Shirzadi and N. C. Nair, “Power system resilience through microgrids: A comprehensive review,” in *2018 IEEE PES Asia-Pacific Power and Energy Engineering Conference (APPEEC)*, pp. 674–679, 2018.
- [19] J. Abdubannaev, Y. Sun, A. Xin, M. U. Jan, N. Makhamadjanova, and S. Rakhimov, “Enhancing power system resilience - a review,” in *2019 IEEE 3rd Conference on Energy Internet and Energy System Integration (EI2)*, pp. 2350–2354, 2019.
- [20] D. K. Mishra, M. J. Ghadi, A. Azizivahed, L. Li, and J. Zhang, “A review on resilience studies in active distribution systems,” *Renewable and Sustainable Energy Reviews*, vol. 135, p. 110201, 2021.
- [21] Q. Shi, W. Liu, B. Zeng, H. Hui, and F. Li, “Enhancing distribution system resilience against extreme weather events: Concept review, algorithm summary, and future vision,” *International Journal of Electrical Power & Energy Systems*, vol. 138, p. 107860, 2022.

- [22] G. Kandaperumal and A. K. Srivastava, “Resilience of the electric distribution systems: concepts, classification, assessment, challenges, and research needs,” *IET Smart Grid*, vol. 3, no. 2, pp. 133–143, 2020.
- [23] United Nations, “The 17 goals,” *United Nations Department of Economic and Social Affairs*.
- [24] A. Kwasinski, “Quantitative model and metrics of electrical grids’ resilience evaluated at a power distribution level,” *Energies*, vol. 9, no. 2, p. 93, 2016.
- [25] A. Kwasinski, V. Krishnamurthy, J. Song, and R. Sharma, “Availability evaluation of micro-grids for resistant power supply during natural disasters,” *IEEE Transactions on Smart Grid*, vol. 3, no. 4, pp. 2007–2018, 2012.
- [26] K. Utkarsh and F. Ding, “Self-organizing map-based resilience quantification and resilient control of distribution systems under extreme events,” *IEEE Transactions on Smart Grid*, vol. 13, no. 3, pp. 1923–1937, 2022.
- [27] “State of reliability: An assessment of 2019 bulk power system performance,” tech. rep., North American Electric Reliability Corporation, USA, July 2020.
- [28] “Maintaining Reliability in the Modern Power System,” tech. rep., U.S. Department of Energy, Dec. 2016.
- [29] M. I. Henderson, D. Novosel, and M. L. Crow, “Electric power grid modernization trends, challenges, and opportunities,” *IEEE Power Energy*, 2017.
- [30] S. Yao, P. Wang, X. Liu, H. Zhang, and T. Zhao, “Rolling optimization of mobile energy storage fleets for resilient service restoration,” *IEEE Transactions on Smart Grid*, vol. 11, no. 2, pp. 1030–1043, 2019.

- [31] S. Nourollah and G. B. Gharehpetian, “Coordinated load shedding strategy to restore voltage and frequency of microgrid to secure region,” *IEEE Transactions on Smart Grid*, vol. 10, no. 4, pp. 4360–4368, 2018.
- [32] F. K. Tuffner, K. P. Schneider, J. Hansen, and M. A. Elizondo, “Modeling load dynamics to support resiliency-based operations in low-inertia microgrids,” *IEEE Transactions on Smart Grid*, vol. 10, no. 3, pp. 2726–2737, 2019.
- [33] T. Ding, Y. Lin, G. Li, and Z. Bie, “A new model for resilient distribution systems by microgrids formation,” *IEEE Transactions on Power Systems*, vol. 32, no. 5, pp. 4145–4147, 2017.
- [34] A. Dubey, A. Bose, M. Liu, and L. N. Ochoa, “Paving the way for advanced distribution management systems applications: making the most of models and data,” *IEEE Power and Energy Magazine*, vol. 18, no. 1, pp. 63–75, 2020.
- [35] J. Carlson, R. Haffenden, G. Bassett, W. Buehring, M. Collins III, S. Folga, F. Petit, J. Phillips, D. Verner, and R. Whitfield, “Resilience: theory and application.,” tech. rep., Argonne National Lab.(ANL), Argonne, IL (United States), 2012.
- [36] P. E. Roege, Z. A. Collier, J. Mancillas, J. A. McDonagh, and I. Linkov, “Metrics for energy resilience,” *Energy Policy*, vol. 72, pp. 249 – 256, 2014.
- [37] P. M. Orencio and M. Fujii, “A localized disaster-resilience index to assess coastal communities based on an analytic hierarchy process (ahp),” *International Journal of Disaster Risk Reduction*, vol. 3, pp. 62 – 75, 2013.

- [38] F. H. Jufri, V. Widiputra, and J. Jung, “State-of-the-art review on power grid resilience to extreme weather events: Definitions, frameworks, quantitative assessment methodologies, and enhancement strategies,” *Applied Energy*, vol. 239, pp. 1049 – 1065, 2019.
- [39] J. Taft, “Electric grid resilience and reliability for grid architecture,” *Pacific Northwest National Laboratory*. [https://gridarchitecture.pnnl.gov/media/advanced/Electric\\_Grid\\_Resilience\\_and\\_Reliability.pdf](https://gridarchitecture.pnnl.gov/media/advanced/Electric_Grid_Resilience_and_Reliability.pdf), 2017.
- [40] M. N. Albasrawi, N. Jarus, K. A. Joshi, and S. S. Sarvestani, “Analysis of reliability and resilience for smart grids,” in *2014 IEEE 38th Annual Computer Software and Applications Conference*, pp. 529–534, 2014.
- [41] M. Ouyang and L. Dueñas-Osorio, “Resilience modeling and simulation of smart grids,” in *Structures Congress ASCE*, pp. 1996–2009, 2011.
- [42] X. Liu, M. Shahidehpour, Z. Li, X. Liu, Y. Cao, and Z. Bie, “Microgrids for enhancing the power grid resilience in extreme conditions,” *IEEE Transactions on Smart Grid*, vol. 8, no. 2, pp. 589–597, 2017.
- [43] M. Bruneau, S. E. Chang, R. T. Eguchi, G. C. Lee, T. D. O’Rourke, A. M. Reinhorn, M. Shinozuka, K. Tierney, W. A. Wallace, and D. von Winterfeldt, “A framework to quantitatively assess and enhance the seismic resilience of communities,” *Earthquake Spectra*, vol. 19, no. 4, pp. 733–752, 2003.
- [44] J.-P. Watson, R. Gutstromson, C. Silva-Monroy, R. Jeffers, K. Jones, J. Ellison, C. Rath, J. Gearhart, D. Jones, T. Corbet, *et al.*, “Conceptual framework for developing resilience metrics for the electricity oil and gas sectors in the United

States,” *Sandia National Laboratories, Albuquerque, NM (United States), tech. rep.*, 2014.

- [45] S. Ma, B. Chen, and Z. Wang, “Resilience enhancement strategy for distribution systems under extreme weather events,” *IEEE Transactions on Smart Grid*, vol. 9, no. 2, pp. 1442–1451, 2016.
- [46] M. Wen, Y. Chen, Y. Yang, R. Kang, and Y. Zhang, “Resilience-based component importance measures,” *International Journal of Robust and Nonlinear Control*, vol. 30, no. 11, pp. 4244–4254, 2020.
- [47] S. Espinoza, A. Poulos, H. Rudnick, J. C. de la Llera, M. Panteli, P. Manarella, R. Sacaan, A. Navarro, and R. Moreno, “Seismic resilience assessment and adaptation of the northern chilean power system,” in *2017 IEEE Power & Energy Society General Meeting*, pp. 1–5, IEEE, 2017.
- [48] S. Poudel and A. Dubey, “Critical load restoration using distributed energy resources for resilient power distribution system,” *IEEE Transactions on Power Systems*, vol. 34, no. 1, pp. 52–63, 2018.
- [49] H. Gao, Y. Chen, Y. Xu, and C.-C. Liu, “Resilience-oriented critical load restoration using microgrids in distribution systems,” *IEEE Transactions on Smart Grid*, vol. 7, no. 6, pp. 2837–2848, 2016.
- [50] D. Anderson, M. Kintner-Meyer, G. Porro, M. Shah, J. Eto, T. Edmonds, S. Folga, S. Hadley, G. Heath, A. Tompkins, A. Eberle, C. Silva-Monroy, E. Vu-grin, M. Yue, and J. Phillips, “Grid modernization: metrics analysis (grid mod-

ernization lab consortium 1.1) reference document, version 2.1,” Tech. Rep. PNNL-28562, Pacific Northwest National Laboratory, 06 2017.

- [51] C. Scawthorn, N. Blais, H. Seligson, E. Tate, E. Mifflin, W. Thomas, J. Murphy, and C. Jones, “Hazus-mh flood loss estimation methodology. i: Overview and flood hazard characterization,” *Natural Hazards Review*, vol. 7, no. 2, pp. 60–71, 2006.
- [52] D. N. Bresch and G. Aznar-Siguán, “CLIMADA v1.4.1: towards a globally consistent adaptation options appraisal tool,” *Geoscientific Model Development*, vol. 14, pp. 351–363, Jan. 2021.
- [53] R. Brown, “Cost-benefit analysis of the deployment of utility infrastructure upgrades and storm hardening programs,” tech. rep., Mar. 2009.
- [54] S. Poudel, A. Dubey, and A. Bose, “Risk-based probabilistic quantification of power distribution system operational resilience,” *IEEE Systems Journal*, pp. 1–12, 2019.
- [55] S. Hanif, V. H. Chalishazar, and D. J. Hammerstrom, “Modeling the functional forms of grid disturbances,” tech. rep., Pacific Northwest National Lab.(PNNL), Richland, WA (United States), 2020.
- [56] C. Wang, P. Ju, F. Wu, X. Pan, and Z. Wang, “A systematic review on power system resilience from the perspective of generation, network, and load,” *Renewable and Sustainable Energy Reviews*, vol. 167, p. 112567, 2022.
- [57] S. Afzal, H. Mokhlis, H. A. Illias, N. N. Mansor, and H. Shareef, “State-of-the-art

review on power system resilience and assessment techniques,” *IET Generation, Transmission & Distribution*, vol. 14, no. 25, pp. 6107–6121, 2020.

- [58] M. Amirioun, F. Aminifar, H. Lesani, and M. Shahidehpour, “Metrics and quantitative framework for assessing microgrid resilience against windstorms,” *International Journal of Electrical Power & Energy Systems*, vol. 104, pp. 716–723, 2019.
- [59] E. Vugrin, A. Castillo, and C. Silva-Monroy, “Resilience metrics for the electric power system: A performance-based approach,” *Report: SAND2017-1493*, 2017.
- [60] L. Schwartz, “Utility investments in resilience of electricity systems,” *Future Electric Utility Regulation Report*, vol. 11, 2019.
- [61] The IEEE PES industry technical support leadership committee task force, “Resilience framework methods, and metrics for the electricity sector,” *IEEE Power & Energy Society Technical Report*, vol. PES-TR83, pp. 1–35, 2020.
- [62] S. Mukhopadhyay and M. Hastak, “Public utility commissions to foster resilience investment in power grid infrastructure,” *Procedia-Social and Behavioral Sciences*, vol. 218, pp. 5–12, 2016.
- [63] F. Petit, G. Bassett, R. Black, W. Buehring, M. Collins, D. Dickinson, R. Fisher, R. Haffenden, A. Huttenga, M. Klett, *et al.*, “Resilience measurement index: An indicator of critical infrastructure resilience,” tech. rep., Argonne National Lab.(ANL), Argonne, IL (United States), 2013.
- [64] D. T. Ton and W. P. Wang, “A more resilient grid: The us department of energy

joins with stakeholders in an r&d plan,” *IEEE Power and Energy Magazine*, vol. 13, no. 3, pp. 26–34, 2015.

- [65] B. Cai, M. Xie, Y. Liu, Y. Liu, and Q. Feng, “Availability-based engineering resilience metric and its corresponding evaluation methodology,” *Reliability Engineering & System Safety*, vol. 172, pp. 216–224, 2018.
- [66] M. Panteli, D. N. Trakas, P. Mancarella, and N. D. Hatziargyriou, “Power systems resilience assessment: Hardening and smart operational enhancement strategies,” *Proceedings of the IEEE*, vol. 105, no. 7, pp. 1202–1213, 2017.
- [67] M. Panteli, C. Pickering, S. Wilkinson, R. Dawson, and P. Mancarella, “Power system resilience to extreme weather: fragility modeling, probabilistic impact assessment, and adaptation measures,” *IEEE Transactions on Power Systems*, vol. 32, no. 5, pp. 3747–3757, 2016.
- [68] S. Hanif, M. Mukherjee, S. Poudel, M. G. Yu, R. A. Jinsiwale, T. D. Hardy, and H. M. Reeve, “Analyzing at-scale distribution grid response to extreme temperatures,” *Applied Energy*, vol. 337, p. 120886, 2023.
- [69] J. Dong, L. Zhu, Y. Su, Y. Ma, Y. Liu, F. Wang, L. M. Tolbert, J. Glass, and L. Bruce, “Battery and backup generator sizing for a resilient microgrid under stochastic extreme events,” *IET Generation, Transmission & Distribution*, vol. 12, no. 20, pp. 4443–4450, 2018.
- [70] J. Zhu, *Uncertainty analysis in power systems*, ch. 1-17, pp. 529–578. Wiley-IEEE Press, 2015.

- [71] North American Electric Reliability Corporation, “Toward ensuring reliability: reliability performance metrics,” tech. rep., Dec. 2007. [Online]. Available: [https://www.nerc.com/docs/pc/rmwg/Reliability\\_Metrics\\_white\\_paper.pdf](https://www.nerc.com/docs/pc/rmwg/Reliability_Metrics_white_paper.pdf).
- [72] K. Gruber, T. Gauster, G. Laaha, P. Regner, and J. Schmidt, “Profitability and investment risk of texan power system winterization,” *Nature Energy*, vol. 7, no. 5, pp. 409–416, 2022.
- [73] P. E. Roege, Z. A. Collier, J. Mancillas, J. A. McDonagh, and I. Linkov, “Metrics for energy resilience,” *Energy Policy*, vol. 72, pp. 249–256, 2014.
- [74] M. M. Hosseini and M. Parvania, “Quantifying impacts of automation on resilience of distribution systems,” *IET Smart Grid*, vol. 3, no. 2, pp. 144–152, 2020.
- [75] C. Poulin and M. B. Kane, “Infrastructure resilience curves: Performance measures and summary metrics,” *Reliability Engineering & System Safety*, vol. 216, p. 107926, 2021.
- [76] C. Nichelle’Le K, I. Dobson, and Z. Wang, “Extracting resilience metrics from distribution utility data using outage and restore process statistics,” *IEEE Transactions on Power Systems*, vol. 36, no. 6, pp. 5814–5823, 2021.
- [77] M. Panteli, P. Mancarella, D. N. Trakas, E. Kyriakides, and N. D. Hatziyriou, “Metrics and quantification of operational and infrastructure resilience in power systems,” *IEEE Transactions on Power Systems*, vol. 32, no. 6, pp. 4732–4742, 2017.

- [78] A. Poudyal, A. Dubey, and S. Poudel, “A risk-driven probabilistic approach to quantify resilience in power distribution systems,” in *2022 17th International Conference on Probabilistic Methods Applied to Power Systems (PMAPS)*, pp. 1–6, 2022.
- [79] S. Zhu, R. Yao, Y. Xie, F. Qiu, and X. Wu, “Quantifying grid resilience against extreme weather using large-scale customer power outage data,” *arXiv preprint arXiv:2109.09711*, 2021.
- [80] P. Teimourzadeh Baboli, “Flexible and overall reliability analysis of hybrid ac–dc microgrid among various distributed energy resource expansion scenarios,” *IET Generation, Transmission Distribution*, vol. 10, no. 16, pp. 3978–3984, 2016.
- [81] M. Panteli, P. A. Crossley, D. S. Kirschen, and D. J. Sobajic, “Assessing the impact of insufficient situation awareness on power system operation,” *IEEE Transactions on Power Systems*, vol. 28, no. 3, pp. 2967–2977, 2013.
- [82] A. Arif, Z. Wang, C. Chen, and J. Wang, “Repair and resource scheduling in unbalanced distribution systems using neighborhood search,” *IEEE Transactions on Smart Grid*, vol. 11, no. 1, pp. 673–685, 2020.
- [83] H. T. Nguyen, M. Parvania, *et al.*, “Assessing impacts of energy storage on resilience of distribution systems against hurricanes,” *Journal of Modern Power Systems and Clean Energy*, pp. 1–10, 2019.
- [84] H. Ji, C. Wang, P. Li, F. Ding, and J. Wu, “Robust operation of soft open points in active distribution networks with high penetration of photovoltaic

integration,” *IEEE Transactions on Sustainable Energy*, vol. 10, no. 1, pp. 280–289, 2019.

- [85] Office of Electricity Delivery & Energy Reliability, “Smart grid investments improve grid reliability, resilience, and storm responses.,” *US Department of Energy*, Nov. 2014. [Online] Available: [https://www.smartgrid.gov/files/documents/B2-Master-File-with-edits\\_120114.pdf](https://www.smartgrid.gov/files/documents/B2-Master-File-with-edits_120114.pdf).
- [86] S. Lei, J. Wang, C. Chen, and Y. Hou, “Mobile emergency generator pre-positioning and real-time allocation for resilient response to natural disasters,” *IEEE Transactions on Smart Grid*, vol. 9, no. 3, pp. 2030–2041, 2016.
- [87] Y. Xu, C.-C. Liu, K. P. Schneider, and D. T. Ton, “Placement of remote-controlled switches to enhance distribution system restoration capability,” *IEEE Transactions on Power Systems*, vol. 31, no. 2, pp. 1139–1150, 2015.
- [88] Y. Tan, F. Qiu, A. K. Das, D. S. Kirschen, P. Arabshahi, and J. Wang, “Scheduling post-disaster repairs in electricity distribution networks,” *IEEE Transactions on Power Systems*, vol. 34, no. 4, pp. 2611–2621, 2019.
- [89] Z. Wang, B. Chen, J. Wang, and C. Chen, “Networked microgrids for self-healing power systems,” *IEEE Transactions on smart grid*, vol. 7, no. 1, pp. 310–319, 2015.
- [90] A. Arif, Z. Wang, J. Wang, and C. Chen, “Power distribution system outage management with co-optimization of repairs, reconfiguration, and dg dispatch,” *IEEE Transactions on Smart Grid*, vol. 9, no. 5, pp. 4109–4118, 2017.

- [91] NOAA research, “Noaa wind forecasts result in \$150 million in energy savings every year,” *National Oceanic and Atmospheric Administration*, May. 2022.
- [92] D. Cerrai, D. W. Wanik, M. A. E. Bhuiyan, X. Zhang, J. Yang, M. E. Frediani, and E. N. Anagnostou, “Predicting storm outages through new representations of weather and vegetation,” *IEEE Access*, vol. 7, pp. 29639–29654, 2019.
- [93] US Department of Energy and US Department of Homeland Security, “Energy sector-specific plan,” tech. rep., US Department of Energy and US Department of Homeland Security, 2015.
- [94] V. H. Chalishazar, S. Poudel, S. Hanif, and P. Thekkumparambath Mana, “Power system resilience metrics augmentation for critical load prioritization,” tech. rep., Pacific Northwest National Lab.(PNNL), Richland, WA (United States), 2021.
- [95] A. Hampson, “Combined heat and power: Enabling resilient energy infrastructure for critical facilities,” tech. rep., Oak Ridge National Lab.(ORNL), Oak Ridge, TN (United States), 2013.
- [96] T. Ding, Y. Lin, Z. Bie, and C. Chen, “A resilient microgrid formation strategy for load restoration considering master-slave distributed generators and topology reconfiguration,” *Applied Energy*, vol. 199, pp. 205 – 216, 2017.
- [97] C. Qin, L. Jia, S. Bajagain, S. Pannala, A. K. Srivastava, and A. Dubey, “An integrated situational awareness tool for resilience-driven restoration with sustainable energy resources,” *IEEE Transactions on Sustainable Energy*, vol. 14, no. 2, pp. 1099–1111, 2023.

- [98] D. Atanackovic and V. Dabic, “Deployment of real-time state estimator and load flow in bc hydro dms-challenges and opportunities,” in *2013 IEEE Power & Energy Society General Meeting*, pp. 1–5, IEEE, 2013.
- [99] S. Bajagain and A. Dubey, “Iterative distribution system state estimation for integrated primary and split-phase secondary feeder monitoring,” *IEEE Transactions on Power Delivery*, 2022.
- [100] Z. Jia, J. Chen, and Y. Liao, “State estimation in distribution system considering effects of ami data,” in *2013 Proceedings of IEEE Southeastcon*, pp. 1–6, IEEE, 2013.
- [101] E. Boardman, “The role of integrated distribution management systems in smart grid implementations,” in *IEEE PES General Meeting*, pp. 1–6, IEEE, 2010.
- [102] J. A. Wischkaemper, C. L. Benner, B. D. Russell, and K. Manivannan, “Application of waveform analytics for improved situational awareness of electric distribution feeders,” *IEEE Transactions on Smart Grid*, vol. 6, no. 4, pp. 2041–2049, 2015.
- [103] Electric Power Research Institute (EPRI), “Improving electric power system situational awareness,” report, Electric Power Research Institute, Palo Alto, CA, Nov. 2015.
- [104] R. J. Campbell, “The smart grid: Status and outlook,” *US Infrastructure: Government Programs and Economic Impacts*, pp. 1–24, 2018.
- [105] G. J. Lim, S. Kim, J. Cho, Y. Gong, and A. Khodaei, “Multi-uav pre-positioning

- and routing for power network damage assessment,” *IEEE Transactions on Smart Grid*, vol. 9, no. 4, pp. 3643–3651, 2018.
- [106] N. Alguacil, A. Delgadillo, and J. M. Arroyo, “A trilevel programming approach for electric grid defense planning,” *Computers & Operations Research*, vol. 41, pp. 282–290, Jan 2014.
- [107] W. Yuan, J. Wang, F. Qiu, C. Chen, C. Kang, and B. Zeng, “Robust optimization-based resilient distribution network planning against natural disasters,” *IEEE Transactions on Smart Grid*, vol. 7, pp. 2817–2826, Nov 2016.
- [108] X. Wang, Z. Li, M. Shahidehpour, and C. Jiang, “Robust line hardening strategies for improving the resilience of distribution systems with variable renewable resources,” *IEEE Transactions on Sustainable Energy*, vol. 10, no. 1, pp. 386–395, 2019.
- [109] A. Arab, A. Khodaei, S. K. Khator, K. Ding, V. A. Emesih, and Z. Han, “Stochastic pre-hurricane restoration planning for electric power systems infrastructure,” *IEEE Transactions on Smart Grid*, vol. 6, no. 2, pp. 1046–1054, 2015.
- [110] G. Zhang, F. Zhang, X. Zhang, Z. Wang, K. Meng, and Z. Y. Dong, “Mobile emergency generator planning in resilient distribution systems: a three-stage stochastic model with nonanticipativity constraints,” *IEEE Transactions on Smart Grid*, vol. 11, no. 6, pp. 4847–4859, 2020.
- [111] M. Jamei, A. Scaglione, C. Roberts, E. Stewart, S. Peisert, C. McParland, and A. McEachern, “Anomaly detection using optimally placed  $\mu$ PMU sensors

- in distribution grids,” *IEEE Transactions on Power Systems*, vol. 33, no. 4, pp. 3611–3623, 2018.
- [112] J. Ingargiola, M. Francis, and et al., “Hurricane Sandy in New Jersey and New York,” Mitigation Assessment Team Report FEMA P-942, Federal Emergency Management Agency, Nov. 2013.
- [113] J. Li, X.-Y. Ma, C.-C. Liu, and K. P. Schneider, “Distribution system restoration with microgrids using spanning tree search,” *IEEE Transactions on Power Systems*, vol. 29, no. 6, pp. 3021–3029, 2014.
- [114] K. P. Schneider, F. K. Tuffner, Y. Tang, N. Radhakrishnan, P. Thekkumparambath, W. Du, J. Kumar, and S. S. Venkata, “Slider-based multi-objective control for resilient microgrids,” *IET Generation, Transmission & Distribution*, vol. 14, no. 13, pp. 2528–2534, 2020.
- [115] L. Che and M. Shahidehpour, “Adaptive formation of microgrids with mobile emergency resources for critical service restoration in extreme conditions,” *IEEE Transactions on Power Systems*, vol. 34, no. 1, pp. 742–753, 2018.
- [116] B. Chen, C. Chen, J. Wang, and K. L. Butler-Purry, “Sequential service restoration for unbalanced distribution systems and microgrids,” *IEEE Transactions on Power Systems*, vol. 33, no. 2, pp. 1507–1520, 2017.
- [117] Y.-J. Kim, J. Wang, and X. Lu, “A framework for load service restoration using dynamic change in boundaries of advanced microgrids with synchronous-machine dgs,” *IEEE Transactions on Smart Grid*, vol. 9, no. 4, pp. 3676–3690, 2016.

- [118] Y. Xu, C.-C. Liu, Z. Wang, K. Mo, K. P. Schneider, F. K. Tuffner, and D. T. Ton, “Dgs for service restoration to critical loads in a secondary network,” *IEEE Transactions on Smart Grid*, vol. 10, no. 1, pp. 435–447, 2017.
- [119] K. P. Schneider, F. K. Tuffner, M. A. Elizondo, C. Liu, Y. Xu, S. Backhaus, and D. Ton, “Enabling resiliency operations across multiple microgrids with grid-friendly appliance controllers,” *IEEE Transactions on Smart Grid*, vol. 9, no. 5, pp. 4755–4764, 2018.
- [120] A. A. A. Mohamed, “On the rising interdependency between the power grid, ict network, and e-mobility: modeling and analysis,” *Energies*, vol. 12, no. 10, 2019.
- [121] Federal Emergency Management Agency, “Power outage incident annex to the response and recovery federal interagency operational plans,” tech. rep., Federal Emergency Management Agency, Jun. 2017.
- [122] S. Sengan, S. V, I. V, P. Velayutham, and L. Ravi, “Detection of false data cyber-attacks for the assessment of security in smart grid using deep learning,” *Computers & Electrical Engineering*, vol. 93, p. 107211, 2021.
- [123] T. O. Olowu, S. Dharmasena, A. Hernandez, and A. Sarwat, *Impact analysis of cyber-attacks on smart grid: a review and case study*, ch. 1, pp. 31–51. Springer Singapore, 2021.
- [124] H. Haggi, R. R. nejad, M. Song, and W. Sun, “A review of smart grid restoration to enhance cyber-physical system resilience,” in *2019 IEEE Innovative Smart Grid Technologies - Asia (ISGT Asia)*, pp. 4008–4013, May 2019.

- [125] G. Huang, J. Wang, C. Chen, and C. Guo, “Cyber-constrained optimal power flow model for smart grid resilience enhancement,” *IEEE Transactions on Smart Grid*, vol. 10, pp. 5547–5555, Sep. 2019.
- [126] D. K. Molzahn, F. Dörfler, H. Sandberg, S. H. Low, S. Chakrabarti, R. Baldick, and J. Lavaei, “A survey of distributed optimization and control algorithms for electric power systems,” *IEEE Transactions on Smart Grid*, vol. 8, no. 6, pp. 2941–2962, 2017.
- [127] W. Wei, D. Wu, Q. Wu, M. Shafie-Khah, and J. P. Catalão, “Interdependence between transportation system and power distribution system: a comprehensive review on models and applications,” *Journal of Modern Power Systems and Clean Energy*, vol. 7, no. 3, pp. 433–448, 2019.
- [128] F. Pérez-Galarce, L. J. Canales, C. Vergara, and A. Candia-Véjar, “An optimization model for the location of disaster refuges,” *Socio-Economic Planning Sciences*, vol. 59, pp. 56–66, 2017.
- [129] Jordan R. Fischbach, Linnea Warren May, Katie Whipkey, Shoshana R. Shelton, Christine Anne Vaughan, Devin Tierney, Kristin J. Leuschner, Lisa S. Meredith, Hilary J. Peterson, “After hurricane maria predisaster conditions, hurricane damage, and recovery needs in puerto rico,” tech. rep., RAND Corporation, 2020. [https://www.rand.org/pubs/research\\_reports/RR2595.html](https://www.rand.org/pubs/research_reports/RR2595.html).
- [130] United States Energy Information Administration , “Use of energy explained energy use in homes,” *U.S. Energy Information Administration*, Jun. 2021. Last accessed 24 Sep 2023.

- [131] Market Monitoring Department, ISO New England, “Final report on electricity supply conditions in new england during the january 14-16, 2004 cold snap,” tech. rep., ISO New England, Oct. 2004.
- [132] Federal Energy Regulation Commission, North American Electric Reliability Corporation, and Regional Entities, “The February 2021 cold weather outages in Texas and the south central United States,” tech. rep., FERC, NERC, and Regional Entities, 2020. <https://shorturl.at/hqvzW>.
- [133] Advanced Network Science Initiative (ANSI), “GasPowerModels.jl,” *Los Alamos National Laboratory*, Jun. 2021. Last accessed 24 Sep 2023.
- [134] O. J. Guerra, B. Sergi, B.-M. Hodge, M. Craig, K. A. Pambour, R. T. Sopgwi, and C. Brancucci, “Electric power grid and natural gas network operations and coordination,” Tech. Rep. NREL/TP-6A50-77096, National Renewable Energy Laboratory, Golden, CO, Sep. 2020.
- [135] R. Bent, S. Blumsack, P. Van Hentenryck, C. Borraz-Sánchez, and M. Shahriari, “Joint electricity and natural gas transmission planning with endogenous market feedbacks,” *IEEE Transactions on Power Systems*, vol. 33, no. 6, pp. 6397–6409, 2018.
- [136] E. C. Portante, J. A. Kavicky, B. A. Craig, L. E. Talaber, and S. M. Folga, “Modeling electric power and natural gas system interdependencies,” *Journal of Infrastructure Systems*, vol. 23, no. 4, p. 04017035, 2017.
- [137] H. Chen and R. Baldick, “Optimizing short-term natural gas supply portfolio

- for electric utility companies,” *IEEE Transactions on Power Systems*, vol. 22, no. 1, pp. 232–239, 2007.
- [138] M. Chertkov, S. Backhaus, and V. Lebedev, “Cascading of fluctuations in interdependent energy infrastructures: Gas-grid coupling,” *Applied Energy*, vol. 160, pp. 541–551, 2015.
- [139] P. Khatavkar and L. W. Mays, “Model for real-time operations of water distribution systems under limited electrical power availability with consideration of water quality,” *Journal of Water Resources Planning and Management*, vol. 144, no. 11, p. 04018071, 2018.
- [140] M. K. Singh, *Optimal operation of water and power distribution networks*. Ph.D. dissertation, Virginia Tech, Dec. 2018.
- [141] K. Oikonomou and M. Parvania, “Deploying water treatment energy flexibility in power distribution systems operation,” in *2020 IEEE Power & Energy Society Innovative Smart Grid Technologies Conference (ISGT)*, pp. 1–5, 2020.
- [142] K. Oikonomou, M. Parvania, and S. Burian, “Integrating water distribution energy flexibility in power systems operation,” in *2017 IEEE Power & Energy Society General Meeting*, pp. 1–5, 2017.
- [143] H. Han, K. Oikonomou, N. Chalapathi, M. Parvania, and B. Wang, “Interactive visualization of interdependent power and water infrastructure operation,” in *2020 IEEE Power & Energy Society Innovative Smart Grid Technologies Conference (ISGT)*, pp. 1–5, 2020.

- [144] S. O. Anne-Sophie Corbeau, Juan Camilo Farfan, “The other European energy crisis: power,” *Center on Global Energy Policy at Columbia/SIPA*, Feb. 2023. Last accessed 6 October 2023.
- [145] Brian Dakss, April Sieze, Alex Sundby, Justin Bey, “Texans face drinking water shortage as power grid returns to normal,” *CBS News*, Feb. 2021. Last accessed 6 October 2023.
- [146] M. T. Van Vliet, D. Wiberg, S. Leduc, and K. Riahi, “Power-generation system vulnerability and adaptation to changes in climate and water resources,” *Nature Climate Change*, vol. 6, no. 4, pp. 375–380, 2016.
- [147] L. Rodriguez-Garcia, M. Parvania, M. M. Hosseini, and T. Mosier, “Resilience analytics for interdependent power and water distribution systems,” *IEEE Transactions on Power Systems*, pp. 1–1, 2022.
- [148] L. Edmonds, M. Derby, M. Hill, and H. Wu, “Coordinated operation of water and electricity distribution networks with variable renewable energy and distribution locational marginal pricing,” *Renewable Energy*, vol. 177, pp. 1438–1450, 2021.
- [149] E. Pournaras, R. Taormina, M. Thapa, S. Galelli, V. Palletti, and R. Kooij, “Cascading failures in interconnected power-to-water networks,” *SIGMETRICS Perform. Eval. Rev.*, vol. 47, p. 16–20, Apr. 2020.
- [150] A. Ferdowsi, A. Sanjab, W. Saad, and N. B. Mandayam, “Game theory for secure critical interdependent gas-power-water infrastructure,” in *2017 Resilience Week (RWS)*, pp. 184–190, 2017.

- [151] J. M. Gonzalez, J. E. Tomlinson, J. J. Harou, E. A. Martínez Ceseña, M. Panteli, A. Bottacin-Busolin, A. Hurford, M. A. Olivares, A. Siddiqui, T. Erfani, K. M. Strzepek, P. Mancarella, J. Mutale, E. Obuobie, A. H. Seid, and A. Z. Ya, “Spatial and sectoral benefit distribution in water-energy system design,” *Applied Energy*, vol. 269, p. 114794, 2020.
- [152] C. Shao, M. Shahidehpour, X. Wang, X. Wang, and B. Wang, “Integrated planning of electricity and natural gas transportation systems for enhancing the power grid resilience,” *IEEE Transactions on Power Systems*, vol. 32, no. 6, pp. 4418–4429, 2017.
- [153] A. Gholami, T. Shekari, F. Aminifar, and M. Shahidehpour, “Microgrid scheduling with uncertainty: The quest for resilience,” *IEEE Transactions on Smart Grid*, vol. 7, no. 6, pp. 2849–2858, 2016.
- [154] B. X. L. Mark Dyson, “Reimagining grid resilience: A framework addressing catastrophic threats to the us electricity grid in an era of transformational change,” tech. rep., 2020 (accessed March 24, 2021). Available at: <http://www.rmi.org/insight/reimagining-grid-resilience>.
- [155] J. Wu, Z. Wu, F. Wu, H. Tang, and X. Mao, “CVaR risk-based optimization framework for renewable energy management in distribution systems with DGs and EVs,” *Energy*, vol. 143, pp. 323–336, Jan. 2018.
- [156] A. Arif, Z. Wang, C. Chen, and B. Chen, “A stochastic multi-commodity logistic model for disaster preparation in distribution systems,” *IEEE Transactions on Smart Grid*, vol. 11, no. 1, pp. 565–576, 2020.

- [157] F. D. Munoz, A. H. van der Weijde, B. F. Hobbs, and J.-P. Watson, “Does risk aversion affect transmission and generation planning? a western north america case study,” *Energy Economics*, vol. 64, pp. 213–225, 2017.
- [158] J. S. Homer, Y. Tang, J. D. Taft, A. C. Orrell, D. Narang, M. Coddington, M. Ingram, and A. Hoke, “Electric distribution system planning with ders-high-level assessment of tools and methods,” tech. rep., Pacific Northwest National Lab.(PNNL), Richland, WA (United States), 2020.
- [159] A. Staid, E. S. Fleming, T. Gunda, and N. D. Jackson, “Critical infrastructure decision-making under long-term climate hazard uncertainty,” Tech. Rep. SAND2021-11394R, Sandia National Laboratories, 2021.
- [160] G. T. Heydt, V. Vittal, S. Malhara, Y. V. Makarov, N. Zhou, and P. V. Etingov, “Characterization and impact of extreme forecast errors on power systems,” *Electric Power Components and Systems*, vol. 39, no. 15, pp. 1685–1700, 2011.
- [161] E. Litvinov, “Computational needs and high-performance computing in power system operation and planning,” tech. rep., ISO New England, 2013. Last accessed Feb. 2022.
- [162] F. Bu, K. Dehghanpour, and Z. Wang, “Enriching load data using micro-pmus and smart meters,” *IEEE Transactions on Smart Grid*, vol. 12, no. 6, pp. 5084–5094, 2021.
- [163] J. Liu, F. Ponci, A. Monti, C. Muscas, P. A. Pegoraro, and S. Sulis, “Optimal meter placement for robust measurement systems in active distribution

- grids,” *IEEE Transactions on Instrumentation and Measurement*, vol. 63, no. 5, pp. 1096–1105, 2014.
- [164] R. Kirkler, “Situational awareness offers grid benefits..,” *T&D World*, Dec. 2016.
- [165] M. Kezunovic, C. Guo, Y. Guan, and M. Ghavami, “New concept and solution for monitoring and control system for the 21 st century substation,” in *2010 International Conference on Power System Technology*, pp. 1–7, IEEE, 2010.
- [166] B. Bhattacharai, V. Chalishazar, D. Hammerstrom, and M. Maharjan, “Transactive energy systems for distributed blackstart and service recovery,” *IET Smart Grid*, vol. 4, no. 5, pp. 489–499, 2021.
- [167] J. Dong, L. Zhu, Q. Dong, P. Kritprajun, Y. Liu, Y. Liu, L. M. Tolbert, J. C. Hambrick, Y. S. Xue, T. B. Ollis, *et al.*, “Integrating transactive energy into reliability evaluation for a self-healing distribution system with microgrid,” *IEEE Transactions on Sustainable Energy*, vol. 13, no. 1, pp. 122–134, 2021.
- [168] A. Poudyal, C. Wertz, A. M. Nguyen, S. U. Mahmud, A. Dubey, and V. Gunturi, “Spatiotemporal impact assessment of hurricanes and storm surges on electric power systems,” in *2023 IEEE Power & Energy Society General Meeting (PESGM)*, pp. 1–5, IEEE, 2023.
- [169] K. Feng, M. Ouyang, and N. Lin, “Tropical cyclone-blackout-heatwave compound hazard resilience in a changing climate,” *Nature communications*, vol. 13, no. 1, p. 4421, 2022.
- [170] R. E. Morss, O. V. Wilhelmi, G. A. Meehl, and L. Dilling, “Improving societal

outcomes of extreme weather in a changing climate: an integrated perspective,” *Annual Review of Environment and Resources*, vol. 36, pp. 1–25, 2011.

- [171] J. Carvallo, F. Hsu, Z. Shah, and J. Taneja, “Frozen out in texas: blackouts and inequity,” *The Rockefeller Foundation*, 2021.
- [172] C.-C. Lee, M. Maron, and A. Mostafavi, “Community-scale big data reveals disparate impacts of the texas winter storm of 2021 and its managed power outage,” *Humanities and Social Sciences Communications*, vol. 9, no. 1, pp. 1–12, 2022.
- [173] Z. Wang, M. Wara, A. Majumdar, and R. Rajagopal, “Local and utility-wide cost allocations for a more equitable wildfire-resilient distribution grid,” *Nature Energy*, pp. 1–12, 2023.
- [174] L. A. Roald, “Sharing the cost of wildfire resilience,” *Nature Energy*, pp. 1–2, 2023.

## CHAPTER 3

### RESILIENCE QUANTIFICATION USING MULTI-CRITERIA DECISION MAKING

#### 3.1 Introduction

This chapter introduces a risk-based resilience metric obtained via a multi-criteria decision-making (MCDM) process. We leverage conditional value-at-risk (CVaR) as the risk measure and Choquet Integral as MCDM method to compute the resilience metric.

##### 3.1.1 Motivation

It is of growing concern to ensure resilience in power distribution systems to extreme weather events. In recent years, weather-related extreme events have severely affected the performance of electric power systems, especially the aging mid-voltage and low-voltage power distribution grid [1]. This calls for proactive threat management of power distribution systems by improving their resilience to high-impact low-probability (HILP) events with the help of new operational procedures and/or hardening of the infrastructure. Planning for resilience requires a metric that can not only quantify the impacts of a future event on the grid but also, help in evaluating/comparing different planning alternatives for their contribution to improving resilience [2]. As discussed in Chapter 2, there are differences between reliability and resilience. Furthermore, resilience cannot be quantified using a single performance index and it requires a holistic study of the electric grid response to extreme conditions to assess its resilience. However, there are no clear methodologies or metrics available

for resilience assessment that allow system planners to assess the impact of appropriate planning measures and new operational procedures for resilience enhancement.

### 3.1.2 Related Literature and Gaps

In literature, multiple articles have sought to define the resilience metrics and have proposed several methods to solve the resilience planning problem. The existing metrics for resilience can be broadly categorized as: a) attribute-based metrics that identify power system attributes such as robustness, resourcefulness, adaptivity, recoverability, and situational awareness [3] and b) performance-based metrics that describe the system's ability to maintain supply (i.e., the system's availability [4]) and often measured using the conceptual resilience curve [5]. Different resilience indicators that are widely used in literature are based on the optimal repair time of critical components [6], energy not served after an extreme event [7], total critical loads supplied during the aftermath of a disaster [8], and in terms of infrastructure recovery [9]. The resilience of power distribution systems is dependent on several factors such as network configuration, available resources and controls, and several other smart grids features such as distributed energy resources (DERs), smart switches, intentional islanding, and self-healing. Towards this goal, references [10, 11] introduce the use MCDM methods to quantify resilience by taking different topological parameters based on graph theory.

Despite these existing approaches, no formal resilience metric is universally accepted. The existing metrics to quantify power distribution system resilience pose one or more limitations including (1) they are post-event measures and mostly evaluated for a single event [12, 8, 6] ; (2) they do not specifically measure the impacts

of HILP events on system performance (kW loss, critical assets without power, total outage duration) [10, 11]; (3) they do not provide additional flexibility to system operators to prioritize one investment decision over the other to evaluate the system resilience [13].

### 3.1.3 Contribution

Contrary to reliability assessment, events with higher impact and lower probability are considered for resilience analysis [14]. Thus, this chapter introduces a probabilistic approach to computing a resilience metric that captures both the system attributes as well as its response to a given extreme event. Prior to this work, our group proposed a framework to evaluate the resilience of power distribution systems using conditional value-at-risk as a risk measure [15]. The specific contributions are listed below:

1. *Multi-criteria Risk-based Resilience Metric:* A novel risk-based resilience metric that considers a comprehensive power system resilience definition. The proposed metric takes multiple resilience-driven parameters – availability, robustness, brittleness, resistance, and resourcefulness to holistically evaluate the power distribution system resilience based on these parameters.
2. *Comprehensive Simulation Framework for Resilience Quantification:* A simulation-based approach that allows system operators to evaluate different mitigating actions. The proposed framework provides additional flexibility to prioritize one investment decision over the others to enhance the system's resilience; The operators can come up with economic investment decisions without compromising the resilience of the system.

## 3.2 Event and Impact Modeling

In this section, we discuss modeling an extreme event and its impact on the distribution grid. For this work, we only consider wind-related events and their impact, which is discussed in the following subsections.

### 3.2.1 Modeling Probabilistic Events

A probabilistic wind event is characterized by the intensity of the wind speed and its probability of occurrence. The intensity here is a function of wind speed,  $v$ . Although wind-related events have spatiotemporal dynamics [16], we assume that for a distribution system, that covers a small region, the wind speed for the entire region is the same. Thus, each of the components in the distribution system experiences a similar wind intensity. The wind speed profile for different intensity levels of the windstorm can be represented by a probability density function (PDF) as discussed in [15].

### 3.2.2 Line Fragility Models

The impact of the wind-related event can be represented by the fragility model of a distribution line [17]. For simplicity, we only consider the impact of wind-related events on the distribution line and not on the other components of the distribution system. The fragility model of any distribution line gives the outage probability of

the line subjected to a particular wind speed and can be represented as:

$$\mathbb{P}_v^l = \begin{cases} \mathbb{F}_n^l & v < v_{cri} \\ \mathbb{P}^l(v) & v_{cri} \leq v < v_{col} \\ 1 & v \geq v_{col} \end{cases} \quad (3.1)$$

where  $\mathbb{F}_n^l$  is the failure rate of line  $l$  in normal weather condition,  $\mathbb{P}^l(v)$  is the failure probability of line  $l$  as a function of  $v$ ,  $v_{cri}$  is the critical wind speed at which line  $l$  experiences failure, and  $v_{col}$  is the wind speed threshold beyond which line  $l$  is guaranteed to fail.

### 3.3 Resilience of Power Distribution Grid

The ultimate goal of a resilient distribution grid is to have a continuous power supply to critical loads (CLs) even during extreme contingencies. In this section we discuss the resilience curve based on number of CLs and resilience-based parameters of a distribution grid.

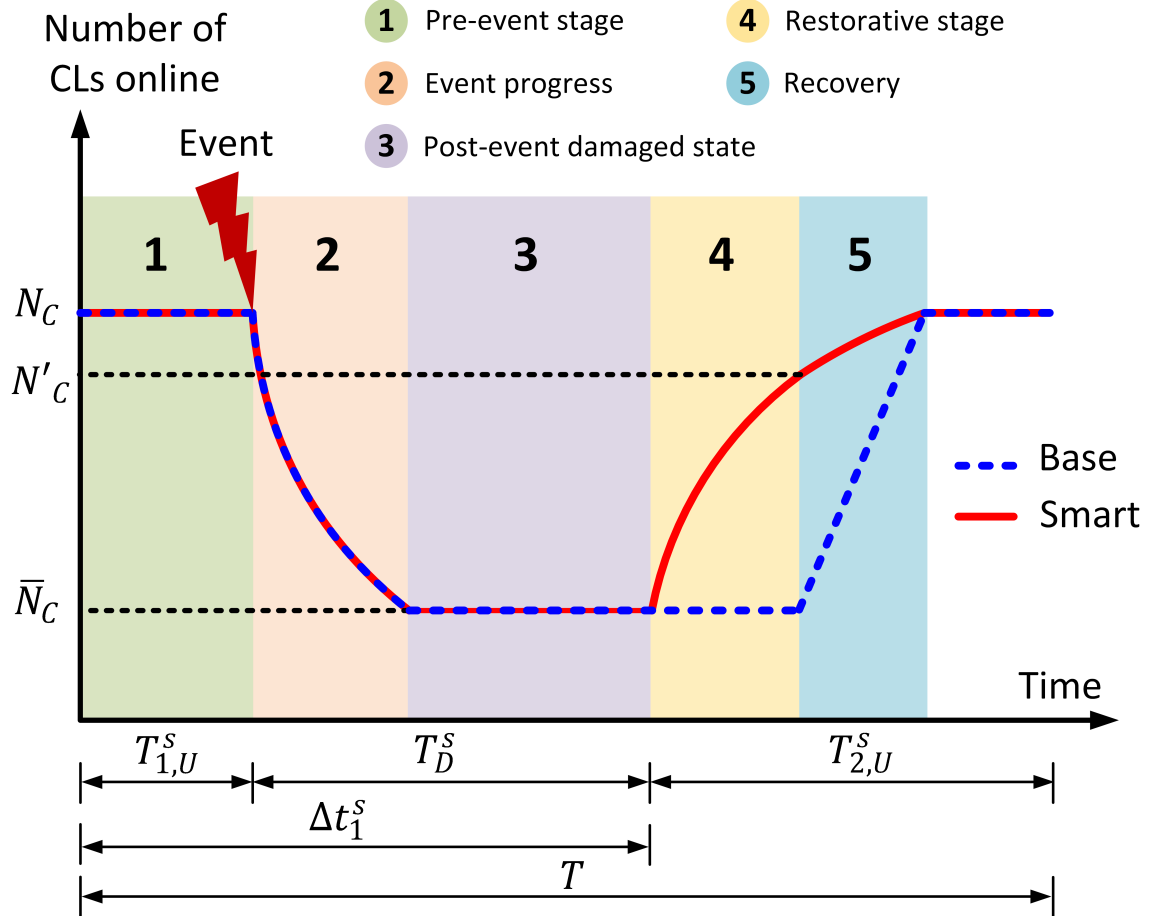
#### 3.3.1 Resilience Curve

Fig. 3.1 shows a typical resilience assessment curve in which the  $x$ -axis represents time whereas the  $y$ -axis represents the number of weighted CLs online. The plot is represented for two cases namely base network, which does not have any restoration strategy once the event occurs and smart network, in which distributed generators (DGs) and smart damage assessment tools are placed for enhanced situational awareness and restoration. To avoid any confusion, the time variables representing only the smart network are used in Fig. 3.1 and are represented with an additional letter  $s$ .

Let  $N_C$  be the total number of CLs that are online at a particular instance of time. The time in which all of the CLs remain online to the time an event occurs is denoted by  $T_{1,U}$  and represented by phase 1. In this work,  $T_{1,U}$  is considered the same for all CLs. The event occurs at the end of  $T_{1,U}$  and sustains for a certain time. The time of event progress depends on the nature and intensity of the event and is denoted by phase 2 of the resilience assessment curve. Some CLs get disconnected due to the severity of the event.  $\bar{N}_C$  be the number of CLs that remain online after an event occurs. Phase 3 denotes the time for damage assessment. Smart networks have smart devices and damage assessment tools that can decrease the damage assessment time significantly. The CLs get disconnected when an event occurs until the point when repair or restoration starts. This is the downtime for CL and is denoted by  $T_D$ .  $\Delta t_1$  is the period from the initial time to the time when repair/restoration begins. For the base case, the repair does not start until the recovery state, phase 5, whereas for the smart network DGs and remote-controlled switches (RCSs) can assist in load restoration, phase 4. At the point of repair/restoration, some of the CLs become online again and remain online for a time  $T_{2,U}$ . Let  $N'_C$  be the number of CLs that are online after the load restoration phase. The total up and downtime of CL for the entire duration is represented by  $T = T_{1,U} + T_D + T_{2,U}$ .

### 3.3.2 Resilience-driven Parameters

In this work, we only consider phases 1 through 4 for quantifying the resilience metric. We will discuss a few parameters that help us define the resilience of a distribution grid as referred to the critical loads and phases described in Fig. 3.1. A detailed explanation of these parameters are given in [18] while some of them are modified as



**Figure 3.1** Typical resilience assessment curve based on the number of weighted CL online. The time variables refer to the smart network [18].

necessary for this work.

### Availability

Let  $i = 1, 2, \dots, N_C$  be the CLs connected in a system,  $T_U^i = T_{1,U}^i + T_{2,U}^i$  be the time period when a CL  $i$  is connected to system (up time), and  $T_D^i$  be the time period when  $i$  is disconnected from the system (down time) due to an extreme event. Hence,

availability refers to the fraction of time when  $i$  is online and is defined as:

$$\mathcal{R}_\psi = \frac{\sum_{i=1}^{N_C} T_U^i}{\sum_{i=1}^{N_C} (T_U^i + T_D^i)} \quad (3.2)$$

Here,  $T_U^i$  and  $T_D^i$  for each  $i$  depends on the type of network. For smart network, some disconnected CLs are restored in phase 4 which increases the overall availability of the system. Here, the choice of  $N_C$  is problem specific and can represent a single customer as well as a particular feeder [18].

### Robustness

Let  $n_0$  be the number of CLs that are disconnected from the system at a given time.

Then the outage incidence,  $\theta$  is defined as:

$$\theta = \frac{n_0}{N_C} \quad (3.3)$$

If  $N_C - \bar{N}_C$  be the maximum number of CLs disconnected from the system and  $\theta_{max}$  is the maximum outage incidence for a given time, then robustness is defined as:

$$\mathcal{R}_\beta = 1 - \theta_{max} = 1 - \frac{N_C - \bar{N}_C}{N_C} = \frac{\bar{N}_C}{N_C} \quad (3.4)$$

### Brittleness

Let  $D$  be the percentage of infrastructure damage in the system. For simplicity, we only consider distribution lines as infrastructures in this work. Brittleness is the level of disruption that occurred in the system with respect to damage. For instance, if the damage of a single distribution line affects the entire system then the system is highly brittle. The brittleness of a system with  $N_C$  critical loads is defined as:

$$\mathcal{R}_\gamma = 100 \times \frac{\theta_{max}}{D} \quad (3.5)$$

## Resistance

According to [18], a system has higher resistance if it can withstand extreme events better and can operate the loads for a longer period before getting disconnected. With this notion, a resistant system should have better physical infrastructures, proper damage assessment methods, and situational awareness in case of extreme events. Furthermore, the resistance is also dependent on the nature of the extreme event. Here,  $\sigma$  is the measure of an extreme event and is obtained as described in [18]. Based on the measure of the event and time before which the repair and restoration begins, the resistance of a system is given by:

$$\mathcal{R}_\xi = \frac{\sigma \sum_{i=1}^{N_C} T_{1,U}^i}{\theta_{max} N_C \Delta t_1} \quad (3.6)$$

## Resourcefulness

Let  $N_{SW}$  be the number of tie-line switches,  $N_S$  be the number of generating sources, and  $N_P$  be the number of simple paths from each of the sources to CLs after an event has occurred in a network. Then the available resources are useful only if their existence is meaningful in system restoration. Thus, resourcefulness is defined as:

$$\mathcal{R}_\delta = \frac{N_P}{(N_{SW} + N_S) \times N_C} \quad (3.7)$$

For the base network, the only available source is the substation so  $N_S = 1$  for the base case. For the smart network,  $N_S$  increases as the number of DG increases. However, the resourcefulness decreases if those DGs are not utilized in network restoration after the event has occurred which is ensured by  $N_C$ . Thus, resourcefulness can be useful for planning the placement and number of DGs to enhance system resilience.

### 3.3.3 Risk-based Resilience Measures

A resilient distribution system should not only handle the expected events but also events with a lower probability of occurrence that might impose a greater impact on the grid. As discussed in [15], we use  $CVaR$  as a risk measure for each of the parameters.  $VaR$  is defined as the specific threshold  $\zeta$ , such that with a specified probability of  $\alpha$   $VaR$  does not exceed  $\zeta$ . On the other hand,  $CVaR$  is the expected value of the distribution that exceeds  $VaR$ . Both of these metrics depend on the value of  $\alpha$  and are commonly represented as  $VaR_\alpha$  and  $CVaR_\alpha$ . If  $p(I)$  be the probability distribution of a random weather event  $I$  then the cumulative probability distribution that the parameter  $\mathcal{R}$  will not exceed  $\zeta$  when impacted by  $I$  is given by:

$$\Psi(\zeta) = \int_{\mathcal{R}(I) \leq \zeta} p(I) dI \quad (3.8)$$

Thus,  $VaR_\alpha$  and  $CVaR_\alpha$  are then defined by:

$$VaR_\alpha(\zeta) = \inf\{\zeta \in \mathbb{R} : \psi(\zeta) \geq \alpha\} \quad (3.9)$$

$$CVaR_\alpha(\zeta) = (1 - \alpha)^{-1} \int_{\mathcal{R}(I) \geq VaR_\alpha} \mathcal{R}(I) p(I) dI \quad (3.10)$$

$CVaR_\alpha$  represents the value of parameter for the extreme  $(1 - \alpha)\%$  of impacts. It is also to be noted that the distribution of parameters below and above the specified threshold  $\zeta$  represent the complete distribution of extreme events with a probability of  $\alpha$  and  $1 - \alpha$  respectively.

## 3.4 Multi-criteria Decision Making using Choquet Integral

All of the parameters defined in Section 3.3.2 are important for enhancing the resilience of a distribution system. Thus, an efficient decision-making strategy is re-

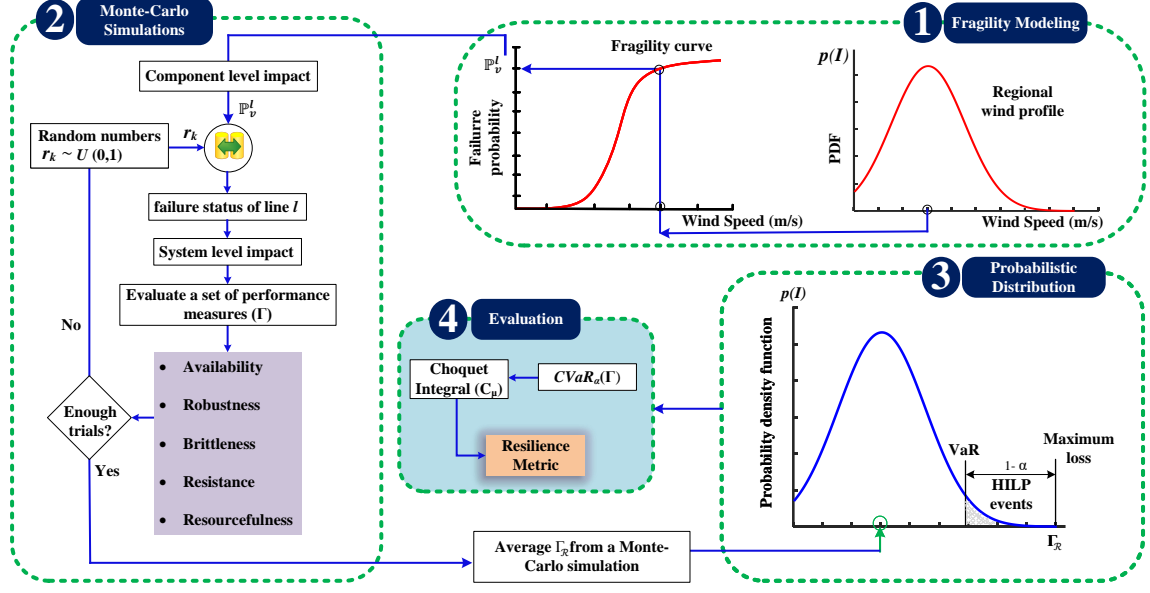


**Figure 3.2** Simulation-based framework for resilience metric computation

quired to identify the important parameters to focus on. The Choquet Integral is an effective method for the MCDM problem [19] and is well suited for our framework.

### 3.4.1 $\lambda$ -Fuzzy Measures

Let a finite universal set be defined by  $\Gamma$ , which has  $N$  parameters;  $\Gamma = \{\mathcal{R}_1, \mathcal{R}_2, \dots, \mathcal{R}_N\}$ .

If  $\mathbb{P}(\Gamma)$  be the power set of  $\Gamma$ , then a fuzzy measure on  $\Gamma$  is defined by,

$$\mu : \mathbb{P}(\Gamma) \rightarrow [0, 1] \quad (3.11)$$

if and only if, a)  $\mu(\phi) = 0$ ,  $\mu(\Gamma) = 1$  and b)  $A \subset B \subset \Gamma \Rightarrow \mu(A) \leq \mu(B)$ . Here, a) ensures that every parameter contributes something and the contribution is maximum when all parameters are included in the set whereas b) shows the monotonic property of fuzzy measures which means that the interaction of parameters should not overshadow the contribution of individual parameters. If  $\lambda$  be the interaction degree

between two disjoint sets  $P$  and  $Q$ , then for  $\lambda > -1$ , the Sugeno  $\lambda$ -fuzzy measure is defined as:

$$\mu(P \cup Q) = \mu(P) + \mu(Q) + \lambda\mu(P)\mu(Q) \quad (3.12)$$

where  $\lambda$  is obtained by solving the first condition of fuzzy measures, i.e.,  $\mu(\Gamma) = 1$ . A detail explanation of calculating  $\lambda$  is given in [20].

### 3.4.2 Behavioral Analysis of Fuzzy Measures

Although  $\lambda$  defines some form of interaction among different parameters, the initial fuzzy weights do not provide concrete evidence on the importance of using one criterion over the other. The Shapely index, also known as the importance index, provides insight into interpreting the fuzzy measures [20]. For any parameter  $\mathcal{R} \in \Gamma$ , the Shapely index of  $\mathcal{R}$  is defined as:

$$\eta_{\mathcal{R}} := \sum_{\mathcal{S} \subset \Gamma \setminus \mathcal{R}} \frac{(N - |\mathcal{S}| - 1)!|\mathcal{S}|!}{N!} [\mu(\mathcal{S} \cup \{\mathcal{R}\}) - \mu(\mathcal{S})] \quad (3.13)$$

where  $|.|$  denotes the cardinality of a set and  $\eta_{\mathcal{R}}$  is the Shapely index of parameter  $\mathcal{R}$ . The Shapely index is based on the interpretation that the weight of a parameter  $\mathcal{R} \in \Gamma$  should not only be defined by its individual fuzzy measure  $\mu(\{\mathcal{R}\})$  but by all  $\mu(\mathcal{S} \cup \{\mathcal{R}\})$  such that  $\mathcal{S} \subset \Gamma \setminus \mathcal{R}$ . The term  $\mu(\mathcal{S} \cup \{\mathcal{R}\}) - \mu(\mathcal{S})$  is defined as the marginal contribution of parameter  $\mathcal{R}$  in  $\mathcal{S}$ . In this work,  $\eta_{\mathcal{R}}$  is used as the initial weight of each  $\mathcal{R}$ .

### 3.4.3 Choquet Integral

If  $\mu$  denote the fuzzy measure on  $\Gamma$  then the discrete Choquet integral of a function  $f : \Gamma \rightarrow \mathbb{R}^+$  with respect to  $\mu$  is defined as [19]:

$$\mathcal{C}_\mu(f) := \sum_{i=1}^n (f(i) - f(i-1))\mu(\{\mathcal{R}_1, \mathcal{R}_2, \dots, \mathcal{R}_n\}) \quad (3.14)$$

where  $f(\cdot)$  are arranged in ascending order of its magnitude and is the  $CVaR_\alpha$  of the parameters calculated using (3.10),  $\mu(\mathcal{R}) = \eta_{\mathcal{R}}$  is obtained from (3.13), and  $f(0) = 0$ . Choquet integral gives the overall score of alternative decisions in problem involving multiple parameters for each decision.

## 3.5 Resilience Metric Evaluation Framework

In this section, we describe the simulation-based framework to quantify the resilience of power distribution systems. First, each resilience parameter is evaluated using a probabilistic method, and a corresponding risk-based metric is defined. Next, these parameters are combined with Choquet integral that evaluates a single value based on multiple different parameters and their associated importance in the decision-making process. Fig. 3.2 shows the overall framework to quantify the system resilience using a stochastic simulation-based approach and is described in detail below. It is to be noted that the smart network contains DG-based restoration and RCS that can improve the damage assessment and restoration phase to enhance the overall resilience of the system.

### 3.5.1 Evaluating Resilience-driven Parameters

The extreme wind event and its impact is characterized using its probability distribution and line fragility model as described in Section 6.2. Since the process of identifying an event and its impact is purely stochastic, Monte-Carlo simulations are conducted to evaluate the probabilistic impacts of the event on the power distribution grid. The approach is generic as each event is simulated for several trials. The fragility models provide the failure probability of any distribution lines. With the increase in wind intensity, the failure probability increases accordingly. Monte-Carlo simulations help us identify the number of lines being failed in each trial, and resilience-driven parameters are evaluated using (3.2) – (3.7). For smart network, the optimization framework using DGs are modeled and simulated as described in [8]. In the optimization model, all the CLs are equally important and a weight factor of 10 is used for CLs and 1 for non-CLs. At the end of each simulation, the average of evaluated parameters for all trials is then mapped with the respective intensity of the events to form a distribution of each parameter corresponding to its intensity.

### 3.5.2 Risk-driven Resilience Quantification

The probability distribution of each of the parameters corresponds to the distribution of the intensity of the event. Thus,  $CVaR_\alpha$  of each of the parameters can be calculated using (3.10). It is to be noted that the value of  $\alpha$  is consistent for each of the parameters. To combine  $CVaR_\alpha$  in the decision-making process, the priorities of each of the parameters are obtained from the system operators and Shapely values of those priorities are evaluated using (3.13). Finally, based on the  $CVaR_\alpha$  of each of the parameters and their Shapely values, Choquet Integral gives an overall score

using (3.14). To identify the interaction of each of the parameters,  $\lambda$  is also considered in the overall calculation process. The overall score obtained from Choquet Integral is the resilience metric for the distribution system. The described process is holistic as it considers all of the resilience-driven parameters (both attribute-based and performance-based) with their priorities in a system along with the associated risk.

### 3.6 Results and Analysis

The proposed method of resilience metric quantification using  $CVaR_\alpha$  of multiple parameters and Choquet Integral is demonstrated on IEEE 123-bus test system, Fig. 4.7. The simulation is carried out for extreme wind-related events. It was experimentally verified that 1000 trials are enough to achieve convergence of MCS for any wind speed scenarios.

#### 3.6.1 Calculating CVaR of Parameters

The five parameters defined in Section 3.3 are calculated based on Fig. 3.1 and using the simulation method described in Section 3.5. Fig. 3.4 shows the PDF of  $\mathcal{R}_\psi$  obtained for each wind speed along with  $VaR_\alpha$  and  $CVaR_\alpha$  values. For all of the cases, the value of  $\alpha$  is set to be 0.95. The  $VaR_\alpha$  and the  $CVaR_\alpha$  are calculated using (3.9) and (3.10). The risk metrics for other parameters are calculated in a similar fashion and are shown in Table 3.1. Each of the parameters are normalized using min-max normalization technique for generality.

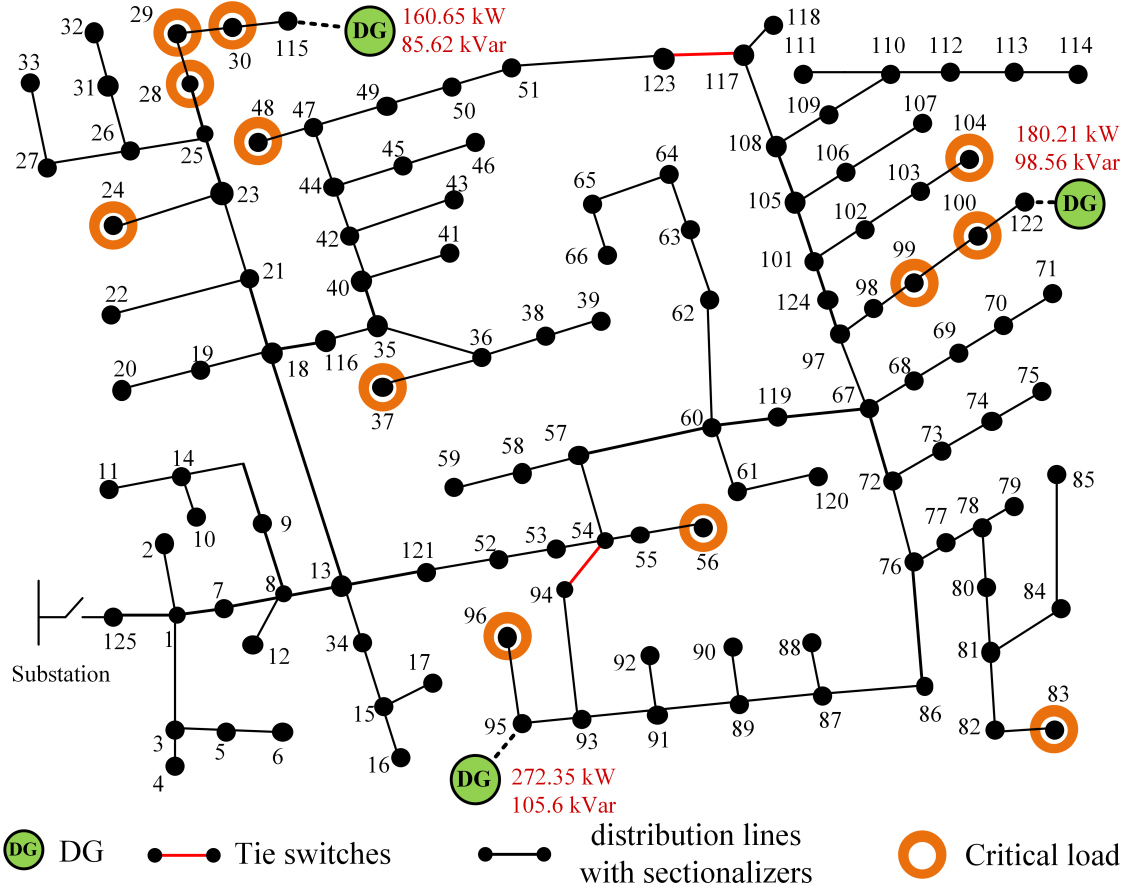


**Figure 3.3** Modified IEEE-123 test case with DGs, tie switches, and CLs.

**Table 3.1**  $CVaR_{\alpha}$  of normalized resilience-based parameters for base and smart network

Cases	$\mathcal{R}_{\psi}$	$\mathcal{R}_{\beta}$	$\mathcal{R}_{\gamma}$	$\mathcal{R}_{\xi}$	$\mathcal{R}_{\delta}$
Base	0.01115	0.00012	0.01656	0.0037	0.00005
Smart	0.01932	0.00012	0.01656	0.0039	0.00314

### 3.6.2 Quantifying Resilience using Choquet Integral

To compute the resilience metric based on the multiple parameters and their respective importance, five different cases are developed. For each of the cases,  $\mu(\cdot)$  is

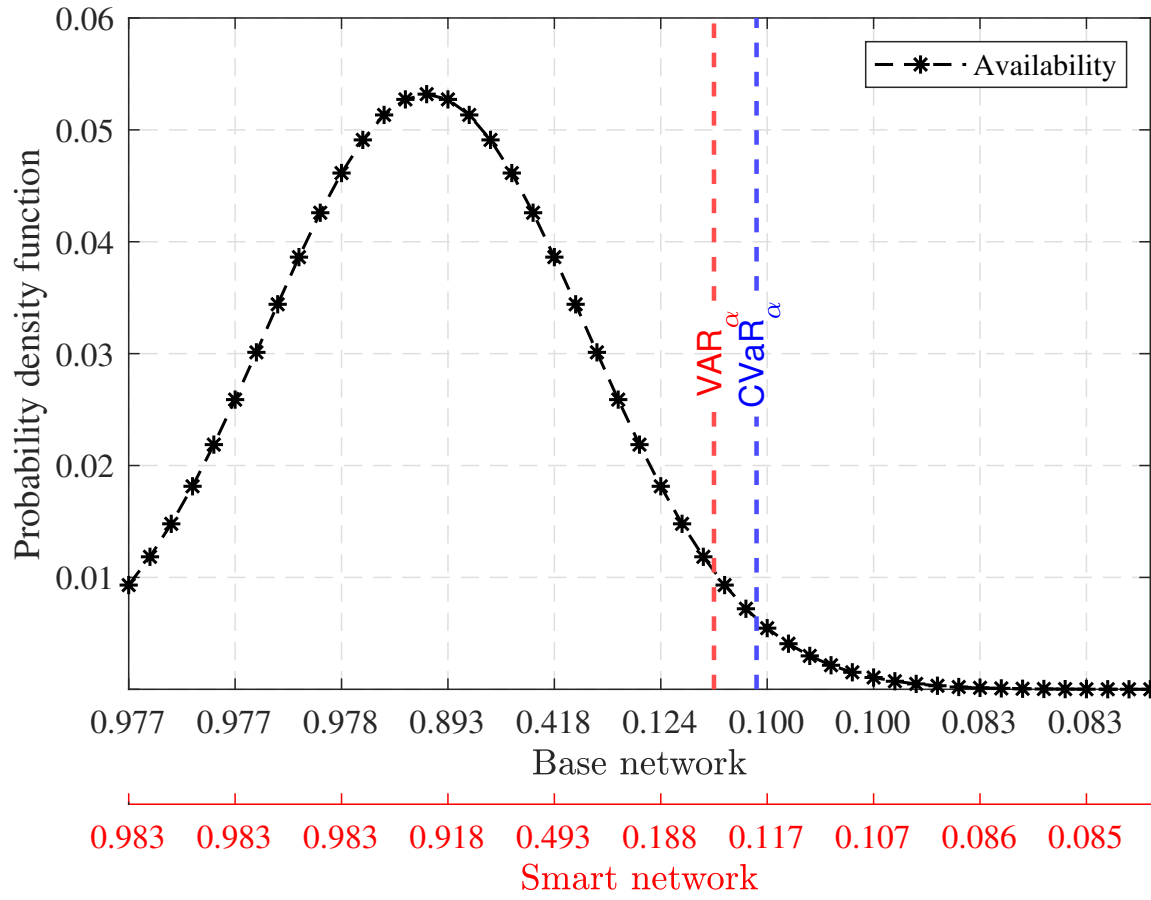


**Figure 3.4** PDF of availability for base and smart network.

assigned for each parameter as shown in Table 3.2. These are the initial fuzzy weights given by the experts or system operators that indicate the priority of one parameter over others.

Table 3.3 shows the Shapely value of each of the parameter calculated using (3.13) from their initial fuzzy weights. These values also indicate the marginal contribution of each of the parameters in the respective cases. For instance, in Case I the importance of  $\mathcal{R}_\psi$  and  $\mathcal{R}_\delta$  are greater than the importance of other parameters. Hence, these two parameters contribute more towards resilience quantification than the others. For different cases, the marginal contribution of each of the parameters differ

**Table 3.2** Initial fuzzy weights of parameters for resilience metric calculation

Cases	$\mu(\mathcal{R}_\psi)$	$\mu(\mathcal{R}_\beta)$	$\mu(\mathcal{R}_\gamma)$	$\mu(\mathcal{R}_\xi)$	$\mu(\mathcal{R}_\delta)$
I	0.9	0.25	0.15	0.6	0.85
II	0.6	0.5	0.45	0.5	0.6
III	0.3	0.8	0.85	0.6	0.2
IV	0.9	0.6	0.6	0.6	0.2
V	0.2	0.6	0.6	0.6	0.9

**Table 3.3** Shapely values of each parameters based of their initial weights.

Cases	$\eta_{\mathcal{R}_\psi}$	$\eta_{\mathcal{R}_\beta}$	$\eta_{\mathcal{R}_\gamma}$	$\eta_{\mathcal{R}_\xi}$	$\eta_{\mathcal{R}_\delta}$
I	0.35235	0.07617	0.04451	0.20400	0.32294
II	0.23225	0.18573	0.16404	0.18573	0.23225
III	0.09441	0.30385	0.33202	0.20849	0.06121
IV	0.34422	0.19903	0.19903	0.19903	0.05869
V	0.05869	0.19903	0.19903	0.19903	0.34422

according to the priority set by the system operator or expert.

The Choquet Integral values for the base and the smart network and each of the cases are shown in Table 3.4. It can be seen that the resilience of the smart network is always greater than that of the base network regardless of individual test cases due to the presence of DGs. However, the resilience for individual networks varies with the Shapely values of each of the parameters. For instance, if we look at the smart network, Case IV is more resilient than any of the other cases as higher priority is given to load availability and infrastructural investments (i.e.,  $\mathcal{R}_\beta$ ,  $\mathcal{R}_\gamma$ , and  $\mathcal{R}_\xi$ ).

**Table 3.4** Choquet Integral values based on Shapely values of each parameters

Network	Case I	Case II	Case III	Case IV	Case V
Base	5.45	6.03	7.36	<b>7.89</b>	4.72
Smart	9.36	8.68	8.36	<b>10.93</b>	6.31

However, this is not true for the base network as loads are not picked up during the restoration phase in the base network making its availability lower than the smart network. It is also interesting to notice that, the resilience for Case I and Case IV does not have a huge difference although for Case I, the priority towards infrastructural investment is less. Hence, the operators can have the flexibility to focus more on less expensive decisions and still enhance the system's resilience.

### 3.7 Summary

In this chapter, we proposed a risk-based resilience metric which incorporates multiple parameters of the distribution grid that can alter the resilience of the grid. A stochastic simulation-based approach is presented to quantify the resilience of the distribution grid. Since resilient systems should be able to withstand extreme events that have a minimum probability of occurrence, the  $CVaR_\alpha$  of the grid parameters for extreme event cases are used to calculate the resilience metric. The simulation results showed that prioritizing one parameter over the others can either enhance or degrade the system's resilience depending upon how the investment decisions are prioritized. Additionally, it was concluded that the framework provides added flexibility to choose economically feasible investments without compromising the resilience of the system.

## REFERENCES

- [1] J. Furman, “Economic benefits of increasing electric grid resilience to weather outages,” *Washington, DC: Executive Office of the President*, 2013.
- [2] J.-P. Watson *et al.*, “Conceptual framework for developing resilience metrics for the electricity oil and gas sectors in the united states,” *Sandia National Laboratories, Albuquerque, NM (United States), Tech. Rep*, 2014.
- [3] G. Kandaperumal and A. K. Srivastava, “Resilience of the electric distribution systems: concepts, classification, assessment, challenges, and research needs,” *IET Smart Grid*, vol. 3, no. 2, pp. 133–143, 2020.
- [4] B. Cai, M. Xie, Y. Liu, Y. Liu, and Q. Feng, “Availability-based engineering resilience metric and its corresponding evaluation methodology,” *Reliability Engineering & System Safety*, vol. 172, pp. 216–224, 2018.
- [5] M. Panteli, D. N. Trakas, P. Mancarella, and N. D. Hatziargyriou, “Power systems resilience assessment: Hardening and smart operational enhancement strategies,” *Proceedings of the IEEE*, vol. 105, no. 7, pp. 1202–1213, 2017.
- [6] M. Wen, Y. Chen, Y. Yang, R. Kang, and Y. Zhang, “Resilience-based component importance measures,” *International Journal of Robust and Nonlinear Control*, vol. 30, no. 11, pp. 4244–4254, 2020.
- [7] S. Espinoza, A. Poulos, and *et al.*, “Seismic resilience assessment and adaptation of the northern chilean power system,” in *2017 IEEE Power & Energy Society General Meeting*, pp. 1–5, IEEE, 2017.

- [8] S. Poudel and A. Dubey, “Critical load restoration using distributed energy resources for resilient power distribution system,” *IEEE Transactions on Power Systems*, vol. 34, no. 1, pp. 52–63, 2018.
- [9] A. Umunnakwe, H. Huang, K. Oikonomou, and K. Davis, “Quantitative analysis of power systems resilience: Standardization, categorizations, and challenges,” *Renewable and Sustainable Energy Reviews*, vol. 149, p. 111252, 2021.
- [10] P. Bajpai, S. Chanda, and A. K. Srivastava, “A novel metric to quantify and enable resilient distribution system using graph theory and choquet integral,” *IEEE Transactions on Smart Grid*, vol. 9, no. 4, pp. 2918–2929, 2018.
- [11] S. Chanda and A. K. Srivastava, “Defining and enabling resiliency of electric distribution systems with multiple microgrids,” *IEEE Transactions on Smart Grid*, vol. 7, no. 6, pp. 2859–2868, 2016.
- [12] H. Gao, Y. Chen, Y. Xu, and C.-C. Liu, “Resilience-oriented critical load restoration using microgrids in distribution systems,” *IEEE Transactions on Smart Grid*, vol. 7, no. 6, pp. 2837–2848, 2016.
- [13] V. Venkataramanan, A. Hahn, and A. Srivastava, “Cp-sam: Cyber-physical security assessment metric for monitoring microgrid resiliency,” *IEEE Transactions on Smart Grid*, vol. 11, no. 2, pp. 1055–1065, 2020.
- [14] M. Panteli and P. Mancarella, “The grid: Stronger, bigger, smarter?: Presenting a conceptual framework of power system resilience,” *IEEE Power and Energy Magazine*, vol. 13, no. 3, pp. 58–66, 2015.

- [15] S. Poudel, A. Dubey, and A. Bose, “Risk-based probabilistic quantification of power distribution system operational resilience,” *IEEE Systems Journal*, vol. 14, no. 3, pp. 3506–3517, 2019.
- [16] A. Poudyal, V. Iyengar, D. Garcia-Camargo, and A. Dubey, “Spatiotemporal Impact Assessment of Hurricanes on Electric Power Systems,” in *2022 IEEE Power Energy Society General Meeting*, 2022 (to appear).
- [17] M. Panteli, C. Pickering, S. Wilkinson, R. Dawson, and P. Mancarella, “Power system resilience to extreme weather: Fragility modeling, probabilistic impact assessment, and adaptation measures,” *IEEE Transactions on Power Systems*, vol. 32, no. 5, pp. 3747–3757, 2017.
- [18] A. Kwasinski, “Quantitative model and metrics of electrical grids’ resilience evaluated at a power distribution level,” *Energies*, vol. 9, p. 93, Feb. 2016.
- [19] Choquet, G., “Theory of Capacities,” *Annales de l’Institut Fourier*, pp. 131–195, 1953.
- [20] M. Grabisch and C. Labreuche, “A decade of application of the choquet and sugeno integrals in multi-criteria decision aid,” *Annals of Operations Research*, vol. 175, no. 1, pp. 247–286, 2010.

## CHAPTER 4

# RISK-BASED ACTIVE DISTRIBUTION SYSTEMS PLANNING FOR RESILIENCE AGAINST EXTREME WEATHER EVENTS

### 4.1 Introduction

This chapter introduces a risk-based active distribution system planning for resilience against extreme weather events. A two-stage risk-averse framework is proposed, and conditional value-at-risk (CVaR) is used as a risk metric. The framework minimizes the weighted sum of the expected load shed and CVaR of the load shed where the investment decisions are DG siting and sizing. The DGs have grid-forming capabilities and can operate in islanded mode.

#### 4.1.1 Motivation

Extreme weather events result in an extended disruption of the electric power supply and severely affect personal safety and national security, thus posing serious concerns for the nation's electric power grid infrastructures. Towards this goal, different utilities have spent millions of dollars deploying smart grid technologies such as distribution automation with automated feeder switching, intentional islanding (microgrid), and upgrading vulnerable feeders and substations [1]. With the increasing frequency and severity of weather-related events, a more systematic approach to smart grid expenditures is required to identify appropriate system upgrade solutions for strengthening system resilience. Upgrading the distribution system infrastructure by system hardening and investing in smart grid technologies effectively enhances grid resilience. Existing distribution system planning methods primarily consider the persistent cost

of the expected events (such as faults and outages likely to occur) and aim at improving system reliability. The resilience to extreme weather events requires reducing the impacts of the high impact low probability (HILP) events characterized by the tail probability of the event impact distribution. Thus, resilience-oriented system upgrade solutions must be driven by the risks imposed by extreme weather events on the power grid infrastructure rather than persistent costs.

#### 4.1.2 Related Literature and Gaps

Strategies for enhancing the resilience of power distribution systems can be classified into short-term (operational) planning and long-term (infrastructure) planning phases. The operational planning aims at making the best use of the existing distribution grid resources (e.g., switches, DGs) to minimize the impacts of an anticipated event in the near term [2]. On the contrary, the infrastructure planning phase targets to optimally upgrade the power systems infrastructure by strategically deploying new resources (e.g., DGs, switches, distribution lines) to improve the system response against possible HILP events [3].

The existing literature on power distribution resilience includes numerous articles on operational planning to mitigate or reduce the impact of an imminent threat such as an upcoming storm [4]. Such solutions build resilience via operational response rather than infrastructural upgrades. In operational planning, decisions are to be made for an upcoming event that is known with a high level of certainty, and thus, a limited number of scenarios are required for decision-making. On the contrary, long-term planning requires a probabilistic analysis over a wider range of scenarios with a higher level of uncertainty for decisions related to system hardening, infrastructure

upgrades, resource allocation, and sizing [5]. These decisions must also connect to the operational problem if and when the events are realized in practice. Thus, the problem is further complicated by additional stages of operational decision-making, leading to an explosion of state space that needs to be considered for decision-making.

In general, hardening the distribution grid and investing in smart grid technologies are effective resilience-oriented designs that need to be adopted in the utilities' portfolio for long-term infrastructure planning to improve the grid's response to extreme weather events. However, infrastructure planning for resilience is challenging mainly as it requires a) to include several different uncertainties (e.g., fault location, load profiles, nature and severity of extreme events, and so forth) in the decision-making process, b) ensure the validity of the planning decisions for the entire profile of weather events, and c) mitigate the critical challenge of achieving a balance between computational cost and accuracy. Thus, long-term infrastructure planning for resilience is conceptually a different problem than the prevalent methods for operational planning solutions [6]. This calls for new methods and contributions to systematically build resilience in active power distribution grid infrastructures against the HILP events [7].

The related literature on resilience-oriented design and pre-disaster resource allocation usually employ a stochastic programming model to minimize the expected cost of the future operational scenarios [8, 9]. For example, in [8], a heuristic search is employed to identify the optimal restoration path and obtain a resource allocation plan. These solutions, however, consider short-term operational requirements for a known HILP event and are not suitable for infrastructure planning. The related work on resilience-oriented distribution system long-term planning also employs stochastic optimization formulations, including a tri-level robust optimization model [10, 12],

**Table 4.1** Summary of existing literature for resilience-oriented planning of power distribution systems

Planning decision	References	Objective	Formulation	Approach
Resource location	[8]	$\text{Max.} (\text{Expected benefit - cost})$	Stochastic NLP	Heuristic search
	[9]	$\text{Min. Cost (operation, action)}$	Two-stage stochastic MILP	Progressive hedging
Line hardening & DG siting	[10]	$\text{Min. Load shedding cost and planning cost}$	Tri-level robust optimization	CCG decomposition
	[11]	$\text{Min. (planning and expected operating cost)}$	Two-stage stochastic	Progressive hedging
	[12]	$\text{Min. Cost (Planning + load shedding)}$	Tri-level robust optimization	Greedy search
	[13]	$\text{Min. Load shedding cost and planning cost}$	Two-stage stochastic	Dual decomposition
Remote controlled switch siting	[14]	$\text{Min. Number of RCS}$	Weighted set cover (WSC)	Greedy algorithm
	[15]	$\text{Min. (Expected loss)}$	Two-stage stochastic	Scenario decomposition
DG siting & sizing	[16]	$\text{Min. (planning and expected operating cost)}$	Two-stage stochastic	Progressive hedging

and a two-stage stochastic optimization model [11, 13, 15]. The tri-level optimization model formulates the resulting problem in a defender-attacker-defender model that is then converted into an equivalent bi-level model and solved using iterative approaches such as CCG or greedy search algorithms [10]. The tri-level approach optimizes for the worst possible outcomes and hence is not suitable for a probabilistic analysis for infrastructure planning that needs to be cost-effective and optimal for a large range of future scenarios. Alternatively, the two-stage stochastic programming method considers the overall impact of stochastic fault scenarios in planning decisions rather than just the worst-case scenarios [11, 16]. The existing two-stage stochastic optimization formulations used in resilience-oriented distribution grid design either assume that all scenarios are observed with equal probability or perform the planning based on only a targeted set of scenarios [17, 18, 19]. While such methods are generally applicable, other approaches such as importance sampling and stratified sampling techniques can be more effective in representing HILP events and their impact probabilities in the optimization process [20, 21]. These techniques are widely adopted in power systems reliability studies [22, 23]. Another approach includes network interdiction models that plan for the worst-case scenarios [5]. However, given the emphasis on the worst-case scenario, these methods may lead to extremely conservative and expensive planning solutions as the worst-case scenario usually occurs with a very small probability. Additionally, related literature obtains planning solutions for persistent costs; they do not explicitly include the risks of extreme events. For a resilience-oriented long-term planning problem, the goal is to determine optimal investments to reduce the consequences (here, customer outages) of the HILP events. Mathematically, this amounts to minimizing the mean of consequences and, more importantly, reducing

the tail of the consequence of the HILP events [1]. Table 4.1 summarizes the existing work in this domain and highlights the problem formulation and solution approaches.

#### 4.1.3 Contribution

To appropriately incorporate the effects of HILP events, the infrastructure planning for resilience needs to be driven by risk rather than pertinent or expected cost [24]. This chapter proposes a risk-based approach for infrastructure planning in active power distribution systems for resilience against extreme weather events. We employ conditional value-at-risk,  $\text{CVaR}_\alpha$ , to quantify the risks of system outages imposed by the HILP events [25, 26]. Related works include using CVaR-metric for robust power grid operations [27, 28, 29]. Here, we employ CVaR-metric for long-term distribution planning, where the goal is to reduce the risks of outages on power distribution systems due to HILP events. A two-stage stochastic optimization framework is proposed to optimize smart grid investments, specifically DG siting and sizing, to enable advanced systems such as DG-assisted restoration and intentional islanding. The proposed model also helps evaluate the trade-off between risk-averse and risk-neutral planning decisions. Note that although in [30], CVaR optimization is used for resilience enhancement, their focus is on reducing the variance of the optimization solution and not on reducing the outage risks of HILP events. The major contributions of this chapter are as follows :

- *Risk-averse Two-stage Stochastic Programming for distribution grid resilience:* Existing literature on resilience-driven planning includes risk-neutral formulations assuming equal probability events. We introduce a risk-based planning approach that appropriately samples the event probabilities and their impacts on the power grid

components and system. The two-stage stochastic programming problem is formulated as a MILP problem where Stage-1 decisions are the infrastructure planning decisions optimized to reduce the risks of outages due to HILP events, assuming optional operational phase decisions. The Stage 2 problem models the operational phase and solves the optimal system response (restoration strategy) for the specified resource allocation (from Stage 1) and a given event realization.

- *Probabilistic scenario generation and smart scenario reduction strategy:* We propose a scenario generation approach using Monte-Carlo simulations that appropriately models a given regional wind profile and its impacts on the distribution system. Next, for scenario reduction, we propose a smart scenario selection strategy based on the average loss of load representing several Monte-Carlo trials. We also extensively validate the robustness of the proposed scenario generation and reduction approach using multiple out-of-sample scenario sets for different simulation case studies.
- *Trade-off analysis on risk minimization vs. expected loss minimization:* Different case studies are presented to identify the trade-off of adopting risk-neutral vs. risk-averse policies in the planning decisions. The analysis can provide insights into adopting risk-driven solutions when the utmost priority is to maintain an uninterrupted power supply to critical customers during extreme weather events. The results suggest that risk-averse planning tends to incur higher costs to meet the resilience objectives during HILP events; however, they are more likely to restore the critical loads during the HILP events. On the other hand, while more cost-efficient, risk-neutral planning decisions end up restoring fewer critical loads during HILP events.

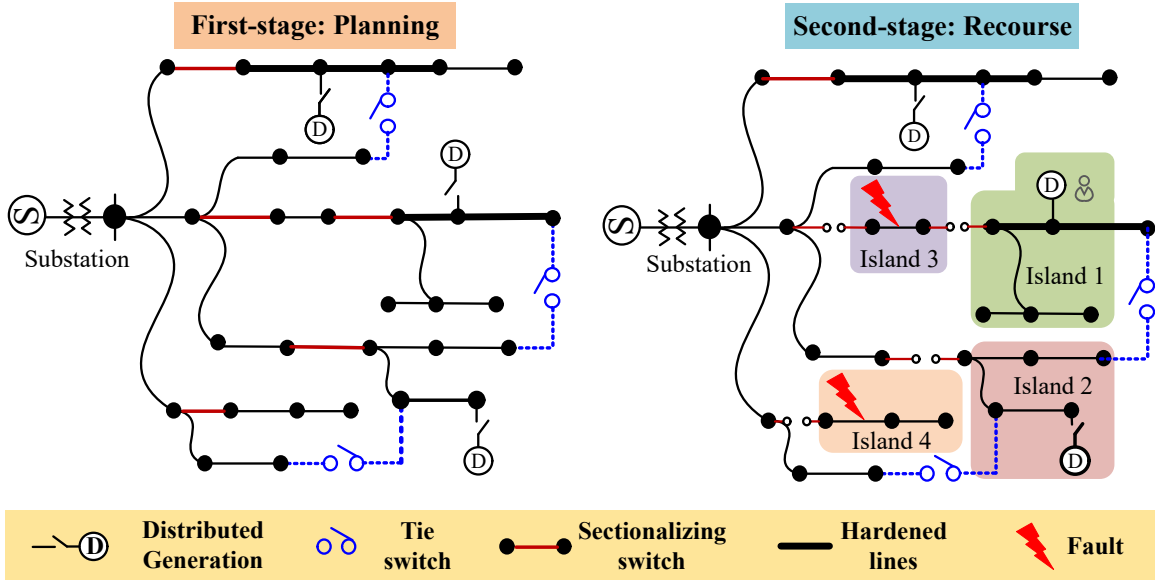


**Figure 4.1** Two-stage planning framework example for a specific scenario.

## 4.2 Mathematical Background

### 4.2.1 Long-Term Planning Model Representation

A power distribution network can be graphically represented as  $G(V, E)$ , where the vertices  $V$  represent the buses or nodes while the distribution lines are represented by the edges  $E$ . Fig. 4.1 shows a general representation of the two-stage planning framework. The overall objective of the two-stage framework is to identify the first-stage optimal planning decisions that minimize the expected operational cost in the second stage. In this work, DG siting and sizing are the planning decisions, whereas the second stage objective is to minimize the prioritized load loss once a scenario is realized. DGs with grid-forming inverters are assumed in this work. Such grid-forming DGs can be used for intentional islanding when some area of the distribution grid gets disconnected from the system due to an extreme event.

It is important to understand that the two stages are not decoupled but rather solved as a single optimization problem. The second stage problem minimizes the operational cost for each scenario and hence its objective function. Note that the two-stage objective function is a random variable. Thus, determining the optimal planning decision is the problem of comparing random cost variables as a function of the planning cost and the operational cost. Furthermore, it is assumed that the uncertain scenario realizations in the second stage have some form of a probability distribution. Here, we use regional wind profiles to demonstrate uncertain fault scenarios. The overall framework should provide planning decisions that remain optimal for every realization of scenarios in the second stage. In Fig. 4.1 it can be seen that once faults occur in the system, the tie switches, and sectionalizing switches are toggled to isolate the faulted sections i.e., Island 3 and Island 4. Furthermore, DGs form two islands i.e., Island 1 and Island 2, and continuously supply the loads inside the island. The connection of DGs is represented by a virtual switch as discussed in [31].

The two-stage problem is formulated as a risk-averse stochastic optimization problem in which the first stage problem minimizes the cost of planning and the weighted combination of the expected value and the *CVaR* of the second stage problem. The second stage problem is the operational stage that minimizes the total prioritized loss of load for every scenario realization.

#### 4.2.2 Two-stage Stochastic Optimization

A general two-stage stochastic integer programming model can be formulated as [32]:

$$f(x) := \min_x c^T x + \mathbb{E}_P[Q(x, \mathcal{E})] \quad (4.1)$$

subject to,

$$Ax = b, \quad x \in \mathbb{R}_{m1}^+ \times \mathbb{Z}_{n1}^+$$

where

$$Q(x, \mathcal{E}) := \min_y q^T y \quad (4.2)$$

subject to,

$$Wy = h - Tx \quad y \in \mathbb{R}_{m2}^+ \times \mathbb{Z}_{n2}^+$$

where  $x$  is the first stage decision variable and  $y$  is the second stage decision variable,  $\mathcal{E}$  refers to the set of uncertain data (or scenarios) with a known probability distribution  $P$ , and  $(q, h, T, W)$  are scenario-dependent variables which vary for each  $\xi \in \mathcal{E}$ . The objective in a general two-stage stochastic optimization is to solve (4.1) which seeks a first-stage decision  $x$  that minimizes the first stage cost and the expected cost of the second stage,  $Q(x, \mathcal{E})$ . The second stage decisions are also known as the recourse decisions and are scenario-dependent. The algorithms and model formulation in two-stage stochastic optimization depends on the stage variable types.

#### 4.2.3 Optimization of Conditional Value-at-Risk

The general stochastic optimization model considers only the expected cost of the second stage as shown in (4.1) and does not directly incorporate the tail of the probability distribution. Unlike routine outages caused by known and credible threats, adequately anticipating and predicting system performance during HILP events is inherently difficult as they are rare [33]. While resilience metrics similar to reliability measures such as expected energy not served (EENS), loss of load expectation (LOLE), and service availability [34, 35, 36] have been investigated, these measures mostly provide a reliability-oriented view and do not explicitly quantify expected

system performance under unseen HILP events. Thus, it is desired to include tail probability events when planning for resilience to reduce the impacts of HILP events on system outages. There are several metrics used to quantify the tail probabilities or risks; VaR and CVaR are commonly used risk metrics in the domain of financial risk management. Fig. 4.2 shows a discrete distribution of a loss function  $L(X)$  along with its VaR and CVaR. VaR is the  $\alpha$ -quantile of the distribution function whereas CVaR is the expected value of the remaining  $1 - \alpha$  region that represents the HILP events. Interestingly, CVaR can be formulated as an optimization problem if the random variable under consideration is discrete [37]. The CVaR optimization problem is shown in (3).

$$CVaR_\alpha(X) = \min \left\{ \eta + \frac{1}{1-\alpha} \mathbb{E}([(X - \eta)]_+ : \eta \in \mathbb{R}) \right\} \quad (4.3)$$

where,  $X$  is a random variable with  $N$  discrete scenarios  $x_1, x_2, \dots, x_n$  each having a probability of  $p_1, p_2, \dots, p_n$  respectively,  $\alpha \in [0, 1)$  is the confidence level which gives the VaR of  $X$  ( $VaR_\alpha$ ), and  $\eta$  be the  $VaR_\alpha$  of  $X$ . Here,  $\eta$  is independent of probability and is the same for each realization of  $X$ . Here,  $[(X - \eta)]_+ = \max\{X - \eta, 0\}$  which represents the point-wise maximum of convex functions and hence, (4.3) can be reformulated using its epigraph form as:

$$CVaR_\alpha(X) = \min \left\{ \eta + \frac{1}{1-\alpha} \sum_{\xi \in \mathcal{E}} p_\xi \nu_\xi \right\} \quad (4.4)$$

subject to,

$$\nu_\xi \geq x_\xi - \eta \quad \eta \in \mathbb{R}, \nu \in \mathbb{R}_+^n \quad (4.5)$$

where,  $p_\xi$  is the discrete probability of each scenario  $\xi$ , and  $\nu_\xi$  is an excess variable which ensures that  $CVaR_\alpha$  is calculated only for realizations beyond  $VaR_\alpha$  for each

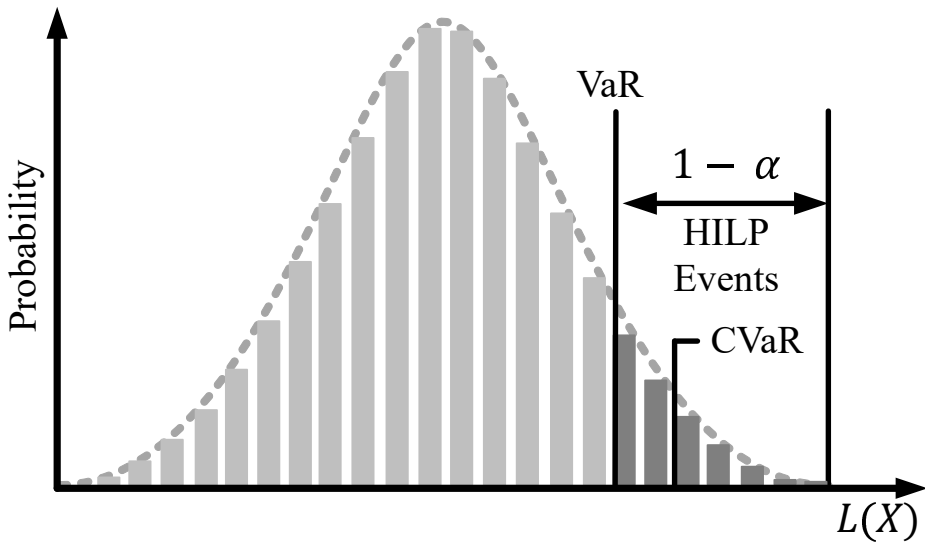


**Figure 4.2** VaR and CVaR representation for a discrete loss function. HILP events are the ones with  $(1 - \alpha)$  probability of occurrence.

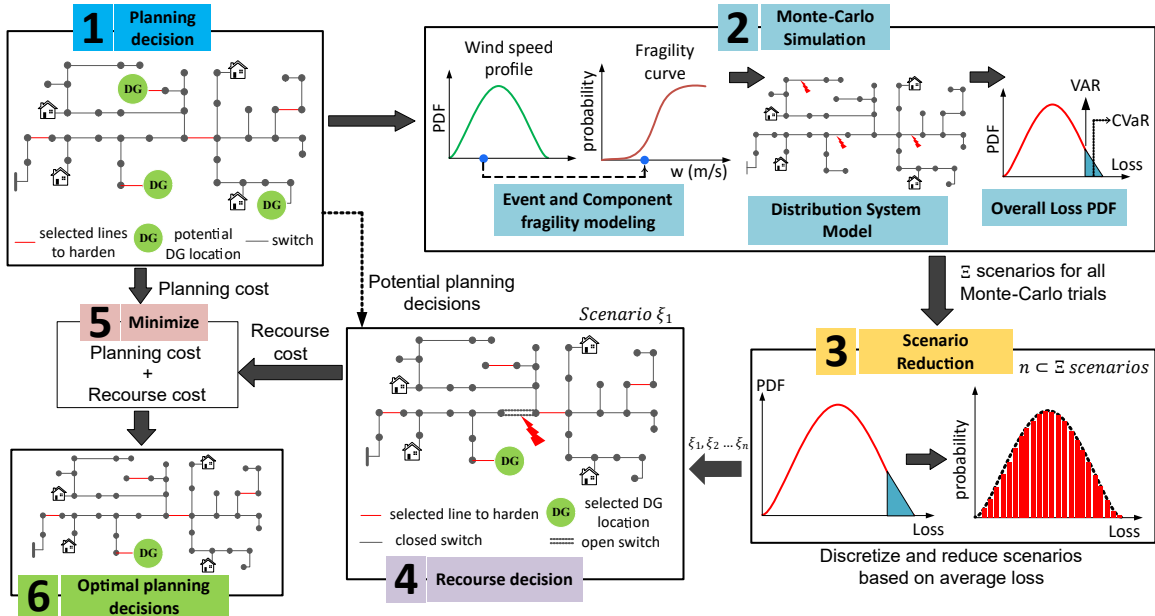


**Figure 4.3** Overall architecture of risk-averse two-stage planning problem.

scenario  $\xi$ . Here, (4.4) is linear and can be solved using existing linear programming techniques.

#### 4.2.4 Risk-based Stochastic Optimization

As discussed earlier, the general two-stage stochastic optimization framework neglects the tail events of the probability distribution that tend to have higher risks in terms of loss in the system.  $CVaR_\alpha$  is the coherent risk metric that can quantify the associated risks given the probability distribution of the losses associated with an event. In (4.4),  $CVaR_\alpha$  is formulated as an optimization problem and hence can be introduced in a general two-stage stochastic optimization framework given in (6)-(7) [38].

$$\min_x c^T x + (1 - \lambda)\mathbb{E}[Q(x, \mathcal{E})] + \lambda CVaR_\alpha(Q(x, \mathcal{E})) \quad (4.6)$$

where

$$\begin{aligned} \mathbb{E}(Q(x, \mathcal{E})) &= \sum_{\xi \in \mathcal{E}} p_\xi Q(x, \xi) \\ CVaR(Q(x, \mathcal{E})) &= \eta + \frac{1}{1 - \alpha} \sum_{\xi \in \mathcal{E}} p^\xi \nu^\xi \end{aligned} \quad (4.7)$$

where  $\lambda \in [0, 1]$  is the risk multiplier or factor that defines the trade-off between  $\mathbb{E}[\cdot]$  and  $CVaR_\alpha(\cdot)$ . By selecting different values of  $\lambda$ , the first stage decisions are termed as either risk-averse ( $\lambda = 1$ ), risk-seeking/mean-risk ( $\lambda = 0.5$ ), or risk-neutral ( $\lambda = 0$ ). The formulation in (4.6) not only minimizes the expected loss but also the  $CVaR_\alpha$  of those loss distributions depending on the value of  $\lambda$ . Hence, with this formulation, one can identify how planning decisions vary with the risk avoidance potential.

### 4.3 Risk-based Resilience-oriented Distribution System Planning

The overall architecture of the proposed method is shown in Fig. 4.3. Only wind-related events are used in this work and the probability distribution of extreme wind events is considered to generate the scenarios. Monte Carlo simulations (MCS) are

conducted to identify the impact of probabilistic events, and an appropriate scenario reduction method is implemented to identify representative scenarios. Finally, the long-term planning problem is solved in a two-stage stochastic optimization setting based on a selected number of scenarios. This section details the overall optimization process along with detailed problem formulations.

#### 4.3.1 Probabilistic scenario generation and reduction

An event is characterized by its intensity and probability of occurrence. Fig. 4.4 shows the event probability distribution for a windfall in three different regions observing extreme, high, and normal wind profiles. The extreme regional wind profile is used to model extreme events in this work. For simplicity, only distribution lines are assumed to be affected by wind in this work. Although wind-related events have spatiotemporal dynamics [39], we assume that for a distribution system, that covers a small region, the wind speed for the entire region is the same. MCS is performed for each wind speed case so as to also include the extreme tail probability events. This process is represented by block 2 in Fig. 4.3. For each wind speed scenario  $u$ , the component level failure probability  $p_f(u)$  determines the operational state of a particular component in the distribution grid. Component level fragility curves [40] or prototype curve fit models [41] can be used to model the impacts of extreme events such as hurricanes or other high-speed wind events on power systems. In this work, we have used the component fragility curve that maps the probability of failure of distribution system components conditioned on the intensity of the hazard (e.g., a wind speed). An example of the fragility curve is shown in Figs. 4.5a and 4.5b. The fragility curve values are randomly selected for simulation purposes; however, if available, empirical

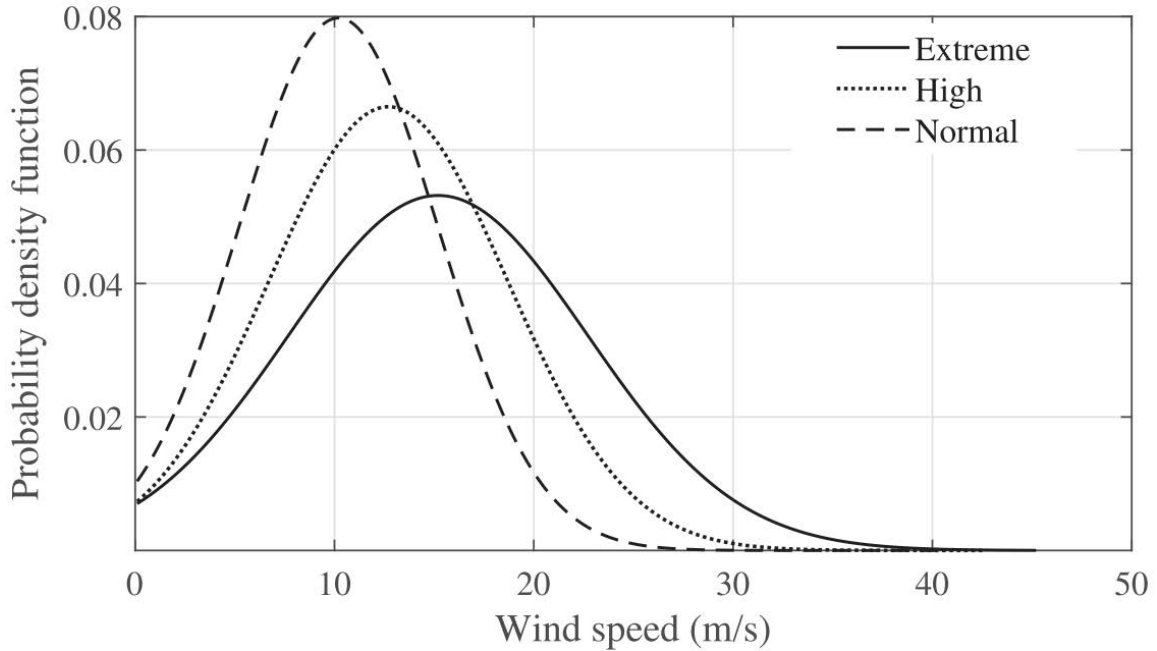


**Figure 4.4** Regional wind profile.

data can be used to adjust the parameters [42].

$$p_f(u) = \begin{cases} P_f^n, & \text{if } u < u_{critical} \\ P_f(u), & \text{if } u_{critical} < u < u_{collapse} \\ 1, & \text{if } u > u_{collapse} \end{cases}$$

where,  $P_f(u)$  is the failure probability of a component as a function of wind speed,  $u$ ;  $P_f^n$  is the failure rate at normal weather conditions;  $u_{critical}$  is the wind speed at which the failure probability rapidly increases. The equipment has a negligible probability of survival at  $u_{collapse}$ . In the problem formulation, the failures due to an extreme event are modeled as open or faulted line/switch variables as discussed later in this section. The location of these faults is determined based on the fragility curve for wind speed greater than  $u_{critical}$ .

Several MCS are conducted to obtain the system loss associated with the fail-

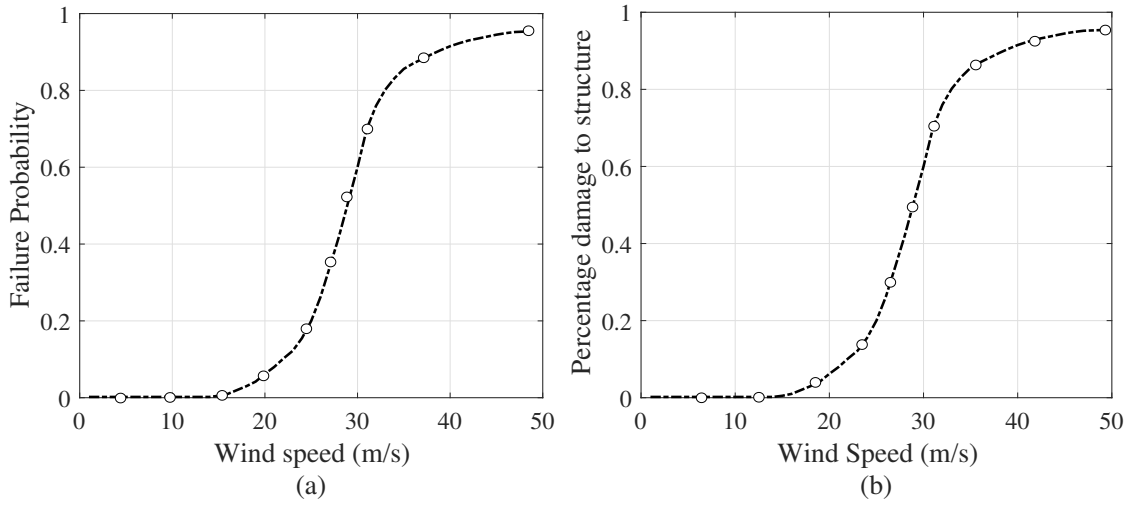


**Figure 4.5** a) Component and b) system-level fragility model for an extreme event

ure probability of a component in the distribution grid. In this work, the amount of active prioritized load ( $kW$ ) disconnected from the system following an event is considered the system loss for a particular wind speed scenario. The critical loads (CL) should always be prioritized in any restoration methods. Hence, higher weights are assigned to the CLs that reflect a higher value of prioritized load loss if any CLs are disconnected and not restored. The average prioritized load loss is then mapped onto the regional wind profile PDF to get a probabilistic representation of the loss in the system when subjected to a given weather event.

MCS provides an extremely large number of scenarios. One major challenge in any stochastic optimization setting is handling many scenarios within the optimization framework. Furthermore, the solution should be optimal for all scenarios that make the stochastic problem computationally intractable. Existing works use special sampling techniques such as stratified sampling [43] or importance sampling [44] to include the tail probability scenarios in the optimization model appropriately.

Distance-based scenario reduction methods have also been used where a probabilistic distance measure is minimized to obtain a reduced scenario distribution that closely represents the overall scenario distribution [45]. We introduce a new approach to scenario reduction inspired by stratified sampling and distance reduction methods. The proposed approach uses stratification to sample representative scenarios for each wind speed and generates a reduced scenario distribution that closely matches the original scenario distribution.

In this work, the overall number of scenarios is reduced by selecting a representative scenario for each wind speed based on the average Monte-Carlo loss. This process is represented by block 3 in Fig. 3. Let  $N_u$  be the total discrete wind speeds under consideration,  $N_{\xi,u}$  be the number of scenarios obtained from MCS for each wind speed  $u$ , and  $L_{avg}^u = \mathbb{E}(L_{\xi,u})$  be the average prioritized load loss in  $kW$  corresponding to  $N_{\xi,u}$  scenarios. Let  $\Xi = N_{\xi,u} \times N_u$  be the total number of scenarios for the entire MCS. Note that we cannot randomly select a subset of these scenarios as it significantly degrades the accuracy of the optimization solutions. Here, we use a unique sampling technique to drastically reduce the number of scenarios while maintaining the representation of the overall scenarios described next. If  $\xi_u$  is a representative scenario for all  $N_{\xi,u}$  scenarios corresponding to  $u$ , then  $\xi_u$  is selected such that the prioritized load loss in the system due to  $\xi_u$  ( $L_{\xi_u}^u$ ) is the one nearest to  $L_{avg}^u$ . In the case of multiple scenarios with losses nearing  $L_{avg}^u$ , one of the scenarios is randomly selected as  $\xi_u$  from the identical scenario representations. The proposed scenario reduction technique reduces the total number of scenarios to  $N_u$  from  $\Xi$  such that  $p_\xi$  corresponds to the wind speed profile. Fig. 4.6 shows a set of  $N_u = 49$  representative scenarios obtained from the overall Monte-Carlo scenarios based on the abovementioned methods.

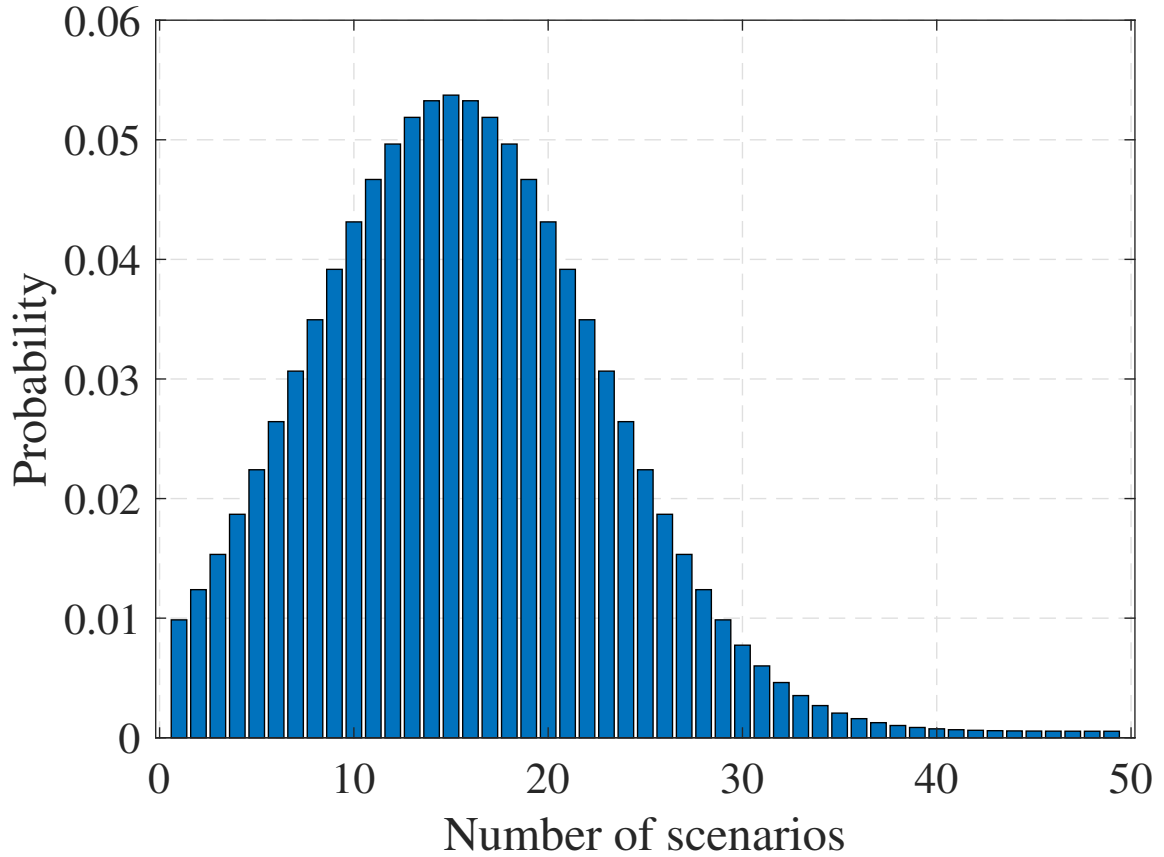


**Figure 4.6** A set of 49 representative scenarios with respective probabilities.

This smart scenario selection strategy ensures the practical realization of the second stage problem while incorporating HILP events within the scenarios. This work does not apply the restoration schemes in the scenario generation and reduction phase. Hence, the obtained scenarios are base case scenarios that only give information on the amount of prioritized load loss in the network based on each of wind scenario.

#### 4.3.2 Two-Stage Stochastic Optimization Problem Formulation

We detail the two-stage stochastic optimization problem for resilient distribution system planning.

## Objective Function

In this paper, the resilience-driven distribution system planning problem is formulated as a two-stage stochastic optimization problem where the overall objective function can be defined as:

$$\min(1 - \lambda)\mathbb{E}(Q(\delta, \mathcal{E})) + \lambda CVaR_\alpha(Q(\delta, \mathcal{E})) \quad (4.8)$$

where,

$$\begin{aligned} \mathbb{E}(Q(\delta, \mathcal{E})) &:= \left( \sum_{\xi \in \mathcal{E}} \sum_{i \in \mathcal{B}_S} \sum_{\phi \in \{a, b, c\}} (1 - s_i^\xi) w_i P_{Li}^{\phi, \xi} \right) \\ CVaR_\alpha(Q(\delta, \mathcal{E})) &:= \left( \eta + \frac{1}{1 - \alpha} \sum_{\xi \in \mathcal{E}} p^\xi \nu^\xi \right) \end{aligned}$$

The problem objective in the first stage is to minimize the weighted sum of expected value and  $CVaR_\alpha$  of the second stage cost, represented by  $Q(\delta, \mathcal{E})$ . To analyze the trade-offs, this formulation has not used minimization of planning cost. Instead, we use a budget constraint and observe the associated trade-offs for risk-averse and risk-neutral decisions when system planners have a limited investment budget. The objective of the second stage of the problem,  $Q(\delta, \mathcal{E})$ , is to minimize the prioritized load loss or maximize the restoration of prioritized loads for each  $\xi \in \mathcal{E}$ . The second stage costs correspond to the optimal restoration decisions once a scenario has been realized. Hence, each variable corresponding to the second stage of the problem is scenario-dependent. Here, DG location ( $\delta_i^{DG}$ ) and size of the DG ( $\beta_i^{DG}$ ) are the first stage decision variables.  $P_{Li}^{\phi, \xi}$  represents the active power demand at node  $i$  for phase  $\phi$  and scenario  $\xi$  and  $s_i^\xi \in \{0, 1\}$  is the load pick-up status variable that determines whether the load at node  $i$  is picked up or not. The CLs are prioritized by a weight

variable  $w_i$ . Since the CLs are critical for any scenario,  $w_i$  remains the same for all scenarios. Furthermore, the scenarios have a specific probability,  $p_\xi$ , associated with them, which comes from the scenario reduction method discussed before. The parameters for  $CVaR_\alpha(Q(\delta, \mathcal{E}))$  are defined similarly as discussed in Section 4.2.

### First Stage Constraints

The first stage constraints correspond to the planning decisions made in the first stage. In this work, the per unit cost for DG installation and sizing is assumed to be the same for each location; these assumptions can be easily relaxed. Constraint (4.9a) ensures that the total cost of DGs should be between  $\$[0, \mathcal{C}_{max}^{DG}]$  regardless of the cost of installation in an individual location. This gives the freedom of utilizing the overall budget for a single big-sized DG or distributing the budget to multiple smaller-sized DGs. Constraint (4.9a) contains a non-linear term  $\delta_i^{DG} \times \beta_i^{DG}$  which is linearized using big-M method as discussed in [46]. Constraint (4.9b) restricts the DG location variable to binary. The DG location variable  $\delta_i^{DG}$  is 1 if a DG is located in node  $i$ , else 0. Furthermore, constraint (4.9c) ensures that  $VaR_\alpha$  for the distribution of load loss in the second stage is a real number. Furthermore,  $VaR_\alpha$  is independent of scenarios and is obtained with the solution of the first stage.

$$\sum_{i \in \mathcal{B}_{DG}} c_i^{DG} \delta_i^{DG} \beta_i^{DG} \leq \mathcal{C}_{max}^{DG} \quad (4.9a)$$

$$\delta_i^{DG} \in \{0, 1\} \quad (4.9b)$$

$$\eta \in \mathbb{R} \quad (4.9c)$$

## Second Stage Constraints

The second stage of the stochastic optimization problem is the operational stage in which DG-assisted restoration is performed for each  $\xi$ . The inner-loop operational stage consists of several constraints corresponding to the restoration problem [31]. Since the second-stage variables change with respect to each scenario, each of these variables has  $\xi$  to differentiate them from the first-stage variables.

### Connectivity constraints:

- Constraint (4.10a) ensures that a load is picked up if and only if it is connected to an energized bus,  $v_i$ . Similarly, based on the constraint (4.10b) loads connected to non-switchable buses will also be picked up if the corresponding bus is energized.
- The line energization status can be observed through the constraints set (4.11). According to constraint (5.12), a switchable line without fault is energized if any of the buses connecting the line is energized. On the other hand, (5.14c) ensures that a non-switchable line connected to any energized bus is also energized. Finally, constraint (4.11c) ensures that a line experiencing a fault is disconnected from the grid.

$$s_i^\xi \leq v_i^\xi, \quad \forall i \in \mathcal{B}_S \quad (4.10a)$$

$$s_i^\xi = v_i^\xi, \quad \forall i \in \mathcal{B} \setminus \mathcal{B}_S \quad (4.10b)$$

$$\delta_e^\xi \leq v_i^\xi, \quad \delta_e^\xi \leq v_j^\xi, \quad \forall e \in \mathcal{L}_S \setminus \mathcal{L}_F^\xi \quad (4.11a)$$

$$\delta_e^\xi = v_i^\xi = v_j^\xi, \quad \forall e \in \mathcal{L} \setminus (\mathcal{L}_S \cup \mathcal{L}_F^\xi) \quad (4.11b)$$

$$\delta_e^\xi = 0, \quad \forall e \in \mathcal{L}_F^\xi \quad (4.11c)$$

**Power Flow Constraints:** In this work, a three-phase unbalanced linearized power flow model is used in the optimization framework [47]. Since we are solving a long-term planning model with CL restoration in the second stage, the linearized model is sufficiently accurate and applicable for our problem [31]. Furthermore, the power flow will only be valid for the energized section of the system. Hence, the power flow equations are coupled with line and bus energization variables to appropriately represent them in the second stage problem.

- Constraints (4.12a) - (4.12d) represent the three-phase unbalanced linearized power flow equations. The equations are coupled with the line decision variable  $\delta_e$  and load-pick variable  $s_i$ . Constraints (4.12a) and (4.12b) represent the active and reactive power flow for each of the energized lines. Constraint (4.12c) is the voltage equation for non-switchable lines whereas (4.12d) represents the voltage equation for a set of lines that are switchable. Constraint (4.12d) is coupled with  $\delta_e$  to ensure that the voltage drop applies only if the switch is closed. The non-linear terms associated with the power flow equations are linearized using the big-M method [46].

$$\sum_{e:(i,j) \in \mathcal{L}} \mathbf{P}_e^\xi = s_j^\xi \mathbf{P}_{Lj}^\xi + \sum_{e:(j,i) \in \mathcal{L}} \mathbf{P}_e^\xi \quad (4.12a)$$

$$\sum_{e:(i,j) \in \mathcal{L}} \mathbf{Q}_e^\xi = s_j \mathbf{Q}_{Lj}^\xi + \sum_{e:(j,i) \in \mathcal{L}} \mathbf{Q}_e^\xi \quad (4.12b)$$

$$\mathbf{U}_i^\xi - \mathbf{U}_j^\xi = 2(\tilde{\mathbf{r}}_e \mathbf{P}_e^\xi + \tilde{\mathbf{x}}_e \mathbf{Q}_e^\xi), \quad \forall e \in \mathcal{L}^\xi \setminus \mathcal{L}_S^\xi \quad (4.12c)$$

$$\delta_e^\xi (\mathbf{U}_i^\xi - \mathbf{U}_j^\xi) = 2(\tilde{\mathbf{r}}_e \mathbf{P}_e^\xi + \tilde{\mathbf{x}}_e \mathbf{Q}_e^\xi), \quad \forall e \in \mathcal{L}_S^\xi. \quad (4.12d)$$

where

$$\tilde{\mathbf{r}}_e = \text{Real}\{\alpha\alpha^H\} \otimes \mathbf{r}_e + \text{Im}\{\alpha\alpha^H\} \otimes \mathbf{x}_e,$$

$$\tilde{\mathbf{x}}_e = \text{Real}\{\alpha\alpha^H\} \otimes \mathbf{x}_e + \text{Im}\{\alpha\alpha^H\} \otimes \mathbf{r}_e,$$

$$\alpha = [1 \ e^{-j2\pi/3} \ e^{j2\pi/3}]^T$$

**Operational Constraints:** The operational constraints of the second stage problem are related to the distribution system topology and voltage limits. The distribution system operates in a radial fashion. Hence, the topology of the distribution grid should be radial at all times. Furthermore, the nodal voltages should be within the specified limits at all times.

- A radial configuration in any distribution system consists of several sectionalizing and tie-line switches. In this work, virtual edges are assumed to supply the power from DGs in case of an islanded mode of operation. In any faulted network, a radial configuration is maintained by toggling any of the switches to avoid the formation of loops or cycles. Constraint (5.16) ensures that at least one of the switches is open in a cycle. In this work, a brute-force approach is applied to count and store the number of cycles in the distribution system and Constraint (5.16) is enforced on each of the cycles so that the system operates in a radial fashion. The process of counting and storing cycles is completely offline and does not affect the computational complexity of the stochastic optimization procedure.
- The voltage limit on each of the buses should be within the ANSI C84.1 standard is ensured by (4.13b). In this work,  $\mathbf{U}^{min}$  and  $\mathbf{U}^{max}$  are set as  $(0.95)^2$  and  $(1.05)^2$  respectively for each of the phases. Since the limits make sense only for the buses that are energized, the limits are coupled with  $v_i^\xi$ .
- For the purpose of reconfiguration, it is required that the power flow through an

open switch is zero. If  $\delta_e^\xi = 0$  for any  $e : i \rightarrow j$  then constraint (5.19) ensures that the power flow through that line is zero. If not, box constraints on the power flow are enforced where  $\underline{M}_p = -\overline{M}_p$  and  $\underline{M}_q = -\overline{M}_q$ .

$$\sum_{e \in \mathcal{L}_c} \delta_e^\xi \leq |\mathcal{L}_c| - 1, \quad \forall e \in \mathcal{L}_c \quad (4.13a)$$

$$v_i^\xi \mathbf{U}^{min} \leq \mathbf{U}_i^\xi \leq v_i^\xi \mathbf{U}^{max}, \quad \forall i \in \mathcal{B} \quad (4.13b)$$

$$\delta_e^\xi [\underline{M}_p \ \underline{M}_q] \leq [\mathbf{P}_e^\xi \ \mathbf{Q}_e^\xi] \leq \delta_e^\xi [\overline{M}_p \ \overline{M}_q], \quad \forall e \in \mathcal{L}_S^\xi \quad (4.14)$$

### DG Constraints:

- Virtual switches represent the connection of DGs in islanded mode. The virtual edge should only be connected if a DG is located at the specific node which is ensured by (4.15a).
- The two stages in any stochastic optimization framework are bound by the non-anticipativity constraints [32]. This means that the location and size of the DGs should be the same for every scenario realized in the second stage of the problem. This non-anticipativity nature of the first stage decision variables is presented in (4.15b).
- The in-flow power of each of the DGs should be less than or equal to the size of the DG. Since the DGs are connected using virtual edges,  $\delta_e^\xi$  is coupled with this constraint as given in (5.20).

$$\delta_e^\xi \leq \delta_i^{DG}, \quad \forall e \in \mathcal{L}_S^v, \quad \forall i \in \mathcal{B}_{DG} \quad (4.15a)$$

$$\begin{aligned} \delta_i^{DG} &= \delta_i^{DG,\xi}, \quad \delta_i^{DG} \beta_i^{DG} = \delta_i^{DG,\xi} \beta_i^{DG,\xi} \\ &\forall i \in \mathcal{B}_{DG}, \forall \xi \in \mathcal{E} \end{aligned} \quad (4.15b)$$

$$\sum_{\phi \in \{a,b,c\}} P_e^{\phi,\xi} \leq \delta_e^\xi \delta_i^{DG} \beta_i^{DG}, \quad \forall e \in \mathcal{L}_S^v, \forall i \in \mathcal{B}_{DG} \quad (4.15c)$$

**$CVaR_\alpha$  Constraints:** The  $VaR_\alpha$  is obtained as a solution in the first stage and is represented by  $\eta$ .  $VaR_\alpha$  and  $CVaR_\alpha$  correspond to the distribution of optimal solutions obtained in the second stage of the problem.  $CVaR_\alpha$  represents  $1 - \alpha$  part of distribution beyond  $VaR_\alpha$ . Hence, as discussed in (4.4) an excess variable is obtained for each scenario  $\nu_\xi$  such that it corresponds  $1 - \alpha$  part of the distribution beyond  $VaR_\alpha$ . Furthermore, this excess variable must be a positive real number. These constraints are represented by (6.20).

$$\nu_\xi \geq x_\xi - \eta, \quad \nu \in \mathbb{R}_+^n \quad (4.16)$$

#### 4.4 Results and Analysis

The effectiveness of the proposed risk-based long-term planning model is verified on a modified IEEE 123-bus case, see Fig. 4.7. Several case studies with multiple DG locations, variable numbers of DGs, and varying risk preferences are presented with detailed analyses of the results. The two-stage problem without DG-based restoration is referred to as the base case which is then compared with other case studies. Furthermore, to analyze the planning decisions better, we create a new test case upon hardening 15 randomly selected lines, as shown in Fig. 4.7. The fragility curves of hardened lines are adjusted so that their outage probability for any extreme event is less than the case when they are not hardened. For CLs,  $w_i = 10$  whereas, for non-critical loads,  $w_i = 1$ . Thus the second stage cost reflects the total amount of prioritized loss of load (in kW). The total non-prioritized demand of the system is

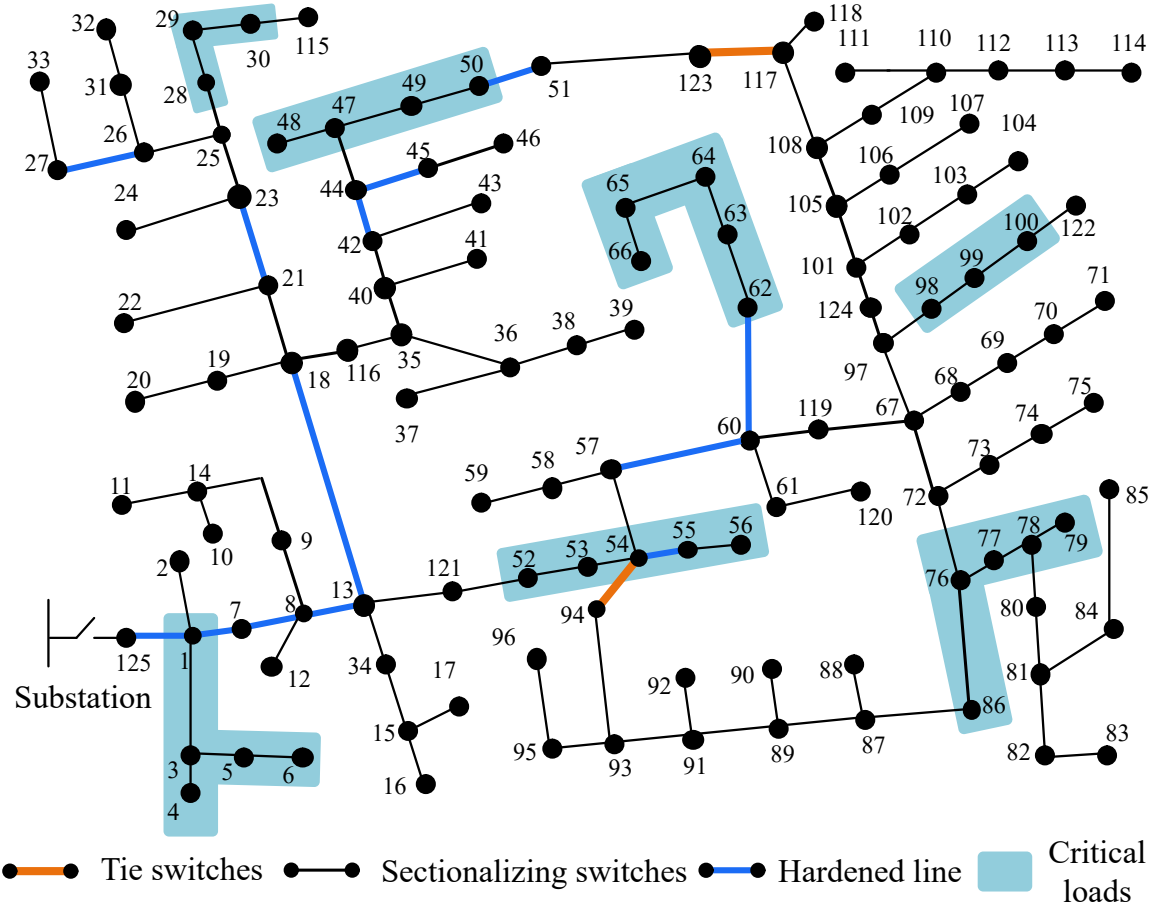


**Figure 4.7** Modified IEEE 123-bus test case

$P_D = 4485 \text{ kW}$  and the prioritized demand is  $\sum_{i \in \mathcal{V}} w_i P_{Li} = 20775 \text{ kW}$ . In this paper, we use prioritized demand to analyze the results for different cases.

The two-stage stochastic integer programming model is formulated using PySP package in Pyomo [48]. Scenario generation and reduction using the Monte-Carlo method are implemented in MATLAB2020a. The entire simulations are carried out on a PC with a 3.4 GHz Intel i7-6700 CPU and 16 GB RAM. The proposed two-stage stochastic problem is solved as a single large mixed-integer linear programming problem for each presented case study.

#### 4.4.1 Scenario Generation and Reduction

The wind event scenarios are generated and reduced using methods discussed in Section 4.3.1. Using the wind speed profile for extreme wind events and failure probability of distribution lines, several trials of MCS simulation are conducted for sampled wind speeds [42]. For this experiment,  $N_u = 49$  wind speeds are sampled from the wind speed profile and it was experimentally verified that 1000 Monte-Carlo trials are enough to obtain a converged value of prioritized loss of load in the distribution grid corresponding to each  $u$ . Fig. 4.8 shows the moving average of prioritized loss of load for 1000 Monte-Carlo trials for the base case without hardening and with hardening. It can be seen that the value of the loss is fairly converged in 1000 trials for both cases. Since 1000 trials are conducted for each  $u$ ,  $N_{\xi,u} = 1000$ . Hence, the total number of scenarios generated through MCS,  $\Xi = 49 \times 1000 = 49000$ .

Fig. 4.9 represents the comparison between  $L_{avg}^u$  and  $L_\xi^u$  for the test case without hardening and with line hardening. The loss due to reduced scenarios is very close to that of the actual representative scenarios for each  $u$ . The y-axis on the right represents the value of  $|L_{avg}^u - L_\xi^u|$ . It can be seen that the maximum difference occurs at  $u = 31m/s$  in Fig. 4.9(a) and has a value of about  $78 kW$  which is  $< 0.5\%$  of total prioritized demand. The difference in their values comes from the fact the  $L_{avg}^u$  is obtained by averaging 1000 different realizations of  $\xi$  for a specific  $u$  whereas  $L_\xi^u$  is the prioritized load loss for a specific failure scenario  $\xi$  corresponding the same  $u$ . Furthermore, it should be noted that HILP events (tail events) are also sampled in this reduction method which makes this approach highly suitable for resilience planning problems.

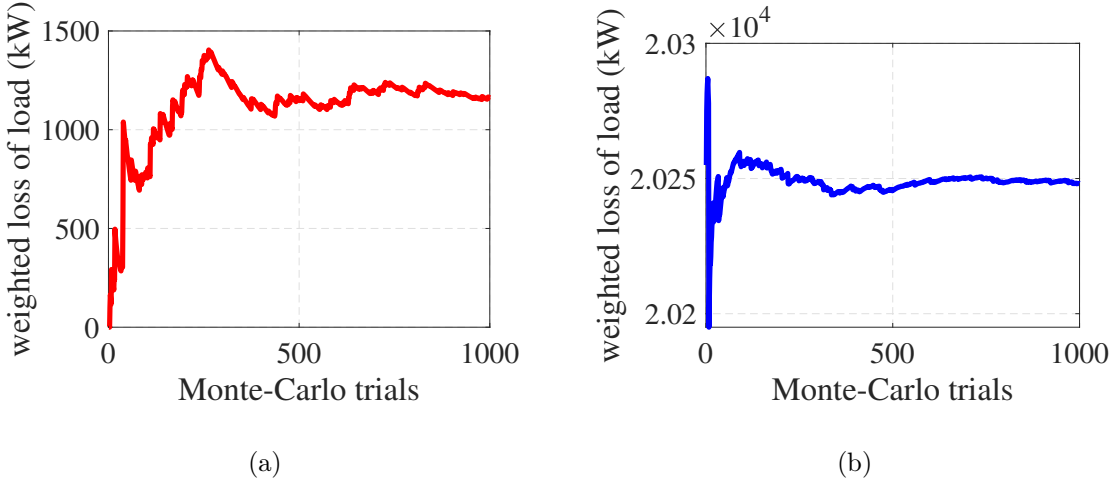


**Figure 4.8** Moving average of loss of load for 1000 Monte-Carlo trials a) without hardening b) with line hardening.

#### 4.4.2 Risk-Averse Long-Term Planning

The reduced scenarios from the method mentioned above represent several scenarios that can occur on the distribution grid. Each scenario represents the line failure status due to a particular wind speed ( $u$ ). In this long-term planning problem, 6 DG locations are pre-selected as potential locations for the placement of DG units. It is to be noted that the candidate locations are not the final DG locations. They are potential locations that can be used to install a DG as per the solution of the proposed optimization framework. The selected potential DG locations are nodes 95, 122, 39, 85, 56, and 66. However, the DG locations are decided by the optimization model and  $\delta_i^{DG} = 1$  if and only if  $\beta_i^{DG} > 0$ . From the operator's perspective, it is often practical to have a limited budget while planning the siting and sizing strategies for DGs. The total budget is constrained so that the sum of the DG units is less than or equal to 900 kW. For risk-driven problems,  $\alpha$  is set at 0.95, meaning that 5% tail

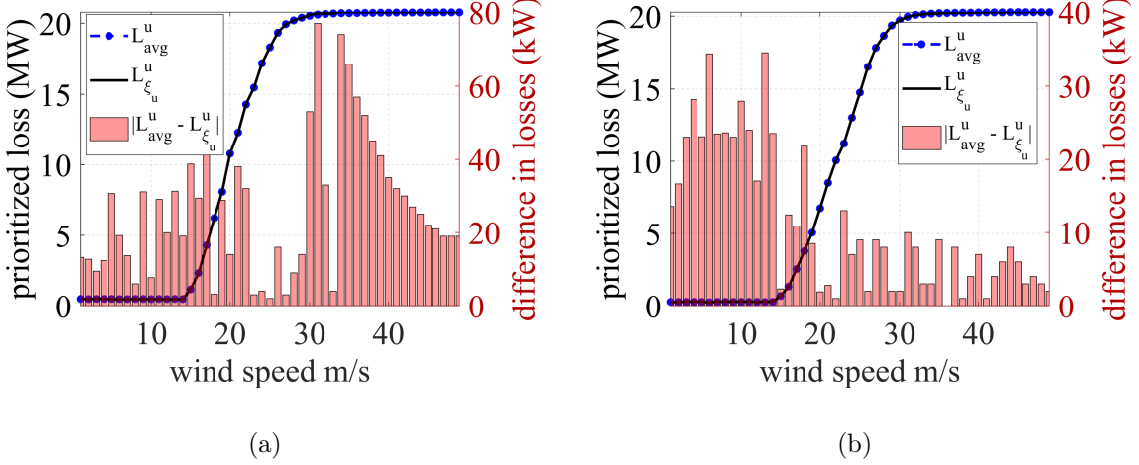


**Figure 4.9** Comparison of prioritized load loss obtained for two sets of reduced scenarios a) without hardening b) with hardening.

scenarios (HILP) are considered to have greater risks.

Table 4.2 shows  $\mathbb{E}(Q(\delta, \mathcal{E}))$  and  $CVaR_\alpha(Q(\delta, \mathcal{E}))$  when no DG-based planning measures are used (base case). Since  $\alpha = 0.95$ , the  $CVaR_\alpha$  represents the 5% of the tail probability cases. This means that when those 5% scenarios are realized, on average, the prioritized loss of load is 20601.58 kW (with no line hardening measures in place). The losses improve to 19839.39 kW when a few lines are hardened, as shown in Fig. 4.7. Furthermore, the expected values of prioritized load loss, calculated over the entire scenarios, are 5982.57 kW and 4541.76 kW for the respective cases mentioned above. However, when an operator is planning to enhance the grid's resilience, the 5% of those scenarios are extremely important because the system needs to withstand or adapt to those events to maintain a constant supply of power to the CLs. Hardening a few lines is already proving to be a potential solution to minimize the expected and  $CVaR_\alpha$  of the prioritized load loss. However, in the case of an islanding situation when CLs are disconnected from the system when a fault occurs, DG-based planning

strategies have proven to be successful in maintaining an uninterrupted power supply to the CLs [3].

**Table 4.2** Base case expected value and  $CVaR_\alpha$  of prioritized load loss.

line hardening	$\mathbb{E}(Q(\delta, \mathcal{E}))$ in kW	$CVaR_\alpha(Q(\delta, \mathcal{E}))$ in kW
No	5982.57	20601.58
Yes	4541.76	19839.39

To identify the trade-off among different DG-based planning strategies, 6 locations — 39, 56, 66, 85, 95, and 122 — are selected as potential DG locations. The planning problem is then solved as a two-stage stochastic problem as discussed in Section 4.3. First, we discuss the results for the risk-neutral case ( $\lambda = 0$ ). The existing resilience-based planning methods, [18, 17, 19], are focused on the risk-neutral case and used as a comparison for this work. The overall capacity of each of the DGs is shown in Table 4.3. For risk-neutral planning without line hardening measures, no DGs are required to be placed on nodes 36 and 95. However, for mean-risk and risk-averse situations, the planning strategies change significantly. For risk-involved strategies, it is required to place DGs on nodes 39 and 95 while reducing the DG sizes for the rest of the nodes as shown in Table 4.3. Hence, the trade-off of including risk minimization in the objective is to increase the number of DG units in the system. This can be fruitful for extreme event scenarios when picking up some of the CLs is required, even though it increases the expected value of prioritized load loss. Table 4.3 also shows the expected value and  $CVaR_\alpha$  of prioritized CLs picked up by different planning strategies. It can be seen that the expected value of prioritized CLs picked up does not change much regardless of the risk preference. However, for risk-based strategies

**Table 4.3** Expected value and  $CVaR_\alpha$  of prioritized load loss and prioritized critical load (PCL) picked up for different values of  $\lambda$ .

	WITHOUT LINE HARDENING						WITH LINE HARDENING					
	Existing methods [18, 17, 19]			Proposed method			Existing methods [18, 17, 19]			Proposed method		
	$\lambda = 0$		$\lambda = 0.5$	$\lambda = 1$	$\lambda = 0$		$\lambda = 0.5$	$\lambda = 1$	$\lambda = 0$		$\lambda = 0.5$	$\lambda = 1$
$\mathbb{E}(Q(\delta, \mathcal{E}))$	3567.12		3586.28		3595.51		2467.46		2463.95		2490.09	
$CVaR_\alpha(Q(\delta, \mathcal{E}))$	19093.89		18885.92		18885.92		18415.04		18160.18		18119.1	
Expectation of PCL picked up	15043.93		15016.64		15006.62		16065.76		16048.17		16026.12	
$CVaR_\alpha$ of PCL picked up	3406.59		3603.06		3603.06		4953.65		5580.72		6295.33	
DG planning strategies	$\beta_{39}^{DG}$	$\beta_{56}^{DG}$	$\beta_{66}^{DG}$	$\beta_{39}^{DG}$	$\beta_{56}^{DG}$	$\beta_{66}^{DG}$	$\beta_{39}^{DG}$	$\beta_{56}^{DG}$	$\beta_{66}^{DG}$	$\beta_{39}^{DG}$	$\beta_{56}^{DG}$	$\beta_{66}^{DG}$
	0	20	370	20	20	340	20	20	370	0	350	330
	$\beta_{85}^{DG}$	$\beta_{95}^{DG}$	$\beta_{122}^{DG}$	$\beta_{85}^{DG}$	$\beta_{95}^{DG}$	$\beta_{122}^{DG}$	$\beta_{85}^{DG}$	$\beta_{95}^{DG}$	$\beta_{122}^{DG}$	$\beta_{85}^{DG}$	$\beta_{95}^{DG}$	$\beta_{122}^{DG}$
	390	0	120	100	300	120	100	270	120	100	0	120
										100	305	0
										100	280	0

(both mean risk and risk-averse),  $CVaR_\alpha$  of prioritized CLs picked up increases by 200 kW compared to the risk-neutral case.

The effect of risk aversion is even more pronounced in the case with the line-hardening strategy. Fig. 4.10 shows a restoration and planning solution for a specific scenario of HILP nature,  $u = 28 m/s$  (see Fig. 4.6). The lines and nodes with black color are the energized section, whereas non-energized sections are represented by gray. Similarly, red lines represent out-of-service lines due to the particular outage scenario. Similar to the restoration for cases without line hardening measures, the risk-neutral solution does not include DGs in nodes 39 and 95. When the objective is risk-neutral ( $\lambda = 0$ ) some of the prioritized critical loads are not picked up in this specific scenario as picking up critical loads in this scenario would not affect

the expected value of load served for the overall scenarios. Since the objective is to minimize the expected value of prioritized load loss for entire scenarios, DG at location 95 is not selected. Note that the probability of HILP scenarios is low. Since the expected value contains the product of this probability with the objective function in the restoration phase, the net value is significantly low to affect the overall expected value. However, when the objective is risk-averse, any prioritized load that the nearest possible DG can pick up is given the top priority for any HILP event. For instance, it can be seen that load at node 62 is picked up by DG at node 95 through path 95-93-94-54-57-60-62. Hence, this draws an important conclusion that risk-averse decisions enhance long-term resilience planning by focusing the extreme HILP events. Contrary to the existing methods in [18, 17, 19], the prioritized CLs have a high chance of being picked up when an HILP event is realized by including risk minimization in the objective. However, when attempting to minimize the risk-averse objective (i.e., the  $CVaR_\alpha$ ), we incur an additional DG cost in the overall planning budget to meet the requirements for risk-averse planning. Thus, through the proposed approach and by including  $CVaR_\alpha$  minimization in the objective function, prioritized critical loads can be properly restored in case of HILP events. Furthermore, with the changing trade-off between the expectation and the  $CVaR_\alpha$  of the prioritized load loss, the expected value *generally* decreases with the increase in  $\lambda$ .

For the case without line hardening, the  $CVaR_\alpha$  does not change when moving from mean-risk to risk-averse setting as shown in Table 4.3. It is important to note that tail probability events are also a part of risk-neutral planning strategies. However, the main focus is to minimize the expected loss over the entire scenario, and hence the effect of those tail events is less prominent. With risk-driven strategies,

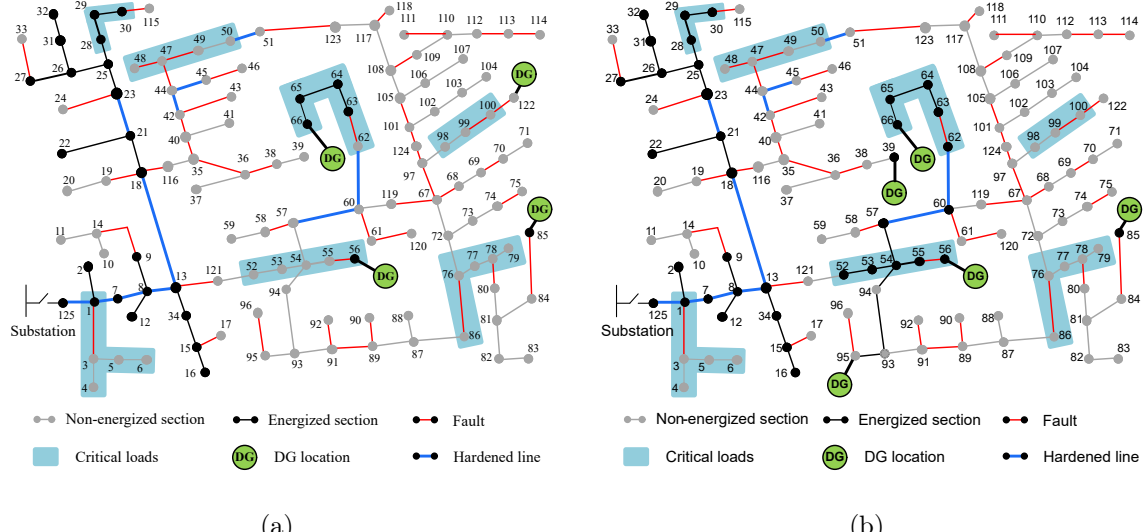


**Figure 4.10** DG sizing and siting solution for a scenario with additional hardening measures for a) risk-neutral and b) risk-averse planning.

$CVaR_\alpha$  of those tail events are also minimized, and hence the value of  $CVaR_\alpha$  decreases with an increase in  $\lambda$ . At some point,  $CVaR_\alpha$  saturates as it is impossible to restore some prioritized loads regardless of the planning strategies. On the other hand, for the case with additional line hardening measures,  $CVaR_\alpha$  of prioritized load loss further decreases with increasing risk-aversion. This is due to the fact that with line hardening measures, the DGs can pick up more CLs during HILP events, which ultimately reduces the prioritized load loss in the system. Hence, it is clear and obvious that with more number of resources, the  $CVaR_\alpha$  can be improved further. However, the trade-off comes with the budget and feasibility. Although it is tempting to harden each and every line and install DGs in each and every location, it is almost impossible for any system operator to allocate the budget accordingly.

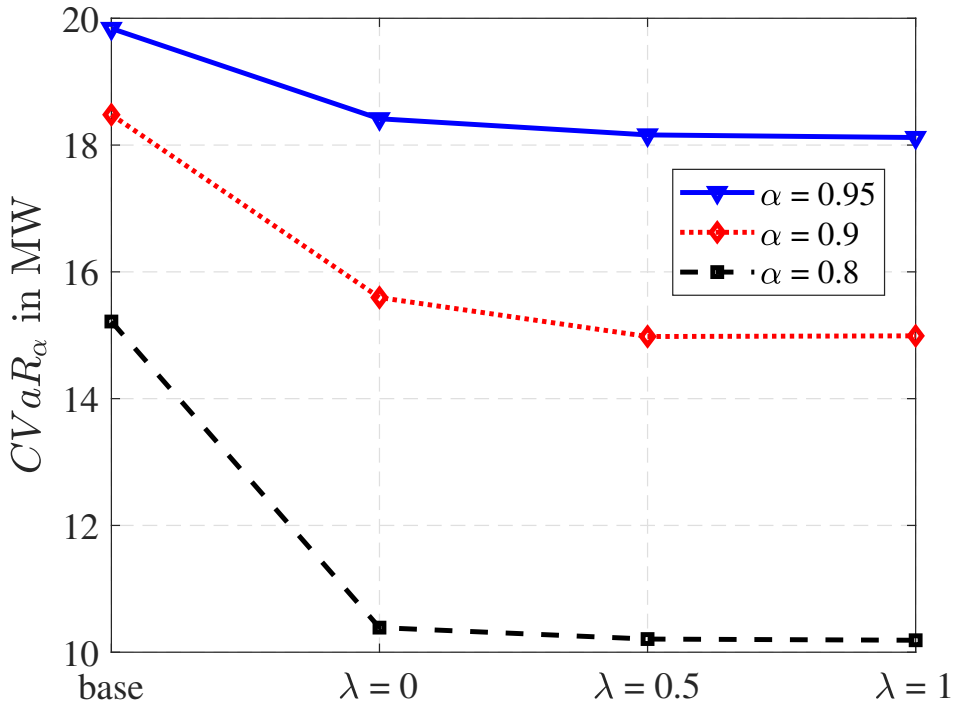
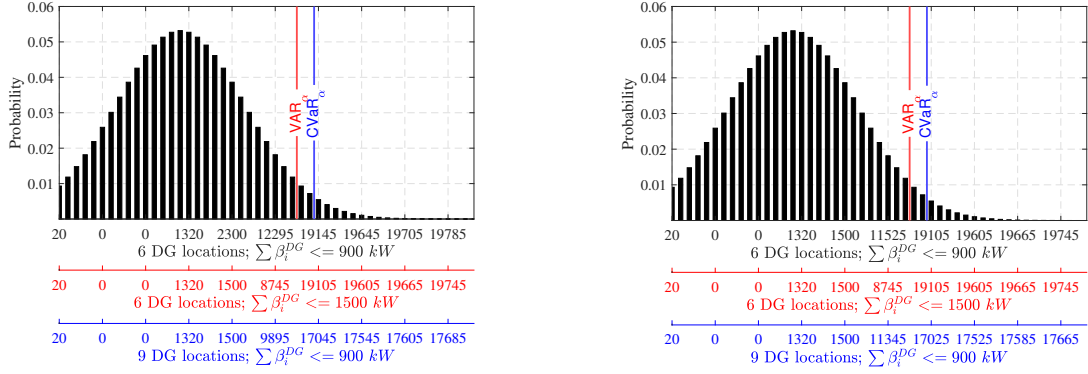


**Figure 4.11** Comparison of  $CVaR_\alpha$  of prioritized loss of load for different values of  $\alpha$  and risk preference.

#### 4.4.3 Sensitivity analysis

The value of  $CVaR$  depends on several factors such as investment decisions, budget, risk preference, and scenarios under consideration. Here, we present a few of the sensitivity analyses and discuss their impacts on  $CVaR$ . For simplicity, the analyses are performed only on the system with additional hardening measures already in place.



(a)

(b)

**Figure 4.12**  $CVaR_\alpha$  for different DG investment strategies for a) risk-neutral and b) risk-averse planning.

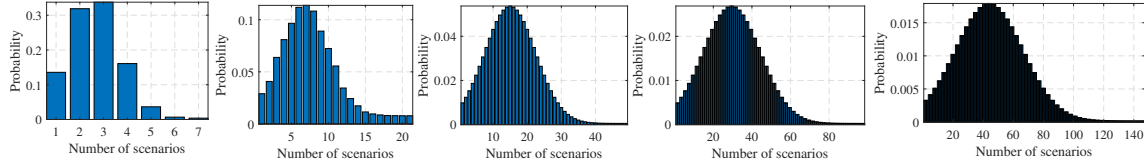


**Figure 4.13** Different number of scenarios with respective probabilities of occurrence: (a) 7, (b) 21, (c) 49, (d) 98, and (e) 147 scenarios.

### Change in confidence level

The risk parameters  $\alpha$  and  $\lambda$  can affect the planning decisions. The value of  $CVaR_\alpha$  highly depends on  $\alpha$  as it defines the number of scenarios to be considered in defining the risk. In other words,  $\alpha$  can also be defined as risk percentage. For a higher value of  $\alpha$ , the value of  $VAR_\alpha$  increases, and hence,  $CVaR_\alpha$  represents the scenarios that create greater losses in the system. Similarly, for a smaller  $\alpha$ ,  $CVaR_\alpha$  incorporates a larger number of scenarios with lower losses in risk quantification. Furthermore, as discussed above, an increasing value of  $\lambda$  denotes an increase in risk aversion towards planning decisions. Fig. 4.11 shows the relation of  $CVaR_\alpha$  for the prioritized loss

of load for different values of  $\lambda$  and  $\alpha$ . As discussed,  $CVaR_\alpha$  decreases when more scenarios are considered as risky (characterized by  $\alpha$ ). Furthermore, for a fixed  $\alpha$ ,  $CVaR_\alpha$  decreases with the increase in the value of  $\lambda$  as more importance are given to risk minimization. Appropriate values for  $\alpha$  and  $\lambda$  need to be selected based on planners' risk aversion criteria.

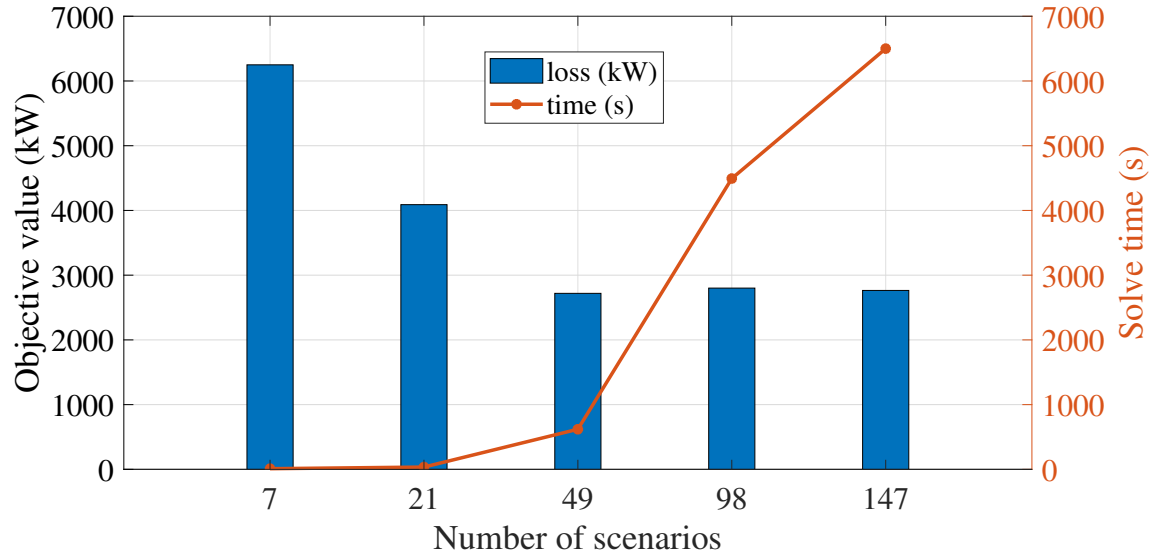
### **Change in investment strategies**

Changing investment strategies and allocating the budget properly can also affect the overall planning cost. First, the overall budget for DG sizing and installation is increased so that  $\mathcal{C}_{max}^{DG}$  corresponds to  $P_{DG}^{max} = 1500 \text{ kW}$  for the same set of DGs and their potential locations. Secondly, 3 additional DG locations (47, 27, and 114) are identified as potential DG placement locations. Fig. 4.12(a) and Fig. 4.12(b) show the distribution of prioritized loss of load when different DG planning measures are taken for risk-neutral and risk-averse cases, respectively. It is interesting to notice that increasing the budget to increase the capacity of DGs has a limited effect on the  $CVaR_\alpha$  minimization. However, the expected value of prioritized load loss decreases to  $2222.43 \text{ kW}$  from  $2467.46 \text{ kW}$ . The conclusion is consistent for the risk-averse case. However, increasing the number of potential DG locations led to significant improvement in  $CVaR_\alpha$  minimization. The change in expected loss is, however, insignificant. For the case with 9 potential DG locations, the value of  $CVaR_\alpha$  decreases from  $18415.04 \text{ kW}$  to  $16385.51 \text{ kW}$ , for the risk-neutral case, and from  $18119.1 \text{ kW}$  to  $15811.59 \text{ kW}$ , for the risk-averse case. Thus, with a limited budget, multiple DG sites with smaller DGs are more effective in improving resilience.

### **Change in number of scenarios and set of scenarios**

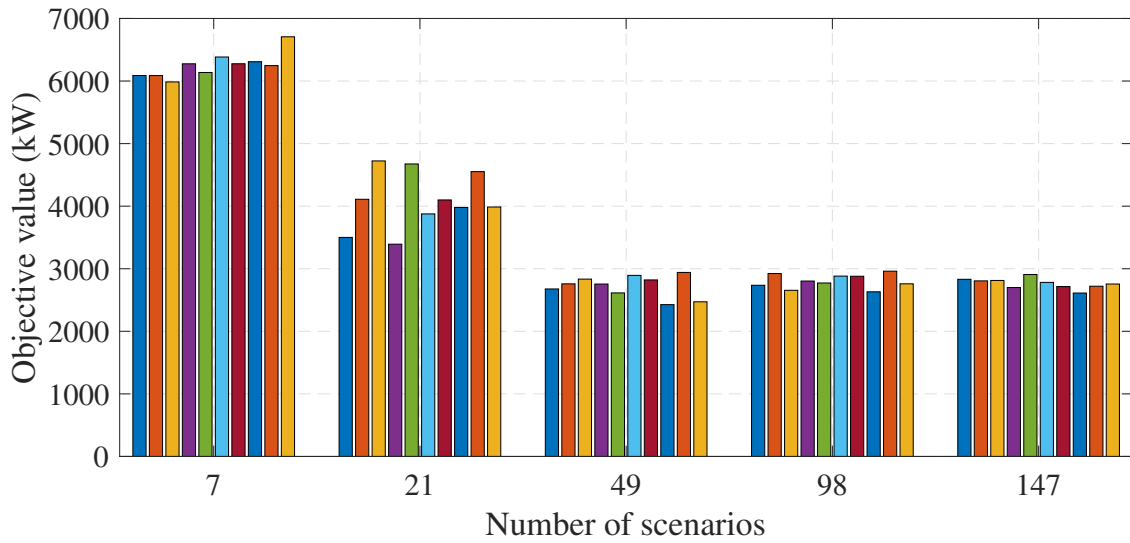
Fig. 4.13 shows five case studies simulated to evaluate the impacts of the number of scenarios (used in optimization) on solution quality and solve time; (a) 7 scenarios, (b) 21 scenarios, (c) 49 scenarios, (d) 98 scenarios, (e) 147 scenarios. Hence, for each case, different scenario sets are obtained using the method discussed in Algorithm 1. Fig. 4.14 shows the objective function value for the different number of scenarios (used in the optimization problem) along with the corresponding solve times. The result for each case is obtained by taking an average of 10 representative scenario sets closest to the average representative scenario. We can clearly observe the trade-off between the number of scenarios, solution quality, and solve time. When a higher number of scenarios are used in optimization, the solution quality improves; however, it also leads to a significant increase in the solve time. It is also interesting to note that the solution obtained for 49 scenarios (2719.17 kW) is very close to the one obtained for 147 scenarios (2764.16 kW). However, the solve time for the problem with 147 scenarios is 11 times greater than that with 49 scenarios. Hence, 49 scenarios work well from the point of view of solution as well as solve time as the additional number of scenarios increases the computational complexity with no significant improvement in the objective value.

Fig. 4.15 shows our simulation results for 10 unique sets of scenarios sampled from the wind profile PDF. The simulations are done for five cases by including a different number of scenarios in the optimization problem, i.e., 7, 21, 48, 98, and 147 (scenarios). For a specific case, it can be observed that the objective function values are very close for all 10 unique scenario sets. Each scenario set is selected based on the closest average Monte-Carlo loss as detailed in Algorithm 1. Hence, the differences in



**Figure 4.14** Comparison of objective value and solve time for a different number of scenarios.

solutions for different scenario sets are not significant. The process is similar to the multiple replication method (MRP) as discussed in [17]. In addition, for each case, Table 4.4 shows the 95% confidence interval for the objective function value along with the average objective value. As expected, including a larger number of scenarios in the optimization problem increases the granularity of information regarding the event and its impacts. As can be seen, the objective function values are consistent with the number of scenarios being considered in the optimization problem. It is interesting to note that the solution quality improves drastically when additional scenarios are considered in the optimization problem. Furthermore, the variation in the optimal function values also reduces as we consider a larger number of scenarios, see Table 4.4. For example, for the simulation case with 147 scenarios, the lower and upper limits of the optimal function values for all 10 unique scenario sets are very close to each other than any other scenarios. However, as shown by the results in Fig. 4.14, the



**Figure 4.15** Comparison of objective value on a different set of scenarios for each number of scenarios sampled.

**Table 4.4** 95% confidence interval of the solution obtained using different scenario sets for each number of scenarios.

Number of scenarios	95% CI (kW)	Average objective value (kW)
7	[6105.95, 6393.99]	6249.57
21	[3764.35, 4414.53]	4089.44
49	[2596.13, 2842.21]	2719.17
98	[2721.20, 2879.54]	2800.37
147	[2705.10, 2823.21]	2764.16

solve time increases drastically with a higher number of scenarios. Thus, as expected, there is a tradeoff between computational complexity and solution quality.

## 4.5 Summary

In this chapter, we present a risk-based planning framework for active power distribution systems to improve their resilience to extreme weather events. Resilience is characterized in a probabilistic sense to quantify the impacts of the HILP events on the system outages. A two-stage stochastic optimization problem is formulated to minimize the risk of system outages as a weighted function of the expected value and CVaR of the probabilistic system outages. The planning decisions include system upgrades by siting and sizing DGs capable of intentional islanding to support CLs. A scenario reduction method is proposed based on realized loss functions that generate representative scenarios for HILP events for computational tractability. The proposed formulation makes it conducive to evaluate the trade-offs between risk-neutral and risk-averse planning decisions. The proposed risk-based planning framework is analyzed for different scenarios. It was observed that the DG-based restoration method with additional hardening measures could effectively minimize both the expectation and  $CVaR_\alpha$  of the prioritized load loss. Furthermore, risk-averse planning measures were highly effective in restoring CLs during HILP events, which is generally not true for risk-neutral policy. It was also observed that it is preferable to site variable-sized DGs at multiple locations rather than a few large DGs under a limited budget. Based on the observations, the proposed risk-based framework provides distribution planners with the much-needed ability to evaluate alternate planning measures for resilience.

## REFERENCES

- [1] R. Moreno, M. Panteli, P. Mancarella, H. Rudnick, T. Lagos, A. Navarro, F. Ordonez, and J. C. Araneda, “From Reliability to Resilience: Planning the Grid Against the Extremes,” *IEEE Power and Energy Magazine*, vol. 18, no. 4, pp. 41–53, 2020.
- [2] Q. Shi, W. Liu, B. Zeng, H. Hui, and F. Li, “Enhancing distribution system resilience against extreme weather events: Concept review, algorithm summary, and future vision,” *International Journal of Electrical Power & Energy Systems*, vol. 138, p. 107860, 2022.
- [3] G. Liu, T. Jiang, T. B. Ollis, X. Li, F. Li, and K. Tomsovic, “Resilient distribution system leveraging distributed generation and microgrids: A review,” *IET Energy Systems Integration*, vol. 2, no. 4, pp. 289–304, 2020.
- [4] A. Arif, S. Ma, Z. Wang, J. Wang, S. M. Ryan, and C. Chen, “Optimizing Service Restoration in Distribution Systems With Uncertain Repair Time and Demand,” *IEEE Transactions on Power Systems*, vol. 33, no. 6, pp. 6828–6838, 2018.
- [5] W. Yuan, J. Wang, F. Qiu, C. Chen, C. Kang, and B. Zeng, “Robust Optimization-Based Resilient Distribution Network Planning Against Natural Disasters,” *IEEE Transactions on Smart Grid*, vol. 7, no. 6, pp. 2817–2826, 2016.
- [6] B. A. J. Conejo *et al.*, “Operations and long-term expansion planning of natural-gas and power systems: A market perspective,” *Proceedings of the IEEE*, vol. 108, no. 9, pp. 1541–1557, 2020.

- [7] A. Stankovic and K. Tomsovic, “The Definition and Quantification of Resilience,” Tech. Rep. PES-TR65, IEEE Power & Energy Society, Apr. 2018.
- [8] H. Gao, Y. Chen, S. Mei, S. Huang, and Y. Xu, “Resilience-oriented pre-hurricane resource allocation in distribution systems considering electric buses,” *Proceedings of the IEEE*, vol. 105, no. 7, pp. 1214–1233, 2017.
- [9] Q. Zhang, Z. Wang, S. Ma, and A. Arif, “Stochastic pre-event preparation for enhancing resilience of distribution systems,” *Renewable and Sustainable Energy Reviews*, vol. 152, p. 111636, 2021.
- [10] W. Yuan, J. Wang, F. Qiu, C. Chen, C. Kang, and B. Zeng, “Robust optimization-based resilient distribution network planning against natural disasters,” *IEEE Transactions on Smart Grid*, vol. 7, no. 6, pp. 2817–2826, 2016.
- [11] S. Ma *et al.*, “Resilience enhancement of distribution grids against extreme weather events,” *IEEE Transactions on Power Systems*, vol. 33, no. 5, pp. 4842–4853, 2018.
- [12] X. Wang, M. Shahidehpour, C. Jiang, and Z. Li, “Resilience enhancement strategies for power distribution network coupled with urban transportation system,” *IEEE Transactions on Smart Grid*, vol. 10, no. 4, pp. 4068–4079, 2018.
- [13] S. Ma *et al.*, “Resilience-oriented design of distribution systems,” *IEEE Transactions on Power Systems*, vol. 34, no. 4, pp. 2880–2891, 2019.
- [14] Y. Xu, C.-C. Liu, K. P. Schneider, and D. T. Ton, “Placement of remote-controlled switches to enhance distribution system restoration capability,” *IEEE Transactions on Power Systems*, vol. 31, no. 2, pp. 1139–1150, 2015.

- [15] J. Liu, Y. Yu, and C. Qin, “Unified two-stage reconfiguration method for resilience enhancement of distribution systems,” *IET Generation, Transmission & Distribution*, vol. 13, no. 9, pp. 1734–1745, 2019.
- [16] Q. Shi, F. Li, T. Kuruganti, M. M. Olama, J. Dong, X. Wang, and C. Winstead, “Resilience-oriented dg siting and sizing considering stochastic scenario reduction,” *IEEE Transactions on Power Systems*, vol. 36, no. 4, pp. 3715–3727, 2020.
- [17] Q. Zhang, Z. Wang, S. Ma, and A. Arif, “Stochastic pre-event preparation for enhancing resilience of distribution systems,” *Elsevier BV*, vol. 152, p. 111636, Dec. 2021.
- [18] S. Ma *et al.*, “Resilience Enhancement of Distribution Grids Against Extreme Weather Events,” *IEEE Transactions on Power Systems*, vol. 33, no. 5, pp. 4842–4853, 2018.
- [19] B. Taheri, A. Safdarian, M. Moeini-Aghetaie, and M. Lehtonen, “Distribution system resilience enhancement via mobile emergency generators,” *IEEE Transactions on Power Delivery*, vol. 36, no. 4, pp. 2308–2319, 2021.
- [20] P. W. Glynn and D. L. Iglehart, “Importance sampling for stochastic simulations,” *Management science*, vol. 35, no. 11, pp. 1367–1392, 1989.
- [21] R. Rush, J. M. Mulvey, J. E. Mitchell, and T. R. Willemain, “Stratified filtered sampling in stochastic optimization,” *Journal of Applied Mathematics and Decision Sciences*, vol. 4, no. 1, pp. 17–38, 2000.

- [22] D. Urgun, C. Singh, and V. Vittal, “Importance sampling using multilabel radial basis classification for composite power system reliability evaluation,” *IEEE Systems Journal*, vol. 14, no. 2, pp. 2791–2800, 2020.
- [23] R. Preece and J. V. Milanović, “Efficient estimation of the probability of small-disturbance instability of large uncertain power systems,” *IEEE Transactions on Power Systems*, vol. 31, no. 2, pp. 1063–1072, 2016.
- [24] F. D. Munoz, A. H. Van Der Weijde, B. F. Hobbs, and J.-P. Watson, “Does risk aversion affect transmission and generation planning? a western north america case study,” *Apollo - University of Cambridge Repository*, 2016.
- [25] S. Poudel, A. Dubey, and A. Bose, “Risk-Based Probabilistic Quantification of Power Distribution System Operational Resilience,” *IEEE Systems Journal*, vol. 14, no. 3, pp. 3506–3517, 2020.
- [26] A. Poudyal, A. Dubey, and S. Poudel, “A risk-driven probabilistic approach to quantify resilience in power distribution systems,” in *2022 17th International Conference on Probabilistic Methods Applied to Power Systems (PMAPS)*, pp. 1–6, 2022.
- [27] R. Khodabakhsh and S. Soroushpour, “Optimal control of energy storage in a microgrid by minimizing conditional value-at-risk,” *IEEE Transactions on Sustainable Energy*, vol. 7, no. 3, pp. 1264–1273, 2016.
- [28] T. Jiang, Q. Xia, Y. Wang, S. Chen, and Z. Wei, “Research on risk-based control strategy for power grid operation,” in *2021 IEEE Sustainable Power and Energy Conference (iSPEC)*, pp. 2815–2820, IEEE, 2021.

- [29] X. Yang, C. Xu, J. Lu, J. Wen, and Y. Zhang, “Risk-averse coordinated economic dispatching and voltage regulation in adns with on-site renewables and soft open points,” in *2021 IEEE Power & Energy Society General Meeting (PESGM)*, pp. 1–5, IEEE, 2021.
- [30] J. Wu and P. Wang, “Risk-averse optimization for resilience enhancement of complex engineering systems under uncertainties,” *Reliability Engineering & System Safety*, vol. 215, p. 107836, Nov. 2021.
- [31] S. Poudel, A. Dubey, and K. P. Schneider, “A generalized framework for service restoration in a resilient power distribution system,” *IEEE Systems Journal*, 2020.
- [32] A. Shapiro, D. Dentcheva, and A. Ruszczynski, *Lectures on stochastic programming: modeling and theory*. SIAM, 2021.
- [33] I. B. Sperstad, G. Kjølle, and E. Ø. Norum, “Accounting for uncertainties due to high-impact low-probability events in power system development,” *Electric Power Systems Research*, vol. 193, p. 107015, 2021.
- [34] D. P. Nedic, I. Dobson, D. S. Kirschen, B. A. Carreras, and V. E. Lynch, “Criticality in a cascading failure blackout model,” *International Journal of Electrical Power & Energy Systems*, vol. 28, no. 9, pp. 627–633, 2006.
- [35] R. N. Allan *et al.*, *Reliability evaluation of power systems*. Springer Science & Business Media, 2013.
- [36] A. Kwasinski, “Quantitative model and metrics of electrical grids’ resilience evaluated at a power distribution level,” *Energies*, vol. 9, no. 2, p. 93, 2016.

- [37] R. T. Rockafellar, S. Uryasev, *et al.*, “Optimization of conditional value-at-risk,” *Journal of risk*, vol. 2, pp. 21–42, 2000.
- [38] N. Noyan, “Risk-averse two-stage stochastic programming with an application to disaster management,” *Computers & Operations Research*, vol. 39, no. 3, pp. 541–559, 2012.
- [39] A. Poudyal, V. Iyengar, D. Garcia-Camargo, and A. Dubey, “Spatiotemporal impact assessment of hurricanes on electric power systems,” in *2022 IEEE Power Energy Society General Meeting (PESGM)*, pp. 1–5, 2022.
- [40] M. Panteli, C. Pickering, S. Wilkinson, R. Dawson, and P. Mancarella, “Power system resilience to extreme weather: fragility modeling, probabilistic impact assessment, and adaptation measures,” *IEEE Trans. Power Syst.*, vol. 32, no. 5, pp. 3747–3757, 2017.
- [41] M. D. Powell, S. H. Houston, and I. Ares, “Real-time damage assessment in hurricanes,” in *Preprints, 21st Conf. on Hurricanes and Tropical Meteorology, Miami, FL, Amer. Meteor. Soc*, pp. 500–502, 1995.
- [42] M. Panteli and P. Mancarella, “Modeling and Evaluating the Resilience of Critical Electrical Power Infrastructure to Extreme Weather Events,” *IEEE Systems Journal*, vol. 11, no. 3, pp. 1733–1742, 2017.
- [43] V. L. Parsons, “Stratified sampling,” *Wiley StatsRef: Statistics Reference Online*, pp. 1–11, Feb. 2017.
- [44] J. Ekblom and J. Blomvall, “Importance sampling in stochastic optimization: An

- application to intertemporal portfolio choice,” *European Journal of Operational Research*, vol. 285, no. 1, pp. 106–119, 2020.
- [45] H. Heitsch and W. Römisch, “A note on scenario reduction for two-stage stochastic programs,” *Operations Research Letters*, vol. 35, no. 6, pp. 731–738, 2007.
- [46] L. C. Coelho, “Linearization of the product of two variables,” *Canada Research Chair in Integrated Logistics*, 2013.
- [47] L. Gan and S. H. Low, “Convex relaxations and linear approximation for optimal power flow in multiphase radial networks,” in *2014 Power Systems Computation Conference*, pp. 1–9, 2014.
- [48] J.-P. Watson, D. L. Woodruff, and W. E. Hart, “Pysp: modeling and solving stochastic programs in python,” *Mathematical Programming Computation*, vol. 4, no. 2, pp. 109–149, 2012.

# CHAPTER 5

## RESILIENCE PLANNING TRADE-OFFS IN POWER DISTRIBUTION SYSTEMS

### 5.1 Introduction

This chapter introduces multi-resource trade-offs in making resilience planning decisions against extreme weather events. Similar to the prior chapter, a two-stage risk-averse framework is proposed, and conditional value-at-risk (CVaR) is used as a risk metric. For planning decisions, we propose using distributed generators (DGs) with grid-forming capabilities, line hardening, and automatic tie-switch placements. For the trade-off analyses, we look into the trade-offs due to data unavailability, budget, resource availability, and risk appetite of the grid planners.

#### 5.1.1 Motivation

Severe weather events, termed high-impact, low-probability (HILP) events, have tremendously affected electric power systems in the last few decades [1, 2]. Power distribution systems are often more affected by such events as they are highly vulnerable to extreme events than the bulk power grid. It is reported that there has been a 67% increase in power outages due to weather-related events since 2000, with 80% - 90% of outages resulting from failures in power distribution systems [3]. This has led to investments from utilities and stakeholders to enhance the resilience of the grid. However, resilience-driven planning remains challenging due to several uncertainties associated with the impact of the extreme weather event and associated trade-offs that the grid planners must navigate to meet the desired resilience goals.

### 5.1.2 Related Literature and Gaps

Existing distribution systems resilience planning models are primarily based on stochastic programming or robust optimization models. In [4], a robust optimization framework is proposed for resilience distribution systems planning against extreme weather events with line hardening and backup distributed generators (DGs). However, details on hardening strategies are lacking, and the work does not model the DG-assisted islanded operations in reducing outage risks. Moreover, planning measures are presented only for worst-case scenarios, potentially leading to overly cautious and costly planning solutions. Other works propose a resilience-driven two-stage stochastic optimization model with multiple planning decisions [5, 6]. The planning problem is formulated to minimize the operational cost and expected value of lost load. However, the DG-assisted island is not modeled. Additionally, both works use a generic fragility model for all line segments, overlooking the component-specific fragility of power conductors and poles subject to wind loading. In contrast, [7] discusses the resilience-oriented design of power distribution systems, including islanded DG operation and automatic switching. However, it introduces a virtual network model to simulate fault isolation, potentially adding complexity to the planning model. The planning models discussed above are based on simplified single-phase power distribution network models, which may not accurately represent the complexities of multi-phase unbalanced systems. Secondly, the works are focused on minimizing the expected cost with an equal probability of occurrence and do not include the risk of observing extreme weather events within the planning framework. Such methods may not adequately address resilience-oriented planning for HILP events.

One commonly used risk-based metric is Conditional value-at-risk (CVaR), widely

adopted in distribution systems planning [8, 9, 10, 11]. Although multiple resilience planning frameworks have been proposed, a majority of them do not analyze the planning trade-offs affecting resilient investment strategies. While some studies discuss the computational complexity related to the number of scenarios in stochastic optimization models, they do not demonstrate how the quality of planning decisions may vary based on the number of scenarios or other stochastic parameters [5]. Others recognize the need for risk-averse planning but do not justify the investment through trade-off analysis [9]. Given that resilience-based investments are costly for system operators, particularly for events that occur infrequently but cause substantial damage, it is essential to assess the trade-offs involved in resilience planning decisions thoroughly. This evaluation is critical for justifying the value of current investments in for potential future extreme weather scenarios. To tackle some of these issues, the work in [11] introduces a risk-based planning framework for power distribution systems with solution portfolios tailored to the risk preferences of the grid planner. However, it does not address the variable probability driven by extreme events within a region, considers a single-phase equivalent model of the distribution grid, and does not provide detailed trade-off analysis on planning decisions.

Grid planners often struggle to determine the best investment strategy for maximum resilience, relying on expert discussions, budget constraints, and the current system needs. While existing works offer planning tools to help operators make preliminary decisions, they often lack insights into why one investment portfolio is superior to another [1]. Additionally, these works are widely disconnected from industry planning practices, specific to grid hardening methods, and fail to address practical concerns that arise when planners must allocate their budget based on policy and

regulations.

### 5.1.3 Contribution

This chapter evaluates how optimal planning decisions vary based on multiple systems and optimization parameters. Detailed trade-off analysis is presented considering system fragility models, allocated budget, multiple planning resources such as grid-forming DGs, tie-switches, and line hardening, and the risk preference of the system operator. A two-stage risk-averse stochastic optimization framework, using CVaR as the risk measure, is formulated for multiple resources-based grid resilience planning for trade-off analysis. The model is validated on realistic historical wind gust data and realistic fragility models for utility wooden poles. This work extends our previous work in [1] and has the following major contributions:

1. Developed a two-stage stochastic programming model for multi-resource risk-based resilience planning in three-phase unbalanced power distribution systems. The planning decision includes siting and sizing grid-forming DGs, placing tie-switches, and installing grid hardening solutions. A heuristic approach is proposed to identify fault sectionalizers in the pre-processing step. A modeling approach is then introduced to incorporate them into the reconfiguration stage if the damaged components associated with the sectionalizers have been hardened.
2. Proposed a method based on kernel density estimation (KDE) to estimate regional wind density and its probability. Realistic fragility models for utility wooden poles are adopted for single and three-phase components to mimic the variation of fragility within a specific system. This work also provides discussion

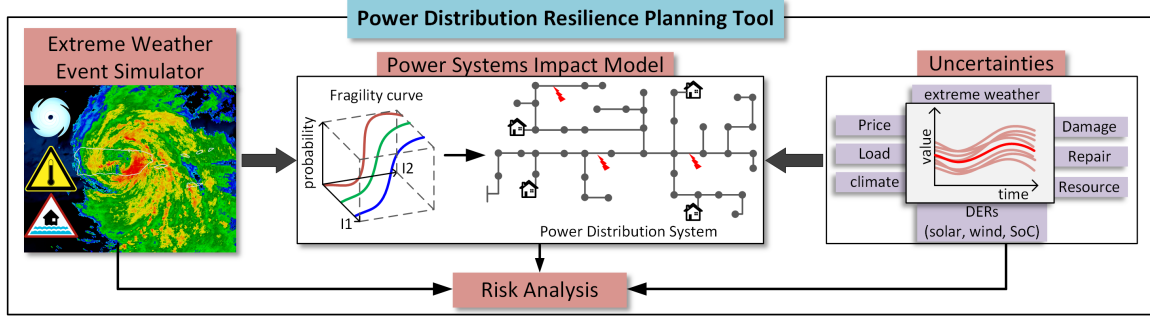


**Figure 5.1** Resilient distribution systems planning framework.

and details on the current and futuristic sustainable grid hardening practices, which can provide valuable insights to the grid planners.

3. Conducted a comprehensive trade-off analysis considering system fragility models, risk preferences, planning resources, and budget allocation.

## 5.2 System Modeling Requirements for Resilience Planning

This section details the system modeling requirements to develop the proposed risk-averse approach for resilient distribution system planning. Fig. 5.1 shows a high-level overview of the proposed resilience planning approach for power distribution systems. Notably, the planning solutions are highly sensitive to each module, and their accurate modeling can drastically improve the quality of the planning solutions.

### 5.2.1 Extreme Weather Events Simulator

Conventional physics and differential equation-based extreme event models can be computationally complex and challenging to integrate into planning tools. Data-driven models offer a promising alternative for creating realistic simulations [12, 13]. Given that most power distribution damages are attributed to wind events [14], we

focus on wind storms as extreme events in this work. Distribution systems cover a small region compared to the bulk power grid, so we assume a uniform wind gust distribution across the distribution grid for each event. Long-term investment planning requires several scenarios to be considered over a longer duration. Considering the lack of weather prediction models for longer horizons, we use regional historical wind gust data that can provide valuable insights into the typical wind patterns and speeds experienced in a region over time. Let  $\mathcal{U}$  represent the daily maximum wind gust as a random variable, then the probability density of  $\mathcal{U}$  can be estimated using Kernel Density Estimation (KDE) as [15]:

$$\hat{p}_{n,h}(\mathcal{U}) = \frac{1}{nh} \sum_{i=1}^n \mathcal{K}\left(\frac{\mathcal{U} - u_i}{h}\right) \quad (5.1)$$

where,  $\hat{p}_{n,h}(\mathcal{U})$  is the probability density estimate of  $\mathcal{U}$  parameterized by number of data points,  $n$ , and a bandwidth factor, also known as the smoothing factor,  $h$ . Here,  $\mathcal{K}(\cdot)$  is a non-negative kernel function. To assess the impact of each wind event scenario, we need to obtain the probability of realizing the corresponding event. Using the KDE from (5.1), the probability density function (PDF) of  $\mathcal{U}$ , can be written as,

$$p[u_a \leq \mathcal{U} \leq u_b] = \int_{u_a}^{u_b} \hat{p}_{\mathcal{U}}(u) du \quad (5.2)$$

where,  $\hat{p}_{\mathcal{U}}$  is the probability density of  $\mathcal{U}$  obtained from (5.1), and  $[u_a, u_b]$  defines the interval containing  $\mathcal{U}$ . Here,  $\mathcal{U}$  is continuous, making it challenging to discretize probability pertaining to wind gust scenarios as the probability of  $\mathcal{U}$  taking any value  $u$  is 0. Therefore, we first discretize the regional wind gust data to their nearest unique integers and consider a constant interval,  $u_b = u_a + \Delta u$ , such that the probability of realizing  $\mathcal{U}$  is the same within the interval  $\Delta u$ . This is a reasonable assumption as

the effect and occurrence of wind gusts are very close within a very small interval. Thus, (5.2) can be re-written to define the scenario probability as:

$$p(u) \approx p_{\mathcal{U}}(u) \times \Delta u \quad (5.3)$$

Eq. (5.3) can provide us with the approximate probability that a wind gust event scenario will be realized with a sustained wind gust value within  $\Delta u$ .

### 5.2.2 Distribution Systems Impact Model

Planning decisions rely heavily on the accuracy of the distribution system impact model, typically achieved through fragility curves. Obtaining accurate data on these factors can be challenging without collaboration with the electric power industry. In [16], component-level fragility models are statistically developed for 1-phase and 3-phase power distribution wooden poles and conductors, considering wind loading and falling trees. The models are based on wooden poles made from southern pine wood and aluminum conductor steel reinforced (ACSR) conductors commonly used in power distribution systems across the United States [17]. This work adopts the wind-loading-based model, where a logistic regression model is defined to obtain the failure probability of a pole or a conductor as:

$$P(u, \psi) = \frac{1}{1 + e^{-l(u, \psi)}} \quad (5.4)$$

where,

$$l(u, \psi) = b_0 + b_1 u + b_2 u \sin(\psi) \quad (5.5)$$

Here,  $b_0$ ,  $b_1$ , and  $b_2$  are regression coefficients corresponding to each component,  $u$  is the wind gust in miles per hour (mph), and  $\psi$  is the angle of attack of the wind gust

to the component. A line segment contains several poles and conductors connected in series. Hence, the line segment is assumed to fail if any conductor or pole within the line segment fails. Let  $P_p(u, \psi)$  be the failure probability of poles and  $P_c(u, \psi)$  be the failure probability of conductors. The line segment failure probability,  $P_l(u, \psi)$ , can hence be calculated using (6).

$$P_l(u, \psi) = 1 - \left( \prod_{p=1}^{N_p} (1 - P_p(u, \psi)) \prod_{c=1}^{N_c} (1 - P_c(u, \psi)) \right) \quad (5.6)$$

### 5.2.3 Modeling Different Uncertainties

Planning for resilience inherently involves appropriately modeling multiple uncertainties, as depicted in Fig. 5.1. Important factors that need to be carefully represented include load variability, the probability of observing an extreme weather event, and power generation from DGs. For instance, predicting load fluctuations requires robust forecasting models, while weather models for extreme events are sophisticated and data-dependent. DGs, affected by weather and consumer behavior, also pose modeling challenges. Damage scenarios, repair time, and resource availability are also uncertain but vital for planning. Obtaining data, such as historical repair time or fuel availability for generators, may be limited for various reasons, including data unavailability and confidentiality issues. This work addresses uncertainty in power distribution component damage due to various weather event scenarios. The weather event is analyzed using the wind profile, while fragility models, as discussed earlier, are used to assess the impact of the wind event on the distribution grid.

#### **5.2.4 Risk Analysis**

Risk analysis is often overlooked in power distribution planning, with grid planners primarily focusing on the expected events or credible scenarios. However, integrating risk analysis into planning tools can significantly improve the resilience of the distribution system [9, 8]. Risk analysis enables decision-makers to identify and prioritize critical areas for system upgrades to specifically reduce the outage risks due to extreme events. However, conducting risk analysis requires accurate data on the likelihood and severity of different events, which may be challenging. Additionally, effective risk analysis relies on modeling techniques that can appropriately incorporate uncertainties and dependencies among different risk factors. Nevertheless, integrating risk analysis into the planning problem is needed to represent stakeholder's interests and cost-benefit tradeoffs appropriately. This work uses CVaR as the risk measure, formulated as a linear and convex optimization model in a two-stage stochastic optimization setting [18]. By incorporating risk within the planning framework, grid planners can evaluate the cost-benefit tradeoffs of different system upgrade solutions in improving grid resilience against extreme weather events.

### **5.3 Methodology**

This section discusses the overall problem formulation and simulation framework for multi-resource resilience planning. The planning decisions and general assumptions made in this work are also discussed.

### 5.3.1 Planning Decisions and Assumptions

This work considers three planning decisions: siting and sizing of grid-forming DGs capable of islanded operation to serve critical loads, installing tie-switches capable of proving alternate restoration paths, and implementing line hardening solutions, as shown in Fig. 5.2. The grid-forming DGs provide voltage slack to the connected microgrid using a concept of virtual edge, which is modeled as a non-physical zero impedance line as proposed in [19]. Fig. 5.2 shows the distribution model representation with the planning decisions. The faults in islands 2 and 3 trigger the operation of DG to pick up loads in island 1. Another planning decision is installing toe-switches. Practically, this decision requires adding a distribution line, which introduces additional cost if the distance between candidate nodes is large. However, we assume the grid planners have identified candidate nodes closer to the system where the distribution lines along with tie-switches can be added. This assumption can be easily relaxed, and distance can be introduced as an additional factor if more information on the grid coordinates is available. In Fig. 5.2, the tie-switches are not activated, either due to fault isolation or to prevent the formation of loops. However, if there was no fault in island 2, closing the bottom two tie switches could allow the substation to pick up loads in both island 1 and island 2.

In [17], two strategies are proposed to enhance the resilience of distribution systems, depicted in Fig. 5.2. Strategy A is to upgrade the existing utility pole to a higher class without changing the pole span, and Strategy B is to decrease the pole span length. Strategy B increases the number of poles in a line segment compared to Strategy A. However, the reduced span length allows the wind load to be distributed among multiple poles and conductors. This enables utilities to use lower-class poles

while maintaining an acceptable bending moment against extreme weather conditions. For instance, according to Rule 250 C, a standard guide for wind loading in utility wooden poles, 40 ft Class 3 poles can withstand extreme wind conditions up to 120 mph with a span of 150 ft. However, with a span of 250 ft., only Class 1 poles can sustain the bending moment of extreme wind events with sustained gusts of 120 mph [17]. The cost per mile and individual pole costs are comparable among higher and lower poles. Hence, the current utility practice leans towards increasing the pole classes for the same span and design grade [17]. In this work, we adhere to this practice and assume all the poles and conductors are upgraded within a hardened line segment. It is important to note that this strategy may change in the future based on the cost-benefit analysis of one strategy over the other, which is beyond the scope of this work.

### 5.3.2 Problem Formulation

Existing works on resilience-driven planning minimize the investment planning cost in the first stage and operational cost in the second stage using the value of lost load (VoLL) to model the cost of load lost due to an extreme event [5]. However, VoLL is multi-dimensional, and a single-point estimate of VoLL cannot fully capture the value of demand lost within the distribution system being studied [20]. Therefore, we propose incorporating planning costs as a constraint to reflect the system operator's budget. This approach allows system operators to identify a portfolio of planning decisions aligned with their budgetary constraints. The multi-resource resilience planning problem against extreme weather events is formulated as a two-stage stochastic MILP model. The overall planning objective is to minimize the weighted

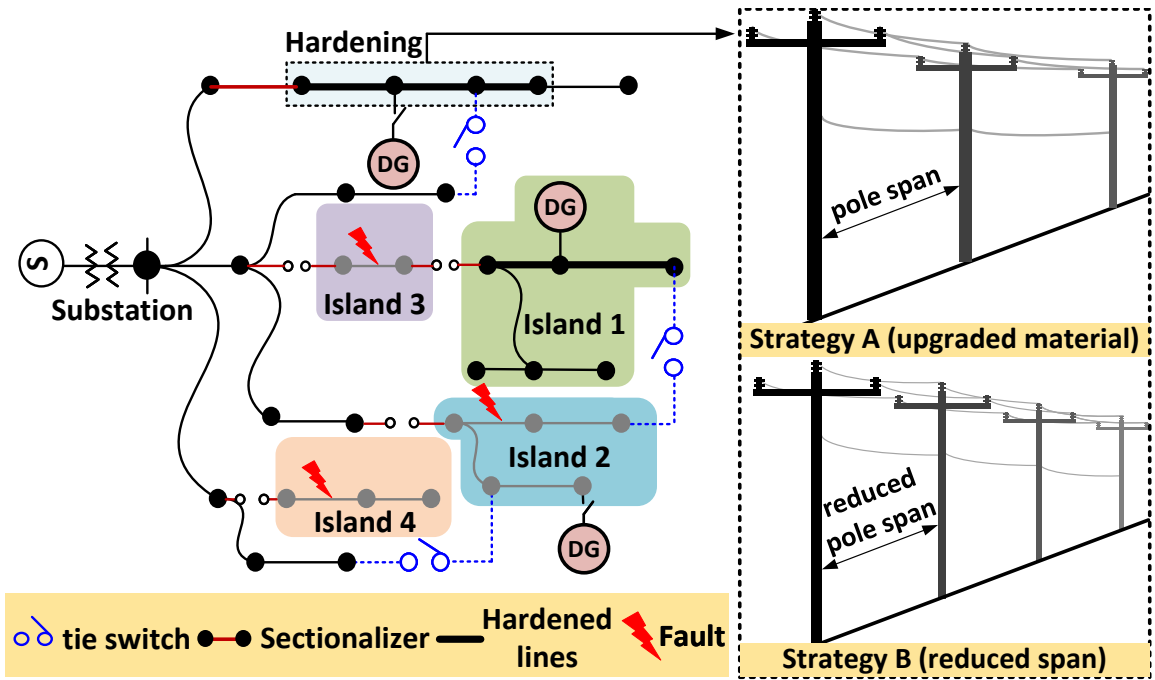


**Figure 5.2** Planning decisions and strategies for resilience enhancement in power distribution systems.

sum of expected value and CVaR of the second stage cost, which can be written as:

$$\min \quad (1 - \lambda) \mathbb{E} \left( Q(\mathbb{X}, \mathcal{E}) + \frac{1}{1 - \lambda} \mathcal{G}(\delta, \mathcal{E}) \right) + \lambda CVaR_\alpha(Q(\mathbb{X}, \mathcal{E})) \quad (5.7)$$

where,

$$\begin{aligned} \mathbb{E}(Q(\mathbb{X}, \mathcal{E})) &:= \left( \sum_{\xi \in \mathcal{E}} \sum_{i \in \mathcal{B}_S} \sum_{\phi \in \{a, b, c\}} p^\xi (1 - s_i^\xi) w_i P_{Li}^\phi \right) \\ CVaR_\alpha(Q(\mathbb{X}, \mathcal{E})) &:= \left( \eta + \frac{1}{1 - \alpha} \sum_{\xi \in \mathcal{E}} p^\xi \nu^\xi \right) \\ \mathbb{E}(\mathcal{G}(\delta, \mathcal{E})) &:= \sum_{\xi \in \mathcal{E}} p^\xi \left( \chi_1 \sum_{e \in \mathcal{L}_S^t \cup \hat{\mathcal{L}}_S^t} \delta_e^\xi + \chi_2 \sum_{e \in \mathcal{L}_S^v} \delta_e^\xi \right) \end{aligned}$$

Here,  $\mathbb{X} = [x_i^{DG} \beta_i^{DG}, x_e^h, x_e^s]$  is a set of first-stage planning decisions for siting ( $x_i^{DG} \in \{0, 1\}$ ) and sizing ( $\beta_i^{DG} \in \mathbb{R}^+$ ) of DGs, line hardening ( $x_e^h \in \{0, 1\}$ ), and

automatic tie switch placements ( $x_e^s \in \{0, 1\}$ ), respectively.  $\mathbb{E}(Q(\mathbb{X}, \mathcal{E}))$  is the expected value of the second stage, which is a prioritized load restoration problem for each scenario  $\xi$ , with an associated probability of occurrence,  $p_\xi$ .  $P_{Li}^\phi$  is the active power demand for each phase  $\phi$  in node  $i$ . Some of the loads are prioritized with a weight variable,  $w_i$ . The variable  $s_i^\xi \in \{0, 1\}$  determines the load pickup status for each  $i$  in  $\xi$ . Similarly,  $CVaR_\alpha(Q(\mathbb{X}, \mathcal{E}))$  is the CVaR of the second stage problem with a confidence level of  $\alpha$ , value-at-risk (VaR)  $\eta \in \mathbb{R}$ , and CVaR excess variable  $\nu^\xi \in \mathbb{R}^+$  for each  $\xi$ . The risk preference factor  $\lambda$  introduces the grid operator's risk appetite within the planning framework. For risk-neutral planning,  $\lambda = 0$  and  $\lambda = 1$  signifies risk-averse planning. Appropriate values of  $\lambda$  can highlight the inclusion of HILP events within the decision-making framework [21]. The term  $\mathbb{E}(\mathcal{G}(\delta, \mathcal{E}))$  in the objective function prevents unnecessary switching of tie and virtual switches for reconfiguration. Assigning very low weights to  $\chi_1$  and  $\chi_2$  ensures that load restoration is prioritized for each  $\xi$  as suggested in [19].

### First-stage constraints

$$\sum_{i \in \mathcal{B}_{DG}} c_i^{DG} x_i^{DG} \beta_i^{DG} + \sum_{e \in \mathcal{L} \setminus \hat{\mathcal{L}}_S^t} c_e^h x_e^h + \sum_{e \in \hat{\mathcal{L}}_S^t} c_e^s x_e^s \leq \mathcal{C}_{max}^T \quad (5.8)$$

$$\begin{aligned} \sum_{i \in \mathcal{B}_{DG}} c_i^{DG} x_i^{DG} \beta_i^{DG} &\leq \mathcal{C}_{max}^{DG}, \quad \sum_{e \in \mathcal{L}} c_e^h x_e^h \leq \mathcal{C}_{max}^h, \\ \sum_{e \in \hat{\mathcal{L}}_S^t} c_e^s x_e^s &\leq \mathcal{C}_{max}^s \end{aligned} \quad (5.9)$$

$$\bar{x}_e^s + x_e^s = \hat{x}_e^s, \quad \forall e \in \mathcal{L}_S \cup \hat{\mathcal{L}}_S^t \setminus \mathcal{L}_S^v, \quad (5.10a)$$

$$x_j^{DG} = \hat{x}_e^s, \quad \forall e \in \mathcal{L}_S^v \quad (5.10b)$$

The first-stage constraints can be represented by (5.8) - (5.10). Constraint (5.8) ensures that the total cost of DG siting and sizing, line hardening, and switch placement does not exceed the total planning budget,  $\mathcal{C}_{max}^T$ . The bi-linear term  $x_i^{DG}\beta_i^{DG}$  is linearized using big-M method as described in [22]. Alternatively, we can constrain each resource's budget individually if requirements are known, as shown in (5.9). This approach allows grid operators the flexibility to prioritize investment in a specific resource, which may be desired due to policy or regulation changes, even if it does not offer the greatest resilience enhancement. In this work, we assume that the investment resources are of the same type, allowing us to cap the number of investments for each resource type and thus limit the budget for the resource. Let  $\mathcal{N}_{max}^h$  be the total number of lines that can be hardened,  $\mathcal{N}_{max}^s$  is the total number of switches that can be installed, and  $\beta_{max}^{DG}$  is the maximum size of a DG unit that can be invested in a location. In (5.10),  $\hat{x}_e^s$  indicates whether a switch exists in a line. Here,  $x_e^s$  is a switch placement decision variable, and  $\bar{x}_e^s$  is an external parameter indicating a pre-existing switch in a line. A similar constraint is represented in (5.10b) for virtual switches; a virtual switch exists if a DG is invested in a node  $j$  such that  $e : \mathbf{i}_{sub} \rightarrow j$ . Here,  $\mathbf{i}_{sub} \in \mathcal{B}_{sub}$  is the substation node and  $j \in \mathcal{B}_{DG}$  is the candidate DG node.

## Second Stage Constraints

The second stage is the prioritized load restoration problem solved for each scenario  $\xi$ . Each of the resources participates in the second stage if they are invested.

### Connectivity constraints:

$$s_i^\xi \leq v_i^\xi, \quad \forall i \in \mathcal{B}_S \quad (5.11a)$$

$$s_i^\xi = v_i^\xi, \forall i \in \mathcal{B} \setminus \mathcal{B}_S \quad (5.11b)$$

$$\delta_e^\xi \leq v_i^\xi, \delta_e^\xi \leq v_j^\xi, \forall e \in \mathcal{L}_S \cup \{\hat{\mathcal{L}}_S^t, \mathcal{L}_S^v\} \quad (5.12)$$

$$\delta_e^\xi \leq \hat{x}_e^s, \forall e \in \mathcal{L}_S \cup \{\hat{\mathcal{L}}_S^t, \mathcal{L}_S^v\} \quad (5.13)$$

- The constraint in (5.11) guarantees that a load is picked up only when its corresponding bus,  $v_i$ , is energized. Similarly, (5.12) ensures the energization of a switchable line if any of its corresponding buses is energized. Here,  $\mathcal{L}$ ,  $\hat{\mathcal{L}}_S^t$ , and  $\mathcal{L}_S^v$  are the set of switchable lines, candidate tie lines, and virtual edges respectively.
- Constraint (5.13) ensures that a switchable line can be toggled if and only if a switch exists. The switch existence variable,  $\hat{x}_e^s$  is guided by (5.10), such that  $\hat{x}_e^s = 1$  if there is a pre-existing switch ( $\bar{x}_e^s = 1$ ), or a new tie-switch is invested ( $x_e^s = 1$ ) or a virtual switch is available due to a DG placement ( $x_i^{DG} = 1, e : \mathbf{i}_{sub} \rightarrow i$ ).

### Fault and Switching constraints:

- Constraint (5.14a) ensures that a line is not damaged if it is hardened. Here,  $\pi_e^\xi$  is an exogenous parameter that determines the line damage status based on an extreme event scenario. If the line is hardened,  $x_e^h = 1$ , then we assume that the line is not damaged  $\gamma_e^\xi = 0$  for scenario  $\xi$ . While hardening improves the fragility of the line segment, it is important to reflect on such an analysis using the concept of endogenous probability, which is beyond the scope of this work. As discussed earlier, upgrading a pole class can significantly improve the bending moment against

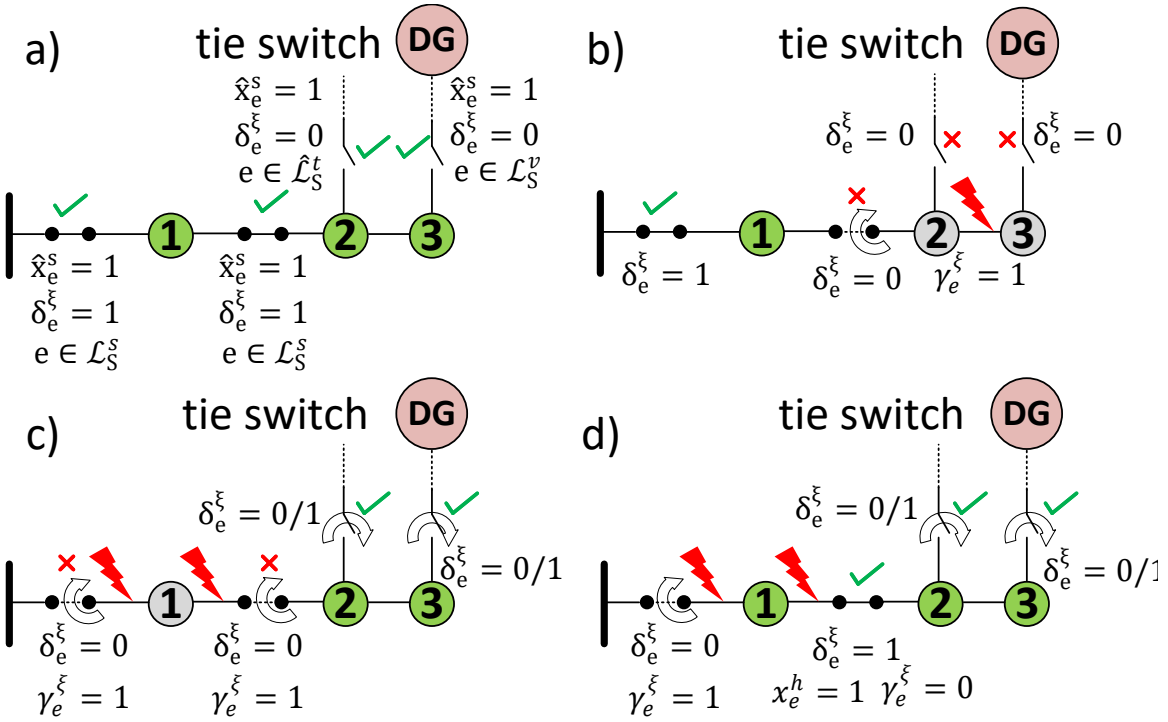


**Figure 5.3** Switch operation and status for normal and damaged conditions.

extreme wind conditions. Hence, the assumption that a hardened line will not be damaged in several extreme wind scenarios is not completely invalid. Constraint (5.14b) ensures that the existing switchable lines with damage can be toggled if they are hardened.

A heuristic method based on graph traversal is developed to obtain switches associated with each line, detailed in Algorithm 1. For each non-switchable line, we traverse upstream and downstream until every switch associated with the line is found. Virtual and candidate tie switches are also considered during fault isolation, as the faulted section should never be energized. Hence, this method prevents newly installed tie switches and DGs from potentially energizing faulted parts of the network for specific scenarios. To incorporate the effect of line hardening, we

---

**Algorithm 1:** Heuristic approach to identify switches associated with each line.

---

1 Model the distribution grid as a graph  $G(N, E)$  with nodes  $N$  and edges

$$E = (a, b)$$

2 Let  $\mathbf{L}_S = \mathcal{L}_S \cup \{\mathcal{L}_S^v, \hat{\mathcal{L}}_S^t\}$

3 **for** each  $(a, b) \in E$  **do**

4     // let the first upstream edge of  $a$  is  $(a', a)$

5     test-edge-up =  $(a', a)$

6     **if**  $test\text{-}edge\text{-}up \in \mathbf{L}_S$  **then**

7         switches[(( $a, b$ )].append = test-edge-up

8     **else**

9         traverse recursively until a switch is found

10   **end**

11   // let the first downstream edge of  $b$  is  $(b, b')$

12   repeat 5-10 for test-edge-down =  $(b, b')$

13 **end**

---

ensure that if the line is hardened, the switches associated with the line can re-participate in network reconfiguration for maximum load restoration. The fault sectionalization logic is represented by constraint (5.14c), ensuring that switches associated with damaged lines must remain open unless the damaged line is hardened or until repaired. Fig. 5.3 a) represents the normal operating condition where the substation serves all the load. In Fig. 5.3 b) line 2-3 is damaged with fault,  $\gamma_{2 \rightarrow 3}^\xi = 1$ . Hence, all the associated switches should remain out of service until the damage is repaired, which puts nodes 2 and 3 out of service. This triggers the sectionalizer between 1 and 2 to open and prevents the flow from the invested line with tie switch and DG. Fig. 5.3 c) and d) represent a multi-fault condition between the substation and node 1 and between node 2 and node 3. The associated sectionalizing switches isolate the faulted section, node 1. However, node 2 and node 3 can get energized via the line with the closed operation of the tie switch or islanded DG operation installed in node 3. If the line between node 1 and node 2 is hardened,  $x_{1 \rightarrow 2}^h = 1$ , then  $\delta_{1 \rightarrow 2}^\xi$  can participate in reconfiguration such that node 1 can be picked up.

$$\gamma_e^\xi = (1 - x_e^h)\pi_e^\xi, \quad \forall e \in \mathcal{L} \setminus (\hat{\mathcal{L}}_S^t \cup \mathcal{L}_S^v) \quad (5.14a)$$

$$\delta_e^\xi \leq (1 - \gamma_e^\xi) + x_e^h, \quad \forall e \in \mathcal{L}_S \quad (5.14b)$$

$$\delta_e^\xi \leq (1 - \gamma_e^\xi) + x_e^h, \quad \forall e \in \mathcal{L} \setminus \mathcal{L}_S, \forall e \in \mathcal{L}_S^e \quad (5.14c)$$

**Power Flow Constraints:** This work uses a three-phase linearized power flow model for an unbalanced distribution system [23]. To ensure the feasibility of our model and prevent power flow in faulted sections of the network, we integrate this power flow model with a range of energization and switch variables.

- The three-phase unbalanced linearized power flow model for power distribution systems is represented by constraints (5.15a) - (5.15d). Constraints (5.15a) and (5.15b) indicate the active and reactive power flow for each line. The per phase demand on each node,  $P_{Lj}^{\Phi,\xi}, Q_{Lj}^{\Phi,\xi}$ , is coupled with the load pick-up variable,  $s_j^\xi$ , such that the incoming flow in each node  $j$  is the sum of its outgoing flow and demand on node  $j$  if  $s_j^\xi = 1$ . Constraint (5.15c) is the voltage balance equation for non-switchable lines, which is coupled with  $\gamma_e^\xi$  such that if a line is damaged,  $\gamma_e^\xi = 1$ , then the voltage on the corresponding node is unconstrained. Similarly, the voltage balance equation in (5.15d) is coupled with two variables,  $\delta_e^\xi$  and  $\hat{x}_e^s$  for switchable lines such that the voltage drop is valid when a switch exists,  $\hat{x}_e^s = 1$ , and it is closed,  $\delta_e^\xi = 1$ .

$$\sum_{e:(i,j) \in \mathcal{L}} \mathbf{P}_e^\xi = s_j^\xi \mathbf{P}_{Lj}^\xi + \sum_{e:(j,i) \in \mathcal{L}} \mathbf{P}_e^\xi \quad (5.15a)$$

$$\sum_{e:(i,j) \in \mathcal{L}} \mathbf{Q}_e^\xi = s_j^\xi \mathbf{Q}_{Lj}^\xi + \sum_{e:(j,i) \in \mathcal{L}} \mathbf{Q}_e^\xi \quad (5.15b)$$

$$\begin{aligned} U_j^\xi - (\tilde{\mathbf{r}}_e \mathbf{P}_e^\xi + \tilde{\mathbf{x}}_e \mathbf{Q}_e^\xi) - \gamma_e^\xi M_U &\leq U_i^\xi \leq U_j^\xi - (\tilde{\mathbf{r}}_e \mathbf{P}_e^\xi + \tilde{\mathbf{x}}_e \mathbf{Q}_e^\xi) \\ &+ \gamma_e^\xi \overline{M}_U, \quad \forall e \in \mathcal{L} \setminus \mathcal{L}_S \cup \{\hat{\mathcal{L}}_S^t, \mathcal{L}_S^v\} \end{aligned} \quad (5.15c)$$

$$\begin{aligned} U_j^\xi - (\tilde{\mathbf{r}}_e \mathbf{P}_e^\xi + \tilde{\mathbf{x}}_e \mathbf{Q}_e^\xi) - (1 - \gamma_e^{s,\xi} + 1 - \hat{x}_e^s) M_U &\leq U_i^\xi \\ &\leq U_j^\xi - (\tilde{\mathbf{r}}_e \mathbf{P}_e^\xi + \tilde{\mathbf{x}}_e \mathbf{Q}_e^\xi) + (1 - \gamma_e^{s,\xi} + 1 - \hat{x}_e^s) \overline{M}_U, \\ &\quad \forall e \in \mathcal{L}_S \cup \{\hat{\mathcal{L}}_S^t, \mathcal{L}_S^v\} \end{aligned} \quad (5.15d)$$

where

$$\tilde{\mathbf{r}}_e = \begin{bmatrix} -2r_{ij}^{aa} & r_{ij}^{ab} - \sqrt{3}x_{ij}^{ab} & r_{ij}^{ac} + \sqrt{3}x_{ij}^{ac} \\ r_{ij}^{ba} + \sqrt{3}x_{ij}^{ba} & -2r_{ij}^{bb} & r_{ij}^{bc} - \sqrt{3}x_{ij}^{bc} \\ r_{ij}^{ca} - \sqrt{3}x_{ij}^{ca} & r_{ij}^{cb} + \sqrt{3}x_{ij}^{cb} & -2r_{ij}^{cc} \end{bmatrix}$$

$$\tilde{\mathbf{x}}_e = \begin{bmatrix} -2x_{ij}^{aa} & x_{ij}^{ab} + \sqrt{3}r_{ij}^{ab} & x_{ij}^{ac} - \sqrt{3}r_{ij}^{ac} \\ x_{ij}^{ba} - \sqrt{3}r_{ij}^{ba} & -2x_{ij}^{bb} & x_{ij}^{bc} - \sqrt{3}x_{ij}^{bc} \\ x_{ij}^{ca} + \sqrt{3}r_{ij}^{ca} & x_{ij}^{cb} - \sqrt{3}r_{ij}^{cb} & -2x_{ij}^{cc} \end{bmatrix}$$

**Operational Constraints:** The operational constraints of the power distribution system relate to the operational topology, power flow limits, and voltage limits in all active nodes of the network.

- In distribution systems, radial configurations are guided by the normally closed sectionalizing switches and tie-switches in the network such that there are no loops in the entire network. In this work, we introduce additional tie-switches and DG-based planning decisions, which can introduce additional loops in the system. Constraint (5.16) ensures that at least one of the switches is open in each cycle. Since we bound the number of tie switches and DG investments with candidate locations, the loop enumeration method can be done offline, which does not affect the optimization procedure.
- The ANSI C84.1 standard limits the voltage in each node to be within [0.95, 1.05]. Constraint (5.17) limits the voltage of each energized node as guided by  $v_i^\xi$ . Similarly, constraint (5.18) maintains a reference voltage in substation nodes.
- Constraint (5.19) ensures zero power flow through an open line. For non-switchable lines, Constraint(5.19a) is coupled with  $\gamma_e^\xi$  such that the flow is zero if  $\gamma_e^\xi = 1$ . Similarly, for switchable lines, the flow limit in (5.19b) is coupled with switch variables such that if a switch exists  $\hat{x}_e^s = 1$  and it is open  $\delta_e^\xi = 0$ , then the power flow in the open line  $e : i \rightarrow j$  is 0. The flow limit is constrained by their respective limits,  $M_p$  and  $M_q$  for closed lines.

$$\sum_{e \in \mathcal{L}_c} \delta_e^\xi \leq |\mathcal{L}_c| - 1, \quad \forall e \in \mathcal{L}_c \quad (5.16)$$

$$v_i^\xi \mathbf{U}^{min} \leq \mathbf{U}_i^\xi \leq v_i^\xi \mathbf{U}^{max}, \quad \forall i \in \mathcal{B} \quad (5.17)$$

$$\mathbf{V}_i^\xi \leq V_{ref}, \quad \forall i \in \mathcal{B}_{sub} \quad (5.18)$$

$$(1 - \gamma_e)^\xi [\underline{M}_p \ \underline{M}_q] \leq [\mathbf{P}_e^\xi \ \mathbf{Q}_e^\xi] \leq (1 - \gamma_e)^\xi [\overline{M}_p \ \overline{M}_q], \quad \forall e \in \mathcal{L} \setminus \mathcal{L}_S \cup \{\hat{\mathcal{L}}_S^t, \mathcal{L}_S^v\} \quad (5.19a)$$

$$(\gamma_e^{s,\xi} + 1 - \hat{x}_e^s) [\underline{M}_p \ \underline{M}_q] \leq [\mathbf{P}_e^\xi \ \mathbf{Q}_e^\xi] \leq (\gamma_e^{s,\xi} + 1 - \hat{x}_e^s) [\overline{M}_p \ \overline{M}_q], \quad \forall e \in \mathcal{L}_S \cup \{\hat{\mathcal{L}}_S^t, \mathcal{L}_S^v\} \quad (5.19b)$$

### DG Constraints:

- The DGs have a grid-forming capability and can form islanded microgrids when the service from the upstream substation is disrupted if required. Constraint (5.20) ensures that the maximum flow on the virtual edge corresponding to each DG unit is less than or equal to its sizing decision,  $\beta_i^{DG}$ , for each scenario  $\xi$ .

$$\sum_{\phi \in \{a,b,c\}} P_e^{\phi,\xi} \leq \delta_e^\xi x_i^{DG} \beta_i^{DG}, \quad \forall e \in \mathcal{L}_S^v, \forall i \in \mathcal{B}_{DG} \quad (5.20)$$

**CVaR <sub>$\alpha$</sub>  Constraints:** Constraint (6.20) bounds the CVaR excess variable,  $\nu$ , to consider scenarios greater than VaR,  $\eta$ . Here,  $\eta$  is the first stage decision variable which is consistent for all scenarios. Hence, the confidence level  $\alpha$  determines the portion of distribution for  $\nu$ . Furthermore,  $\nu$  must be a positive real number for loss-based distributions.

$$\nu_\xi \geq Q(\mathbb{X}, \xi) - \eta, \quad \nu \in \mathbb{R}_+^n \quad (5.21)$$

### 5.3.3 Scenario Generation and Reduction

This section discusses the process of generating stochastic damage scenarios. The regional historical wind gust data are collected from the weather station database, and an appropriate PDF is estimated using (5.1) and (5.2). The wind event scenarios and respective probability of occurrence are obtained from (5.3). Then, fragility models are developed for each line segment based on (5.4)-(5.6). Selective Monte Carlo simulations (MCS) are conducted to observe failure scenarios due to the probabilistic nature of damage scenarios and extreme wind conditions. While traditional scenario generation methods primarily rely on random sampling of extreme wind events, they often overlook wind events corresponding to tail events due to their lower probability. To address this limitation, various sampling techniques, such as stratified and importance sampling, have been proposed to sample HILP events [24]. This work uses an event-driven scenario generation and selection approach as proposed in [10]. First, MCS is conducted for each wind gust  $u$  to generate damage scenarios. This is similar to creating strata of each wind gust and conducting simulations. This ensures that all wind gust conditions are included in the scenario generation phase. Let  $N_{\xi,u}$  be the total number of Monte-Carlo trials for each  $u$  and  $\mathcal{L}_u = \mathbb{E}(\mathcal{L}_{\xi,u})$  be the expected system loss corresponding to each  $u$ . The loss refers to the total prioritized load isolated from the system as a result of faults due to component damages. Unlike our previous work in [1], we introduce the operation of sectionalizing switches, which can isolate the faulted parts of the network. The prioritized load loss is calculated for nodes isolated from the main network. These scenarios represent base case scenarios without additional planning measures. A total of  $N_{\xi,u} \times N_u$  scenarios are generated, where  $N_u$  corresponds to the number of unique discrete wind gust values in a region

and is automatically identified from the probability assessment method discussed in Section 5.2.1. Hence,  $N_u$  is larger for regions with higher variation in wind conditions than regions with very low variation in wind conditions. Next, for each  $u$ , a representative scenario  $\xi_u$  is selected to be closest to the converged Monte-Carlo loss for the specific  $u$ . In other words, the objective for scenario selection is to select a scenario  $\xi_u$  for each  $u$  such that  $|\mathcal{L}_u - \mathcal{L}_{\xi}|$  is minimum. In the case of multiple selections, one scenario is selected randomly. Hence, this method reduces the number of scenarios to  $N_u$  from  $N_{\xi,u} \times N_u$  scenarios. More discussions on scenario generation and selection strategy with detailed case studies are presented in [10].

#### 5.4 Results and Analysis

In this section, we discuss the validation of the proposed approach and conduct an in-depth trade-off analysis of the resilience planning decisions. The proposed approach is validated on a modified IEEE-123 bus system, as shown in Fig. 5.4. The test case contains two existing tie-switches, and we include 13 sectionalizing switches that can assist in fault isolation and reconfiguration of the networks. The system also consists of underground lines, which are assumed to be insusceptible to wind damage. The system's total non-prioritized active power demand is 4485 kW whereas the prioritized active power demand,  $\sum_i w_i P_{Li}$ , is 11725 kW for  $w_i = 5$ . The risk-averse two-stage optimization model is formulated using the PySP module in Pyomo [25] and solved as a large MILP problem using off-the-shelf solvers with mipgap of  $1e^{-3}$ .

For investment, five candidate lines are selected for tie-switch placement. Due to the lack of geographical coordinates information on the test case, we assume a constant length of 150 ft for the distribution line that should be installed along with

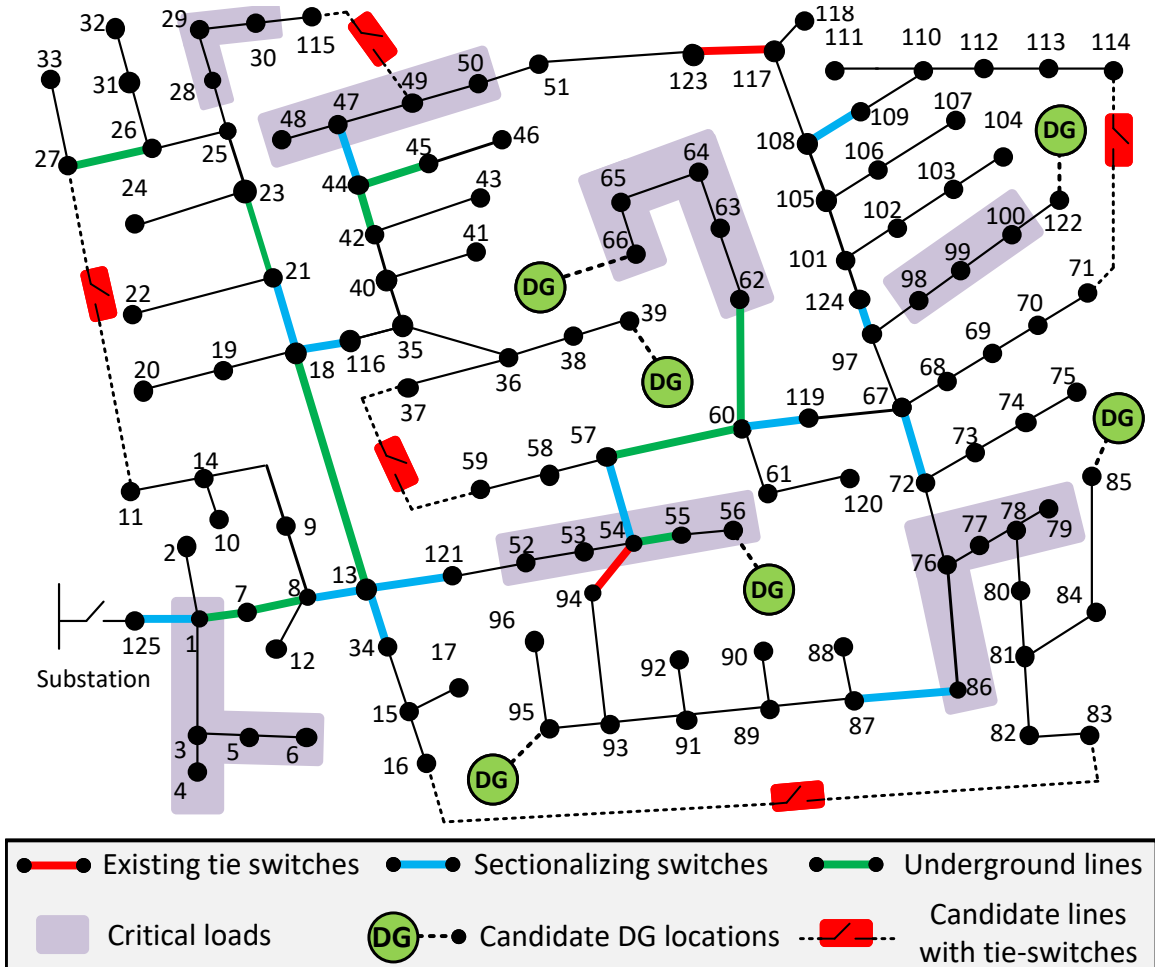


**Figure 5.4** Modified IEEE-123 bus test system.

tie-switches. Similarly, we assume candidate DG locations where grid-forming DGs with islanding capabilities can be sited. For line hardening, we assume each line is a potential candidate for hardening. The poles in each line segment are assumed to have a constant span of 150 ft. Considering that most utility wooden poles in the United States are 40 ft Class 4 (40/4) [16], in which more than 80% are made from Southern Yellow Pine [17], we assume all the poles in the system are of Class 40/4 made from the same material. For upgrading the pole, we propose upgrading each of the poles

**Table 5.1** Resilience Planning Investment Costs

Investment Strategy		Cost (\$)	Ref
Distribution lines with tie-switches	line installation	100/ft.	-
	tie-switch placement	15000/unit	[5]
Line Hardening	1-phase segment	75/ft.	-
	3-phase segment	126/ft.	[26, 17]
DG installation	Natural gas microturbine units	920/kW	[27]

to Class 40/3 such that the upgrades also require the reconductoring of conductors. Table 5.1 provides the cost breakdown of each resource investment. The DGs and tie-switches are assumed to be of a 3-phase configuration. The DGs are assumed to be natural gas microturbine units with variable capacity for demonstration. For 1-phase segments, the cost of hardening is assumed to be 60% of the cost for 3-phase segments, considering the similar amount of labor hours.

#### 5.4.1 Wind and Fragility Models

The region of study is focused in Fort Myers, Florida, where the wind gust data from January 1, 2010, to December 31, 2023, is obtained using a historical weather API platform [28]. We extract daily maximum wind gusts above 10 meters from the ground. The probability density of the wind gust data is estimated using (5.1) with Gaussian kernels and  $h = 0.35$ . Upon testing different values of  $h$ ,  $h = 0.35$  provided a better trade-off on smoothness vs fit on the actual data distribution. Fig. 5.5(a) represents the histogram and KDE of the wind gusts with a few days having maximum

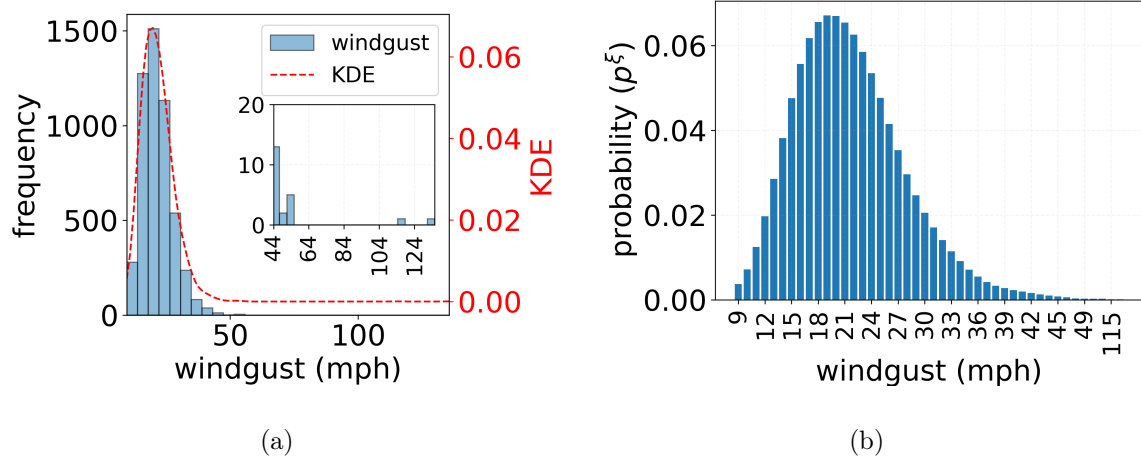


**Figure 5.5** a) Historical wind gust data in Fort Myers, Florida, and its density estimate with Gaussian kernel. b) Wind gust scenario probability estimation.

wind gusts above 100 mph, representing HILP scenarios. The probability of the wind gust scenarios, represented in Fig. 5.5(b), is obtained using (5.3). We consider  $\Delta u = 1$  mph to compute  $p(u)$  assuming that the variation and impact of the wind gust event remain the same within a range of 1 mph. The fragility of 1-phase and 3-phase line segments with Class 40/4 wooden poles and ACSR conductors are shown in Fig. 5.6(a). The fragility models for poles and conductors are separately derived using (5.6) based on their individual coefficients presented in [16], which are modified slightly for simulation purposes. In this study, we consider  $\psi = 90^\circ$  such that the components incur maximum impact during wind events.

#### 5.4.2 Planning Model Trade-offs

The planning decision trade-offs are based on several parameters that can affect the decisions. The simulations for trade-off analyses are conducted with  $\alpha = 0.95$ ,  $\mathcal{N}_{max}^h = 10$ , and  $\mathcal{C}_{max}^T = \$1 M$  for consistency, unless specified otherwise.

## Fragility Model

Fig. 5.6(b) shows a comparative study between risk-neutral and risk-averse cases when using identical vs non-identical fragility models for each line segment. To generate an identical model for each segment, we use the average fragility shown in Fig. 5.6(a). For non-identical cases, each segment has its own fragility curve defined by its configuration, number of phases, number of poles, and conductors. Interestingly, the case with identical fragility overestimates  $CVaR_{0.95}$  for the risk-neutral case and underestimates it for the risk-averse case compared to the case with non-identical fragility models. The average model increases the fragility of robust segments and decreases the ones of non-robust segments in a network. Thus, such approximation can cause misjudgment in identifying the risk of extreme events within the planning framework. It is to be noted that the average is still a representative fragility of overall components in the network. A worse analysis could be in a case where steel pole fragility is approximately used in a system with wooden poles and vice-versa. This highlights the importance of accurate fragility models and data availability in power distribution systems.

## Risk preference

The risk-based decisions in CVaR-based planning problems have two different risk parameters,  $\alpha$ , and  $\lambda$ . Here,  $\alpha$  determines the confidence level in  $CVaR_\alpha$  and defines the proportion of scenarios to consider when defining the system risk. For instance,  $\alpha = 0.95$  means that only 5% of the tail event scenarios are risky, and the risk-averse policies are defined for those representative events. However, for lower alpha values, the value of  $VAR_\alpha$  decreases, and more scenarios are considered risky as  $CVaR_\alpha$

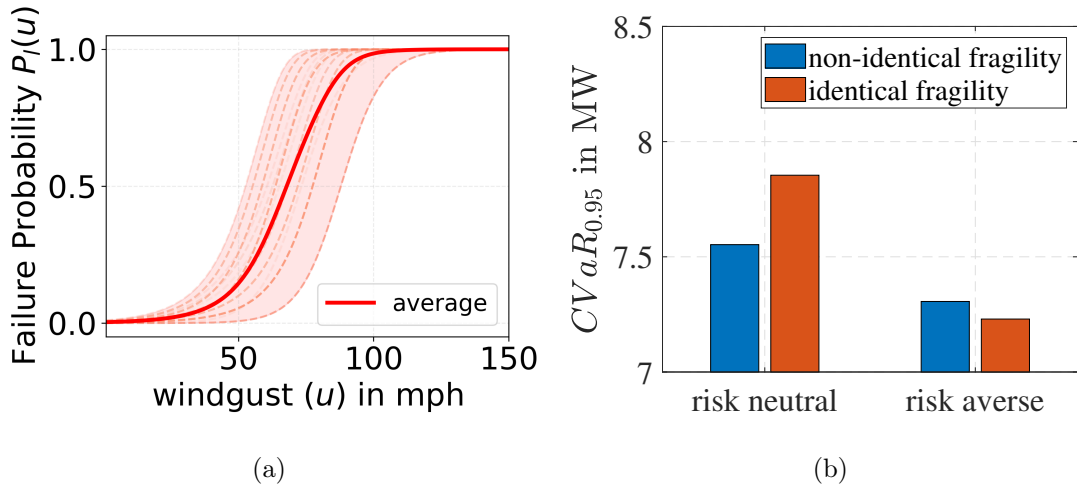


**Figure 5.6** a) Fragility models of 1-phase and 3-phase line segments. b) Sensitivity of  $CVaR_\alpha$  with change in fragility models.

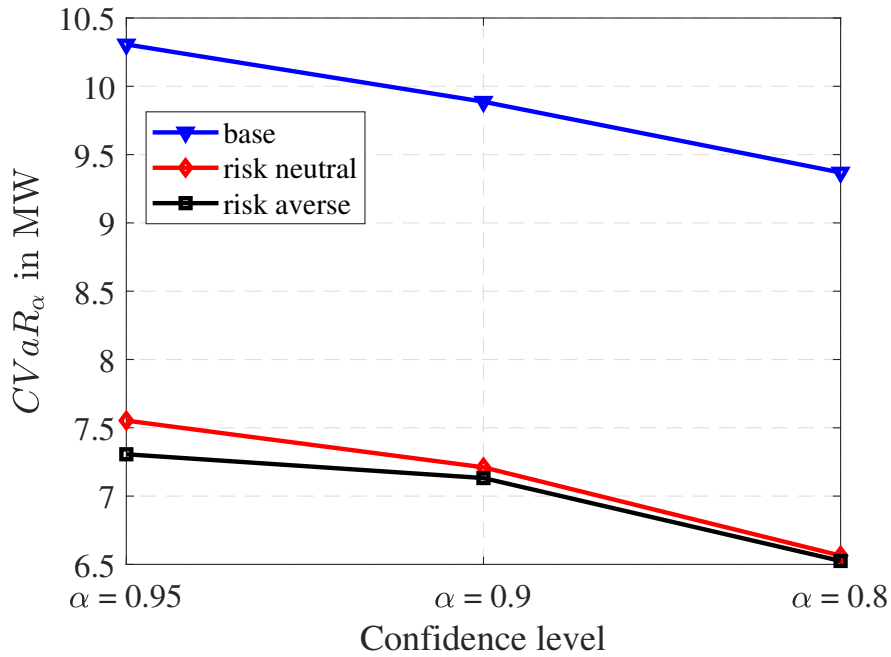


**Figure 5.7** Sensitivity of  $CVaR$  of the prioritized load loss with respect to  $\alpha$  and risk preference.

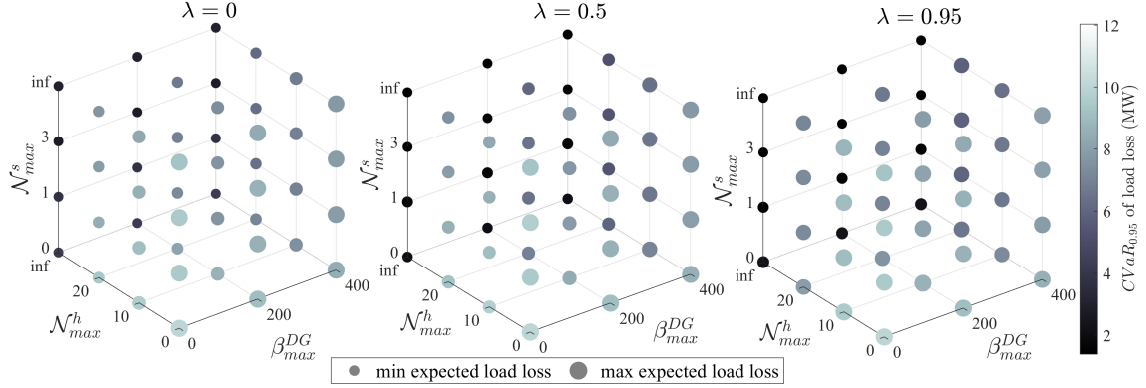


**Figure 5.8** Multi-resource trade-offs for  $C_{max}^T = \$2$  M. The size represents the expected, whereas the color represents the  $CVaR_{0.95}$  of load loss.

represents the expected value of losses beyond  $VaR_\alpha$ . This can increase the planning expenses as the system operators have to plan for more events considered as “risk” to the system. Fig. 5.7 shows the  $CVaR_\alpha$  of prioritized load loss for different values of  $\alpha$  and risk considerations. It can be observed that with higher values of  $\alpha$ , the  $CVaR_\alpha$  decreases as the  $VaR_\alpha$  decreases, which shifts the  $CVaR_\alpha$  to the lower side. Additionally, the  $CVaR_\alpha$  decreases with an increase in risk aversion of the system operator. Although the change in CVaR looks smaller at first glance, it is important to note how the restoration of critical loads is affected by risk aversion. For  $\alpha = 0.95$ , the risk-neutral solution ( $\lambda = 0$ ) picked up 670.45 kW while the risk-averse solution ( $(\lambda \approx 1)$  picked up 822.5 kW of prioritized critical load on average during the HILP events. In Fig. 5.8, it can be seen that risk aversion can indeed reduce the  $CVaR_\alpha$  of load loss. Furthermore, it is important to note that being too conservative on the risk minimization can affect the system’s normal operation, which is reflected by increased expected load loss in Fig. 5.8. Hence, it is important to identify a balance and analyze such trade-offs when making planning decisions. Thus, it is essential to identify appropriate values of  $\alpha$  and the  $\lambda$  of the system operator to better analyze

the resilience planning tool.

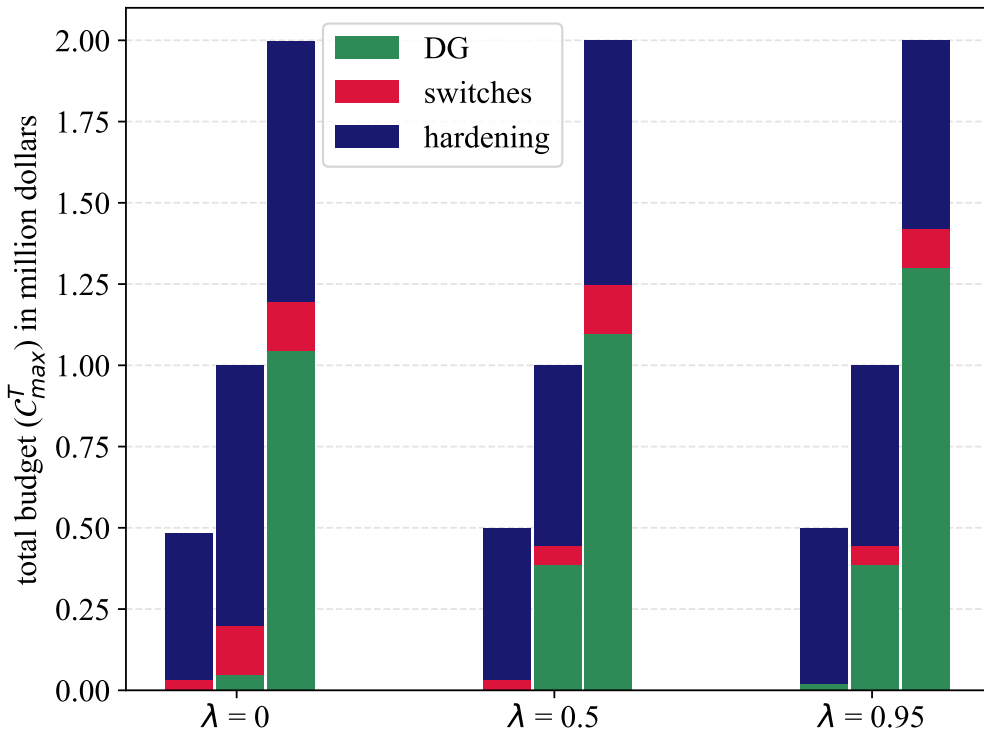
## Multiple Resources

Fig. 5.8 shows the multiple resources trade-offs for a planning budget of  $\mathcal{C}_{max}^T = \$2 M$ . The size of the data points refers to the expected load loss, and their color represents the  $CVaR_{0.95}$  of the load loss. For each data point, the combination of resources can be represented as a tuple  $(D, h, s)$  where  $D$  represents DG,  $h$  represents line hardening, and  $s$  represents tie switches. The DG can be installed with a maximum capacity of either 200 kW or 400 kW in each location. Similarly, the number of lines that can be hardened or the number of tie switch investments are limited with  $\mathcal{N}_{max}^h$  and  $\mathcal{N}_{max}^s$ , respectively. Here,  $inf$  refers to the maximum number of investments i.e., all the lines can be hardened, and all candidate switches can be installed, if needed. It is to be noted that limiting the number of investments in one resource over the other can provide biased planning decisions. However, such a method provides flexibility to grid planners when the budget is restricted towards one investment over the others. For instance, grid planners may be required to spend the majority of \$2M for DG installations as required by the budget policy. However, it is observable from Fig. 5.8 that  $(400, 0, 0)$  only provides a slight improvement on  $CVaR_{0.95}$  but little to no improvement on the expected load loss. However, if the grid planners optimize the budget to install a single unit of DGs and redistribute the budget to line hardening and switch investments i.e.,  $(200, \cdot, \cdot)$ , then the planners can improve both the expected load loss and  $CVaR_{0.95}$  of the load loss for various such combinations while respecting the budget policy. It is also interesting to notice that line hardening provides maximum resilience as investing the entire budget in line hardening decreases the expected loss

and risk for any risk preference. The reason behind minimal improvement with DGs and tie switch investment is due to the fact that the solver avoids connecting sections that are out of service due to a faulted region to prevent the faulted region from being energized. However, line hardening can re-energize the faulted section as additional sectionalizers can participate in network reconfiguration due to the hardening of the faulted lines within the region. Hence, it is important to identify the right combination of resources based on the policy, regulations, and planning objectives.

## Planning Budget

Fig. 5.9 represents the budget distributions for  $\mathcal{N}_{max}^h$  and various values of  $\mathcal{C}_{max}^T$  and  $\lambda$ . Interestingly, most of the budget is spent on line hardening for low-budget situations, i.e.,  $\mathcal{C}_{max}^T = \$0.5$  M. At the same time, a small proportion is allocated to investment in remote-controlled tie-switches. The decision is somewhat consistent for risk-neutral planning for  $\mathcal{C}_{max}^T = \$1$  M. However, the budget distribution shifts towards DGs as the risk aversion parameter  $\lambda$  increases (where  $\lambda > 0$ ). DGs dominate the distribution regardless of risk preference in situations with a high budget. This analysis is crucial because hardening more lines would connect the unserved loads to the substation in scenarios with a lower budget. Given the high number of damages in the HILP scenarios, the budget constraint makes investing in DGs and tie lines challenging. These investments could only pick up a fraction of the loads to avoid energizing the faulted parts of the network. However, with an increased budget, there are more options to harden a few lines within the several areas served by the DGs as microgrids. Therefore, these combined investment strategies can enhance the resilience of the grid.



**Figure 5.9** Budget distribution in various planning decisions with respect to risk preferences.

## 5.5 Summary

This chapter presented a comprehensive trade-off analysis in resilience planning decisions for power distribution systems. We considered the planning trade-offs with the fragility models of the components, risk preference, planning resources, and budget allocation. The results conclude that considering extreme event risk within the planning framework can focus on critical load pickup during HILP conditions, which fails to get picked up when the decisions are made considering expected events only. However, the results also suggest that being too conservative on the risk may hamper the decisions for expected conditions. Hence, it is important to identify the balance in

the risk preference for power distribution systems planning. This study also provides an interesting direction in identifying system-level models and data requirements to develop resilience planning tools for power distribution systems.

## REFERENCES

- [1] A. Poudyal and A. Dubey, “Understanding trade-offs in resilience planning decisions for power distribution systems,” in *2023 IEEE Industry Applications Society Annual Meeting (IAS)*, pp. 1–6, IEEE, 2023.
- [2] NOAA National Centers for Environmental Information (NCEI), “U.s. billion-dollar weather and climate disasters,” Aug. 2013.
- [3] J. Furman, “Economic Benefits of Increasing Grid Resilience to Weather Outages,” tech. rep., US Department of Energy, Aug. 2013.
- [4] W. Yuan, J. Wang, F. Qiu, C. Chen, C. Kang, and B. Zeng, “Robust optimization-based resilient distribution network planning against natural disasters,” *IEEE Transactions on Smart Grid*, vol. 7, no. 6, pp. 2817–2826, 2016.
- [5] S. Ma, L. Su, Z. Wang, F. Qiu, and G. Guo, “Resilience enhancement of distribution grids against extreme weather events,” *IEEE Transactions on Power Systems*, vol. 33, no. 5, pp. 4842–4853, 2018.
- [6] M. Ghasemi, A. Kazemi, E. Bompard, and F. Aminifar, “A two-stage resilience improvement planning for power distribution systems against hurricanes,” *International Journal of Electrical Power & Energy Systems*, vol. 132, p. 107214, 2021.
- [7] S. Ma, S. Li, Z. Wang, and F. Qiu, “Resilience-oriented design of distribution systems,” *IEEE Transactions on Power Systems*, vol. 34, no. 4, pp. 2880–2891, 2019.

- [8] R. Khodabakhsh and S. Soroushpour, “Optimal control of energy storage in a microgrid by minimizing conditional value-at-risk,” *IEEE Transactions on Sustainable Energy*, vol. 7, no. 3, pp. 1264–1273, 2016.
- [9] J. Wu and P. Wang, “Risk-averse optimization for resilience enhancement of complex engineering systems under uncertainties,” *Reliability Engineering & System Safety*, vol. 215, p. 107836, Nov. 2021.
- [10] A. Poudyal, S. Poudel, and A. Dubey, “Risk-based active distribution system planning for resilience against extreme weather events,” *IEEE Transactions on Sustainable Energy*, pp. 1–14, 2022.
- [11] A. Moreira, M. Heleno, A. Valenzuela, J. H. Eto, J. Ortega, and C. Botero, “A scalable approach to large scale risk-averse distribution grid expansion planning,” *IEEE Transactions on Power Systems*, 2023.
- [12] A. Poudyal, A. Dubey, V. Iyengar, and D. Garcia-Camargo, “Spatiotemporal impact assessment of hurricanes on electric power systems,” in *2022 IEEE Power & Energy Society General Meeting (PESGM)*, pp. 1–5, 2022.
- [13] D. N. Bresch and G. Aznar-Siguan, “CLIMADA v1.4.1: towards a globally consistent adaptation options appraisal tool,” *Geoscientific Model Development*, vol. 14, pp. 351–363, Jan. 2021.
- [14] NOAA National Centers for Environmental Information (NCEI), “U.S. Billion-Dollar Weather and Climate Disasters.” <https://www.ncei.noaa.gov/access/billions/>, 2024.

- [15] Y.-C. Chen, “Stat 425: Introduction to nonparametric statistics winter 2018 lecture 6: Density estimation: Histogram and kernel density estimator.” Lecture, Winter 2018. Course Lecture.
- [16] G. Hou and K. K. Muraleetharan, “Modeling the resilience of power distribution systems subjected to extreme winds considering tree failures: An integrated framework,” *International Journal of Disaster Risk Science*, vol. 14, no. 2, pp. 194–208, 2023.
- [17] H.M. Rollins, P.E., “Sustainable wood pole design for overhead systems,” North American Wood Pole Council Technical Bulletin No. 21-D-205, H.M. Rollins Company, Inc., 2021.
- [18] R. T. Rockafellar, S. Uryasev, *et al.*, “Optimization of conditional value-at-risk,” *Journal of risk*, vol. 2, pp. 21–42, 2000.
- [19] S. Poudel, A. Dubey, and K. P. Schneider, “A generalized framework for service restoration in a resilient power distribution system,” *IEEE Systems Journal*, vol. 16, no. 1, pp. 252–263, 2020.
- [20] W. Gorman, “The quest to quantify the value of lost load: A critical review of the economics of power outages,” *The Electricity Journal*, vol. 35, no. 8, p. 107187, 2022.
- [21] R. Moreno, M. Panteli, P. Mancarella, H. Rudnick, T. Lagos, A. Navarro, F. Ordonez, and J. C. Araneda, “From reliability to resilience: Planning the grid against the extremes,” *IEEE Power and Energy Magazine*, vol. 18, no. 4, pp. 41–53, 2020.

- [22] L. C. Coelho, “Linearization of the product of two variables,” *Canada Research Chair in Integrated Logistics*, 2013.
- [23] L. Gan and S. H. Low, “Convex relaxations and linear approximation for optimal power flow in multiphase radial networks,” in *2014 Power Systems Computation Conference*, pp. 1–9, IEEE, 2014.
- [24] Q. Chen and L. Mili, “Composite power system vulnerability evaluation to cascading failures using importance sampling and antithetic variates,” *IEEE Transactions on Power Systems*, vol. 28, no. 3, pp. 2321–2330, 2013.
- [25] J.-P. Watson, D. L. Woodruff, and W. E. Hart, “Pysp: modeling and solving stochastic programs in python,” *Mathematical Programming Computation*, vol. 4, no. 2, pp. 109–149, 2012.
- [26] “Technical guidance cost matrix for integrating der - updated and combined.” Joint Utilities of New York, Aug 2022.
- [27] “Construction cost data for electric generators installed in 2021.” U.S. Energy Information Administration. Release date: September 21, 2023.
- [28] P. Zippenfenig, “Open-meteo.com weather api,” 2023.

## CHAPTER 6

# RESILIENCE PLANNING OF BULK POWER SYSTEMS AGAINST EXTREME WEATHER EVENTS

### 6.1 Introduction

This chapter introduces a two-stage stochastic planning model for bulk power systems where the generation dispatch, line hardening, line capacity expansion, and distributed generation sizing and siting decisions are proactively decided to minimize the overall load shed and its risk for extreme weather scenarios. The risk of extreme weather events is modeled using conditional value-at-risk, and a representative scenario sampling method is used to alleviate computational complexity without sacrificing solution quality over a wide range of scenarios. Finally, the overall framework is tested on a standard IEEE reliability test system to evaluate the effectiveness of the proposed approach. Several planning portfolios are presented that can help system planners identify trade-offs between system resilience, planning budget, and risk aversion.

#### 6.1.1 Motivation

In recent years, the frequency of severe weather events, such as hurricanes, flooding, wildfires, and heat/cold waves, has risen significantly as a result of climate change. The annual average number of disasters exceeding \$1 billion from 1980 to 2022 is 8.1, whereas the most recent five years, from 2018 to 2022, has an average of 18 [1]. Approximately 83% of all major outages reported in the U.S. between 2000 and 2021 were weather-related [2].

The aftermath of such events incurs significant socio-economic losses to the end users and an economic burden on the grid operators. For example, the economic losses due to Hurricane Ida were more than \$55 billion in Louisiana alone due to wind and storm surge damage, with an additional \$23 billion flooding damage in the Northeastern US [3]. The unusually cold weather event that hit Texas in 2021, the coldest weather event in Texas since 1989, caused more than 10 million customers without power and caused a financial impact of \$ 4 billion [4]. The occurrences and severity of such events are more likely to increase in the future as a result of global warming and climate change. All these facts illustrate the importance of increasing the power system's resilience.

One way to increase the system's resilience is by implementing short-term actions during/after disasters, and many works focus on this domain. A post-event islanded grid operation with load criticality is considered in [5]. [6],[7] have studied the proactive operation of the grid where various resources are scheduled to ensure the feasible operation during the event progressing. Siting and sizing of available resources might not be sufficient to support the resilient-oriented operation of the system, and long-term resilience-based planning of the system needs to be done. Traditional-based long-term planning of power systems considers the contingency of one (N-1) or two (N-2) equipment where the system should survive fully even if there is failure of one or two components [8] respectively. It is not economically feasible to go for a higher contingency value due to budget limitations, and consequently, it fails to consider the impact of extreme weather events while planning.

### 6.1.2 Related Literature and Gaps

There are several works focusing on resilience enhancement transmission planning. In [9], a two-stage stochastic model is developed for transmission expansion and generation installation. The study presented in [10] introduces a data-driven planning model for transmission systems. This model aims to identify the most effective portfolio for enhancing resilience against extreme weather events in the power system. However, the above works only focus on the worst-case scenario. Such kind of planning is too conservative as such a scenario occurs barely and resources might be underutilized most of the time.

A resilient network investment model, considering many possible scenarios, that co-optimizes substation hardening and transmission expansion to protect the system against extreme events is proposed in [11]. Resilience-based planning of distributed series reactors is proposed in [12]. However, the above works have restricted themselves, either to one or two types of investment decisions which might not give the optimal utilization of budget as the advantages of combining different types of investments is higher which is illustrated in our work. [13] implemented the two-stage stochastic model to identify the optimal combination of line expansion, substation hardening, and DG installation but did not consider the impact of planning during the normal operation of the system.

Moreover, most of all of these works consider the DC optimal power flow (DCOPF) model, which is a decent approximation model for ACOPF. However, DCOPF does not necessarily have resilience considerations when the generator dispatch decisions are made. The work in [14] addresses this issue by formulating a resilience-driven proactive dispatch model. However, the approach only considers a targeted number

of outage scenarios, which is inappropriate for planning purposes. For instance, ten different line outages might incur no loss in a meshed network. However, the outage of even two lines connecting the generator to the load can instigate a blackout in the system. Additionally, none of the above-mentioned works consider risk minimization and only focus on expected outcomes, which often fail to characterize and incorporate system resilience within the optimization.

### 6.1.3 Contribution

This chapter proposes a resilience-driven two-stage stochastic planning model where generation proactive dispatch, line hardening, line capacity upgrading, DG siting, and sizing decisions are decided to minimize the expected load loss and generation curtailment while minimizing the risk of load loss. The risk is modeled using conditional value-at-risk (CVaR), which has been widely used in other risk-based planning models [15]. The generation dispatch and line hardening decisions are proactively decided so as to minimize the total load shed and generation curtailment for extreme weather scenarios. A similar planning model is presented in [14] where the planning decisions are based on a targeted number of outage scenarios. However, such a scenario selection method is not appropriate for planning purposes. For instance, ten different line outages might incur no loss in a meshed network. However, the outage of even two lines connecting the generator to the load can instigate a blackout in the system. Hence, scenario selection based on a targeted number of outages will be difficult to justify in a planning model. Furthermore, this work has not included risk metrics for the planning decision. A regional wind profile represents the extreme wind storm event, and the impact on the grid is observed using component-level fragility

curves. Such a regional wind profile-based method is appropriate for long-term planning methods. However, for short-term and operational planning, it is desired to plan according to the nature of an upcoming event. Based on the regional wind profile and component level, the failure probability of the component is obtained based on its fragility curve and the wind speed experienced by it. Since the event is not deterministic, many scenarios need to be taken. The number of scenarios is chosen in such a way that convergence is obtained when the system is exposed to such scenarios. The damage scenarios are generated using Monte-Carlo simulation, and to alleviate the computational complexity, a strategic representative scenario selection method is utilized as described in [15]. Finally, a two-stage risk-averse stochastic problem is formulated where the first stage involves planning and proactive generator dispatch decisions, whereas the second stage facilitates optimal operation of the power grid based on the planning decision for every scenario. The overall contributions of this chapter are:

1. *A risk-based resilience planning model for electric power systems:* We propose a two-stage risk-based mixed integer linear programming (MILP) model for resilience planning in the power grid. The planning decisions include proactive generator dispatch decisions, line hardening, line capacity upgrade, and DG siting and sizing. The effectiveness of the proposed resilience-driven planning model is tested on the IEEE Reliability Test System [16]
2. *Trade-off analysis on multiple planning portfolios:* A comprehensive trade-off analysis is presented on several resource portfolios compared to the planning budget and risk aversion. The grid operators can effectively utilize the trade-off in making planning decisions based on the planning objective and availability

of the budget and resources.

## 6.2 Resilience-driven Planning Modeling

### 6.2.1 Two-stage Stochastic Planning Model

The DCOPF model obtains the cost-economical generation dispatch decisions. However, DCOPF-based dispatch decisions do not consider system resilience and future extreme events within its model. Furthermore, once the dispatch decisions are identified, generators are constrained by their ramp rates, which makes it challenging to re-dispatch in case of extreme weather events. The proposed two-stage stochastic planning model provides generation dispatch, and investment planning decisions to minimize the total load shed and risk due to extreme weather scenarios. The two-stage problems are described below.

#### First Stage Problem

The overall planning decisions obtained after solving the first stage problem are the line hardening decision ( $x^h$ ), line capacity expansion decision ( $x^u$ ), DG sizing ( $x^{DG}$ ), and siting ( $\zeta^{DG}$ ) decisions, and proactive generator dispatch decision ( $P_G$ ). The objective function in (6.1) minimizes the weighted sum of expected load shed ( $\hat{P}_i^{D,\xi}$ ) and CVaR and an additional generation curtailment ( $\hat{P}_{i_G}^\xi$ ) for a set of extreme weather event scenarios,  $\xi \in \mathcal{E}$ . The generation curtailment term, weighed by  $\gamma$ , is introduced to maintain a feasible power flow solution in cases when there are islands with more generation than load. The value of  $\gamma$  is set very low to ensure higher priority to minimize the weighted sum of expected load shed and CVaR. CVaR has been widely adopted as a risk metric for resilience planning and quantification in power

systems and can be easily integrated with stochastic models [15] and is described in detail in [17]. The weighing term  $\lambda \in [0, 1]$  represents the risk aversion of the system planner, which increases monotonically with  $\lambda$ .

Eqs. (6.2) - (6.6) represent first-stage DCOPF constraints for identifying generator dispatch decisions to minimize (6.1) for all scenarios. Constraint (6.2) ensures the power balance in each bus such that the generation and incoming power on the bus are equal to the outgoing power, demand ( $P_i^D$ ), and shunt conductance ( $G_i$ ) on the same bus  $i \in \mathcal{B}$ . The line flow is maintained by (6.3), which is the product of line susceptance  $B_e = x_e^{-1}$  and angle ( $\theta$ ) difference between the two buses connected by the line. For transformers, the line flow is also guided by their turn ratio ( $N_e^T$ ) or phase shift angle ( $\Phi_e^T$ ) as shown in (6.5). Constraints (6.4) - (6.6) bound the active power flow from the generators ( $\mathcal{P}_{\mathcal{G}}$ ), active power flow on the lines( $P_e$ ) based on their thermal limits ( $P_e^{max}$ ), and angle difference between two buses in a line respectively. For economic and physical operating reasons, some generators should have a minimum generation level below which they cannot operate. Hence,  $P_{i_G}^{min}$  ensures that for such generators, a minimum generation level is always maintained if operated. Eqs. (6.7) - (6.9) represent constraints for first-stage investment decisions. Constraint (6.7) ensures that the investment on hardening, capacity upgrade, and DGs do not exceed the maximum planning budget of  $\mathcal{C}_T^{max}$ , (6.8) restricts the maximum number of investment for each investment decision, and (6.9) constraints the size of DG unit that can be placed in each bus. It is done to decrease the computational complexity. In this work, the amount of connected bus load and utilization factor of DG units guide the maximum capacity of the DG unit at that bus.

$$\min(1 - \lambda)\mathbb{E} \left( \mathcal{F}(\mathbf{x}, \mathcal{E}) + \frac{\gamma \hat{P}_{\mathcal{G}}^{\mathcal{E}}}{1 - \lambda} \right) + \lambda CVaR_{\alpha}(\mathcal{F}(\mathbf{x}, \mathcal{E})) \quad (6.1)$$

where,

$$\begin{aligned} \mathbf{x} &\in \{x^h, x^u, x^{DG}, \zeta^{DG}, P_{\mathcal{G}}\} \\ \mathbb{E}(\mathcal{F}(\mathbf{x}, \mathcal{E}) + \gamma \hat{P}_{\mathcal{G}}^{\mathcal{E}}) &:= \sum_{\xi \in \mathcal{E}} p^{\xi} \left( \sum_{i \in \mathcal{B}} \hat{P}_i^{D, \xi} + \gamma \sum_{i_G \in \mathcal{G}} \hat{P}_{i_G}^{\xi} \right) \\ CVaR_{\alpha}(\mathcal{F}(\mathbf{x}, \mathcal{E})) &:= \left( \eta + \frac{1}{1 - \alpha} \sum_{\xi \in \mathcal{E}} p^{\xi} \nu^{\xi} \right) \end{aligned}$$

subject to,

$$\sum_{i_G \in \mathcal{G}_{\mathcal{B}}} P_{i_G} + \sum_{e: (j, i) \in \mathcal{L}} P_e - \sum_{e: (i, j) \in \mathcal{L}} P_e = P_i^D + G_i \quad (6.2)$$

$$\forall i, j \in \mathcal{B}, \mathcal{G}_{\mathcal{B}} \in \mathcal{G}$$

$$P_e = \frac{B_e}{N_e^T} (\theta_i - \theta_j - \Phi_e^T) \quad \forall e : (i, j) \in \mathcal{L}, i, j \in \mathcal{B} \quad (6.3)$$

$$P_{i_G}^{min} \leq P_{i_G} \leq P_{i_G}^{max} \quad \forall i_G \in \mathcal{G} \quad (6.4)$$

$$-P_e^{max} \leq P_e \leq P_e^{max} \quad \forall e : (i, j) \in \mathcal{L} \quad (6.5)$$

$$-\theta_e^{max} \leq \theta_i - \theta_j \leq \theta_e^{max} \quad \forall e : (i, j) \in \mathcal{L}, i, j \in \mathcal{B} \quad (6.6)$$

$$\sum_{e \in \mathcal{L}} c_e^h x_e^h + \sum_{e \in \mathcal{L}} c_e^u x_e^u + \sum_{i \in \mathcal{B}} c_i^{DG} x_i^{DG} \leq \mathcal{C}_T^{max} \quad (6.7)$$

$$\forall e : (i, j) \in \mathcal{L}$$

$$\sum_{e \in \mathcal{L}} x_e^h \leq N_h, \sum_{e \in \mathcal{L}} x_e^u \leq N_u, \sum_{i \in \mathcal{B}} \zeta_i^{DG} \leq N_{DG} \quad \forall e : (i, j) \in \mathcal{L} \quad (6.8)$$

$$0 \leq x_i^{DG} \leq \zeta_i^{DG} P_i^{DG,max} \quad \forall i \in \mathcal{B} \quad (6.9)$$

### Second Stage Problem:

For the given first stage decision, this stage solves for the optimal operation considering each scenario. Since, the second-stage problem is solved for each scenario, the second-stage variables are parameterized by  $\xi$  throughout this paper. The objective function in (6.10) minimizes the load shed ( $\hat{P}_i^{D,\xi}$ ) and an additional generation curtailment ( $\hat{P}_{i_G}^\xi$ ) for a scenario,  $\xi \in \mathcal{E}$ .

Constraint (6.11) restricts the generation re-dispatch within its maximum and minimum ramping ability based on the first stage proactive dispatch. Generators are limited in terms of active power modulation by their ramp rate, which is usually based on their maximum and available capacity once they are dispatched. Therefore, it is desired to carefully decide the optimal generation dispatch to enhance the system's resilience. The power balance at each bus for each scenario is maintained by (6.12), where generation curtailment and load shedding variables are introduced. Here,  $x_i^{DG}$  supplies additional generation to minimize the load shed. Constraint (6.13) decides the line connectivity based on the outage and hardening decision. Here,  $\pi_e^\xi$  is an exogenous parameter and is known when a scenario is realized such that when  $x_e^h = 0$ ,  $\delta_e^\xi = \pi_e^\xi$  and when  $x_e^h = 1$ ,  $\delta_e^\xi = 1$ . Constraints (6.14) - (6.16) ensure that the power flow in a line is 0 for out-of-service lines for every scenario. When  $\delta_e = 0$ , the power flow through the open line becomes 0,  $P_e^\xi = 0$ , which makes  $\theta_i - \theta_j$  unconstrained.

For normal conditions, the flow is constrained by a large number  $\mathbf{M}$ . The first-stage capacity upgrade decision  $x_e^u$  is incorporated in (6.15), such that if  $x_e^u = 1$  then the existing line capacity will be upgraded by a factor of  $\phi_e^u$ , which is a known parameter. The capacity upgrade decision will still depend on whether the line is in-service ( $\delta_e = 1$ ) or out-of-service ( $\delta_e = 0$ ). Eq. (6.15) is non-linear and hence is linearized using the Big-M method as suggested in [18].

$$\min \left( \sum_{i \in \mathcal{B}} \hat{P}_i^{D,\xi} + \gamma \sum_{i_G \in \mathcal{G}} \hat{P}_{i_G}^\xi \right) \quad (6.10)$$

$$-P_{i_G}^R \leq P_{i_G} - P_{i_G}^\xi \leq P_{i_G}^R \quad \forall i_G \in \mathcal{G}, \forall \xi \in \mathcal{E} \quad (6.11)$$

$$\begin{aligned} \sum_{i_G \in \mathcal{G}_B} (P_{i_G}^\xi - \hat{P}_{i_G}^\xi) + \sum_{i \in \mathcal{B}} x_i^{DG} + \sum_{e:(j,i) \in \mathcal{L}} P_e^\xi - \sum_{e:(i,j) \in \mathcal{L}} P_e^\xi = \\ P_i^D + G_i - \hat{P}_i^{D,\xi} \quad \forall i, j \in \mathcal{B}, \forall \xi \in \mathcal{E}, \mathcal{G}_B \in \mathcal{G} \end{aligned} \quad (6.12)$$

$$\delta_e^\xi = \pi_e^\xi + x_e^h - \pi_e^\xi \times x_e^h \quad \forall e : (i, j) \in \mathcal{L}, \forall \xi \in \mathcal{E} \quad (6.13)$$

$$\begin{aligned} -(1 - \delta_e^\xi) \mathbf{M} \leq \frac{P_e^\xi \times N_e^T}{B} - (\theta_i^\xi - \theta_j^\xi - \phi_e^T) \leq (1 - \delta_e^\xi) \mathbf{M} \\ \forall e : (i, j) \in \mathcal{L}, i, j \in \mathcal{B}, \forall \xi \in \mathcal{E} \end{aligned} \quad (6.14)$$

$$\begin{aligned} -\delta_e^\xi (1 - x_e^u) P_e^{max} - (1 + \phi_e^u) x_e^u \delta_e^\xi P_e^{max} \leq P_e^\xi \leq \delta_e^\xi (1 - x_e^u) P_e^{max} \\ +(1 + \phi_e^u) x_e^u \delta_e^\xi P_e^{max} \quad \forall e : (i, j) \in \mathcal{L}, \forall \xi \in \mathcal{E} \end{aligned} \quad (6.15)$$

$$\begin{aligned} -\theta_e^{max} - \mathbf{M}(1 - \delta_e^\xi) \leq \theta_i^\xi - \theta_j^\xi \leq \theta_e^{max} + \mathbf{M}(1 - \delta_e^\xi) \\ \forall e : (i, j) \in \mathcal{L}, i, j \in \mathcal{B}, \forall \xi \in \mathcal{E} \end{aligned} \quad (6.16)$$

$$P_{i_G}^{min} \leq P_{i_G}^{\xi} \leq P_{i_G}^{max} \quad \forall i_G \in \mathcal{G}, \quad \forall \xi \in \mathcal{E} \quad (6.17)$$

$$0 \leq \hat{P}_i^{D,\xi} \leq P_i^D \quad \forall i \in \mathcal{B}, \quad \forall \xi \in \mathcal{E} \quad (6.18)$$

$$0 \leq \hat{P}_{i_G}^{\xi} \leq P_{i_G}^{\xi} \quad \forall i_G \in \mathcal{G}, \quad \forall \xi \in \mathcal{E} \quad (6.19)$$

$$\nu^{\xi} \geq \mathcal{F}(\mathbf{x}, \xi) - \eta, \quad \nu \in \mathbb{R}_+^n, \quad \forall \xi \in \mathcal{E} \quad (6.20)$$

Constraints (6.17) - (6.19) limit the active power generation from a generator to its maximum capacity, load shedding limit to the maximum demand per bus, and generation curtailment to the maximum generation dispatch per generator in each scenario. The CVaR-based constraint is represented by (6.20), which ensures that  $\nu^{\xi}$  is greater than or equal to the load-shed at  $\eta$  for each scenario  $\xi \in \mathcal{E}$ .

### 6.3 Probabilistic Scenario Generation and Selection

This section describes the scenario generation and selection procedure for resilience-based planning. It describes how an event and its impact on the power grid is modeled. A representative scenario selection method is also discussed. The overall planning framework is shown in Fig. 6.1.

#### 6.3.1 Scenario Generation

An event can be defined by its probability of occurrence and the corresponding intensity. One such example of an event related to wind profile in three different regions

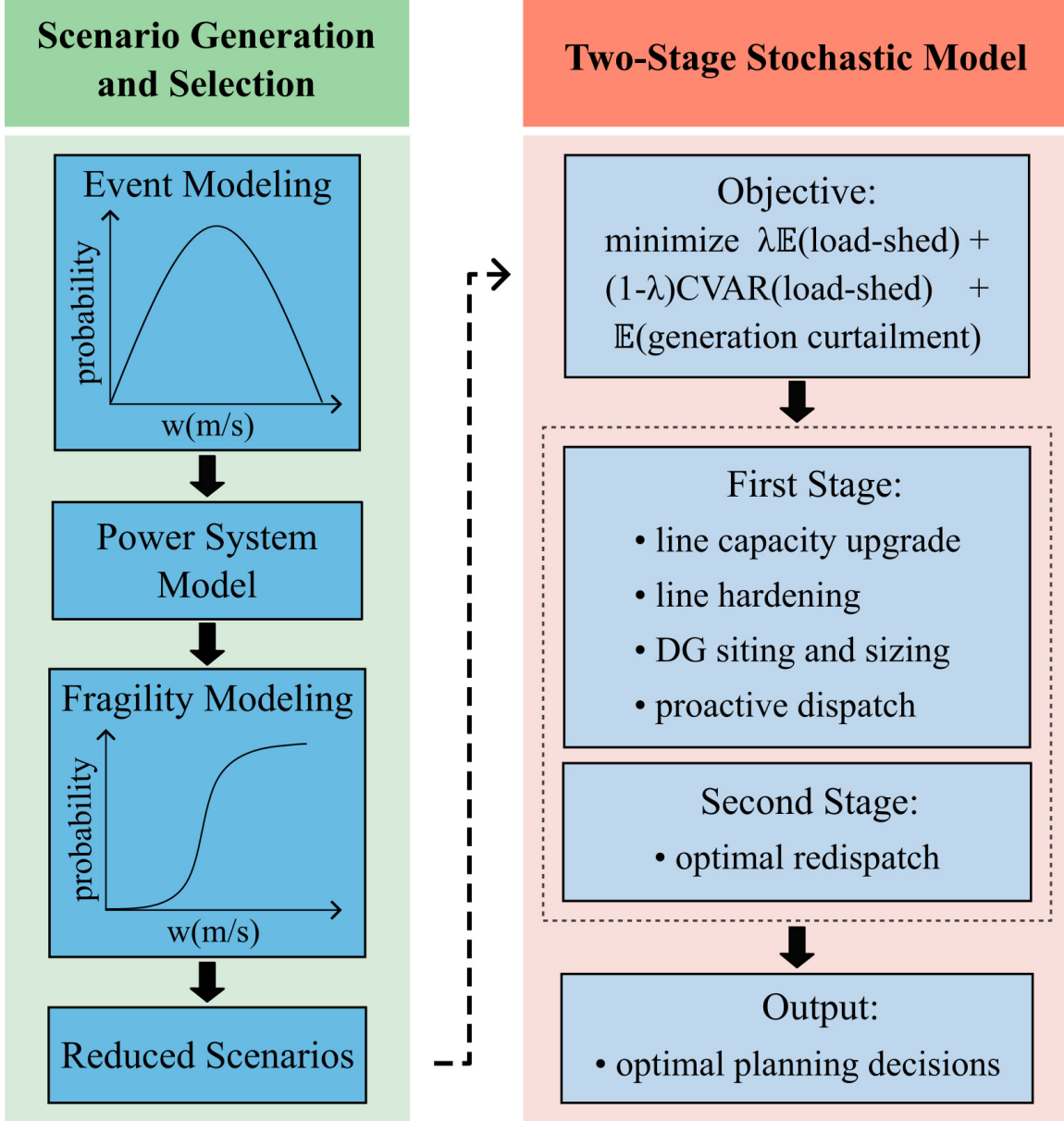


**Figure 6.1** Overall framework of risk-based planning model.

observing extreme, high, and normal wind profiles is shown in Fig. 6.2. Component level fragility curve or prototype curve fits model can be used to assess the damage in the system due to hazards [19]. For each wind speed, the component level fragility

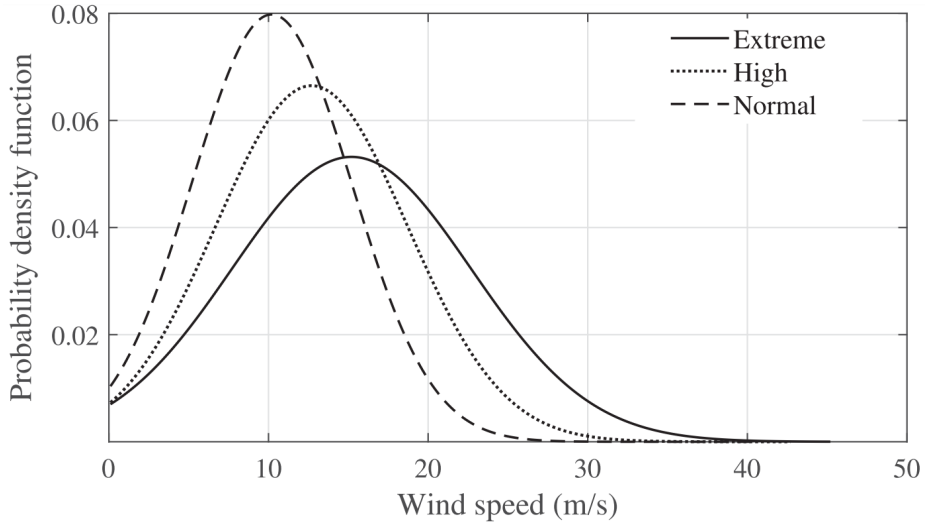


**Figure 6.2** Regional wind profile [19].

curve determines the operational state of the component. The fragility curve maps the wind speed to the damage probability of the component and thus can be used to determine the impacts of the event on the power system. Here, we use an empirical component-level fragility curve and assume that only transmission lines will be damaged due to extreme wind events. The empirical model can be replaced with known fragility models if the data is available. The mathematical relation to map wind speed to the fragility curve is given below:

$$p_f(v) = \begin{cases} P_f^n, & \text{if } v < v_{\text{critical}} \\ P_f(v), & \text{if } v_{\text{critical}} < v < v_{\text{collapse}} \\ 1, & \text{if } v > v_{\text{collapse}} \end{cases}$$

where,  $P_f(v)$  is the failure rate of the component as a function of wind speed  $v$ ,  $P_f^n$  is the failure rate at normal weather conditions,  $v_{\text{critical}}$  is the wind speed at which failure probability rapidly increases and beyond  $v_{\text{collapse}}$ , the component fails.

To evaluate the impact of wind-induced damages on the power system, Monte-

Carlo simulations (MCS) are conducted for each wind speed to determine the system loss until the moving average loss converges. In steady-state conditions, before the system is subjected to an event, we run DCOPF on the model to mimic the normal and economic operating conditions of the generators. When an extreme event is realized, it is assumed that the available capacity to each generator is fixed to this pre-dispatched value as it is difficult to adjust the dispatch depending on the ramp rate and type of generator. During or after the grid disruption due to an extreme event, the network may become disconnected, resulting in the formation of many islands. Loads on a particular island can get power only from generators available within the island and any mismatch between load and generation within an island is considered a load shed. In this work, we do not consider the dynamics of the grid and assume that each island is operationally stable. The converged load loss of each wind speed is then mapped to the regional wind profile probability density function.

### 6.3.2 Scenario Selection

In MCS, a large number of scenarios need to be generated so that it can represent all possible circumstances. However, it is computationally challenging to incorporate all of the scenarios in the stochastic model. Hence, to solve the problem efficiently, scenario reduction methods are proposed to select representative scenarios from a large set of scenarios [20]. Some other works propose sampling techniques like importance sampling [21], stratified sampling [22], and probabilistic-distance reduction [23]. These methods have their own trade-off regarding solution time and quality. In this work, we use a method that is closely related to stratified sampling and distance reduction methods.

Let us consider that  $N_v^\xi$  is the total number of scenarios generated for a corresponding wind speed,  $v$ , with  $N_v$  discrete samples of wind speed. Let  $L_v^{avg}$  represent the converged MCS loss for each  $v$ . Then, the total number of scenarios can be represented as  $\Xi = N_v^\xi \times N_v$ . The representative scenario,  $\xi_v$ , is chosen such that the distance, here loss, between  $\xi_v$  and average value  $L_v^{avg}$  will be smallest. Thus, one representative scenario out of  $N_v^\xi$  scenarios is chosen corresponding to each  $v$ . In total, we have  $N_v$  representative scenarios out of total  $\Xi$  scenarios. The method is described in detail in [15]. Once the representative scenarios are selected, the two-stage stochastic planning model discussed in Section 6.2 is then optimized for the selected range of scenarios to enhance the overall resilience of the system.

## 6.4 Results and Analysis

### 6.4.1 Test Case and Parameters

The effectiveness of the proposed resilience-driven planning model is tested on the IEEE Reliability Test System-GMLC [16]. The test system is a 73-bus system having 158 generators with a total generation capacity of 14.55 GW, 120 branches with realistic branch parameters, and a total demand of 8.55 GW. The two-stage stochastic MILP model is formulated using Pyomo [24] and solved using Gurobi [25]. Scenario generation and scenario reduction methods are implemented in MATLAB2023a, and DCOPF is solved using MATPOWER [26]. All experiments are simulated on a PC with 16 GB RAM and Intel i7-6700 CPU @3.4GHz.

The factor of generation curtailment in (6.1),  $\gamma$ , is selected as 0.001 to prioritize minimizing the weighted sum of expected load shed and CVaR. The confidence level for CVaR is taken as  $\alpha = 0.95$ . The risk-neutral solution is represented by  $\lambda = 0$ ,

**Table 6.1** Cost for each planning measure.

Planning Measure	Cost × (\$1 mil)
upgrade 138 kV line	1.5 per mile [27]
upgrade 230 kV line	1.8 per mile [28]
harden 138 kV line	7.5 per mile
harden 230 kV line	9 per mile
DG unit installation	1.8 per MW [29]

and the risk-averse solution is represented by  $\lambda = 0.95$ . The test case has different types of generator units with their corresponding ramp rates. We assume that the generators can ramp up or down to a maximum of 5 minutes, corresponding to their ramp rate. For capacity upgrade,  $\phi_e^u$  is chosen as 1, which means that if a line is decided to be upgraded, then the line capacity is doubled. For each bus, the size of the DG unit is limited to 50% of the total load, and a utilization factor of 50% is assumed. This means that for each bus  $i \in \mathcal{B}$ ,  $P_i^{DG,max} \leq 0.25 \times P_i^D$ . The individual cost of other investment measures are given in Table 6.1. The cost of hardening a line (undergrounding) is assumed to be five times greater than the upgrade cost for the same line rating. The overall planning budget  $\mathcal{C}_T^{max}$  is varied from \$0.5 billion to \$3 billion.

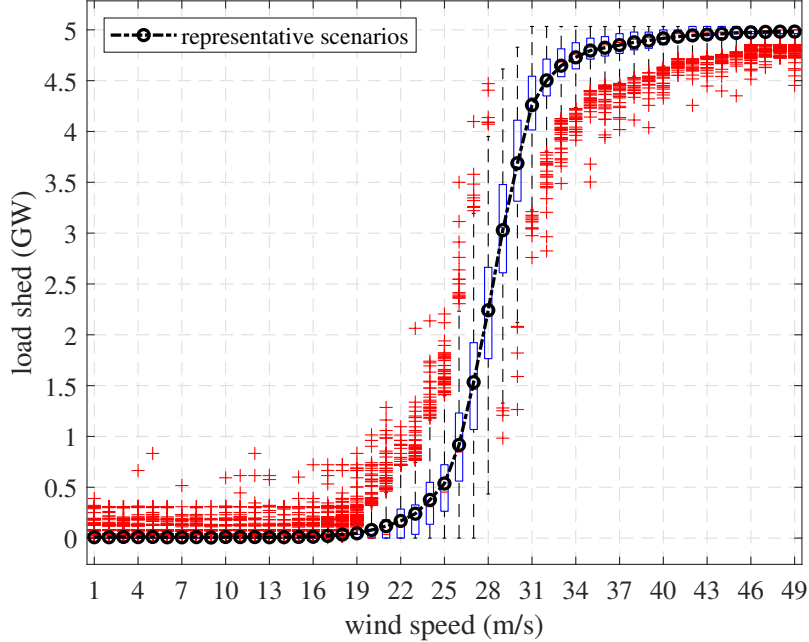
#### 6.4.2 Scenario Generation and Selection

Wind events scenarios are generated using method detailed in Section III-A. We sample  $N_v = 49$  distinct wind speeds to represent extreme wind events, and conduct 1000 MCS trials for each wind speed considering the fragility model of transmission

lines, thus resulting in a total of  $\Xi = 49000$  scenarios. The rationale behind choosing 1000 trials is that it ensures enough convergence for the moving average load loss in this experiment. Fig. 6.3 shows the box plot of load loss for all scenarios with outliers denoted by red marks. At a windspeed of  $v = 49 \text{ m/s}$ , it is observed that the system experiences a maximum load loss of 5.033 GW, equivalent to 58.8% of the total load. The reason for not having total blackouts even at tail-end events stems from the network topology of the transmission system and multiple generator availability at many buses. These generators create isolated islands that continue to supply power to local loads. A total of  $N_v$  representative scenarios are selected based on the method described in Section III-B. The corresponding plot of reduced scenarios is shown in the black curve in Fig. 6.3. It is worth mentioning that this reduction method incorporates the sampling of HILP events, which enhances its suitability for addressing resilience planning problems.

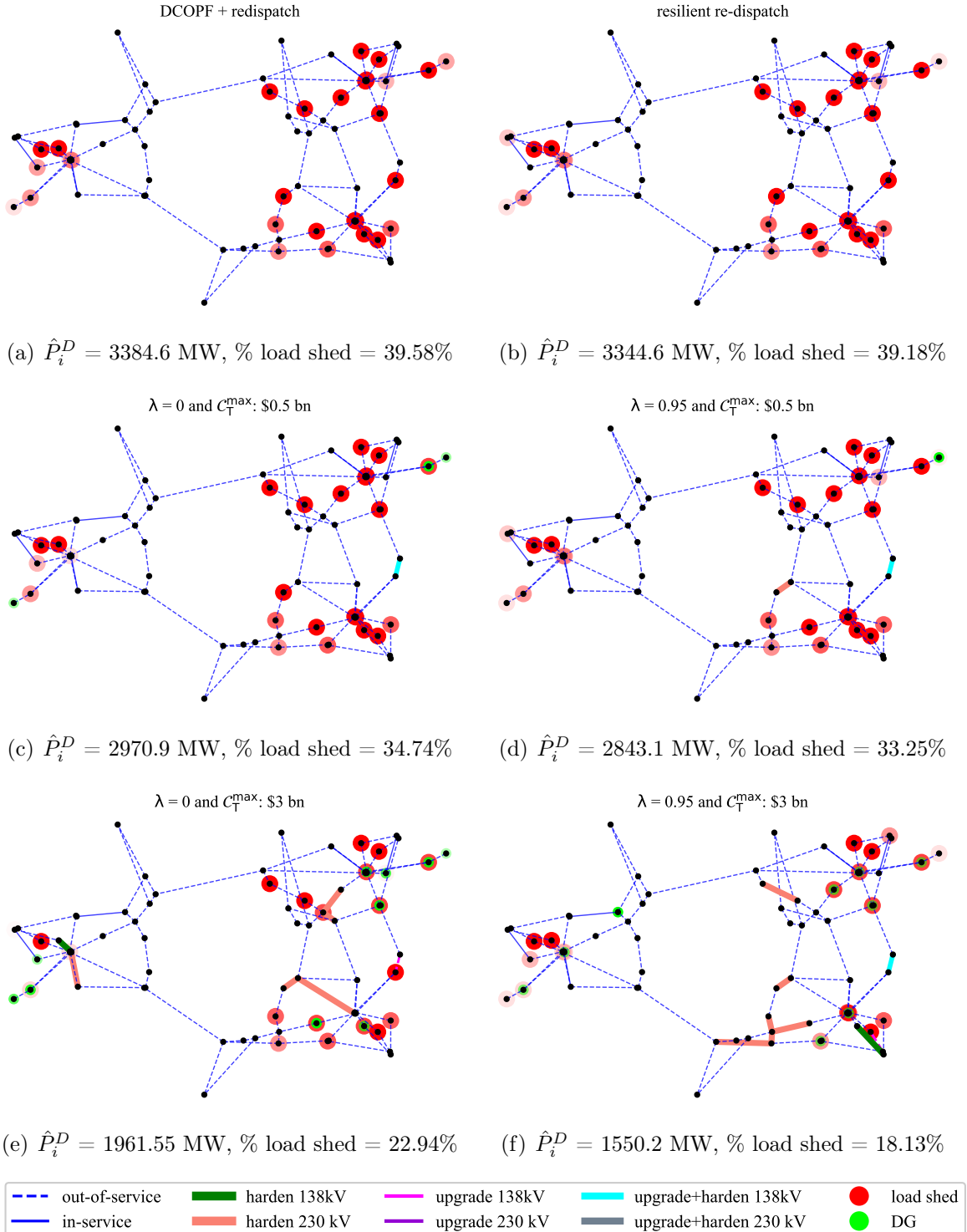
#### 6.4.3 Resilience Planning

Table. 6.2 compares the expected load shed and CVaR for various planning strategies, budget, and risk aversion. For the base case, scenarios obtained from the scenario selection method are considered to calculate the expected load shed and CVaR. In this case, no operational decisions are carried out. For the DCOPF + re-dispatch case, generator dispatch decisions are obtained by solving the DCOPF problem without damage scenarios. Then, the dispatch decisions are fixed as the first stage dispatch decisions in the optimization model with no other planning decisions. The optimization model is then solved to consider re-dispatch decisions corresponding to each scenario. For the resilient re-dispatch case, the first-stage dispatch decisions are also



**Figure 6.3** Loss distribution of overall scenarios for each wind speed.

obtained from the optimization model, contrary to the prior cases, where the first-stage generator dispatch decisions were fixed. The remaining cases consider resilient re-dispatch of generators along with hardening, upgrade, and DG decisions. In these cases, the maximum number of investments for each decision is fixed to 10. It can be observed that CVaR is minimum when considering all investment decisions for  $\lambda = 0.95$ ,  $\mathcal{C}_T^{max} = \$ 3$  bil, which is an improvement of 68.32% from the baseline case. However, the expected load loss is minimal when considering all investment decisions for  $\lambda = 0$ ,  $\mathcal{C}_T^{max} = \$ 3$  bil, which is an improvement of 81.79% from the baseline case. There is a slight trade-off observed in the expected load shed when the risk aversion increases, irrespective of budget. This is normal as the optimization model focuses on investing more to minimize the impact of HILP events, which can lower the performance slightly during expected conditions.

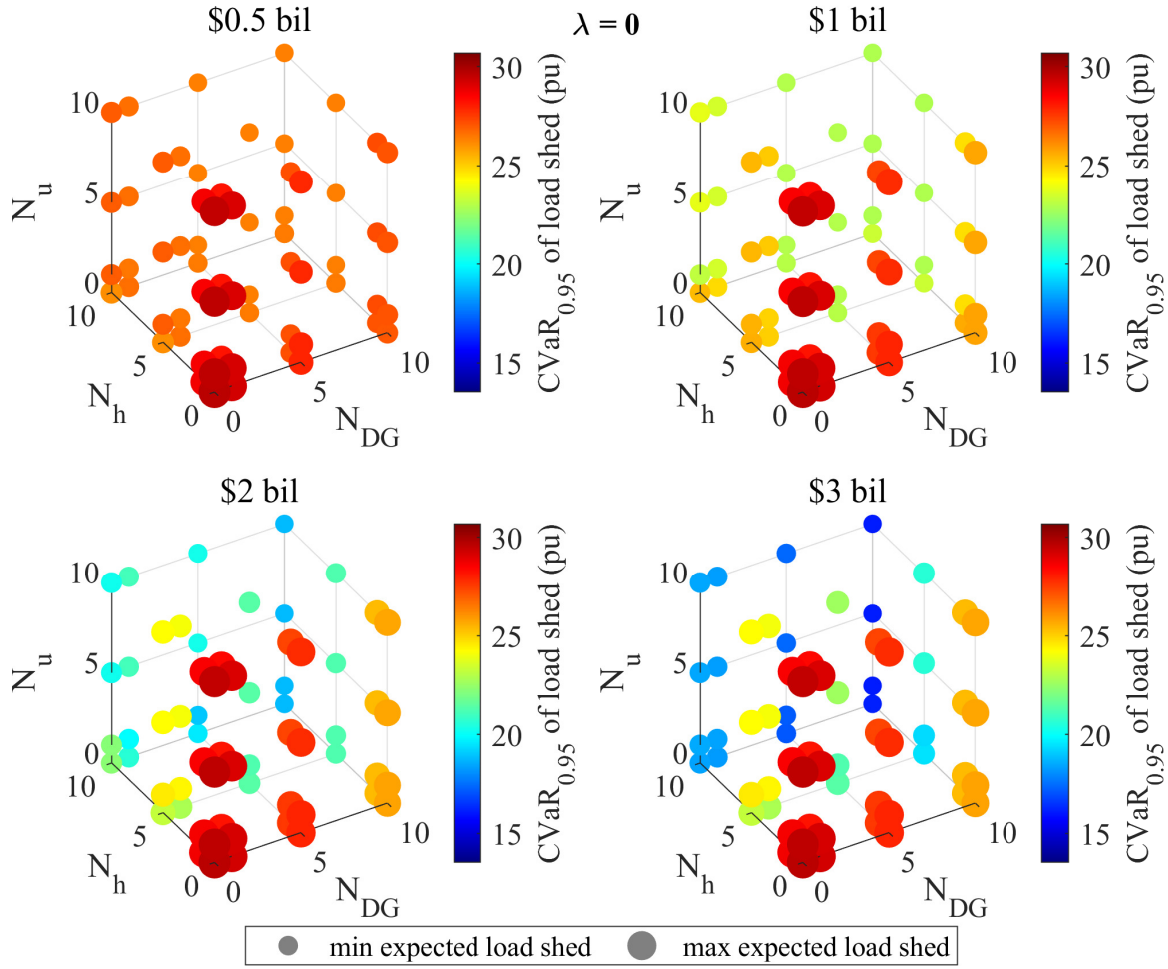


**Figure 6.4** Comparison of total and % load shed for various planning strategies.

**Table 6.2** Expected load shed and CVaR for various planning strategies, risk aversion, and budget.

$\lambda$	$C_T^{\max}$	Planning Strategy	$\mathbb{E}(\mathcal{F}(\mathbf{x}, \mathcal{E})$		$\text{CVaR}_{0.95}(\mathcal{F}(\mathbf{x}, \mathcal{E})$	
			Value (MW)	Change (%)	Value (MW)	Change (%)
-	-	DCOPF (base case)	318.68	-	4588.07	-
-	-	DCOPF + re-dispatch	162.14	49.12	3028.22	34
-	-	resilient re-dispatch	158.87	52.34	2966.17	35.35
0	\$0.5 bil	$N_h, N_u, N_{DG} = 10$	119.78	62.41	2634.85	42.57
0.95	\$0.5 bil	$N_h, N_u, N_{DG} = 10$	128.23	59.76	2544.01	44.55
0	\$3 bil	$N_h, N_u, N_{DG} = 10$	<b>50.01</b>	<b>81.79</b>	1612.12	64.86
0.95	\$3 bil	$N_h, N_u, N_{DG} = 10$	77.68	75.62	<b>1453.48</b>	<b>68.32</b>

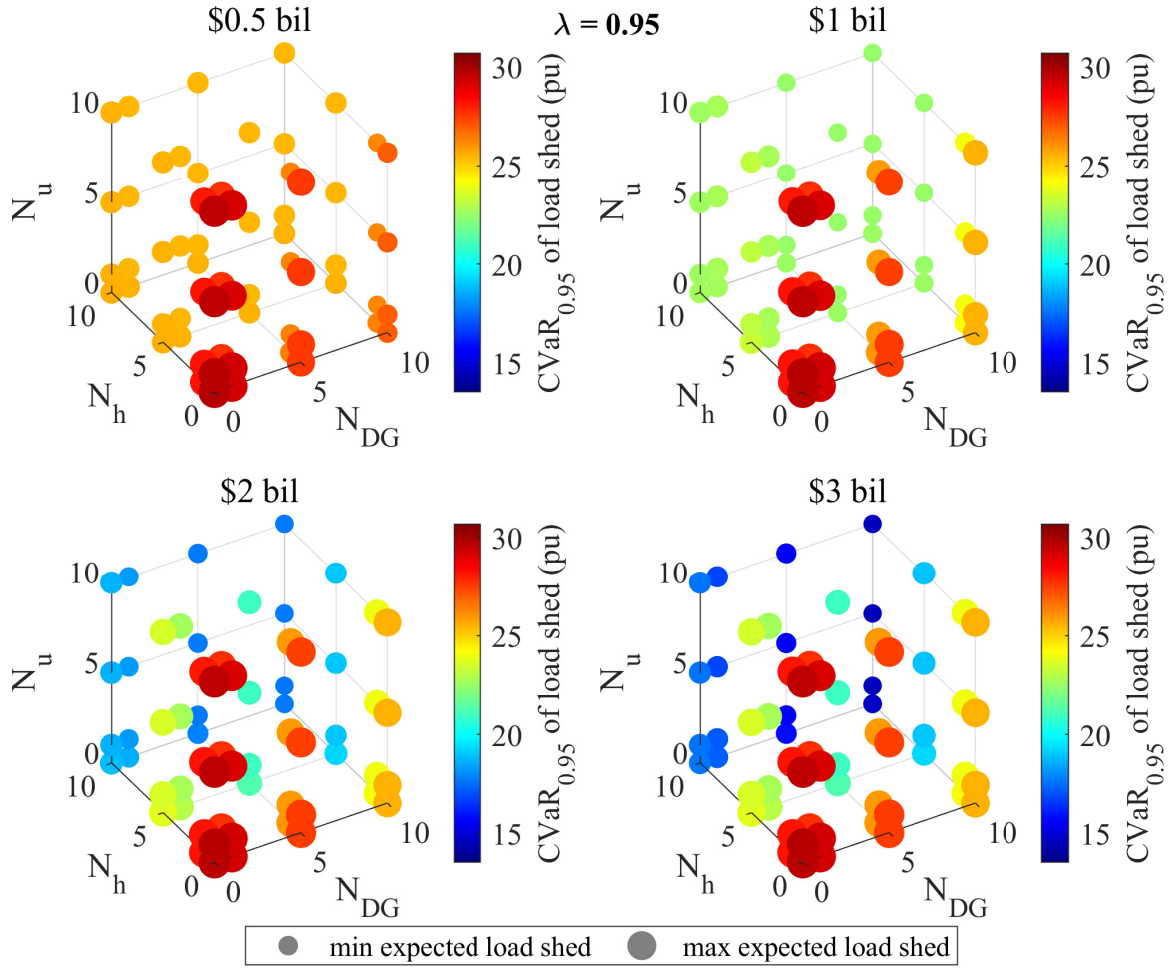
The justification above is further clarified by Fig. 6.4, which shows the optimization decisions for a HILP scenario where  $v = 41 \text{ m/s}$  and  $p^\xi = 0.000672$ . Although multiple lines are out-of-service in this particular scenario, the system contains several generators that can serve the load in the respective buses. However, the generators are constrained by their ramp rates and dispatch set points, which is the first-stage decision. The DCOPF + re-dispatch case is assumed as the base case here. The resilient re-dispatch model has minimal improvement over the former model in terms of load-shed minimization for this scenario. It is to be noted, however, that these decisions were made considering the entire range of scenarios, and considering all scenarios, the resilient re-dispatch model has an improvement of over 3% in expected load shed minimization as compared to DCOPF + redispatch model, as shown in Table 6.2. However, it is evident that the resilient re-dispatch model does not perform well in HILP conditions. For the rest of the cases, the overall planning decisions change drastically depending upon the budget and objective. For this HILP scenario,



**Figure 6.5** Variation of expected load shed and CVaR of load shed for varying planning portfolios risk-neutral decisions.

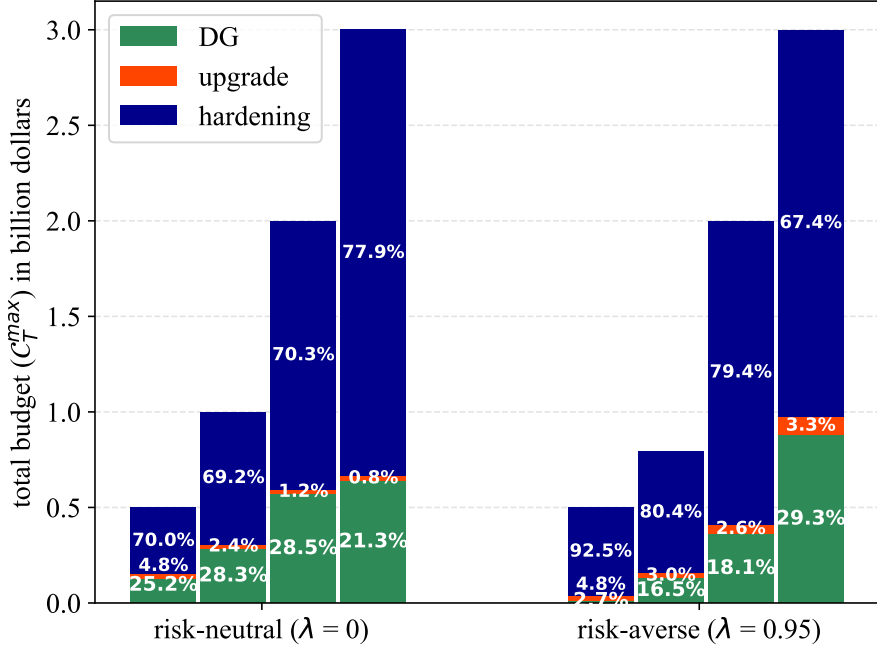
the minimal load shed condition is achieved by the risk-averse model with \$3 billion investment. Hence, this is an important conclusion that it is essential to minimize CVaR when we want to minimize load shed for HILP scenarios. Interestingly, risk-averse models tend to invest more in hardening 230 kV lines since these lines have higher power-carrying capability and can serve more loads in case of failure of other lines.

Fig. 6.5 and Fig. 6.6 presents a variation of expected and CVaR of load shed for



**Figure 6.6** Variation of expected load shed and CVaR of load shed for varying planning portfolios risk-averse decisions.

various planning portfolios. The circle size represents the expected load shed for each combination, whereas the color of the circles represents CVaR. The maximum cap on each investment decision varies within  $[0, 1, 5, 10]$ , where 0 represents the case when no other planning decisions, other than generator dispatch decisions, are considered i.e., resilient re-dispatch case. For a constant budget, increasing  $N_u$  has minimal impact in minimizing both the CVaR and expected load shed, whereas increasing  $N_h$  has the maximum impact in all conditions. The improvement when increasing



**Figure 6.7** Budget distribution for multiple planning decisions.

$N_{DG}$  is less than the line hardening but better than the capacity upgrade. When considering capacity upgrades only, the improvement is minimal, even if the budget is increased. In fact, increasing  $N_u$  in combination with other investments shows a slight increment in risk for risk-neutral cases. However, the proper combination of line upgrade, hardening, and DG can effectively minimize the expected load shed and CVaR. Consistent with the prior results, CVaR is minimum when  $\lambda = 0.95$ ,  $C_T^{max} = \$ 3$  bil whereas the expected load shed is minimum when  $\lambda = 0.95$ ,  $C_T^{max} = \$ 3$  bil.

The planning decisions corresponding to the  $N_u, N_e, N_{DG} = 10$  are taken, and the overall budget distribution for each case is shown in Fig. 6.7. Interestingly, for lower budget cases until  $C_T^{max} = \$1$  billion, the risk-averse model puts a significant amount of budget in line hardening compared to other decisions. For  $C_T^{max} = \$3$  billion, a considerable amount of the budget is shifted towards DGs. For the risk-neutral case,

the budget proportion is almost the same for the first three budgets. However, when  $\mathcal{C}_T^{max} = \$3$  billion, the risk-neutral model increases the investment in line hardening. For almost all cases, the capacity upgrade is least adopted and is only considered once the budget for other investments has been fulfilled and the remaining budget can no longer make those investments for a given objective.

## 6.5 Summary

This chapter presented a resilience-driven proactive generation dispatch and multi-resource investment planning model using a two-stage stochastic optimization framework. The proposed model can identify the optimal generation dispatch, lines to harden, upgrade, and DG siting and sizing decisions, which can assist in minimizing the expected load shed and CVaR of the load shed when extreme weather scenarios are realized. The resilient re-dispatch model allows the generator to achieve a certain set point from which they can modulate within the ramp rate constraints to minimize the load shedding for a range of scenarios effectively. Detailed simulations and analysis verified that the proposed method behaves considerably well compared to DCOPF-based methods, which do not have resilience considerations. Furthermore, risk-averse decisions for the same investment budget can significantly reduce load shedding in HILP scenarios compared to other cases. It was also observed that line hardening is the most effective, and line capacity upgrade is the least effective method to minimize the load shed when considered as two independent investments. However, it was also observed that an effective planning strategy can enhance the power grid's resilience against extreme weather events.

## REFERENCES

- [1] A. B. Smith, “2022 U.S. billion-dollar weather and climate disasters in historical context,” *NOAA National Centers for Environmental Information (NCEI)*, 2023.
- [2] Climate Central, “Surging power outages and climate change,” *Climate Central*, Sep. 2022.
- [3] J. L. B. II, A. Hagen, and R. Berg, “National hurricane center tropical cyclone report,” *Hurricane Ida*, 2022.
- [4] G. S. Poulos, W. Johnson, J. Crescenti, M. Stoelinga, and J. Bosche, “Ercot market cold weather failure 10-19 february 2021: wind energy financial loss and corrective actions,” *ArcVera Renewables*, 2021.
- [5] H. Farzin, M. Fotuhi-Firuzabad, and M. Moeini-Aghetaie, “Enhancing power system resilience through hierarchical outage management in multi-microgrids,” *IEEE Transactions on Smart Grid*, vol. 7, no. 6, pp. 2869–2879, 2016.
- [6] C. Wang, Y. Hou, F. Qiu, S. Lei, and K. Liu, “Resilience enhancement with sequentially proactive operation strategies,” *IEEE Transactions on Power Systems*, vol. 32, no. 4, pp. 2847–2857, 2016.
- [7] M. H. Amirioun, F. Aminifar, and H. Lesani, “Towards proactive scheduling of microgrids against extreme floods,” *IEEE Transactions on Smart Grid*, vol. 9, no. 4, pp. 3900–3902, 2017.
- [8] E. Heylen, M. Ovaere, S. Proost, G. Deconinck, and D. Van Hertem, “A multi-

- dimensional analysis of reliability criteria: From deterministic n- 1 to a probabilistic approach,” *Electric Power Systems Research*, vol. 167, pp. 290–300, 2019.
- [9] F. Verástegui, A. Lorca, D. E. Olivares, M. Negrete-Pincetic, and P. Gazmuri, “An adaptive robust optimization model for power systems planning with operational uncertainty,” *IEEE Transactions on Power Systems*, vol. 34, no. 6, pp. 4606–4616, 2019.
- [10] J. Yan, B. Hu, K. Xie, J. Tang, and H.-M. Tai, “Data-driven transmission defense planning against extreme weather events,” *IEEE Transactions on Smart Grid*, vol. 11, no. 3, pp. 2257–2270, 2019.
- [11] D. Alvarado, R. Moreno, A. Street, M. Panteli, P. Mancarella, and G. Strbac, “Co-optimizing substation hardening and transmission expansion against earthquakes: A decision-dependent probability approach,” *IEEE Transactions on Power Systems*, vol. 38, no. 3, pp. 2058–2070, 2023.
- [12] A. Soroudi, P. Maghouli, and A. Keane, “Resiliency oriented integration of DSRs in transmission networks,” *IET Generation, Transmission & Distribution*, vol. 11, no. 8, pp. 2013–2022, 2017.
- [13] T. Lagos, R. Moreno, A. N. Espinosa, M. Panteli, R. Sacaan, F. Ordonez, H. Rudnick, and P. Mancarella, “Identifying optimal portfolios of resilient network investments against natural hazards, with applications to earthquakes,” *IEEE Transactions on Power Systems*, vol. 35, no. 2, pp. 1411–1421, 2020.
- [14] M. Bynum, A. Staid, B. Arguello, A. Castillo, B. Knueven, C. D. Laird, and J.-P. Watson, “Proactive operations and investment planning via stochastic op-

timization to enhance power systems' extreme weather resilience," *Journal of Infrastructure Systems*, vol. 27, no. 2, 2021.

- [15] A. Poudyal, S. Poudel, and A. Dubey, "Risk-based active distribution system planning for resilience against extreme weather events," *IEEE Transactions on Sustainable Energy*, vol. 14, no. 2, pp. 1178–1192, 2022.
- [16] C. Barrows, A. Bloom, A. Ehlen, J. Ikäheimo, J. Jorgenson, D. Krishnamurthy, J. Lau, B. McBennett, M. O'Connell, E. Preston, *et al.*, "The ieee reliability test system: A proposed 2019 update," *IEEE Transactions on Power Systems*, vol. 35, no. 1, pp. 119–127, 2019.
- [17] R. T. Rockafellar, S. Uryasev, *et al.*, "Optimization of conditional value-at-risk," *Journal of risk*, vol. 2, pp. 21–42, 2000.
- [18] L. C. Coelho, "Linearization of the product of two variables," *Canada Research Chair in Integrated Logistics*, 2013.
- [19] M. Panteli, C. Pickering, S. Wilkinson, R. Dawson, and P. Mancarella, "Power system resilience to extreme weather: Fragility modeling, probabilistic impact assessment, and adaptation measures," *IEEE Transactions on Power Systems*, vol. 32, no. 5, pp. 3747–3757, 2016.
- [20] W. Römisch, "Scenario reduction techniques in stochastic programming," in *International Symposium on Stochastic Algorithms*, pp. 1–14, Springer, 2009.
- [21] J. Ekblom and J. Blomvall, "Importance sampling in stochastic optimization: An application to intertemporal portfolio choice," *European Journal of Operational Research*, vol. 285, no. 1, pp. 106–119, 2020.

- [22] V. L. Parsons, “Stratified sampling,” *Wiley StatsRef: Statistics Reference Online*, pp. 1–11, 2014.
- [23] H. Heitsch and W. Römisch, “A note on scenario reduction for two-stage stochastic programs,” *Operations Research Letters*, vol. 35, no. 6, pp. 731–738, 2007.
- [24] W. E. Hart, C. D. Laird, J.-P. Watson, D. L. Woodruff, G. A. Hackebeil, B. L. Nicholson, J. D. Siirola, *et al.*, *Pyomo-optimization modeling in python*, vol. 67. Springer, 2017.
- [25] L. Gurobi Optimization, “Gurobi optimizer reference manual,” 2021.
- [26] R. D. Zimmerman, C. E. Murillo-Sánchez, and R. J. Thomas, “Matpower: Steady-state operations, planning, and analysis tools for power systems research and education,” *IEEE Transactions on power systems*, vol. 26, no. 1, pp. 12–19, 2010.
- [27] Valley Electric Association (VEA), “VEA 2022 Final Per Unit Cost Guide,” *California ISO*, 2022.
- [28] Pacific Gas and Electric (PG&E), “PG&E 2022 Final Per Unit Cost Guide,” *California ISO*, 2022.
- [29] K. Anderson, X. Li, S. Dalvi, S. Ericson, C. Barrows, C. Murphy, and E. Hotchkiss, “Integrating the value of electricity resilience in energy planning and operations decisions,” *IEEE Systems Journal*, vol. 15, no. 1, pp. 204–214, 2020.

## CHAPTER 7

### SCALABLE PLANNING FRAMEWORK FOR RESILIENCE PLANNING IN POWER DISTRIBUTION SYSTEMS

#### 7.1 Introduction

This chapter introduces a scalable resilience planning framework. As discussed in the previous chapter, a two-stage risk-averse framework is proposed. This chapter aims to test the scalability of the planning model in terms of model complexity and scenarios. Hence, all performance experiments are conducted with random line outage scenarios for expected load loss minimization. We use distributed generators (DGs) with grid-forming capabilities and line-hardening decisions for planning decisions.

##### 7.1.1 Motivation

In power engineering, the resource planning framework is divided into two categories — long-term investment planning and short-term operational planning. Due to both frameworks' stochastic nature, planning models are significantly challenging to solve with the increase in the number of scenarios. Although there have been modeling improvements in the past, planning models for a size comparable with utility-scale feeders are still unsolvable [1]. Hence, there is a need for a scalable framework for grid planners to identify reasonable planning solutions in polynomial time. Moreover, the complexity of the planning models, both due to model complexity and a high number of scenarios, makes it increasingly difficult to obtain the planning solutions, let alone assess their quality. This chapter discusses using a dual-decomposition approach to scale the resilience planning model. For simplicity, we verify the proposed approach

to the distribution systems model. However, the model is generic and applies to transmission studies as well.

### 7.1.2 Related Literature and Gaps

Existing distribution systems resilience planning models suffer from the curse of dimensionality, where a marginal number of scenarios can increase the problem size significantly [2]. Furthermore, most planning models are validated on smaller test cases with several assumptions, making such models less accurate for real-world problems [3]. A few other works have developed frameworks for large-scale problems but these works either compromise on the solution quality [4] or make several assumptions to solve the problem [5]. Some of the scalability issues are readily solved via modeling innovations [1], whereas other works follow an approach of scenario reduction [6] or the use of advanced computing resources [7]. Nevertheless, there is a significant gap in existing works that can address the issue of scalability in power systems planning.

### 7.1.3 Contribution

This chapter proposes a framework for large-scale planning problems in power systems using dual decomposition techniques and high-performance computing architectures. Specifically, the progressive hedging (PH) algorithm and its extensions are leveraged to decompose the two-stage planning problem into scenario-based sub-problems by relaxing the non-anticipativity constraints. The framework is tested on a realistic 9500-node distribution system for several scenarios. In this chapter, we develop a two-stage stochastic programming model with grid-forming DERs and hardening decisions for a 9500-node system. The problem is further decomposed into several sub-problems

based on the number of damage scenarios in the model. The proposed approach can solve a relatively complex stochastic optimization problem in significantly reduced time and with reasonable accuracy compared to the extensive form version of the problem.

## 7.2 Scalable Framework for Power Systems Planning

### 7.2.1 Dual-decomposition with Progressive Hedging

The compact version of a general two-stage stochastic programming model is extensively discussed in Chapter 4 and can be written as

$$\min c^T x + \mathbb{E}(Q(x, \mathcal{E})) \quad (7.1)$$

$$s.t. Ax \geq b \quad (7.2)$$

$$x \in \mathbb{R} \times \mathbb{Z} \quad (7.3)$$

Generally, these problems are solved as a single significant problem known as the extensive form (EF) of the overall stochastic programming problem. Hence, it is computationally challenging to build and solve such models for problems with many scenarios, a large system model, or both. The problem complexity is due to the non-anticipative nature of first-stage variables,  $x$ . In [8], a dual-decomposition technique known as Progressive Hedging (PH) decomposes each scenario by relaxing the problem's non-anticipation and introducing the objective's dual variable and penalty function. The non-anticipativity relaxation makes each scenario-based subproblem independent, which is naturally parallelizable, as shown in Fig. 7.1. PH has been proven to solve stochastic problems of any number of stages and with optimality in-

volving continuous decisions. However, for problems with mixed-integers or binary variables, PH has successfully been used as an excellent heuristic to get to a reasonable approximation of the overall solution [9].

The following equation defines the overall objective of the PH algorithm:

$$x_\xi^{k+1}, Q(x_\xi, \xi)^{k+1} = \operatorname{argmin}_{x_\xi, Q(x_\xi, \xi)} (c^T x + Q(x, \mathcal{E} + (\tau_\xi^k)^T x_\xi + \rho^k \|x_\xi - \bar{x}^k\|_2^2)) \quad (7.4)$$

where  $\tau$  is the dual weight variable,  $\rho$  is the penalty factor, and  $\bar{x}$  is the average value of first-stage decisions obtained through a consensus. A common way to get the consensus is through  $\bar{x} = \sum_\xi p_\xi^k x_\xi^k$ , i.e., get the average of first-stage decisions in each scenario. Here,  $k$  is the number of iterations, and the first-stage decisions and duals are iteratively updated until convergence. The convergence of the PH algorithm is determined either by the maximum number of iterations  $k$  or through the normalized term difference coefficient metric as given by:

$$\frac{\sum_{\xi \in \mathcal{E}} \frac{p_\xi \|x_\xi^{k+1} - \bar{x}^{k+1}\|_2^2}{\bar{x}^{k+1}}}{|\mathcal{E}|} \leq \epsilon_t \quad (7.5)$$

Fig. 7.2 shows the summarized version of the PH algorithm. In every iteration, the dual weight variable is updated based on the first-stage decisions and penalty factor  $\rho$ .

### 7.2.2 Progressive Hedging Extensions

PH is a heuristic approach, especially for stochastic mixed-integer problems. Hence, the solution quality and solve time significantly depend on the parameters that guide the algorithm's convergence. The methods to accelerate the convergence of the PH

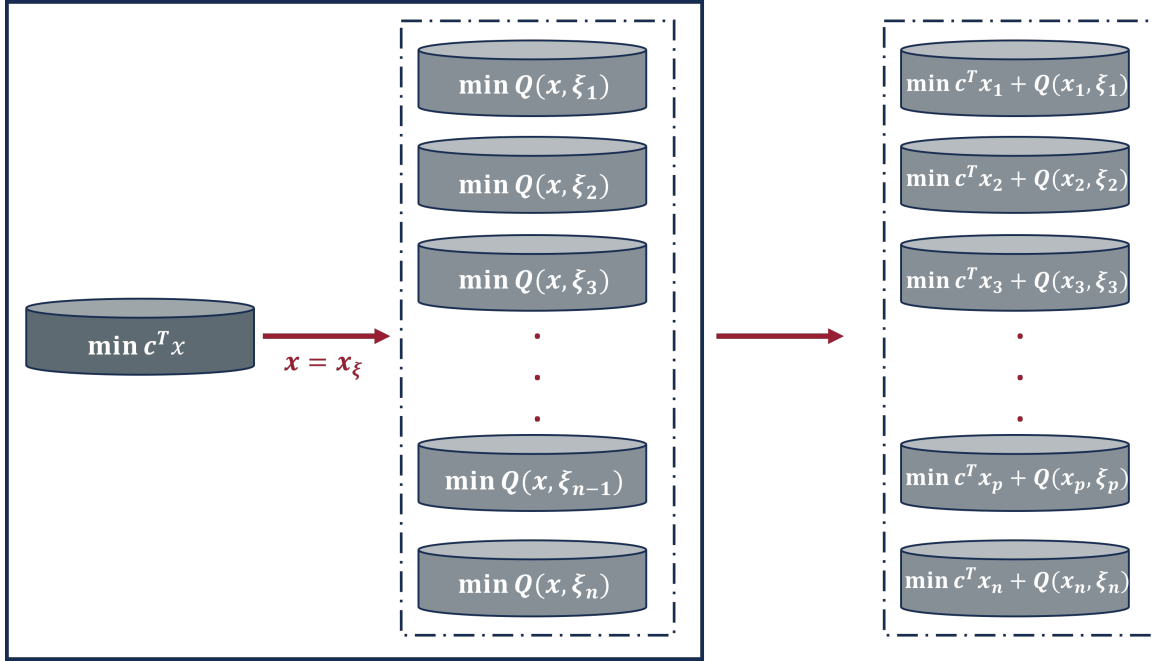


**Figure 7.1** Scenario decomposition and non-anticipativity relaxation

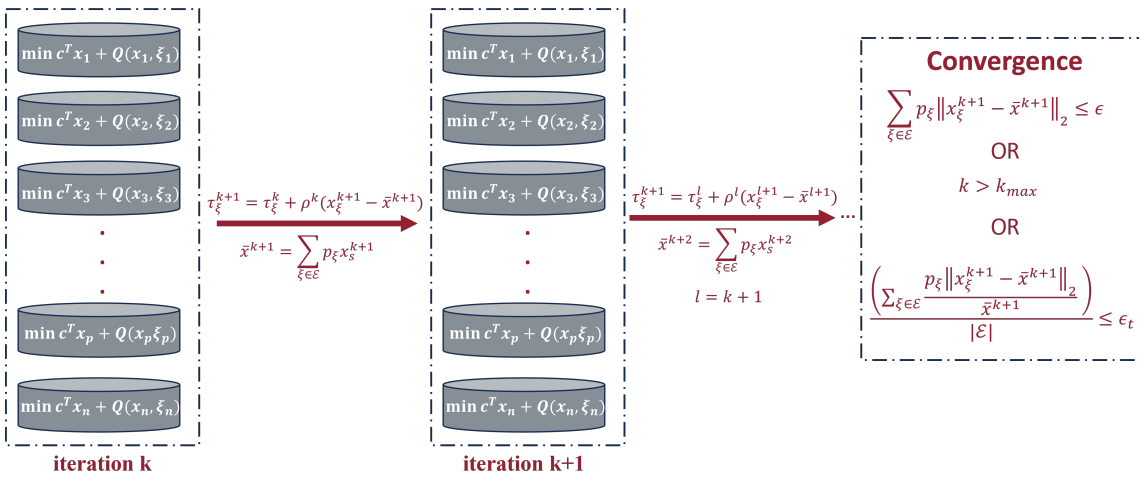


**Figure 7.2** Progressive Hedging Algorithm

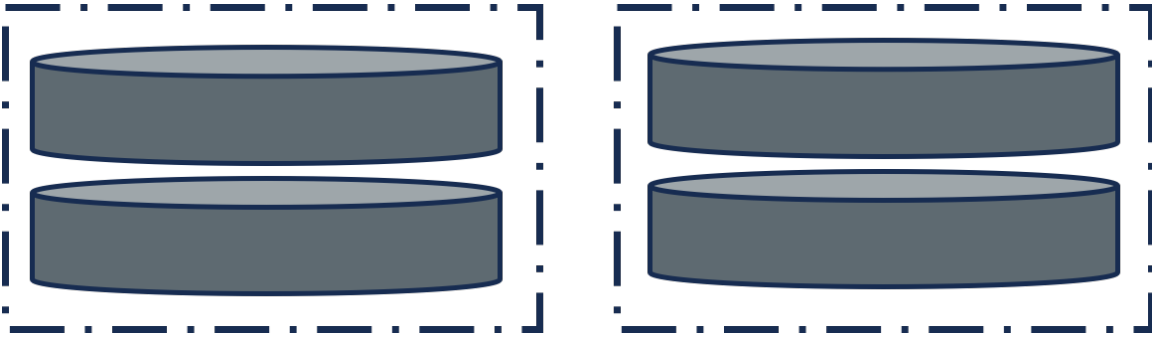


**Figure 7.3** Two scenario bundles with two scenarios each

algorithm and improve the solve time are discussed in [9]. We briefly discuss some of those innovations that apply to our planning problem.

### Scenario Bundling

The concept of scenario bundling is to bundle some of the independent scenario sub-problems and solve the extensive form for each bundle. Each bundle then acts as one sub-problem for the PH algorithm. Fig. 7.3 represent an example of two scenario bundles each with two independent scenarios. Bundling scenarios can significantly improve the quality of the solution. However, the solve time can increase significantly depending on the number of bundles or scenarios per bundle since we are solving extensive forms for each bundle [10, 11, 12]. In this work, we randomly bundle an equal number of scenarios in different bundles.

### Variable Fixing and Slammering

During early PH iterations, certain decision variables can converge to a fixed value for all scenarios and do not change in subsequent iterations [9]. A lag parameter  $\mu$  is introduced as a user parameter that defines the variable fixing strategy if the

decision variables remain unchanged for  $\mu$  number of PH iterations. Furthermore, an aggressive approach of variable slamming can be taken for mixed integer problems, which can suffer cyclic behavior due to integer decisions. Some decision variables can be fixed to their nearest lower or upper bound to avoid cyclic behavior. Additionally, when most decisions have been fixed, PH can still take longer to reach convergence. Hence, the remaining variables are slammed to get the current solution. These approaches can drastically minimize the overall solve time with a slight compromise on the solution quality [9, 13].

## Penalty Factor

The penalty factor,  $\rho$  is the most important parameter to accelerate the convergence of PH algorithm [9, 12]. A usual approach is to select a fixed value of  $\rho$  for all variables in entire PH iterations. However, several other approaches exist to select the penalty factor's value as suggested in [9]. The lower value of  $\rho$  facilitates slower convergence with better solution accuracy, whereas the higher value of  $\rho$  does the opposite. Hence, it is important to identify a proper value of  $\rho$  that can improve the convergence time and solution quality of the overall problem. One approach other than the fixed value approach is to select  $\rho$  proportional to the cost of the first stage decisions. With this approach, the value of  $\rho$  will differ for each first-stage decision. Existing works have shown that this method of  $\rho$  selection has significantly improved the solution quality of problems solved via PH [12]. However, some problems suffer from premature convergence and do not behave well with such approaches [9]. Hence,  $\rho$  selection is problem-specific and should be carefully selected to improve the solution time and quality.

## Lagrangian Lower Bound

The PH algorithm is a heuristic approach and can only provide the primal solution. Often, the accuracy of primal solutions can only be assessed if they can be compared with other solutions of the problem obtained through alternative approaches. A general way to do that is to solve the extensive form of the overall problem and compare the primal solution of the PH with the current solution of the extensive form problem. However, such a method can only provide a range of solution regions, not its bounds. In [12], the dual bound of the PH problem is mathematically derived such that the dual weight variable  $\tau(\xi) \in \mathbb{R}^n$  satisfies  $\sum_{\xi \in \mathcal{E}} p_\xi \tau(\xi) = 0$ . Obtaining explicit bounds on the stochastic problem will help assess the solution quality. Let  $D_\xi(\tau(\xi))$  represent the objective term without penalty function such that,

$$D_\xi(\tau(\xi)) := \min_{(x, Q(x, \xi))} (c^T x + Q(x, \xi) + \tau(\xi)^T x) \quad (7.6)$$

then the lower bound (upper for maximization problem) is given by,

$$D(\tau) := \sum_{\xi \in \mathcal{E}} p_\xi D_\xi(\tau(\xi)) \leq z^* \quad (7.7)$$

## PH as heuristic for Extensive Form

As a heuristic, the PH algorithm can only improve the solution convergence as much. The solution is obtained in the first few iterations, and the further iterations are just fine-tuning the algorithm to reach a better solution. However, in certain instances, the problem does not improve further and fails to reach convergence. In such situations, PH can be used as an initial heuristic to reach a solution, and the results can then

be used as a warm start solution to solve the overall problem using the extensive form. This way, the final bounds of the problem can be obtained quickly through a branch-and-bound algorithm for the resulting MILP model.

### 7.3 Results and Analysis

This section discusses the results and analysis of the proposed framework for scalable planning in power distribution systems. Since this Chapter highlights the planning framework’s scalability, we simplify the scenario generation and reduction approach with randomly generated fault scenarios to mimic the threat model. Furthermore, the planning model discussed in Chapter 5 is leveraged with line hardening, DER siting, and sizing decisions. The second stage of the problem is modeled using LinDis-TRestoration package [14]. The overall problem is solved using the PySP package in Pyomo using Gurobi [15, 16, 17]. The PH algorithm is solved in parallel in WSU’s Kamiak high-performance computing environment with up to 55 cores using Python Remote Objects (PYRO) [18]. The extensive form of the problem is solved in the Intel Xeon Gold 6230 @2.10 GHz Workstation with 32 GB RAM and 20 physical cores. All of the physical cores are utilized for branch-and-bound through Gurobi.

#### 7.3.1 9500-Node Model

The 9500-node test system is the modified version of the IEEE-8500-node test system [19]. It is a comprehensive, futuristic utility-sized system with three feeders connected to a 69 kV sub-transmission line. The overall system supplies a total load of 12236.73 kW, consisting of 7 tie-switches and 101 sectionalizing switches. Furthermore, eight utility-scale DERs can be operated in an islanded mode. Fig. 7.4

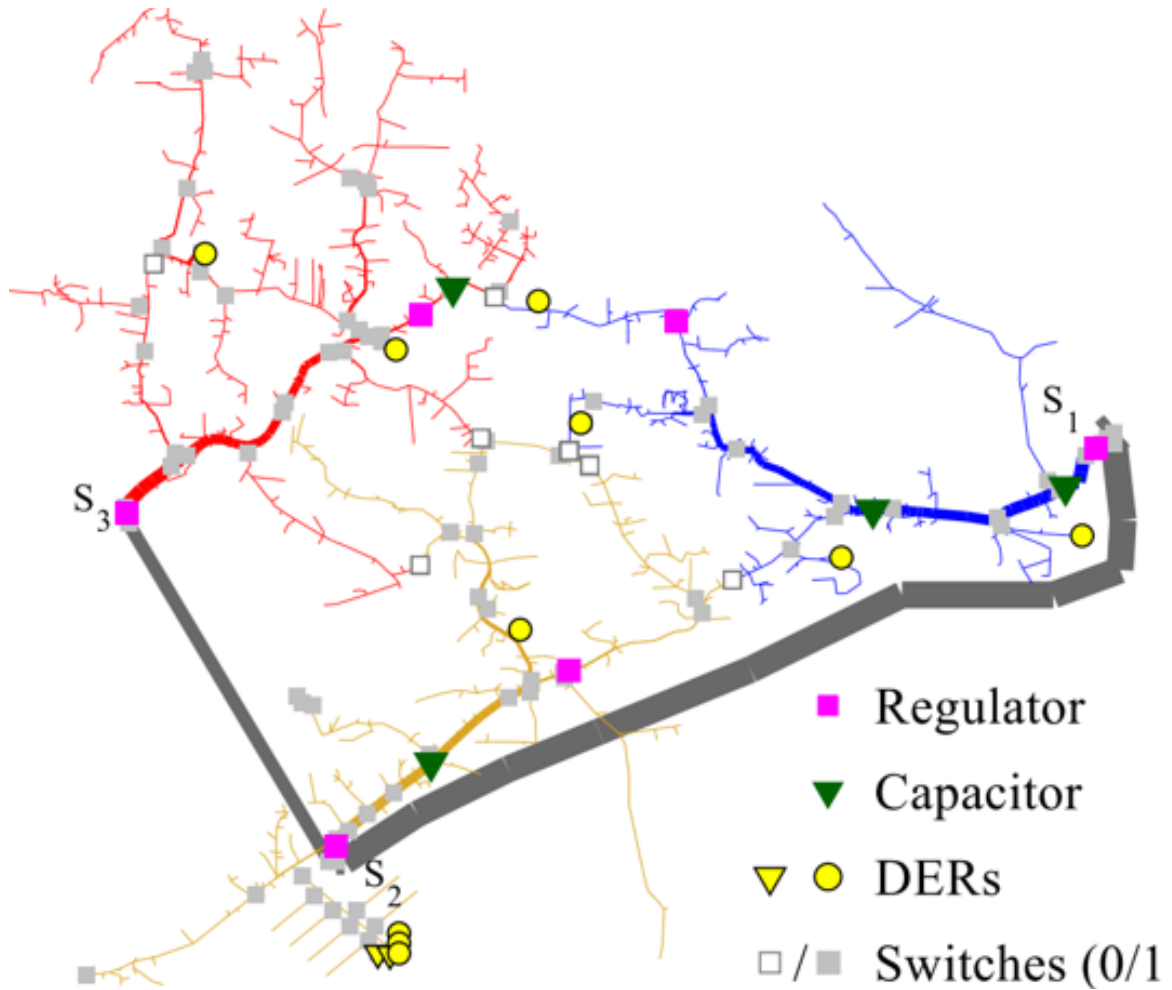


**Figure 7.4** 9500-node test system.

represents the schematic of the 9500-node system.

In this work, we consider all the tie-switches as candidate tie-switch locations and assume that all the existing DERs are candidate locations to site the DERs. For their sizing, each DER can be sized to a maximum of the provided capacity of the DERs in [19]. Furthermore, we do not consider the backup DGs in this work; every branch is a potential candidate for line hardening. The maximum number of DER sites and lines available for hardening is limited to two and five, respectively. All the secondary

**Table 7.1** Comparison of model complexities with the number of scenarios.

Scenarios	Number of Constraints	Number of Variables		
		Continuous	Binary	Total
5	522581	14600	82485	97085
10	1045161	283750	164970	448720
20	2090321	559250	329940	889190
50	5225801	1385750	824850	2210600

lines are referred back to their primary, and hence, the system contains 2745 nodes and 2773 branches, where some of the nodes are three phases. For each scenario, the maximum damage is also limited to 5% of the overall system.

### 7.3.2 Analysis of Model Complexities

As discussed earlier, the increase in the number of scenarios can significantly increase the complexity of the stochastic model. Table. 7.1 shows the number of constraints and variables in the stochastic model with the number of scenarios. Just with five scenarios, the model has over half a million constraints and about 100k variables. The size increases exponentially with over 5.2 million constraints and 2.2 million variables when the number of scenarios increases to 50.

Fig. 7.5 represents the factor of increase in the number of scenarios in the horizontal axis, and the increase in the factor of constraints and variables is represented by the vertical axis, where the base number is represented for cases with five scenarios. It can be seen that although the increase in the number of constraints is almost linear, the number of variables increases exponentially with the increase in the number of

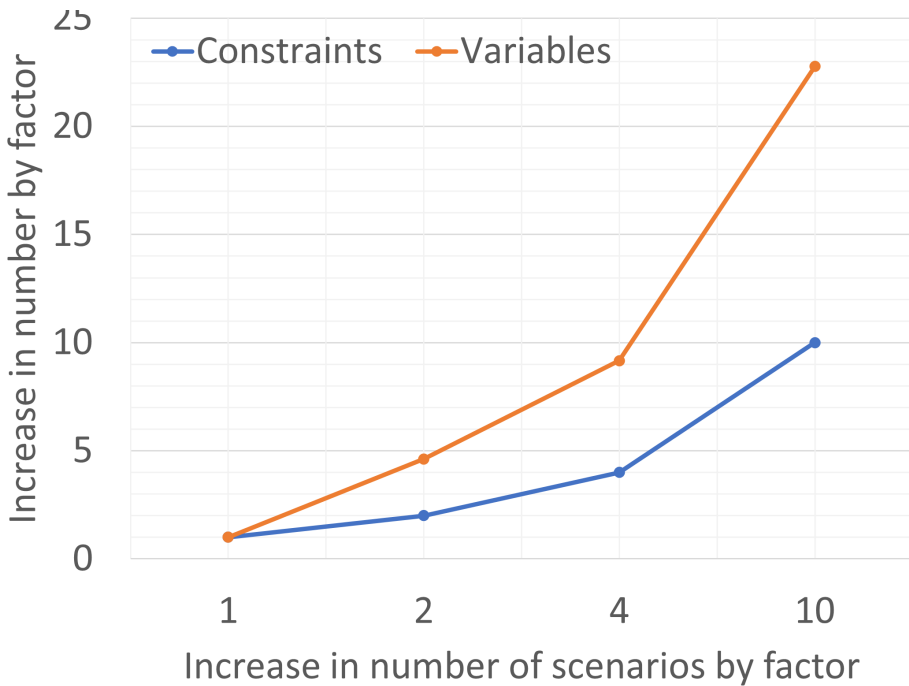


**Figure 7.5** Increase in model complexity with the increase in the number of scenarios. The base with factor 1 is represented by 5 scenarios.

scenarios.

### 7.3.3 Scalability of Planning Models

Table. 7.2 shows the results of EF and PH algorithms to solve the planning model with varying numbers of scenarios for each algorithm. For PH, each experiment was run with 20 core machines, and the number of threads available for branch and bound was limited to 2. The EF of the problem was solved in less than an hour for five scenarios, but the solving time increased significantly for a higher number of scenarios. For 20 scenarios, the problem was solved optimally in around 10 hours. However, with 50 scenarios, the problem was not solved in over 53 hours and still had a mip gap of about 17%. For the PH algorithm, the maximum number of iterations was set to

**Table 7.2** Solve time and solution for EF and solution with relative gap and parameters for PH algorithm.

Scenario	Method	Objective	Time (hrs)	Rel Gap (%)	Rho	iterations	converged
5	EF	5499.038	0.113	-	-	-	Yes
	PH	5126.08	0.744	6.78	10	100	No
	PH	5366.408	0.005	2.41	10	1	No
	20	EF	3622.9	10.708	-	-	Yes
		PH	3363.47	1.390	7.16	1	No
	50	EF	2887.1 (UB)	53	17	-	No
		EF	2460.8 (LB)	53	17	-	No
		PH	2136.2	2.478	26.01 (UB)	1	No
		PH	2095.65	1.904	27.41 (UB)	0.1	No
		PH	2104.38	3.989	27.11 (UB)	10	No
		PH	2136.2	2.478	13.19 (LB)	1	No

100 for convergence, and the term-difference convergence metric threshold was set to 1e-6. The PH algorithm took less than an hour for five scenarios case. However, the objective was very close to the optimal objective obtained through EF in the first iteration. PH finds a reasonably good solution in the first few iterations and fine-tunes the model in the subsequent iterations. For all experiments, the PH algorithm terminated due to the end of a maximum number of iterations. The solve time is significantly less than EF for the higher number of scenarios. For 20 iterations, PH solves the problem 7.6 times faster than EF with a relative gap of 7.16%. For the problem with 50 scenarios, the best solution is given by PH with  $\rho = 1$  with a relative gap of 26% with the upper bound and 13.19% with the lower bound with a speedup of about 25 times. All the PH experiments are performed with the base model of PH,

with the number of compute cores limited to 20.

#### 7.3.4 PH Extensions

The extensions discussed above are now applied to the PH algorithm. Furthermore, we increase the number of cores to 55 for each experiment with PH. The first extension is scenario bundling. We create 25 bundles, each with 2 randomly grouped scenarios, and solve the problem with PH. Each bundle, however, will have an extensive form problem to solve with 2 scenarios each. The value of  $\rho$  is set to a constant value of 1. The objective improved to 2163.95 kW with a solve time of 9.89 hours. We did not decrease the number of bundles as with just 2 scenarios per bundle, the solve time is increasing significantly.

Next, we use an adaptive rho converger so that the selected rho value minimizes the primal and dual residuals. We fix the variables with a lag factor of 5 and slam the variables if a cycle is detected after 30 iterations. Finally, after obtaining the PH solution, we use it as a warm start with fixed variables for the EF problem, which can then solve the problem using branch and bound. The objective was improved to 2244.19 kW, and the PH algorithm terminated in 74 iterations. However, the EF problem did not further improve the objective. Fig. 7.6 a. shows the normalized term-difference convergence metric and Fig. 7.6 b. shows the primal-dual residual convergence metric.

Finally, using a heuristic approach, we determine a variable value of  $\rho$  for each iteration based on their first-stage solution. Then, the value is fixed for subsequent iterations. We also obtain Lagrangian lower bounds to assess the quality of the solution. Fig. 7.7 shows the upper and lower bounds of the problem. The horizontal

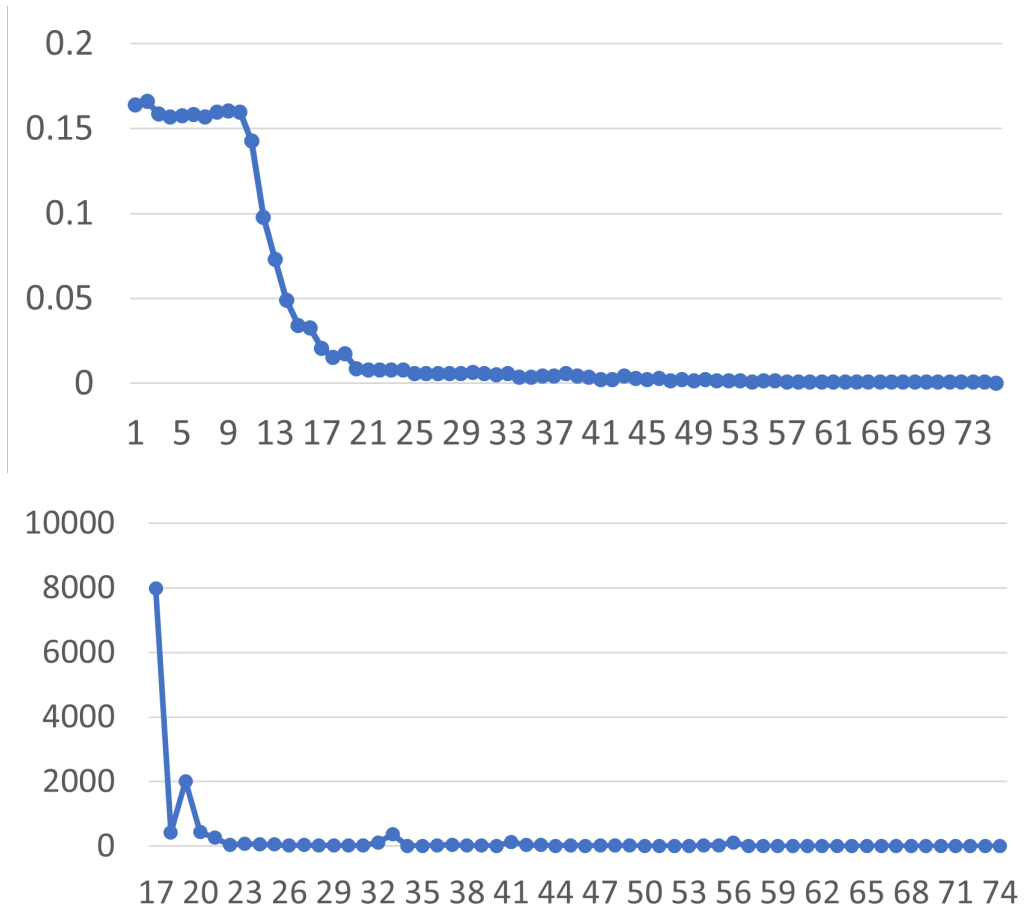


**Figure 7.6** a) Normalized term-difference convergence metric b) Primal-dual residual convergence metric.

axis until 100 shows the number of PH iterations, and beyond 100, we solve the problem using EF with warm start solutions from PH. The PH algorithm solved in 1297.57 seconds with an objective of 2317.34 kW, and after solving the problem with EF, we reached a gap of 2444.37 kW with an additional 90 seconds. The problem's relative gap with the extensive form's lower bound solution is 0.66%. Hence, the heuristic approach to obtain the value of  $\rho$  performed best for DG siting, sizing, and line hardening decisions in the 9500-node model.

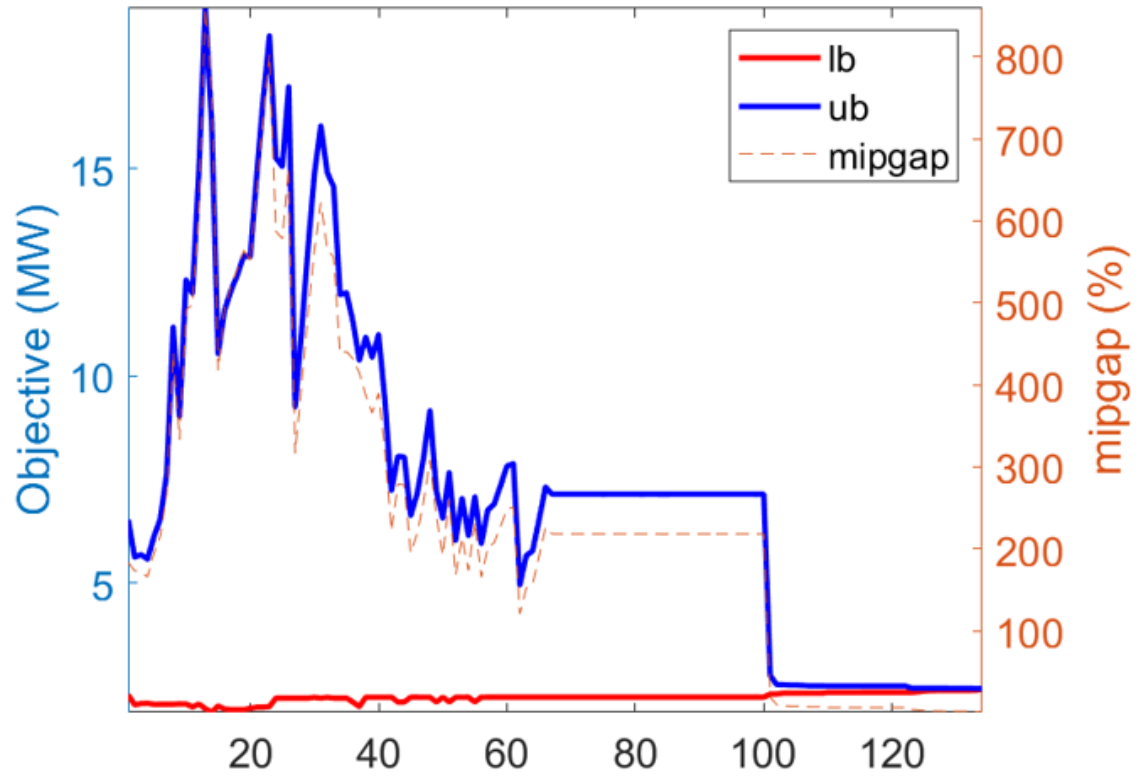


**Figure 7.7** Convergence bounds and mip gap for PH and post PH operation.

## 7.4 Summary

This chapter presented a framework for resilience planning in large-scale distribution system models. The stochastic models suffer from the curse of dimensionality with the increase in the number of scenarios. However, a wider range of scenarios increases the robustness of the planning models compared to decisions made with a small number of scenarios. It was observed that a minimal increase in the number of scenarios could significantly affect the solving time of stochastic models. In most cases, EF fails to solve the problem within polynomials. This work shows that the dual decomposition algorithm, PH, can be an effective strategy to improve the scalability of the planning model with minimal effect on solution quality with careful model and algorithm considerations. With careful parameters, PH solved the model 25 times faster than EF with reasonable solution quality. However, it is also important to note that PH is a heuristic algorithm, and there is no one-size-fits-all model configuration applicable to any application. Hence, planners should carefully assess several methods before reaching a conclusion regarding resilience investments.

## REFERENCES

- [1] B. Knueven, J. Ostrowski, and J.-P. Watson, “On mixed-integer programming formulations for the unit commitment problem,” *INFORMS Journal on Computing*, vol. 32, no. 4, pp. 857–876, 2020.
- [2] S. Ma, S. Li, Z. Wang, and F. Qiu, “Resilience-oriented design of distribution systems,” *IEEE Transactions on Power Systems*, vol. 34, no. 4, pp. 2880–2891, 2019.
- [3] M. Ghasemi, A. Kazemi, E. Bompard, and F. Aminifar, “A two-stage resilience improvement planning for power distribution systems against hurricanes,” *International Journal of Electrical Power & Energy Systems*, vol. 132, p. 107214, 2021.
- [4] Q. Zhang, Z. Wang, S. Ma, and A. Arif, “Stochastic pre-event preparation for enhancing resilience of distribution systems,” *Renewable and Sustainable Energy Reviews*, vol. 152, p. 111636, 2021.
- [5] A. Moreira, M. Heleno, A. Valenzuela, J. H. Eto, J. Ortega, and C. Botero, “A scalable approach to large scale risk-averse distribution grid expansion planning,” *IEEE Transactions on Power Systems*, 2023.
- [6] A. Poudyal, S. Poudel, and A. Dubey, “Risk-based active distribution system planning for resilience against extreme weather events,” *IEEE Transactions on Sustainable Energy*, pp. 1–14, 2022.
- [7] B. Knueven, D. Mildebrath, C. Muir, J. D. Siirala, J.-P. Watson, and D. L. Woodruff, “A parallel hub-and-spoke system for large-scale scenario-based optimi-

- mization under uncertainty,” *Mathematical Programming Computation*, vol. 15, no. 4, pp. 591–619, 2023.
- [8] R. T. Rockafellar and R. J.-B. Wets, “Scenarios and policy aggregation in optimization under uncertainty,” *Mathematics of operations research*, vol. 16, no. 1, pp. 119–147, 1991.
- [9] J.-P. Watson and D. L. Woodruff, “Progressive hedging innovations for a class of stochastic mixed-integer resource allocation problems,” *Computational Management Science*, vol. 8, pp. 355–370, 2011.
- [10] L. F. Escudero, M. A. Garín, G. Pérez, and A. Unzueta, “Scenario cluster decomposition of the lagrangian dual in two-stage stochastic mixed 0–1 optimization,” *Computers & Operations Research*, vol. 40, no. 1, pp. 362–377, 2013.
- [11] T. G. Crainic, M. Hewitt, and W. Rei, “Scenario grouping in a progressive hedging-based meta-heuristic for stochastic network design,” *Computers & Operations Research*, vol. 43, pp. 90–99, 2014.
- [12] D. Gade, G. Hackebeil, S. M. Ryan, J.-P. Watson, R. J.-B. Wets, and D. L. Woodruff, “Obtaining lower bounds from the progressive hedging algorithm for stochastic mixed-integer programs,” *Mathematical Programming*, vol. 157, pp. 47–67, 2016.
- [13] K. Cheung, D. Gade, C. Silva-Monroy, S. M. Ryan, J.-P. Watson, R. J.-B. Wets, and D. L. Woodruff, “Toward scalable stochastic unit commitment: Part 2: solver configuration and performance assessment,” *Energy Systems*, vol. 6, pp. 417–438, 2015.

- [14] A. Poudyal, “Lindistrestoration.” <https://github.com/abodh/LinDistRestoration>, 2024. Accessed: April 21, 2024.
- [15] J.-P. Watson, D. L. Woodruff, and W. E. Hart, “Pysp: modeling and solving stochastic programs in python,” *Mathematical Programming Computation*, vol. 4, pp. 109–149, 2012.
- [16] M. L. Bynum, G. A. Hackebeil, W. E. Hart, C. D. Laird, B. L. Nicholson, J. D. Siirola, J.-P. Watson, D. L. Woodruff, *et al.*, *Pyomo-optimization modeling in python*, vol. 67. Springer, 2021.
- [17] Gurobi Optimization, LLC, “Gurobi Optimizer Reference Manual,” 2023.
- [18] I. de Jong, “Pyro4.” <https://github.com/irmen/Pyro4>, 2022.
- [19] A. A. Anderson, S. V. Vadari, J. L. Barr, S. Poudel, A. Dubey, T. E. McDermott, and R. Podmore, “Introducing the 9500 node distribution test system to support advanced power applications: An operations-focused approach,” tech. rep., Pacific Northwest National Laboratory (PNNL), Richland, WA (United States), 2022.

# CHAPTER 8

## EXTREME WEATHER EVENTS-INDUCED OUTAGES AND THEIR SOCIOECONOMIC IMPACT

### 8.1 Introduction

This chapter introduces a spatiotemporal impact assessment framework of hurricanes and storm surges on the electric power grid and proposes an integrated community vulnerability index due to the induced power outages. The quasi-static state of the hurricanes is modeled using statistical methods, whereas a probabilistic storm surge model is adopted to assess the compound effect of these two events. The social vulnerability is combined with the outage vulnerability to obtain the integrated vulnerability index. The proposed framework is tested on a synthetic Texas system with historical hurricane scenarios. It was observed that the vulnerability of the community is shifted towards the coastal region due to the impact of weather events.

#### 8.1.1 Motivation

Hurricanes, one of the most severe conditions of *tropical storms* with wind speed exceeding 75 miles per hour (mph), are reported to be the primary cause of power outages due to extreme weather events resulting in an economic loss of over \$1.5 trillion in the US alone [1]. For example, Hurricane Ida is estimated to have cost \$16 to 24 billion in flooding damage in the Northeastern US. About 1.2 million customers were left without power – it took almost 15 days to restore the electric power entirely. These events are categorized as high impact, low probability (HILP) or black swan events. However, the frequency of the events carrying the highest impacts has dras-

tically increased, costing around \$22 billion in climate-related disasters in 2020 alone in the USA [2]. Thus, with the growing intensity and frequency of extreme weather events, there is a critical need to characterize and quantify the impacts of these HILP events on the electric power grid.

Although long-range weather prediction models have improved in recent years, they have not been adequately utilized to evaluate climate impacts on the power grid. For example, there have been significant efforts to forecast the hurricane's tracks, where the forecast error for the tracking has reduced from 300 nautical miles (nm) in 1990 to about 100 nm in 2016 [3]. A weather-grid impact model provides a much-needed capability to the grid planners in adapting the existing grid to become a resilient grid [4, 5]. Without a weather-grid impact model, planning for long-term grid resilience may not be well-informed or effective. Thus, there is a critical need to develop an appropriate weather-impact model for the power grid by adequately modeling the associated spatiotemporal properties of the extreme weather event.

Unfortunately, the communities at the forefront of these natural disasters are often the most vulnerable. Outages that are 8+ hours - often caused by these high-impact, low-probability (HILP) events - are experienced mostly by highly vulnerable communities [6]. During Hurricane Harvey in 2007, it was found that households with a lower socioeconomic status faced more extensive flooding than those of higher incomes [7]. Additionally, the Federal Emergency Management Administration (FEMA) has been criticized for having regressive policies regarding restoration allocation after major power outages [8]. Hence, it is essential to analyze the impact of such extreme events on both the power grid and the socioeconomic status of the community as a result of power outages.

### 8.1.2 Related Literature and Gaps

A large body of existing work studies the effects of hurricanes on the power grid, as reviewed below. A majority of the existing work considers hurricanes as a function of the wind speed; however, other dynamics associated with the hurricanes that are crucial to analyze their impacts on the power grid are ignored [9, 10]. A grid resilience model considering hurricane-induced damages and integrated renewable resources is presented in [11]. However, the approach is not generic as it considers a single case study on Hurricane Harvey. In [12], a data-driven outage prediction method is proposed, which uses a decision boundary method to identify the operational state of grid components. However, the authors do not report any analysis to quantify the damages or impacts on the grid. Authors in [13] present a framework to analyze energy storage's impacts on improving distribution systems' resilience against hurricanes. However, since the hurricane's radius is greater than an entire distribution grid at any instant time, such analysis would not be meaningful for a distribution grid alone. Finally, [14] introduces a community and customer-based perspective on improving the power grid's resilience against hurricanes; however, the spatiotemporal effects of hurricanes are not modeled.

The existing literature lacks in adequately modeling the spatio-temporal impacts of dynamic hurricane events and their impacts on the large power grid. The impact assessment model should capture different uncertainties associated with the stochastic nature of the event and their impacts on the individual power grid components and the power system as a whole. With these considerations, this paper aims to develop a probabilistic weather-impact assessment framework that appropriately models the stochastic nature of hurricanes and their time-varying impacts on the large-scale

power grid. First, we present an approach to generate dynamic hurricane scenarios considering different hurricane tracks that are mapped onto a transmission grid with geospatial information. The hurricane parameters are sampled from actual hurricanes that have previously occurred in the USA. Next, we develop a probabilistic weather-impact assessment model using Monte-Carlo simulations considering a large number of hurricanes with different tracks and at different time steps. The damage levels are mapped with the respective fragility curves of the transmission lines to visualize the spatiotemporal effects of the event. Finally, a spatiotemporal loss metric is proposed to quantify the impacts of probabilistic hurricane scenarios on the power grid.

Additionally, none of these works model the impact of storm surges on the power grid. In [15], a power system impact assessment framework is presented to identify potential mitigation strategies and enhance resilience against floods. A stochastic optimization framework for substation hardening against storm surge is presented in [16]. [17] evaluated the impacts of tropical cyclones and heatwaves on the power grid. The existing work, however, lacks the spatiotemporal impacts analysis of hurricanes characterizing the compound effects of high-speed wind and flooding. Other studies have analyzed power system impact from hurricane-flood events [15, 18]. There is minimal literature that combines community impact evaluation with power system impact. Energy equity metrics are still underdeveloped [19], despite it being well-documented that inequities are apparent in outages from HILP events. In [20] analysis regarding the infrastructure losses due to Hurricane Harvey is investigated and identifies impacted communities. However, the work is based on critical infrastructural information, affecting the extension of the work to other regions.

### 8.1.3 Contribution

## 8.2 Extreme Weather Events and Impact Model

### 8.2.1 Hurricane Wind Field Model

The damage created by the hurricane is due to high-intensity wind speed, spread around the region of its eye, that changes along its path as it moves inland from the location of its landfall [21]. With hurricane eye as the reference, the static gradient wind field model of the hurricane is defined using three variables — maximum sustained wind speed of the hurricane ( $v_{max}$ ) in knots, the distance to  $v_{max}$  from the hurricane eye ( $R_{v_{max}}$ ) in nautical miles (nmi), and the radius of the hurricane from the hurricane eye ( $R_s$ ) in nmi [22]. The static model represents the wind field model of a hurricane at a particular instance of time as shown in Fig. 8.1. A piecewise mathematical function of the gradient wind field model shown in Fig. 8.1 can be represented using (1) [23].

$$v(x) = \begin{cases} K \times v_{max}(1 - \exp[-\Psi x]) & 0 \leq x < R_{v_{max}} \\ v_{max} \exp[-\Lambda(x - R_{v_{max}})] & R_{v_{max}} \leq x \leq R_s \\ 0 & x > R_s \end{cases} \quad (8.1)$$

$$\Psi = \frac{1}{R_{v_{max}}} \ln \left( \frac{K}{K-1} \right), \quad K > 1; \quad \Lambda = \frac{\ln \beta}{R_s - R_{v_{max}}}$$

where,  $x$  is the distance from the hurricane eye ,  $K$  is a constant depending on the nature of the hurricane,  $\beta$  is the factor by which the maximum sustained wind speed decreases at the boundary of the hurricane,  $R_s$ . It is also assumed that the hurricane has no effect outside of its boundary.

The dynamic behavior of a hurricane can be incorporated by simulating the static

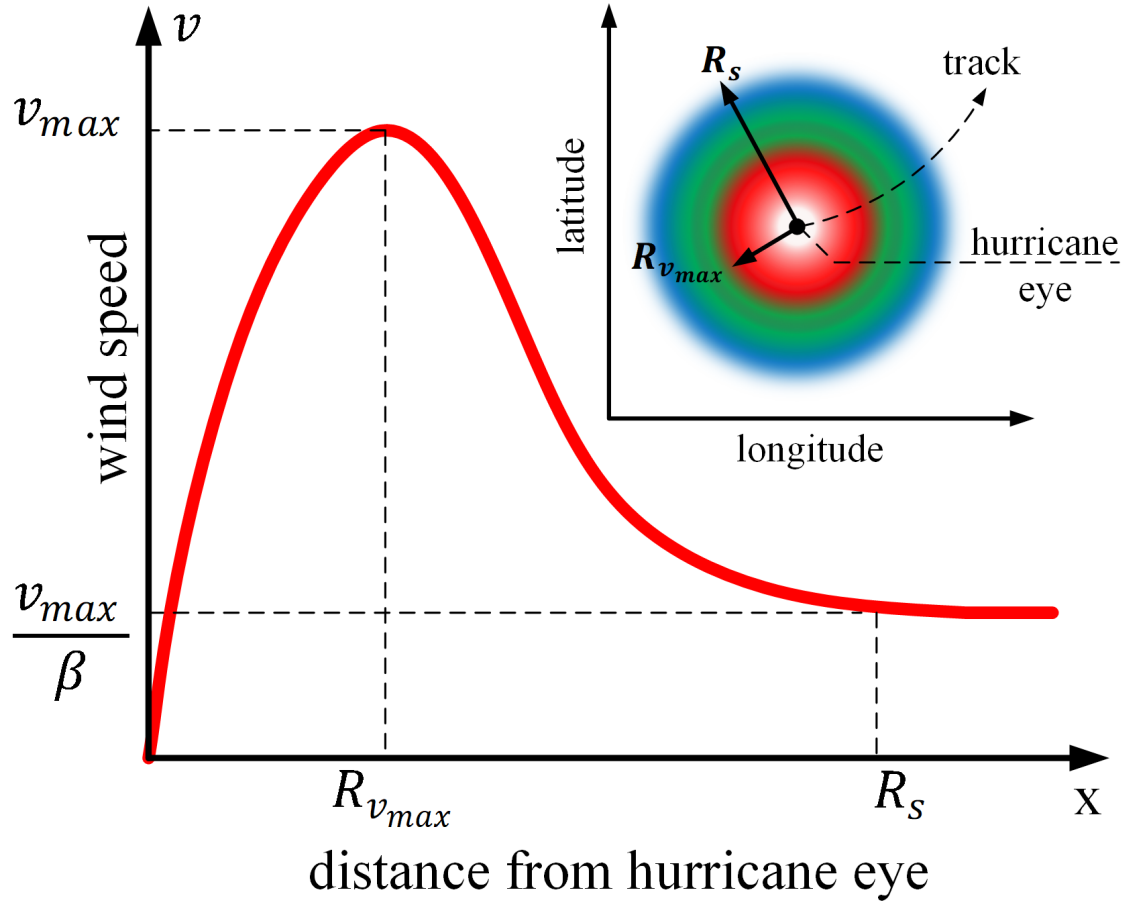


**Figure 8.1** Distribution of wind field of a hurricane at a fixed time.

model at several discrete time intervals. Having this dynamic wind field allows us to track the severity of a hurricane as it moves along its path after landfall. The hurricane has minimum wind speed and maximum pressure at the location of the eye given by [22]:

$$\Delta P_h^{0,\zeta} = \sqrt{\frac{2.636 + 0.0394899\phi^{0,\zeta} - \ln(R_{v_{max,h}}^{0,\zeta})}{5.086 \times 10^{-4}}} \quad (8.2)$$

where,  $\phi^{0,\zeta}$  is the latitude of the location of landfall for track  $\zeta$ , and  $\Delta P_h^{0,\zeta}$  is the pressure of the hurricane eye at time step  $t = 0$  for hurricane  $h$  and track  $\zeta$ . Here, it

is assumed that the landfall always occurs at time step  $t = 0$  for each  $\zeta$ . Thus, for each hurricane  $h$ , the pressure at the eye location for each time step  $t$  and track  $\zeta$  can then be calculated as:

$$\Delta P_h^{t,\zeta} = \Delta P_h^{0,\zeta} e^{-\alpha t} \quad (8.3)$$

Here, (8.3) represents the hurricane decay model with land decay parameter  $\alpha$ . Using the above equations and for each  $t$ , new values of  $\{R_{v_{max}}^{t,\zeta}, R_s^{t,\zeta}, v_{max}^{t,\zeta}\}_h$  are obtained for each hurricane scenario,  $h$ , based on their values in the previous time step and the known coordinates of the forecasted hurricane tracks obtained for each  $\zeta$ . Using these new values, a static wind field is generated for each  $t$  and  $\zeta$ , resulting in a dynamic wind field model [23].

### 8.2.2 Storm Surge Model

In this work, we use SLOSH (Sea, Lake, and Overland Surge from Hurricanes) model to generate probabilistic storm surge scenarios. SLOSH is a numerical storm surge model that provides surge heights around the coastal regions from historical or hypothetical hurricanes based on parameters such as atmospheric pressure, hurricane tracks, forward speed, and so forth [24]. It was developed by National Oceanic and Atmospheric Administration (NOAA) and is currently being used by several federal agencies, including the national hurricane center (NHC) and the federal emergency management agency (FEMA), for flood advisories and evacuation. Furthermore, NHC provides a SLOSH Display Package (SDP) tool in which users can generate flooding scenarios based on the direction, forward speed, and intensity of the hurricane followed by the sea tide level [25]. The provided surge heights are above the elevation

referenced in the North American Vertical Datum of 1988 (NAV88). The tool also has an added functionality to subtract land elevations so that the surge level is referenced above the ground level. Details on the SDP tool and other surge-related products from NOAA can be found at [25].

SDP contains several coastal basins on which surge scenarios can be created. Furthermore, SDP provides two different surge analyses based on hurricane simulations: Maximum Envelope of Water (MEOW) and Maximum of the MEOWs (MOM). The MEOWs reflect the worst-case snapshots of the storm surge for hurricanes of particular intensity and forward direction but with different landfall locations. This work uses MEOW for storm surge scenarios to identify potential flooding locations. The MEOW scenarios from SDP provide the inundation level for each defined grid in a basin. Let  $\mathcal{X}_S$  be the geographical coordinate of a substation  $S$ . Then, we define  $\mathcal{X}_{S,h}^B$  as the inundation level,  $h$ , for substation  $S$  situated at  $\mathcal{X}$  for basin  $B$ . Since the inundation level is spatially distributed, the expected value of inundation around 0.5 miles of  $\mathcal{X}_S$  is assumed to be  $\mathcal{X}_{S,h}^B$ .

### 8.2.3 Power Systems Impact Model

The hurricane model described above will have a spatiotemporal effect on the power grid. That is, each of the spatially distributed power grid components will experience different wind speeds at time instances. To capture spatiotemporal effects, we modify the hurricane impact model presented in [23] by introducing additional time and track variables. Accordingly, the wind speed experienced by the transmission line  $l$ , at discrete time-interval  $t$  and track  $\zeta$  is given by (4).

$$\Gamma_{l,h}^{t,\zeta} = \begin{cases} v_{max_h}^{t,\zeta} & d_{\min}^{t,\zeta}(l, h) \leq R_{v_{max_h}}^{t,\zeta} \leq d_{\max}^{t,\zeta}(l, h) \\ \max \left( \begin{array}{c} v^{t,\zeta}(\gamma_1) \\ v^{t,\zeta}(\gamma_2) \end{array} \right) & \text{otherwise} \end{cases} \quad (8.4)$$

$$\gamma_1 = d_{\min}^{t,\zeta}(l, h) \mid \{R_s^{t,\zeta}, R_{v_{max}}^{t,\zeta}, v_{max}^{t,\zeta}\}_h$$

$$\gamma_2 = d_{\max}^{t,\zeta}(l, h) \mid \{R_s^{t,\zeta}, R_{v_{max}}^{t,\zeta}, v_{max}^{t,\zeta}\}_h$$

where,  $\Gamma_{l,h}^{t,\zeta}$  is the maximum wind speed experienced by line  $l$  for the hurricane scenario,  $h$ , in track  $\zeta$  and at time step  $t$ .  $d_{\min}^{t,\zeta}(\cdot)$  and  $d_{\max}^{t,\zeta}(\cdot)$  represent the minimum and maximum distance of  $l$  from the eye of the hurricane  $h$  for track  $\zeta$  at time step  $t$ .  $v^{t,\zeta}(\cdot)$  is calculated using (8.1). For simplicity, the lines connected between any two buses are assumed to be straight lines and the wind speed across the entire section of a single transmission line is assumed to be the same.

#### 8.2.4 Power Systems Impact Model

Fragility curves are proposed to assess the impact of extreme weather events on the power grid [26]. The component fragility models provide the probability of failure of a component as a function of hazard intensity. In this work, we use the fragility of line segments, as a combined fragility of line and tower, as a function of  $v_{max}$  experienced by the line segment in a power grid. The value of  $v_{max}^t$  experienced by each line segment is obtained by a method discussed in [27]. The structure and strength of lines and towers differ by voltage level in a transmission grid. Hence, we modify the fragility of each line segment based on its voltage level,  $\mathcal{V}$ .

$$\mathbb{P}_{out}^{t,\zeta}(l_{\mathcal{V}}) = \begin{cases} 0 & \Gamma_{l_{\mathcal{V}}}^{t,\zeta} < v_{cri}^{l_{\mathcal{V}}} \\ \frac{\Gamma_{l_{\mathcal{V}}}^{t,\zeta} - v_{cri}^{l_{\mathcal{V}}}}{v_{col}^{l_{\mathcal{V}}} - v_{cri}^{l_{\mathcal{V}}}} & v_{cri}^{l_{\mathcal{V}}} \leq \Gamma_{l_{\mathcal{V}}}^{t,\zeta} < v_{col}^{l_{\mathcal{V}}} \\ 1 & \Gamma_{l_{\mathcal{V}}}^{t,\zeta} \geq v_{col}^{l_{\mathcal{V}}} \end{cases} \quad (8.5)$$

where,  $\mathbb{P}_{out}^{t,\zeta}(l_{\mathcal{V}})$  is the outage probability of line  $l$  with voltage level  $\mathcal{V}$  for hurricane  $\zeta$  at time step  $t$ , and  $\Gamma_{l_{\mathcal{V}}}^{t,\zeta}$  is the maximum sustained wind speed experienced by  $l_{\mathcal{V}}$  due to  $\zeta$  at  $t$ . Here,  $v_{cri}^{l_{\mathcal{V}}}$  is the wind speed beyond which a branch is affected, and  $v_{col}^{l_{\mathcal{V}}}$  is the wind speed above which a branch collapses. The values of  $v_{cri}^{l_{\mathcal{V}}}$  and  $v_{col}^{l_{\mathcal{V}}}$  differ for each  $l_{\mathcal{V}}$ . If  $\delta_l^{t,\zeta} \in \{0, 1\}$  denotes the line status of line  $l$  at time  $t$  for hurricane in track  $\zeta$ , then  $\delta_l^{t+1,\zeta} \leq \delta_l^{t,\zeta}$ . This ensures that if a line  $l$  experiences an outage at time  $t$ , it remains out of service for the remaining duration of the hurricane.

The substation failure probability depends on the corresponding inundation level. The storm surge impact on the substation is determined using the following Weibull stretched exponential function [27].

$$\mathbb{P}_{out}^{\mathcal{S}}(\mathcal{X}_{\mathcal{S},D_{\mathcal{S}}}^{\mathcal{B}}) = 1 - \exp \left[ - \left( \frac{\mathcal{X}_{\mathcal{S},D_{\mathcal{S}}}^{\mathcal{B}}}{a} \right)^b \right] \quad (8.6)$$

where  $\mathbb{P}_{out}^{\mathcal{S}}(\mathcal{X}_{\mathcal{S},D_{\mathcal{S}}}^{\mathcal{B}})$  is the probability of experiencing the inundation level around 0.5 miles of  $\mathcal{S}$  having inundation of  $D_{\mathcal{S}}$  for any  $\mathcal{B}$ . The fragility model includes two constants  $a \in \mathbb{R}^+$  and  $b > 2$  with known values. Suppose a substation experiences an outage due to flooding. In that case, the transmission lines linked to that substation, inward or outward, are also considered out-of-service for the rest of the storm period. If  $\delta_{l,\mathcal{S}}^{t,\zeta} \in \{0, 1\}$  denotes the line status of line  $l$  connected to substation  $\mathcal{S}$  at time  $t$  for hurricane in track  $\zeta$ , then  $\delta_{l,\mathcal{S}}^{t+1,\zeta} \leq \delta_{l,\mathcal{S}}^{t,\zeta}$ . This ensures that if a line  $l$  experiences

an outage at time  $t$  due to a storm surge, it remains out of service for the remaining event duration. Let  $\mathcal{L}_{Total}^t = \mathcal{L}_{\mathcal{W}}^t \cup \mathcal{L}_{\mathcal{F}}^t$  be a set of lines that are out of service due to the combined effect of hurricane wind and flood damage at every time step  $t$ . Here,  $\mathcal{L}_{\mathcal{W}}^t$  and  $\mathcal{L}_{\mathcal{F}}^t$  refer to the set of outage lines due to hurricane wind damage and flood-induced substation outages, respectively.

Due to the disruption of branches, several buses are islanded from the grid either without generators (offline buses) or with generators that can fully or partially meet the demand of the islanded grid. Islands with more generation than load require generation curtailment, while those with loads higher than generation require load curtailment. The load shed from each bus is based on priorities set by the operators on load criticality. If the information on load criticality is missing, then the load in each bus will be curtailed by a uniform percentage, reflected by the load deficit relative to the total load demand on the corresponding island.

### 8.2.5 Community Impact Assessment

In order to assess the impact on the community, it is essential to know the geographical distribution of load losses due to hurricanes. The synthetic test cases identify the buses and substations based on zip codes [28]. This work correlates bus load loss with zip code locations. Multiple substations may exist in cities with greater load density. The losses at the zip code level are aggregated into city load loss by summing the losses from all zip codes belonging to the same city. Furthermore, a county-level analysis is proposed to alleviate the concern of loads being served from the buses in one city to the neighboring cities. After identifying cities and their associated load loss, cities within the same county, as indicated by United States Postal Service

data [29], are aggregated to find the county-level load loss. Cities that reside in multiple counties have their load distributed based on the percentage of the city's population residing in each county. Let  $\mathcal{P}_C^D$  be the total load demand in each county ( $C$ ) and the load loss in  $C$  at each time step  $t$  due to corresponding  $\zeta$  is represented by  $\hat{\mathcal{P}}_C^{t,\zeta}$ . If  $\mathcal{T}^\zeta$  is the total time step of each  $\zeta$ , then the corresponding load loss associated with every  $C$  is obtained as,

$$\hat{\mathcal{P}}_C^\zeta = \max\{\hat{\mathcal{P}}_C^{t,\zeta}\} \quad \forall t \in \mathcal{T}^\zeta \quad (8.7)$$

## 8.3 Vulnerability Assessment

### 8.3.1 Power System Vulnerability

In this work, we assess the power system's vulnerability, which is the vulnerability of the branches and substations due to hurricanes and storm surge scenarios. Although hurricane tracks are obtained from IBTrACS, the storm surge scenarios are probabilistic, considering several similar hurricane scenarios. Due to a lack of surge data for hurricanes with lower intensity, we assume that such scenarios do not trigger any surge and the impact is due to the hurricane alone. The spatiotemporal outage probabilities of branches and substations are obtained for all the hurricanes and storm surges. The maximum outage probability experienced by each branch for each hurricane is observed to determine the vulnerability of these components. For substations, we observe the maximum outage probability averaged over all basins.

When the hurricane moves inland,  $\Gamma_l^{t,\zeta}$  is obtained for each  $l$  and  $\mathcal{X}_{S,h}^B$  is obtained for each  $S$  from the MEOW maps. It is assumed that all substations at the coast are elevated at 3 ft from the ground level. Fig. 8.2 shows the wind field of Hurricane

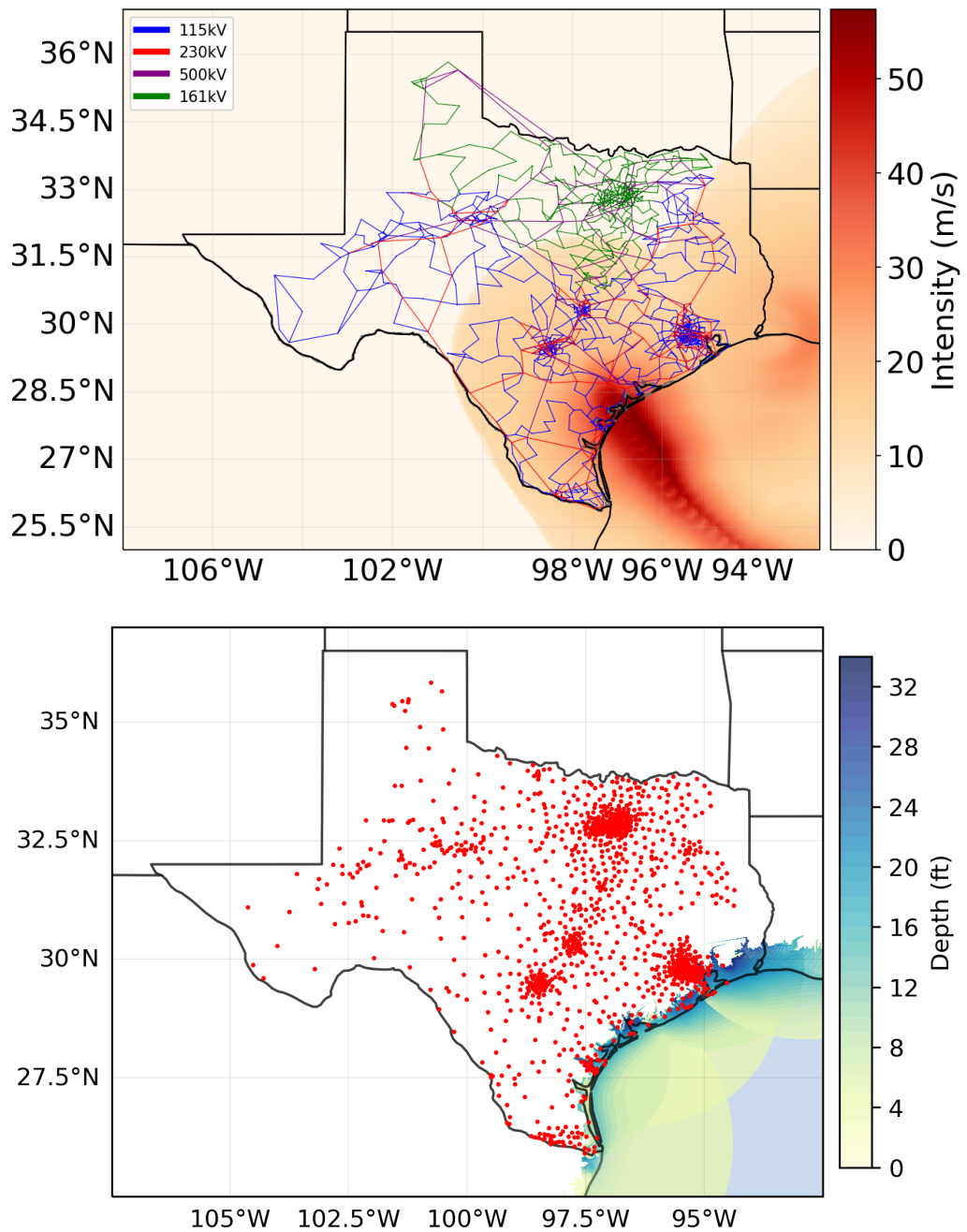


**Figure 8.2** a) Wind field of Hurricane Harvey and b) Substation flooding scenario, above ground level, for Texas basins.

Harvey and MEOW maps on five different basins on the footprint of Texas. For each  $\zeta$ ,  $\mathcal{B}$ , and  $t$ , MCS is performed for several trials. For each trial,  $\mathbb{P}_{out}^{t,\zeta}(l)$  and  $\mathbb{P}_{out}^{\mathcal{S}}(\mathcal{X}_{\mathcal{S},h}^{\mathcal{B}})$  is compared with a uniform random number,  $r \sim U(0, 1)$ , to identify  $\mathcal{L}_{\mathcal{H}}^t \cup \mathcal{L}_{\mathcal{S}}^t$ . As discussed before, MEOW maps are time-independent. However, we define an activation flag  $\mathcal{S}_{\mathcal{B},h}^{t,\zeta} \in \{0, 1\}$  such that  $\mathcal{S}_{\mathcal{B},h}^{t,\zeta} = 1$  makes the substation  $\mathcal{S}$  inundated with depth  $h$  above the ground elevation for hurricane track  $\zeta$ , SLOSH basin  $\mathcal{B}$ , and time  $t$ . In this work, we do not model any drainage system; hence, it is assumed that the inundation level is the same for future time steps  $t + 1$ . The objective is to identify the time stamp when the substation gets flooded to analyze the compound spatiotemporal impact of two different hazards at that time step. The information,  $\mathcal{L}_{\mathcal{H}}^t \cup \mathcal{L}_{\mathcal{S}}^t$ , is then sent to the power grid simulator to remove the respective branches from the system. Finally, the loss for the particular  $t$  is observed as the total load disconnected from the main grid. The MCS trial is conducted until the loss converges to some value.

We assume that the inundation scenarios for each  $\mathcal{B}$  and each hurricane tracks  $\zeta$  are equally likely. If  $N_{\zeta}$  is the total number of tracks under consideration and  $N_{\mathcal{B}}$  is the total number of basins, then the system level load loss at each time step  $t$  is given by (8.8)

$$loss_t = \frac{1}{N_{\zeta} \times N_{\mathcal{B}}} \sum_{\zeta=1}^{N_{\zeta}} \sum_{\mathcal{B}} loss_{\mathcal{B}}^{t,\zeta} \quad (8.8)$$

Finally, the vulnerability percentile rank is computed for each branch and substation to obtain the branch vulnerability index (BVI) and substation vulnerability index (SSVI) once the outage data is mapped to the county-level data.

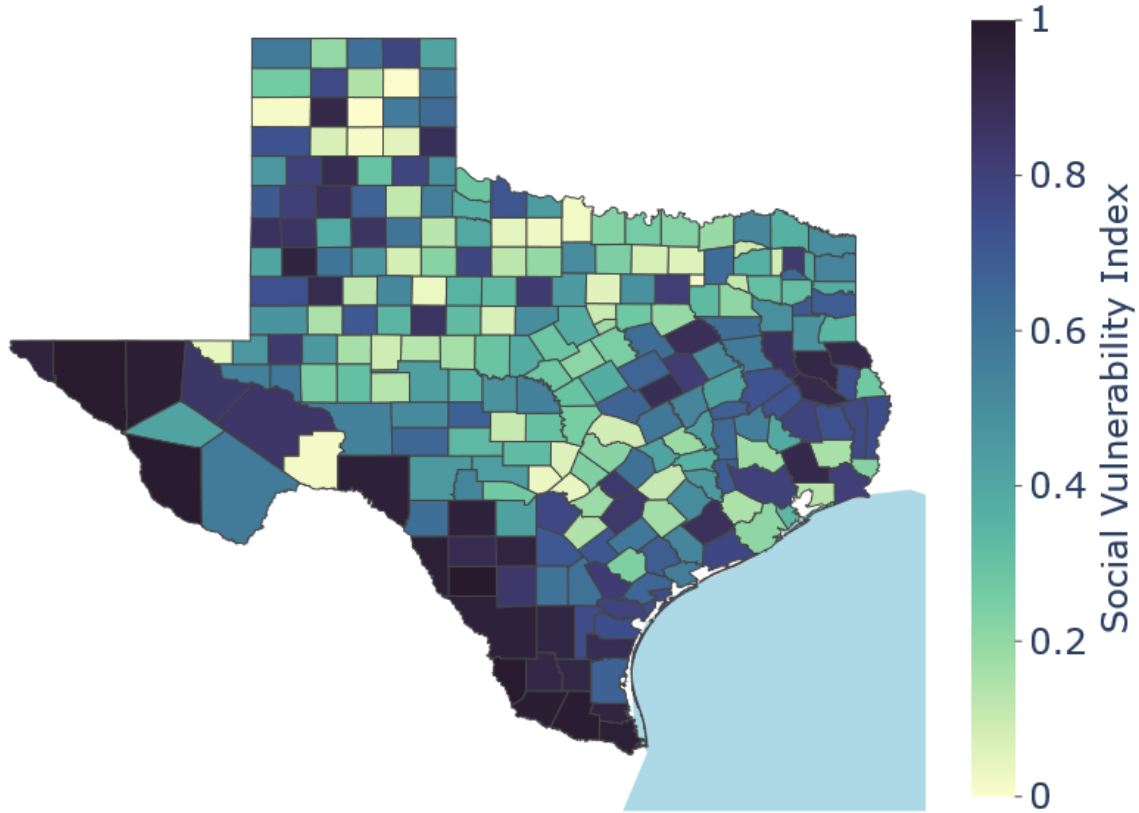


**Figure 8.3** CDC's social vulnerability index

### 8.3.2 Community Vulnerability

To observe the community vulnerability due to the impact of hurricanes and storm surges on the power grid, we obtain the value of  $\hat{\mathcal{P}}_C^\zeta$  and normalize the load loss using  $\mathcal{P}_C^D$  to get the vulnerability of the community in each  $C$  for each  $\zeta$ . We then define expected vulnerability of each  $C$  based on all  $\zeta$  as  $\hat{\mathcal{P}}_C = \mathbb{E}_\zeta \left( \frac{\hat{\mathcal{P}}_C^\zeta}{\mathcal{P}_C^D} \right)$  and term the outage vulnerability index (OVI) as

$$OVI = \text{percentile.rank} \left( \hat{\mathcal{P}}_C \right) \quad (8.9)$$

Although OVI defines the propagating impact of hurricanes and storm surges on

the community through their grid impact, it does not incorporate a socioeconomic impact. To address this concern, we leverage the Centers for Disease Control and Prevention (CDC)'s Social Vulnerability Index (SVI) for socioeconomic analysis [30], see Fig. 8.3. The SVI metric aggregates vulnerability based on four major themes: socioeconomic status, racial/ethnic minority, household characteristics, and housing/transportation type. These themes are then normalized and ranked by percentile into an encompassing index, SVI, that ranges between 0 and 1 (1 being the highest vulnerability). SVI has been widely adopted in relating infrastructure losses due to HILP events to their associated socioeconomic vulnerabilities [31]. Further documentation on SVI can be found at [30]. Each of SVI's four themes are comprised of socioeconomic variables in sum of percentile  $\mathbb{S}_i$ , where  $i$  denotes each theme. All four themes are summed together to create  $\mathbb{S}$ , then finally percentile-ranked again to achieve the Social Vulnerability Index seen in (8.10).

$$SVI = \text{percentile.rank}\left(\sum_{i=1}^4 \mathbb{S}_i\right) \quad (8.10)$$

The social and outage vulnerability metrics are compounded to create a new measurement, the Integrated Community Vulnerability Index (ICVI), a modified SVI that accounts for power system losses. The percentage of county population without power is treated as a 5th theme to SVI; therefore, it is min-max normalized and added to the min-max normalized  $\mathbb{S}_i$ , then percentile ranked between 0 and 1. This adjusts the original SVI with sensitivity to the outage analysis obtained.

$$ICVI = \text{percentile.rank}\left(\left\|\sum_{i=1}^4 \mathbb{S}_i\right\| + \left\|\hat{\mathcal{P}}_c\right\|\right) \quad (8.11)$$

Finally, with (8.11), we can simultaneously analyze the socioeconomic and power

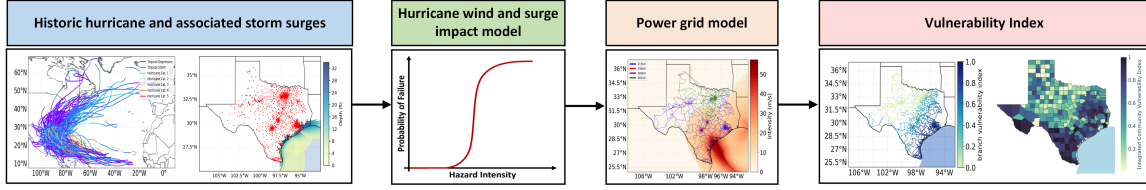


**Figure 8.4** Overall framework of assessing hurricane and storm surge-induced power system vulnerabilities and their socioeconomic impact.

system impacts.

#### 8.4 Simulation Framework

To observe the overall vulnerability due to the impact of hurricanes and storm surges on the power grid, the parameters for historical hurricanes are obtained from IB-TrACS, and storm surge scenarios are generated based on the hurricane parameters in SDP. The time-varying outage probability for each of the power system components is obtained using (8.5) and (8.6). Several MCSs are conducted to obtain the  $\hat{\mathcal{P}}_C^\zeta$  based on the methods described in Section 8.2. Finally, the community-level vulnerability due to the impact of extreme weather events on the power grid is quantified as ICVI, using (8.11). This section details the overall simulation framework, as shown in Fig. 8.4.

Initially, historical hurricanes that made landfall in the Texas coastal area from 2000 to 2018 were obtained using IBTrACS. There were a few hurricanes that did not affect the region of interest. Hence, we set a boundary region and filter the hurricanes that impact the boundary region at any point during its occurrence. Within the investigation region, 97 storms were identified within the Gulf of Mexico region, of which 26 showed activity within the boundary region. Furthermore, there were a few hurricanes with missing information on  $R_{v_{max}}$  and  $R_s$ . In such cases, the parameters

were estimated from their kernel density estimates as described in [32]. As per NHC’s guidelines, all storms are labeled from category -1 to 5 on the Saffir-Simpson hurricane wind scale, where categories -1 and 0 refer to tropical depression and tropical storm, respectively.

SDP can only provide the storm surge information for category 1 and higher. Hence, we identify 11 storms out of 26 that trigger storm surges on the coast and are considered to have an inundation impact in this study. MEOW data are generated from SDP for each of these 11 historic hurricanes at five basins of Texas — namely Corpus, Galveston, Laguna, Matagorda, and Sabine. Each basin’s inundation level depends on the category, landfall direction, hurricane’s translational speed, and mean to high tide conditions.

The wind and storm surge scenarios are then integrated into the geographical footprint of Texas with a synthetic ERCOT 2000-bus system [28]. The power grid model comprises 1250 substations and 1918 transmission lines operating at different voltage levels: 115kV, 161kV, 230kV, and 500kV, with a total load of 67.11 GW and a generation capacity of 96.29 GW. The load substations are clustered based on geographical and average load consumption, and the buses have additional information on the zip code or the city name in Texas, which we leverage to map the load associated with each county. The value of  $\hat{\mathcal{P}}_{\mathcal{C}}^{\zeta}$  is computed using MCS conducted on each  $\zeta$  and  $\mathcal{B}$ . As discussed, only 11 out of 26 hurricanes instigate storm surges. Hence, we only consider obtaining  $\mathcal{L}_{\mathcal{W}}^t$  for the remaining 15 hurricanes. Since storm surges are static models, we use a surge activation flag that gets triggered once the hurricane is within 6 hours from landfall. We only consider the impact of storm surge beyond this time frame for any  $\zeta$  with additional surge impact. It is assumed that substations

**Table 8.1** voltage level-based critical and collapse sustained wind speed values for each line segment for fragility analysis

Voltage level (kV)	$v_{cri}^{lv}$ (m/s)	$v_{col}^{lv}$ (m/s)
115	25	55
161	30	60
230	35	65
500	45	75

in the coastal regions are elevated at a height of 3 meters as an additional planning measure. MCS provides several outage scenarios corresponding to branch and substation outages. For each MC scenario, DC optimal power flow is conducted to obtain the load loss associated with that scenario at each  $t$ , and the loss is then mapped back to the county using the method described in Chapter 8.2. The community-level vulnerability is quantified as ICVI. Initially, OVI is calculated to assess the outage vulnerability due to hurricanes and storm surges using (8.9). We then blend outage likelihood with SVI to compute ICVI based on (8.11).

## 8.5 Results and Analysis

In this work, the hurricanes are extracted from IBTRaCS and analyzed using CLIMate ADAptation (CLIMADA) package [33]. The synthetic 2000-bus ERCOT system [28] is modeled in MATPOWER, which is further utilized for DC power flow. The fragility model discussed in (8.5) is based on the voltage level of the branches. Table. 8.1 presents the values of  $v_{cri}^{lv}$  and  $v_{col}^{lv}$  used in this work. These values are arbitrarily selected for simulation and can be modified based on data availability.

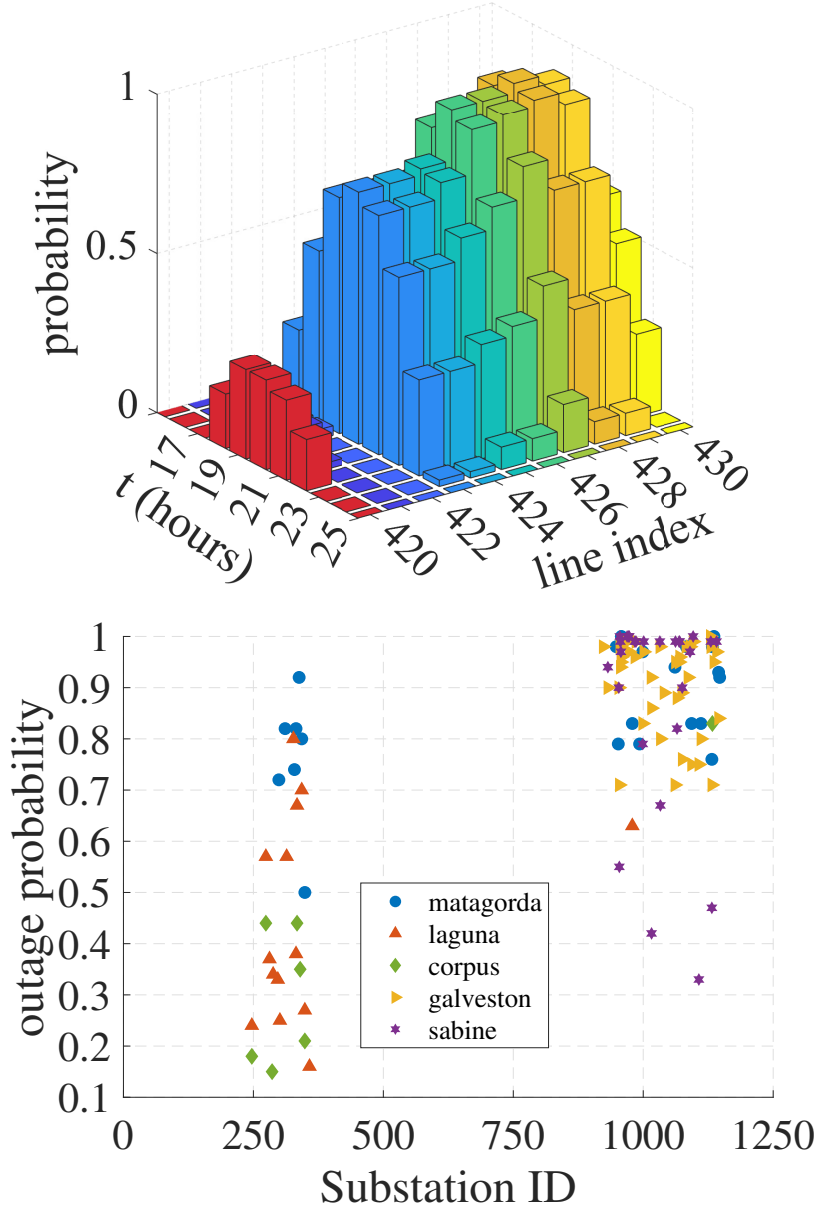
### 8.5.1 Hurricane and Storm Surges Impact Assessment

### 8.5.2 Vulnerability Assessment

From the IBTrACS, the hurricane's initial location is in the North Atlantic Ocean, which is observed at “2017 – 08 – 16 06 : 00 : 00” and hence creates no impact on the power grid. Thus, the simulation for the impact assessment begins at the 100<sup>th</sup> time step, i.e., at the advisory of “2017 – 08 – 24 12 : 00 : 00”. To avoid any confusion, this timestamp is referred to as  $t = 0$  hours for the rest of the paper. Fig. ?? a) shows the outage probability of a set of transmission lines due to the original Hurricane Harvey track. It can be observed that with the moving nature and intensity of the hurricane, the outage probability of each line changes. The probability is maximum when the line experiences wind speed closer to  $v_{col}$  and gradually decreases as the hurricane decays while moving inland. Fig. ?? b) represents the outage probability of substations for five different Texas basins. It is seen that the substation's vulnerability depends on the location and basin.

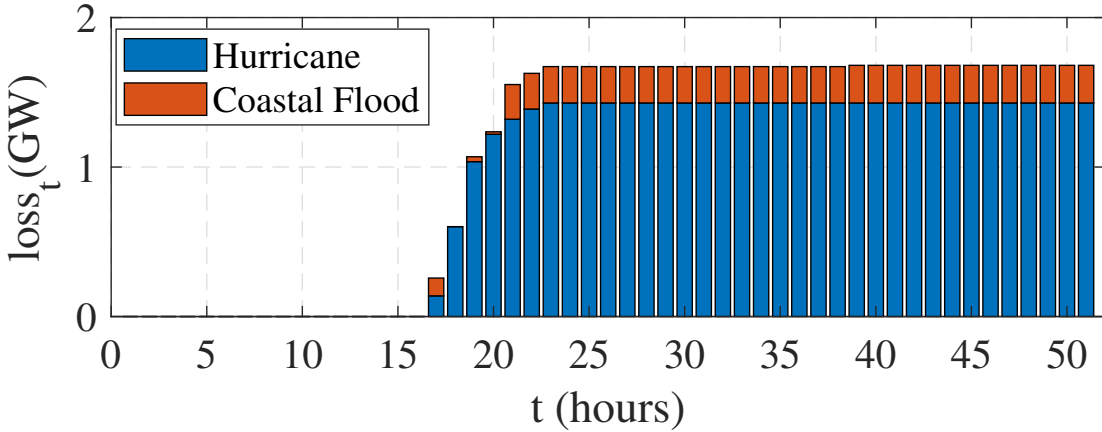
It was found that 800 Monte Carlo trials are enough to achieve convergence for any simulation case [32]. Hence, for each  $\zeta$ ,  $\mathcal{B}$ , and  $t$ , 800 Monte Carlo trials are conducted. Fig. 8.6 shows the comparison of losses when considering the impact of the hurricane alone with the compound effect of the hurricane and the coastal flood for  $\zeta = 1$ . It can be observed that considering substation flooding scenarios incur an additional loss of 250 MW by  $t = 50$  hours due to substation outages.

Fig. 8.7 represents the spatiotemporal loss for the compound impact of hurricane and storm surge. The dashed curves represent the loss for all basins for each track, whereas the solid blue curve represents  $loss_t$  obtained from (8.8). The loss is not



**Figure 8.5** a) Line outage probability for selected lines Harvey's track. b) Substation outage probability for all storm surge scenarios.

incurred until  $t = 12$  for any  $\zeta$  under consideration, and the increase is significant once the hurricane moves inland, followed by the compounded impact of storm surge.

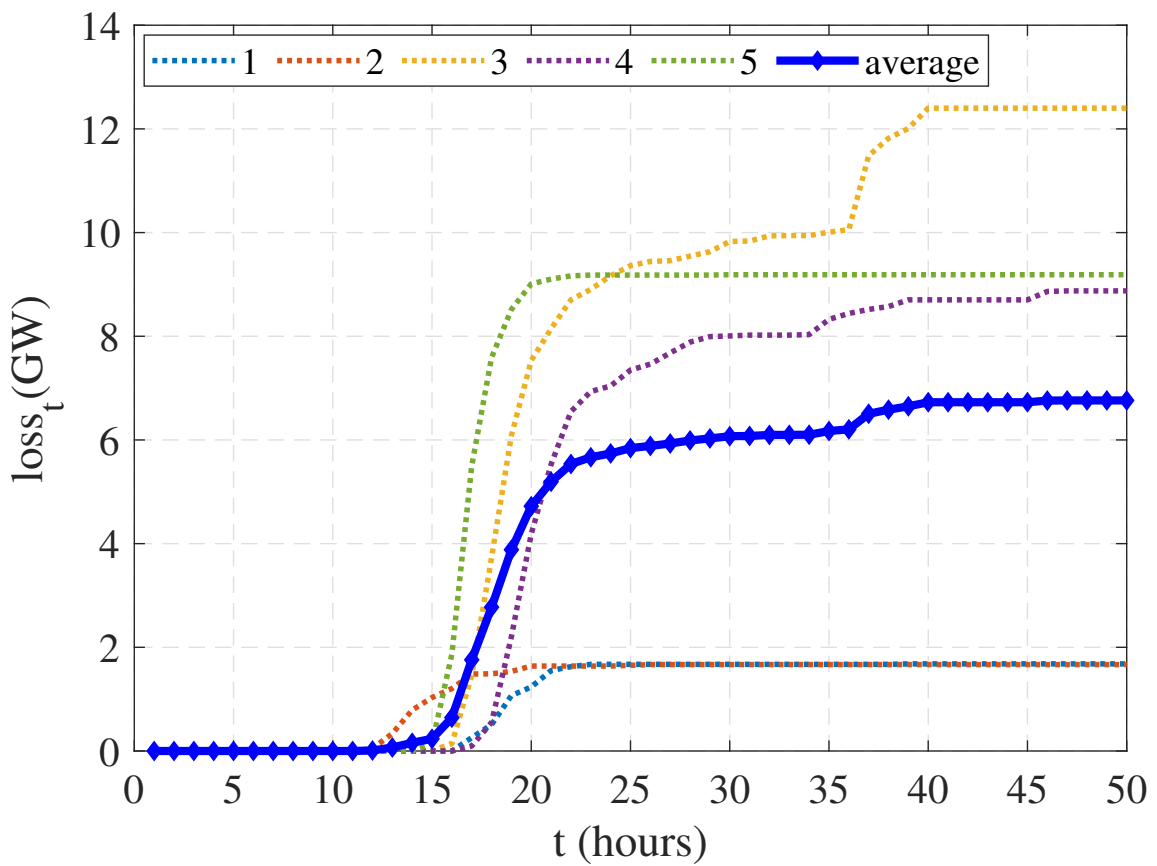


**Figure 8.6** Overall loss comparison between the impact of hurricane alone and the compound impact of the hurricane and coastal flood for  $\zeta = 1$ .

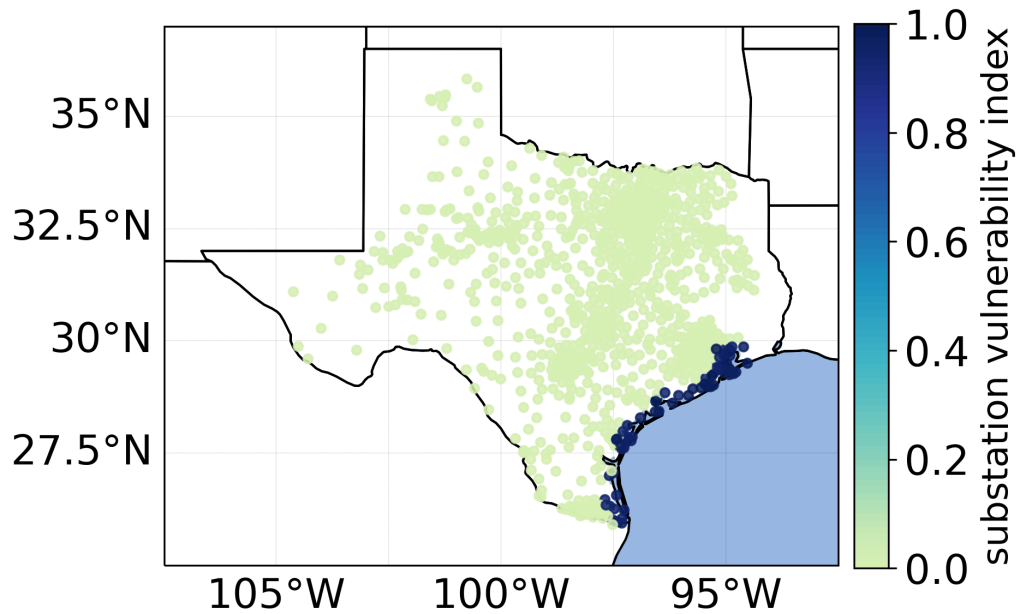
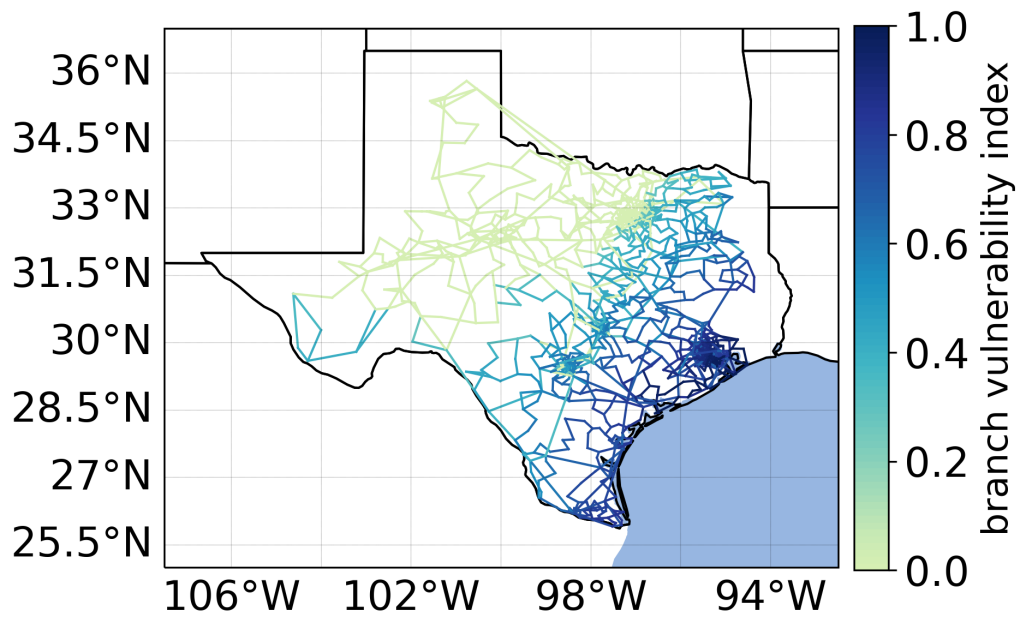
The loss increases from  $loss_{12} = 9.4072$  MW to  $loss_{22} = 5536.1$  MW before saturating at  $loss_{40} = 6761.97$  MW as the intensity of the extreme events decreases.

Fig. 8.8 represents the branch and substation vulnerability index for all  $\zeta$  and  $\mathcal{B}$ . Since hurricanes and storm surges have the highest impact on the coastlines, the most vulnerable components lie around the coastal regions. The vulnerability of inner coastal regions depends on the fragility of the branches. It is to be noted that branch and substation vulnerabilities, in Fig. 8.8, are based on outage probability rather than the load loss they incur in the system if they are damaged.

Fig. 8.9 shows a bar chart illustrating the overall load loss across the system attributed to historical hurricanes with their respective category. It can be seen that hurricanes Rita, Ike, and Harvey, with respective indices of 12, 4, and 26, exhibit substantial impact on the system, resulting in losses of 10.2 GW, 14.67 GW, and 15.2 GW. These are the three most formidable hurricane events ever recorded in Texas [34]. Interestingly, it is observed that some hurricanes with lower categories exhibit more significant effects, such as Hurricane Allison (index=3), than those with



**Figure 8.7** Time-varying loss for each hurricane track. The loss at each time step also includes the expected value of loss over entire flood basins.



**Figure 8.8** Vulnerability indices based on the percentile rank of the average outage probability of a) branches and b) substations for all hurricanes.

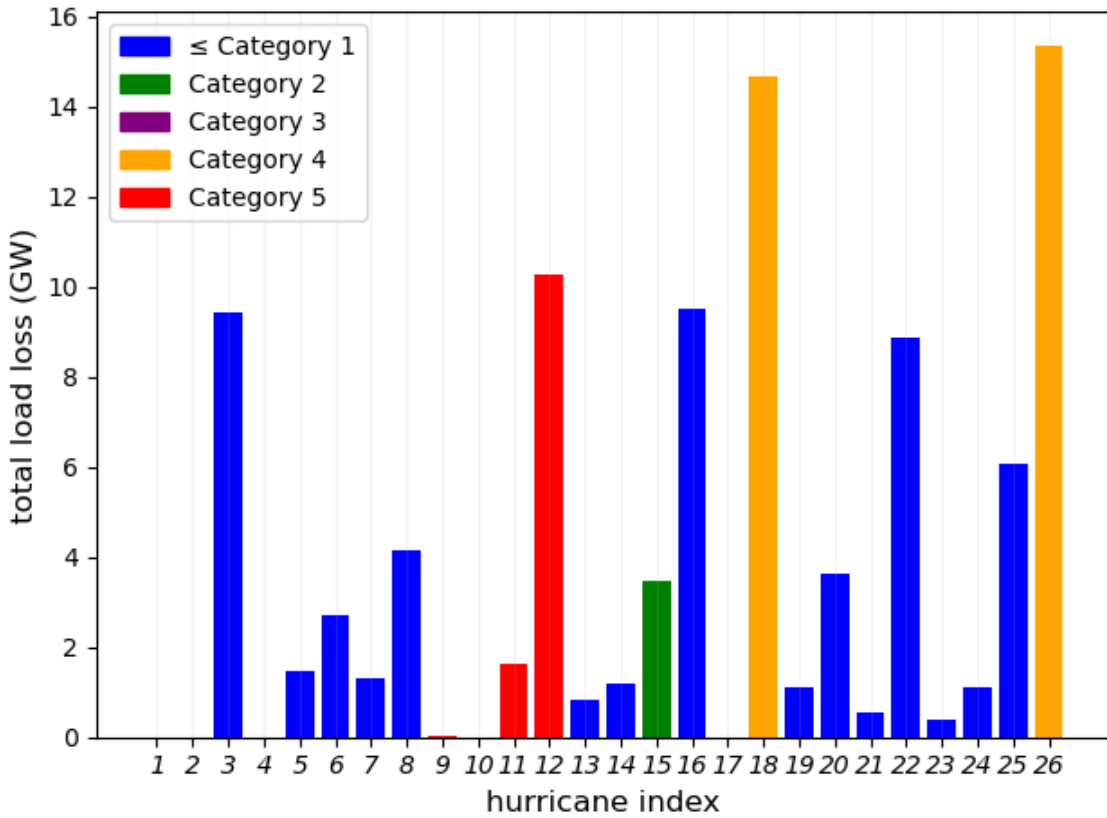


**Figure 8.9** Bar chart depicting an overall load loss in the study area caused by historical hurricanes

higher categories, such as Hurricane Ivan (index=9). This discrepancy is attributed to the fact that hurricane Allison, despite its 0 category, generates heavy flooding over coastal Texas. In contrast, by the time Hurricane Ivan reached Texas, it had significantly weakened, leading to a reduced load loss, while its substantial impact was observed in a location other than Texas.

Fig. 8.10a shows the OVI obtained using (8.9). It is evident that communities with higher outage vulnerability from hurricanes and storm surges are predominantly situated along the coastline. However, because of the grid's architecture, communi-

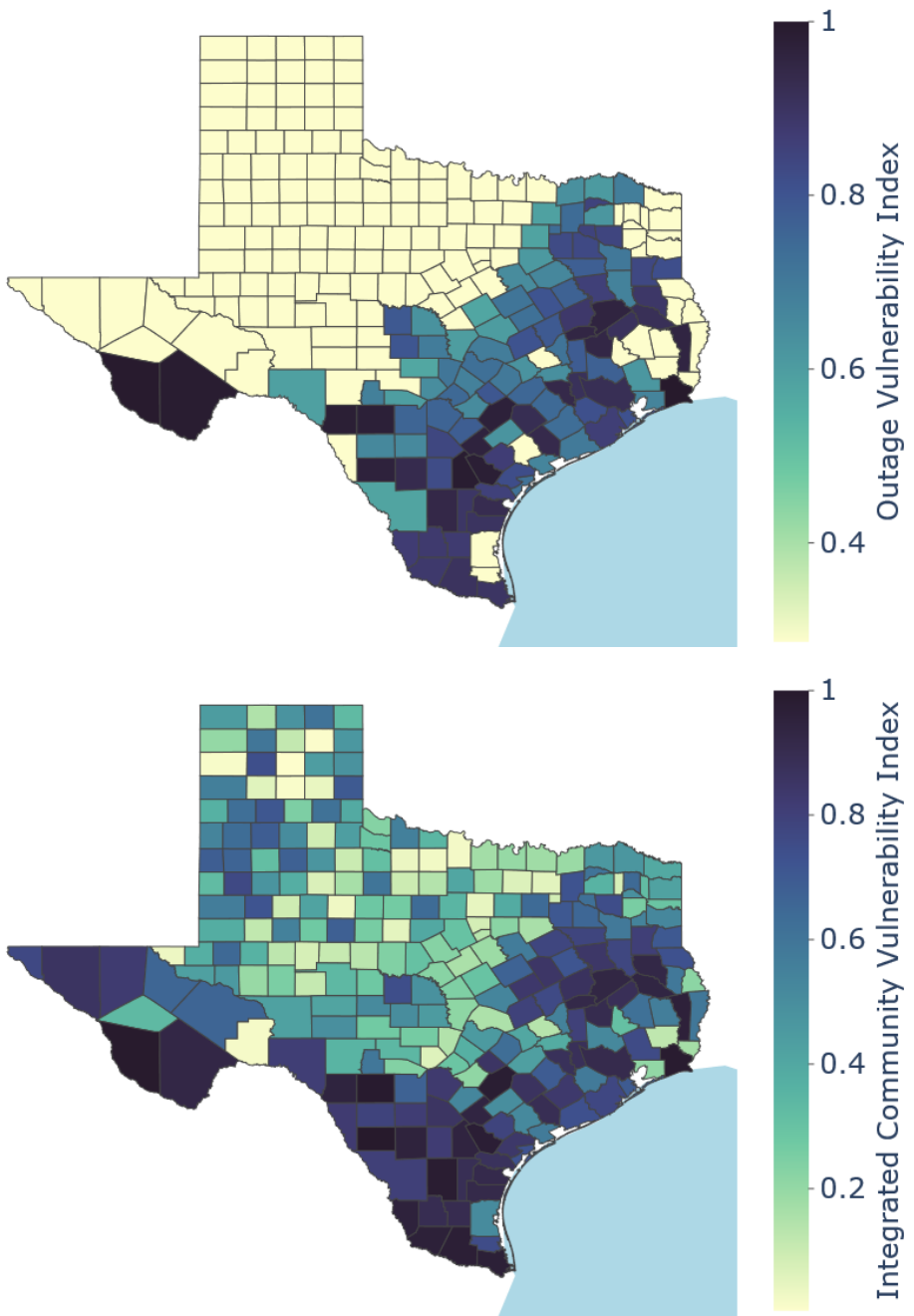


**Figure 8.10** a) Outage Vulnerability Index (OVI) and b) Integrated Community Vulnerability Index (ICVI) around the ERCOT region.

ties farther from the coastline can still affect a hurricane-induced outage, as seen in Fig. 8.10. The compounded effect of their social vulnerability amplifies this impact, highlighting the need for infrastructure improvement in these regions. This can be useful knowledge for transmission planners when determining vulnerable components to future climate events. In Fig. 8.10b, the ICVI can be compared to results of SVI in Fig. 8.3 and OVI in Fig. 8.10a. ICVI reflects the socioeconomic disparities from SVI and highlights communities disproportionately impacted by hurricane and storm surge-induced outage events. There is a shift in vulnerability towards the coastline in ICVI compared to SVI. This gives important insights to grid operators on allocating resources during future hurricane events because we know communities of different vulnerabilities respond differently to outages. A limitation in this analysis is that some counties with very low populations do not have outage data as they are served from different regions; also, counties not within ERCOT territory are not analyzed. However, most of these counties are in regions further from the coastline and less likely to be affected.

## 8.6 Summary

This chapter presents the compounded spatiotemporal impact assessment of hurricanes and storm surges on the power grid and the induced socioeconomic vulnerabilities. A spatiotemporal loss metric is identified based on a probabilistic model. Simulations showed that storm surges could flood the coastal substations to incur an additional loss in the system. The hurricane intensity decays and the overall loss saturates at some point, after which system restoration is required to restore the power to unserved parts of the grid. This chapter also introduces a community vulnerability

metric that integrates the CDC's SVI with the outage factor derived from the impact assessment results. Simulation results show that a hurricane of a higher category does not necessarily entail higher impacts on the system; the landfall location and associated storm surge also influence it. The communities farther from the coast are not immediately perceived as high-risk due to their distance from the coast and often get less attention in storm management strategies. However, the community could have higher socioeconomic vulnerability exacerbated by the outage vulnerability. Hence, ICVI provides a holistic assessment of vulnerable communities by incorporating the effect of extreme weather events and their impact on power outages and associated communities. The proposed methodology can assist planners in identifying the vulnerable system components and vulnerable communities, enabling strategic planning to minimize outages or expedite the restoration while considering energy equity as an additional dimension. In the future, we aim to observe the impact of changing climate on the extreme event scenarios, how other HILP events impact disadvantaged communities, and evaluate the underlying assumption that load and population are highly correlated.

## REFERENCES

- [1] NOAA National Centers for Environmental Information (NCEI), “U.s. billion-dollar weather and climate disasters,” 2021.
- [2] Office for Coastal Management, “Hurricane costs,” 2021.
- [3] C. W. Landsea and J. P. Cangialosi, “Have We Reached the Limits of Predictability for Tropical Cyclone Track Forecasting?,” *Bulletin of the American Meteorological Society*, vol. 99, pp. 2237–2243, Nov. 2018.
- [4] A. Kwasinski, F. Andrade, M. J. Castro-Sitiriche, and E. O’Neill-Carrillo, “Hurricane maria effects on Puerto Rico electric power infrastructure,” *IEEE Power and Energy Technology Systems Journal*, vol. 6, no. 1, pp. 85–94, 2019.
- [5] H. Zhang, L. Cheng, S. Yao, T. Zhao, and P. Wang, “Spatial-temporal reliability and damage assessment of transmission networks under hurricanes,” *IEEE Transactions on Smart Grid*, vol. 11, no. 2, pp. 1044–1054, 2019.
- [6] V. Do, H. McBrien, N. Flores, A. Northrop, J. Schlegelmilch, M. Kiang, and J. Casey, “Spatiotemporal distribution of power outages with climate events and social vulnerability in the usa,” *Nature Communications*, vol. 14, p. 2470, 2023.
- [7] T. W. Collins, S. E. Grineski, J. Chakraborty, and A. B. Flores, “Environmental injustice and hurricane harvey: A household-level study of socially disparate flood exposures in greater houston, texas, usa,” *Environmental Research*, vol. 179, p. 108772, 2019.

- [8] “Let the rich be flooded; the distribution of financial aid and distress after hurricane harvey,” *Journal of Financial Economics (JFE)*, 2019.
- [9] M. Panteli and P. Mancarella, “Modeling and evaluating the resilience of critical electrical power infrastructure to extreme weather events,” *IEEE Systems Journal*, vol. 11, no. 3, pp. 1733–1742, 2015.
- [10] S. Poudel, A. Dubey, and A. Bose, “Risk-based probabilistic quantification of power distribution system operational resilience,” *IEEE Systems Journal*, vol. 14, no. 3, pp. 3506–3517, 2020.
- [11] E. B. Watson and A. H. Etemadi, “Modeling electrical grid resilience under hurricane wind conditions with increased solar and wind power generation,” *IEEE Transactions on Power Systems*, vol. 35, no. 2, pp. 929–937, 2019.
- [12] R. Eskandarpour and A. Khodaei, “Machine learning based power grid outage prediction in response to extreme events,” *IEEE Transactions on Power Systems*, vol. 32, no. 4, pp. 3315–3316, 2016.
- [13] H. T. Nguyen, J. W. Muhs, and M. Parvania, “Assessing impacts of energy storage on resilience of distribution systems against hurricanes,” *Journal of Modern Power Systems and Clean Energy*, vol. 7, no. 4, pp. 731–740, 2019.
- [14] A. C. Reilly, G. L. Tonn, C. Zhai, and S. D. Guikema, “Hurricanes and power system reliability—the effects of individual decisions and system-level hardening,” *Proceedings of the IEEE*, vol. 105, no. 7, pp. 1429–1442, 2017.
- [15] L. Souto, J. Yip, W.-Y. Wu, B. Austgen, E. Kutanoğlu, J. Hasenbein, Z.-L. Yang, C. W. King, and S. Santoso, “Power system resilience to floods: Modeling,

impact assessment, and mid-term mitigation strategies,” *International Journal of Electrical Power & Energy Systems*, vol. 135, p. 107545, 2022.

- [16] A. Shukla, J. Hasenbein, and E. Kutanoglu, “A scenario-based optimization approach for electric grid substation hardening against storm surge flooding,” in *IIE Annual Conference. Proceedings*, pp. 1004–1009, Institute of Industrial and Systems Engineers (IISE), 2021.
- [17] K. Feng, M. Ouyang, and N. Lin, “Tropical cyclone-blackout-heatwave compound hazard resilience in a changing climate,” *Nature Communications*, vol. 13, Jul. 2022.
- [18] M. Panteli and P. Mancarella, “Influence of extreme weather and climate change on the resilience of power systems: Impacts and possible mitigation strategies,” *Electric Power Systems Research*, vol. 127, pp. 259–270, 2015.
- [19] B. W. Tarekegne, B. G. R. Pennell, D. C. Prezioso, and R. S. O’Neil, “Review of energy equity metrics,” tech. rep., Pacific Northwest National Lab.(PNNL), Richland, WA (United States), 2021.
- [20] N. Coleman, A. Esmalian, A. Mostafavi, M., “Equitable resilience in infrastructure systems: Empirical assessment of disparities in hardship experiences of vulnerable populations during service disruptions,” *American Society of Civil Engineers*, vol. 21, no. 4, 2020.
- [21] National Hurricane Center, “Hurricane Basics,” tech. rep., National Oceanic and Atmospheric Administration, May 1999.

- [22] Y. Wang and D. V. Rosowsky, “Joint distribution model for prediction of hurricane wind speed and size,” *Structural Safety*, vol. 35, pp. 40–51, Mar. 2012.
- [23] P. Javanbakht and S. Mohagheghi, “A risk-averse security-constrained optimal power flow for a power grid subject to hurricanes,” *Electric Power Systems Research*, vol. 116, pp. 408–418, Nov. 2014.
- [24] B. Glahn, A. Taylor, N. Kurkowski, and W. A. Shaffer, “The role of the slosh model in national weather service storm surge forecasting,” *National Weather Digest*, vol. 33, no. 1, pp. 3–14, 2009.
- [25] “Slosh display package.”
- [26] A. Serrano-Fontova, H. Li, Z. Liao, M. R. Jamieson, R. Serrano, A. Parisio, and M. Panteli, “A comprehensive review and comparison of the fragility curves used for resilience assessments in power systems,” *IEEE Access*, 2023.
- [27] A. Poudyal, C. Wertz, A. M. Nguyen, S. U. Mahmud, A. Dubey, and V. Gunturi, “Spatiotemporal impact assessment of hurricanes and storm surges on electric power systems,” in *2023 IEEE Power & Energy Society General Meeting (PESGM)*, pp. 1–5, IEEE, 2023.
- [28] A. B. Birchfield, T. Xu, K. M. Gegner, K. S. Shetye, and T. J. Overbye, “Grid structural characteristics as validation criteria for synthetic networks,” *IEEE Transactions on Power Systems*, vol. 32, no. 4, pp. 3258–3265, 2017.
- [29] Simplemaps, “Us zip codes database,” *Simplemaps*, 2023.
- [30] “Cdc/atsdr svi 2020 documentation,” tech. rep., Center for Disease Control, 2020.

- [31] J. Montoya-Rincon, S. Mejia-Manrique, S. Azad, M. Ghandehari, E. Harm-sen, R. Khanbilvardi, and J. Goncalves-Cruz, “A socio-technical approach for the assessment of critical infrastructure system vulnerability in extreme weather events,” *Nature Energy*, vol. 8, p. 1002–1012, 2023.
- [32] A. Poudyal, A. Dubey, V. Iyengar, and D. Garcia-Camargo, “Spatiotemporal impact assessment of hurricanes on electric power systems,” in *2022 IEEE Power & Energy Society General Meeting (PESGM)*, pp. 1–5, 2022.
- [33] D. N. Bresch and G. Aznar-Siguan, “CLIMADA v1.4.1: towards a globally consistent adaptation options appraisal tool,” *Geoscientific Model Development*, vol. 14, pp. 351–363, Jan. 2021.
- [34] “U.s. billion-dollar weather and climate disasters (2023).”

## CHAPTER 9

### CONCLUSIONS AND FUTURE WORK

The power grid is one of the most essential infrastructures in any country, as other critical infrastructures are highly dependent on it. Extreme weather events have significantly increased in frequency and intensity, creating a serious concern for the security and resilience of the power grid. This dissertation provides an in-depth insight into the resilience assessment and planning of electric power grids against extreme weather events through mathematical modeling and optimization techniques.

#### 9.1 Summary of Contributions

This dissertation primarily focuses on resilience assessment, planning, and enhancement of electric power systems against extreme weather events using mathematical modeling techniques and optimization. Broadly, the contributions are categorized as (i) highlight the need for resilience assessment and planning, resilience metric, resilience analysis process, and interdependence with other critical infrastructures in electric power systems; (ii) develop a holistic resilience quantification approach that incorporates both the performance and attribute-based resilience metrics followed by multi-criteria decision-making process to quantify the resilience; (iii) formulate risk-based planning model to enhance the resilience of power distribution systems against extreme weather events; (iv) formulate multi-resource resilience planning model for power distribution and conduct decision trade-off analyses; (v) develop risk-based planning model against extreme weather events for bulk power systems; (vi) decompose the large-scale planning model to alleviate computational complexity and solve

time of planning models; (vii) propose a spatiotemporal impact and vulnerability assessment framework for hurricane and storm surge-induced vulnerabilities for bulk power systems and socioeconomic conditions of the customers.

### **9.1.1 Resilience Assessment and Planning for Power Distribution**

The first contribution is to comprehensively describe the resilience assessment and planning process in power distribution systems. Resilience Assessment and analysis is a holistic approach, and towards this goal, we detail the process and characterize resilience along with several attributes and performance-based resilience metrics. Secondly, an important contribution of this work is also to characterize the need for resilience assessment with other critical infrastructures.

### **9.1.2 Risk-based Planning Framework of Electric Power Systems**

The second contribution is developing a risk-based planning framework for power distribution and bulk power systems using a two-stage stochastic programming model. For the distribution system, we model the problem as a three-phase unbalanced power flow. The proposed risk-based planning model allows utility planners to exercise their risk appetites when planning. Secondly, we also provide a comprehensive trade-off analysis on various planning decisions and system data requirements that can directly or indirectly affect the planning solutions. The scenarios are generated using Monte-Carlo simulations and reduced using a stratified sampling approach. The proposed approaches are validated on a modified IEEE-123 bus system with DG siting and sizing, line hardening, and tie-switch placement decisions. We demonstrate the proposed model on the RTS-GMLC test case for the bulk power system with DG

siting sizing, line capacity upgrade, and line hardening decisions.

### **9.1.3 Large-Scale Planning using Dual Decomposition Approach**

The third contribution is expanding the planning framework for large-scale models. Stochastic programming models are inherently difficult to solve with the increase in the number of scenarios or size of the system model. We propose a dual decomposition-based progressive hedging (PH) framework to decompose the planning model into scenario-based sub-problems so that each problem can be solved independently. With more scenarios, the proposed approach can leverage more compute cores through high-performance computing environments. The proposed framework is validated on a 9500-node test system with three feeders and numerous switches for facilitating reconfiguration. Through experiments, we showed that the PH-based stochastic planning model solves 25 times faster than traditional approaches with reasonable solution quality.

### **9.1.4 Spatiotemporal Impact Assessment of Hurricanes and Storm Surges**

Finally, we developed a spatiotemporal hurricane and storm surges impact assessment framework in bulk power systems. We further extend the work to assess the socioeconomic vulnerabilities of the communities affected by power outages due to hurricanes and storm surges. The hurricane is modeled using a statistical model, whereas storm surges are obtained through NOAA’s SLOSH models. The proposed framework is tested on geographical footprint of Texas with synthetic ERCOT grid. We obtain several outage scenarios for each time step using Monte Carlo simulations. and assess the time-varying outages for each county in Texas. For vulnerability assessment, we

leverage the CDC’s social vulnerability index (SVI) and obtain an integrated community vulnerability index (ICVI) by combining the vulnerability due to power outages. Results show that the vulnerability of specific communities worsens when integrating outages within SVI, and the vulnerabilities shift towards the coast where the impact of hurricanes and storm surges is significant.

## 9.2 Future Research Directions

The current work aims to scale the resilience planning framework to solve large-scale optimization models regarding resources, networks, and scenarios under consideration. As discussed in our existing work, the scenarios are time and space-varying; hence, such details must be incorporated into the planning model for better accuracy. Additionally, solving the extensive form of the problem is suffered by the curse of dimensionality. Hence, off-the-shelf solvers are more likely to crash or provide high optimality gap solutions when a high dimensional extensive form of the model is fed to the solvers. Thus, solving a large-scale stochastic optimization problem has several challenges and is an active area of research that motivates us in our future work. In addition, operational planning strategies like defensive islanding would be studied to better prepare for the upcoming hurricane storms. Such a proactive islanding method can prevent the propagation of cascading failure effects in the power system.

### 9.2.1 Modeling Critical Infrastructures Interdependence

As discussed in Chapter. 2.4 power distribution systems and bulk power systems are interdependent with other critical infrastructures such as natural gas, water, cyber security, and so forth. This dissertation does not include the interdependency in the

resilience metric or planning. It is essential to accurately model these interdependencies to represent a single or aggregated system's resilience. For example, a certain region might have a high dependency on natural gas-fired generators, and a shortage of natural gas can pose a risk of outages. Hence, it is essential to plan other backup resources or create another generation mix in the region to minimize the impact due to the shortage of natural gas.

### **9.2.2 Multi-stage Planning**

The core planning model presented in this dissertation is based on a two-stage stochastic programming model where the first-stage decisions are the planning or investment decisions, whereas the second-stage decisions are the recourse. However, additional complexities cannot be represented via a two-stage model. For example, the invested DG in the first stage depends on other resources, such as fuel in the second stage, whose uncertainty is not considered in the planning model. When fuel uncertainties are considered, the model expands to three stages or even multiple stages, where the fuel uncertainty is then incorporated into the second stage. Additionally, energy storage systems introduce charging uncertainties in the model and can be extended to even multi-stage multi-period optimization [1].

### **9.2.3 Defensive Islanding and Restoration of Electric Power Systems**

#### **Against Extreme Weather Events**

Extreme weather events, such as hurricanes and storm surges, can have devastating impacts on the power grid and can result in cascading failures of the resources if not handled properly. During an upcoming storm, it is typically challenging to address the

operational decisions considering the timescale of the events and resources required. However, it is possible to minimize the impact of these events if the grid is split into multiple self-sustaining islands ahead of the event. Some existing works propose the idea of defensive islanding [2]. However, the event scenarios in these works are non-realistic, as the spatiotemporal impact of these events is not considered. Hence, future directions in this area can explore ways to identify proactive islanding strategies to minimize the impact of extreme weather events on the grid.

#### **9.2.4 Use of Artificial Intelligence Techniques for Realistic Scenario Generation**

Recently, artificial intelligence (AI) models, especially machine learning (ML) models, have gained significant popularity. ML models are widely used in forecasting, even in practical power systems applications [3, 4]. With the rapid proliferation of large language models, researchers have pivoted their focus on how to leverage ML tools to solve complex engineering problems, including decision-making under uncertainty [5]. One such application could be using graph neural networks (GNNs) to identify grid vulnerability by leveraging the graph-driven training feature of GNNs. Once trained, ML models are incomparable with model-based approaches regarding solving time. However, the major challenge is that such models are highly data intensive and depend on high-quality data to train on. Future advancements in ML models can open new doors for power system applications.

### 9.3 Publications and Software Packages

#### 9.3.1 Journals

1. A. Poudyal, S. Poudel, and A. Dubey, “**Large-scale Resilience Planning in Power Distribution Systems against Extreme Weather Events**,” *IEEE Transactions on Power Systems* (in preparation)
2. A. Poudyal, S. Lamichhanne, J. Campos do Prado, and A. Dubey, “**Resilience-driven Planning of Electric Power Systems Against Extreme Weather Events**,” *Sustainable Energy, Grids and Networks* (in preparation)
3. A. Poudyal, and A. Dubey, “**Multi-resource Trade-offs in Resilience Planning Decisions for Power Distribution Systems**,” *IEEE Transactions on Industry Applications* (under review)
4. A. Poudyal, S. Paul, S. Poudel, and A. Dubey, “**Resilience assessment and planning in power distribution systems: Past and future considerations**,” *Renewable and Sustainable Energy Reviews*, Jan. 2024
5. A. Poudyal, S. Poudel, and A. Dubey, “**Risk-Based Active Distribution System Planning for Resilience Against Extreme Weather Events**,” *IEEE Transactions on Sustainable Energy*, Nov. 2022

#### 9.3.2 Conferences

1. A. Poudyal, S. Lamichhane, C. Wertz, S. Uddin Mahmud, and A. Dubey. “**Hurricane and Storm Surges-Induced Power System Vulnerabilities and**

**their Socioeconomic Impact,” 2024 IEEE Power & Energy Society General Meeting**, Seattle, WA, Jul. 2024 (accepted)

2. A. Poudyal, and A. Dubey. “**Understanding Trade-Offs in Resilience Planning Decisions for Power Distribution Systems,” 2023 IEEE Industry Applications Society Annual Meeting (IAS)**, Nashville, TN, Oct. 2023.
3. A. Poudyal, C. Wertz, A. Mi Nguyen, S. Uddin Mahmud, V. Gunturi and A. Dubey. “**Spatiotemporal impact assessment of hurricanes and storm surges on electric power systems,” 2023 IEEE Power & Energy Society General Meeting**, Orlando, FL, Jul. 2023.
4. A. Poudyal, V. Iyengar, D. Garcia-Camargo, and A. Dubey. “**Spatiotemporal Impact Assessment of Hurricanes on Electric Power Systems,” 2022 IEEE Power & Energy Society General Meeting**, Denver, CO, Jul. 2022.
5. A. Poudyal, S. Poudel, and A. Dubey. “**A risk-driven probabilistic approach to quantify resilience in power distribution systems,” 2022 17th international conference on probabilistic methods applied to power systems (PMAPS)**, Manchester, UK, Jun. 2022.

### 9.3.3 Software Packages

1. <https://abodh.github.io/LinDistRestoration/>
2. <https://github.com/abodh/LinDistRestoration>
3. [https://github.com/abodh/proactive\\_resilience\\_planning](https://github.com/abodh/proactive_resilience_planning)

## REFERENCES

- [1] S. Zeynali, N. Rostami, A. Ahmadian, and A. Elkamel, “Two-stage stochastic home energy management strategy considering electric vehicle and battery energy storage system: An ann-based scenario generation methodology,” *Sustainable Energy Technologies and Assessments*, vol. 39, p. 100722, 2020.
- [2] M. Panteli, D. N. Trakas, P. Mancarella, and N. D. Hatziargyriou, “Boosting the power grid resilience to extreme weather events using defensive islanding,” *IEEE Transactions on Smart Grid*, vol. 7, no. 6, pp. 2913–2922, 2016.
- [3] “Load forecasting for adms and aems.” <https://www.ge.com/digital/applications/advanced-distribution-management-solutions-adms/load-forecasting-adms-and-aems>.
- [4] B. V. Lundin, “National grid eso deploys ml-based inertia forecasting,” *EE Powers*, April 2022.
- [5] J. Wendel, “Chatgrid: A new generative ai tool for power grid visualization,” *PNNL News*, February 2024. Accessed: April 23, 2024.